Thèse n° 8397

Large charge, semiclassics and superfluids : from broken symmetries to conformal field theories

Présentée le 24 septembre 2020

à la Faculté des sciences de base
Laboratoire de physique théorique des particules
Programme doctoral en physique

pour l'obtention du grade de Docteur ès Sciences

par

Gabriel Francisco CUOMO

Acceptée sur proposition du jury

Prof. F. Carbone, président du jury
Prof. R. Rattazzi, directeur de thèse
Prof. A. Nicolis, rapporteur
Dr A. Zhiboedov, rapporteur
Prof. J. M. Penedones, rapporteur

École
polytechnique
fédérale
de Lausanne

2020

El mundo era tan reciente, que muchas cosas carecían de nombre,
y para mencionarlas había que señarlarlas con el dedo.
— Gabriel Garcia Marquez

A Mariela e Massimo, i miei genitori

Acknowledgements

I can hardly imagine a fully personal achievement in life. This certainly holds in science, whose progress largely relies on the exchange of ideas among different people. This is also true for such an apparently small thing as getting a title or a degree. If in few months I will earn the privilege of being called "doctor" (dear committee members, please don't fail me), I cannot forget that this will be largely due to all the amazing people who accompanied and guided me during the last four years. These perhaps obvious, but very sincere pages want to be a small, though awkwardly incomplete, tribute to them.

The first obvious, but sincere, acknowledgements are for my advisor, Riccardo Rattazzi. Having him as a guide in the last four years was a privilege far beyond what one might expect from his well known scientific achievements. Indeed, not only he is an exceptional scientist, but he is also a true *maestro.* I learned some physics (and not only) from every single discussion with him, including those on politics. Each of his sentences is able to explain something while, at the same time, pointing at some question lying slightly beyond the current discussion; this always motivated me to go deeper into the subject and keep asking questions. Perhaps most importantly, he taught me the importance of always having a critical perspective on my own work. As if all of this was not enough, he is also an exceptional person. He honestly cared about me in the last four years and he was incredibly supportive during the stressful time when I was applying for jobs. His importance on my personal development in the last four years, as a scientist and as a person, can hardly be overestimated. These few acknowledgments and the (I hope not too crappy) thesis which follows them cannot make justice to that. For what matters, sincerely, thanks.

Most students would call themselves lucky for having one such supervisor. I was even luckier in that I effectively had two more! I wish to acknowledge them here. One was/is Andrea Wulzer, who I work with for my more phenomenological research. From him I learned an incredible amount of physics, both on phenomenology and formal topics. Our ongoing research is certainly the one of most direct relevance for particle physics among the projects I worked on so far, and I hope to be able to keep contributing to that in the future. With him, I also learned how different can be the first formulation of an idea from its final version in a draft (after all, research can be described as the amazing

transformation process of blackboard scribbles and swear words into elegant and detailed derivations). The other effective advisor of mine was Sasha Monin, who I worked with for most of my projects. His lucid perspective is invaluable in assessing the validity of an idea. He taught me the importance of the details, behind which, often, something not yet understood is hiding. Luckily, I could partially pay him back for what he taught me in physics with some proper ping-pong lessons (Sasha, you're welcome for that).

In my still short research experience, I already had the chance to collaborate and discuss ideas with many other researchers and professors at EPFL and not only. An incomplete list includes Gil Badel, Anton De La Fuente, Angelo Esposito, Emanuele Gendy, Denis Karateev, Andrei Khmelnitsky, Petr Kravchuk, Alberto Nicolis, Joao Penedones, David Pirtskhalava, Lorenzo Ricci, Marco Serone, Emmanuel Stamou, Luca Vecchi, Alessandro Vichi. From each of them I learned something. Special thanks to Andrei, Angelo and Luca for their crucial support, not only concerning physics, during the two longest projects of my PhD. I would also like to mention Marco Serone, without whose help I would have never had to chance to pursue my doctoral studies in Lausanne.

Doing a PhD can be stressful at times, and I devoted to it more resources, in terms of energy and time, than I like to admit. Luckily, things were made better by the possibility of sharing this demanding experience with many other students: Aditya, Adrien, Alfredo, Andrea, Andrei, Bernardo, Davide, Francisco, Gil, Jeanne, Joao, Kamran, Kin, Lorenzo, Marten, Miguel, Misha, Siyu. With them I did not only share the difficulties of doing a PhD, but also concerts, ski trips (in which I risked my life), movie nights, football games, jokes (mostly racist ones) and much more. Special thanks also to my amazing housemates, Max, Michele, Seb and Vlado, who made me live many "Big Bang Theory" moments in real life (too bad we missed a proper Penny though). It is also thanks to all of these people that I enjoyed the last four years in Lausanne.

It's been six years since I left Acireale and Catania, but I cannot stop thinking of them as "home". This is largely due to the many friends which I still have there, too many to be mentioned here. The time spent with them during holidays, quarantine (mostly playing "scopone" telematically) and not only has always been the best way to "recharge the battery" and forget about papers, equations and all that.

The last acknowledgements are for my family. I cannot but thank my parents for their support and encouragement throughout these years. It is them who instilled in me the curiosity, and perhaps the workaholic attitude, that led me to the choice of this path. I would like to devote a thought to my grandmother Ruby, whose love certainly cannot be stopped just by an ocean. Finally, thanks to Maria Vittoria, for always being close to me, for the last years spent together. This achievement also belongs to her.

Sincerely, Gabriel

Foreword

The material of the thesis is schematically organized as follows.

- Chapter 1 is an orginal presentation of existing results on Goldstone bosons for spontaneously broken symmetries at finite density.
- Chapter 2 is based on [1]:
  G. Cuomo, A. Esposito, E. Gendy, A. Khmelnitsky, A. Monin and R. Rattazzi, "Gapped Goldstones at the cutoff scale: a nonrelativistic EFT",
  e-Print: arXiv:2005.12924 [hep-th] .
- Chapter 3 reviews the large charge expansion in conformal field theories with $U(1)$ symmetry, including some unpublished results.
- Chapter 4 discusses the large charge expansion in conformal field theories invariant under general symmetry groups and mostly presents original unbpublished material.
- Chapter 5 is based on [2]:
  G. Cuomo, A. de la Fuente, A. Monin, D. Pirtskhalava, and R. Rattazzi, "Rotating superfluids and spinning charged operators in conformal field theory", Phys. Rev.D 97 (2018) no. 4, 045012, e-Print: arXiv:1711.02108 [hep-th] .
- Chapter 6 is based on [3]:
  G. Cuomo, "Superfluids, vortices and spinning charged operators in 4d CFT", JHEP 2002 (2020) 119, e-Print: arXiv:1906.07283 [hep-th] .
- Chapter 7 is based on [4]:
  G. Badel, G. Cuomo, A. Monin, and R. Rattazzi, "The epsilon expansion meets semiclassics", JHEP 1911 (2019) 110, e-Print: arXiv:1909.01269 [hep-th] .
- Chapter 8 is based on [5]:
  G. Badel, G. Cuomo, A. Monin, and R. Rattazzi, "Feynman diagrams and the large charge expansion in $3-\varepsilon$ dimensions", Phys. Lett. B802 (2020) 135202, e-Print: arXiv:1911.08505 [hep-th] .

Our presentation includes some additional material with respect to the published papers; notably, section 5.2 and most of section 5.6 did not appear in [2]. Appendices contain additional details not included in the main text.

Abstract

This thesis explores the application of semiclassical methods in the study of states with large quantum numbers for theories invariant under internal symmetries.

In the first part of the thesis, we study zero-temperature superfluids. These provide a general description of many systems at finite charge density. In particular, we derive a universal effective field theory description for non-Abelian superfluids. Such construction illustrates the role of gapped Goldstones, Goldstone modes whose gap is fixed by the symmetry, and may be as large as the strong coupling scale of the system.

The second and third part of the thesis are devoted to the study of operators with large internal charge in strongly coupled conformal field theories. Using effective field theory techniques, we derive universal results for the spectrum of scaling dimensions and the OPE coefficients in a large charge expansion, both for theories invariant under Abelian and non-Abelian symmetry groups. We also extend these results to operators with large spin as well as large internal charge.

The last part of this thesis studies operators with large internal charge within the ε-expansion. We show how, using a semiclassical approach, one can overcome the breakdown of diagrammatic perturbation theory for the multi-legged amplitudes associated with these operators. These results provide a concrete illustration of the systematic large charge expansion discussed in the previous parts.

Riassunto

In questa tesi si studia l'applicazione di metodi semiclassici nello studio di stati caratterizzati da grandi numeri quantici per teorie invarianti sotto una simmetria interna.

Nella prima parte della tesi, si studiano superfluidi a temperatura zero. Questi costituiscono una descrizione generale di molti sistemi a densità di carica finita. In particolare, viene derivata una teoria di campo effettiva per superfluidi non-Abeliani. Tale descrizione illustra il ruolo dei Goldstone gappati, modi di Goldstone il cui gap è fissato dalla simmetria e può essere dello stesso ordine della scala a cui il sistema diventa fortemente interagente.

La seconda e la terza parte della tesi sono dedicate allo studio di operatori con grande carica per simmetria interna in teorie di campo conformi fortemente interagenti. Tramite teorie di campo effettive, si derivano risultati universali per lo spettro delle dimensioni conformi e i coefficienti di fusione in un'espansione di grande carica, sia per teorie invarianti per simmetrie Abeliane che per teorie invarianti per simmetrie non-Abeliane. Tali risultati vengono anche estesi al caso di operatori con grande momento angolare oltre che carica interna.

La quarta parte della tesi studia operatori con grande carica interna nell'espansione in ε. Si dimostra come, tramite un approccio semiclassico, è possibile superare le difficoltà legate al fallimento dell'espansione perturbativa in diagrammi per le ampiezze a molte gambe legate a questi operatori. Tali risultati illustrano altresì l'espansione a grande carica, discussa in precedenza nel caso generale, tramite un esempio concreto.

Contents

Acknowledgements **i**

Foreword **iii**

Abstract **v**

Riassunto **vii**

Introduction **1**

I Aspects of spontaneous symmetry breaking at finite density **9**

1 Goldstone bosons at finite density **11**
- 1.1 Goldstone theorem at finite density 11
- 1.2 Examples 17

2 Non-Abelian superfluids: gapped Goldstones at the cutoff scale **26**
- 2.1 Interactions of slow gapped Goldstones in the linear triplet 28
- 2.2 The Nonrelativistic EFT: the universal description of slowly moving gapped Goldstones 30
- 2.3 Integrating out the gapped Goldstone: a less effective field theory 46

Conclusions to Part I **50**

II Superfluids and the large charge sector of strongly coupled CFTs **55**
- Invitation: the hydrogen atom at large angular momentum 56

3 The large charge expansion in $U(1)$-invariant CFTs **60**
- 3.1 Path-integral at fixed charge 60
- 3.2 The spectrum of $U(1)$-invariant CFTs at large global charge 63
- 3.3 Correlation functions from EFT in $U(1)$-invariant CFTs 69

4 The large charge expansion in CFTs: general symmetry groups 77
4.1 Operators with lowest dimensions at large charge 78
4.2 Charged operators in the critical $O(N)$ models 83
4.3 CFT data from a gapped Goldstone resonance 89

Conclusions to Part II 100

III Rotating superfluids and spinning charged operators in CFTs 105

5 Spinning charged operators and vortices in $3d$ CFTs 107
5.1 Summary of Results 107
5.2 Spinning superfluid: vortices and singularities 108
5.3 Formulation of the EFT 111
5.4 From vortices to spinning charged operators 114
5.5 Correlators 119
5.6 Discussion and generalizations 120

6 Spinning charged operators and vortices in four dimensions 127
6.1 Summary of results 127
6.2 Formulation of the EFT in four dimensions 130
6.3 Scaling dimensions from vortices in four dimensions 133
6.4 Correlators 142
6.5 Vortices in arbitrary dimensions 144

Conclusions to Part III 146

IV The ε-expansion meets semiclassics 149
Invitation: perturbation theory for an ordinary integral 150

7 Large charge operators and multi-legged amplitudes at the Wilson-Fisher fixed point 152
7.1 Perturbation theory around the vacuum 154
7.2 Semiclassical approach 157
7.3 Finite λn on the cylinder 162
7.4 Discussion 171

8 Feynman diagrams and the large charge expansion in $3-\varepsilon$ dimensions 174
8.1 Lagrangian and Feynman diagrams 175
8.2 Semiclassical computation 176
8.3 Analysis of the result 179

Conclusions to Part IV 182

V Appendix **185**

A Appendices to Part I **186**
A.1 Dimensionless coefficients in the model of two complex doublets 186
A.2 Details on amplitudes in the triplet model 187
A.3 Spacetime coset construction for the $SU(2)$ superfluid 190
A.4 NREFT details 195

B Appendices to Part II **204**
B.1 Basics of Conformal Field Theories 204
B.2 Conformal superfluid from the coset construction 211
B.3 Casimir energy of the $U(1)$-conformal superfluid 214
B.4 Details on correlation functions in the large charge EFT 218
B.5 Continuum approximation and thermalization in the CFT spectrum . . 226

C Appendices to Part III **231**
C.1 Nambu-Goto action for superfluid vortices from the coset construction . 231
C.2 Photon propagator on the sphere 234
C.3 Vortex energy in 4d via dimensional regularization 235

D Appendices to Part IV **240**
D.1 Diagrammatic two loop computation in $\lambda|\phi|^4$ 240
D.2 One loop computation on the cylinder in $\lambda|\phi|^4$ 243

Bibliography **247**

Curriculum Vitae **265**

Introduction

Feynman's "sum over paths" epitomizes the striking difference between classical and quantum mechanics. The physical evolution of a classical system is determined by the condition that the trajectory $q_{classical}(t)$ be a stationary point of the action functional $S[q]$. Instead, quantum-mechanical amplitudes are determined by an "average over all possible paths" $q(t)$ weighted by a factor $e^{iS[q]}$. This defines the *path integral*:

$$\langle q_f|e^{-iH(t_f-t_i)}|q_i\rangle = \int_{q_i}^{q_f} \mathcal{D}q\, e^{iS[q]}\,,$$

where the initial and final state of the system specify the boundary conditions for the functional integration.

The different regimes of quantum systems are readily classified through the properties of the corresponding path integral. The latter of course depends not only on the dynamics but also on the boundary conditions and, somewhat equivalently, on the operator insertions. Path integrals can be broadly divided into two classes, Weakly Coupled (WC) and Strongly Coupled (SC). A path integral is weakly coupled when it can be approximated by a loop expansion around some leading classical trajectory γ. A SC path integral instead occurs when no saddle point approximation is possible.

When considering systems with a large number of degrees of freedom, such as those naturally described by quantum field theory (QFT), our predictive ability largely relies on the existence of a WC path integral. Most notably, a WC path integral describes collisions between Standard Model particles at center of mass energy $E \gg 1$ GeV. An example of a SC case is instead given by QCD processes around the GeV. Even in the presence of SC path integrals, one can often find a subset of the variables, normally associated to long distance physics, whose quantum fluctuations are small around some trajectory. In that case, one can first integrate out the variables with large quantum fluctuations and derive an effective WC description for the remaining variables. In the case of QCD, the latter correspond to the low energy excitations of the pions.

In the WC case the contribution to physical observables $\mathcal{O}$ consists of the sum of two terms

$\mathcal{O} = \mathcal{O}_\gamma + \mathcal{O}_q$, a classical one $\mathcal{O}_\gamma$, determined by the value of physical variables along the leading trajectory, and a quantum one, $\mathcal{O}_q$, determined by quantum fluctuations around γ. One can then distinguish classical and quantum observables depending respectively on whether $\mathcal{O}_\gamma \gg \mathcal{O}_q$ or not. For instance, the path integral for the harmonic oscillator is always weakly coupled, by definition, while the corresponding ground state energy is a quantum observable, and one can consider states (for instance coherent states) where to find classical observables. For a SC path integral all observables are quantum mechanical.

Observables describing small fluctuations of the vacuum state are always quantum in nature. Generically, they are amenable to a WC description only if the system is well approximated by a free theory, such as the harmonic oscillator, up to corrections proportional to a small coupling $\lambda \ll 1$. Instead, semiclassical observables are normally associated with states made of *many quanta*, therefore very different from the vacuum.

Observables with large quantum numbers under the conserved charges of the theory are naturally semiclassical. Irrespectively of the existence of a small coupling, we generically expect the existence of a WC semiclassical path integral in that case, even if only as an effective description for a subset of the variables. This entails substantial simplifications in the description of the sectors of the theory with large quantum numbers. The present thesis will deal with some instances of this general phenomenon.

Large quantum numbers and semiclassics

As a simple illustration of the emergence of classical physics in the limit of large quantum numbers, consider the Hydrogen atom system in quantum mechanics. In the limit of infinite proton mass, the electron Hamiltonian is given by

$$H = \frac{\boldsymbol{p}^2}{2M} - \frac{\alpha}{r}\,,$$

where M denotes the mass of the electron, $\boldsymbol{p}$ its momentum and α the fine structure constant. As well known, the bound states of the system are found solving the Schrödinger equation. They have energy $E_n = -\frac{M\alpha}{2n^2}$ and are labeled by three integer quantum numbers n, ℓ, and m, with $n \geq \ell + 1$. In particular ℓ and m specify, respectively, the angular momentum $\boldsymbol{J}^2 = \ell(\ell+1)$ and its projection $J_3 = m$ on the third axis. The minimal energy state at fixed angular momentum m on the third axis has energy $E_0(m) = -\frac{M\alpha}{2(m+1)^2}$, corresponding to $m = \ell = n - 1$.

For $m \gg 1$, the value of $E_0(m)$ is well approximated by the classical result. To see this, we observe that the (classical) *effective* potential at fixed angular momentum $\ell = m$ is given by:

$$V_{eff}(r) = \frac{m^2}{2Mr^2} - \frac{\alpha}{r}\,.$$

Upon minimizing this expression, we find that the minimal energy solution at fixed angular momentum corresponds to a circular orbit at radius $r_{class.}=\frac{m^2}{M\alpha}$. Computing the Hamiltonian on this configuration, we find

$$E_0^{class.}(m)=-\frac{M\alpha}{2m^2}\qquad\Longrightarrow\qquad\frac{E_0(m)-E_0^{class.}(m)}{E_0(m)}\simeq\frac{2}{m}\,,\quad m\gg 1\,.$$

As anticipated, we see that the classical approximation becomes exact in the infinite angular momentum limit.

Why does classical physics emerge at large angular momentum? Let us of focus on the radial wave-function for concreteness. According to the standard WKB procedure [6], the quasi-classical treatment holds for $d\lambda_r/dr\ll 1$, where the radial wave-length is given by $\lambda_r=2\pi\hbar/|\boldsymbol{p}|\sim r/m$, thus reproducing the condition $m\gg 1$. Physically, the centrifugal force keeps r localized on the classical trajectory for $m\gg 1$; indeed, it can be checked that the spread of the exact expression of the wave-function scales as $\Delta r^2/r^2_{class.}\propto 1/m$. This implies that the exact result can be computed expanding the corresponding path-integral around the classical trajectory. We shall discuss in detail the systematic calculation of $1/m$ corrections to the classical result in the introduction to part II.

Let us now discuss the case of a quantum field theory at large quantum numbers. In this case, while the basic picture is similar, the presence of an infinite number of degrees of freedom makes things more involved. In general, the WC semiclassical description takes the form of an effective field theory for certain light degrees of freedom. That such light modes generically exist follows from the fact that a state with large charge density unavoidably breaks certain (spacetime and often also internal) symmetries. The long distance dynamics of the system is thus described by the associated Nambu-Goldstone modes [7,8]. The prototypical example of this scenario is given by the relativistic effective string theory (EST) describing meson resonances with large spin, which we illustrate below.

A meson can be thought as a bound state made of a quark-antiquark pair, held together by a tube of chromoelectric flux. This leads to a potential linearly increasing with the distance between the two quarks, in agreement with lattice calculations [9]. The development of this model led to the formulation of the first string theory [10] as an attempt to describe the strong interactions. Nowadays we understand that the correct theory to describe hadron physics is given by QCD, while, much more ambitiously, we consider string theory as the most promising framework where to find a consistent theory for quantum gravity and all other interactions. Nonetheless, EST can still be used to describe the dynamics of a sufficiently long flux tube.

Let us consider first a simple a toy model describing a meson: a rotating string with constant angular velocity around its center, such that its endpoints move at the speed of light. A simple classical analysis reveals that the angular momentum J and the energy E

of the string are related to its length R and tension T by [11]

$$J = \frac{\pi}{8} T R^2 \,, \qquad\qquad E = \frac{\pi}{2} T R \,.$$

Identifying E with the mass M of the meson, we find the celebrated Regge relation between the mass and the spin of the lightest mesons:

$$M^2 = \frac{J}{\alpha'} \,, \qquad\qquad \alpha' = \frac{1}{2\pi T} \,.$$

Perhaps surprisingly, such a simple linear relation between the spin and the mass of the resonances is indeed approximately observed in nature [12], with the string tension given by $T \simeq 0.2\,\text{GeV}^2$ [13].

We would like to promote the previous toy model to a systematic effective description of the flux tube dynamics. To this aim, we should identify the variables describing the system. In general, the string degrees of freedom include its coordinates in the transverse direction, called *branons*, as well as other degrees of freedom determining the microscopic structure of the tube. The latter will in general be strongly coupled and we do not expect to be able to describe them via a WC path integral. However, on dimensional grounds, such microscopic variables will generically describe fluctuations on short scales, of order $\sqrt{\alpha'}$. [1] Instead, the branon modes can be thought as the Goldstone bosons for the translations broken by the string; thus they are always light, corresponding to long wavelength fluctuations, and weakly interacting at low energies. Therefore, to describe the dynamics of a sufficiently long string $R \gg \sqrt{\alpha'}$, we can integrate out the microscopic modes and consider a long distance effective theory for the branons only. According to the previous discussion $R \sim \sqrt{\alpha' J}$ and such description applies for $J \gg 1$. As anticipated, we see that the large angular momentum limit entails the existence of a WC description.

The most general Lagrangian for EST was constructed in [16, 17] (see also [18, 19] for a covariant formulation). Calling X^m with $m = 2, 3$ the transverse coordinates of the string, the action to leading order is just given by the Nambu-Goto action [20]:

$$S_{string} = -T \int d^2\sigma \sqrt{-\det\left(\eta_{\alpha\beta} + \partial_\alpha X^m \partial_\beta X^m\right)} + \ldots \,,$$

where $\alpha, \beta = 0, 1$ and $\{\sigma_0, \sigma_1\}$ parametrize the string worldsheet. The structure of the action follows simply from the nonlinearly realized Poincaré symmetry, all the information on the microscopic details of the theory being encoded in the value of the string tension T. The dots stand for higher derivative terms, possibly including boundary terms for open strings, suppressed by powers of $1/(TR^2) \sim 1/J$ with respect to the leading order.

---

[1] Interestingly, lattice data suggest that this expectation is not entirely correct due to the existence of a light *string axion* on the worldsheet [14]. We shall neglect this complication in our analysis, referring the reader to [15] for an effective field theory including the latter.

As an illustration, let us discuss the basic predictions for an open string with free endpoints (Neumann boundary conditions). Quantizing the action around a rotating solution we find the existence of states with $\alpha' M^2 = J + N$, $N = 0, 1, 2 \ldots$, in agreement with the classical analysis discussed before for $N = 0$. Furthermore, we may compute corrections to this formula in a $1/J$ expansion. For the ground state of the string, this was done in [13]. The result reads:

$$M^2 = \frac{J}{\alpha'} + c_q J^{1/4} - \frac{1}{12} + \mathcal{O}\left(J^{-1}\right) ,$$

where c_q is the Wilson-coefficient of a certain boundary operator, physically parametrizing the contribution of the quark masses.[2] Interestingly, the value of the Regge intercept, the term proportional to J^0, corresponds to the Casimir energy of the branons and it is hence independent of the coefficients of the effective theory. In other words, such contribution takes the same value for all meson families and it is hence *universal.* This illustrates the predictive power of EST at large angular momentum.

Plan of the thesis

Most interesting theories are not only invariant under the spacetime Poincaré symmetry, but also under additional internal symmetries, the conserved charges often associated with the number of particles of a certain species. In this thesis we will study certain aspects of the limit of large internal charge.

Physically, a system at finite charge density can be associated with a certain *condensed matter phase* of the theory. From the field theoretical point of view, a condensed matter phase is a state in which the Poincaré and the internal symmetries are spontaneously broken, preserving at large distances some form of spatial translations, time-translations, and possibly spatial rotations [22]. The simplest option is that the ground state of the system at fixed charge density induces the symmetry breaking pattern which defines a superfluid phase [23]. Motivated by this observation, in part I of this thesis we study the basic features of zero-temperature superfluids from the field theoretical viewpoint, focusing in particular on systems at large non-Abelian charge density.

In the rest of the thesis, we will focus on conformal field theories (CFTs), QFTs invariant under scale transformations. CFTs are of general interest since, given an arbitrary theory, whenever there is a large separation between two relevant scales $\Lambda_1 \ll \Lambda_2$, the system can be described as an approximate scale-invariant theory at intermediate scales $\Lambda_1 \ll E \ll \Lambda_2$. They also describe critical points in statistical mechanics and provide a non-perturbative definition of quantum gravity through the AdS/CFT correspondence [24].

The vast majority of CFTs does not possess a small coupling. Therefore, the physics of the vacuum and of the lowest energy excitations is described by a SC path integral. We hence have to rely on numerical techniques to study them, such as Monte-Carlo simulations or the conformal bootstrap [25], and most of our knowledge is limited to specific examples. However, things simplify for states with large internal charge, in which case we expect that the system is found in a superfluid phase. In parts II and III of this thesis we will study the consequences of this idea for the spectrum of three- and four-dimensional CFTs, partly relying on the effective field theory techniques discussed in part I.

---

[2] In the Polchinski-Strominger formalism, boundary operators were classified in [21]).

Finally, we will study the limit of large internal charge for fixed points in the ε-expansion in part IV of this thesis. Such theories are always described by a WC path integral and therefore we will not need to resort to an effective field theory description. Nonetheless, in agreement with our general discussion, we will find that certain observables can only be computed expanding the path integral around a non-trivial semiclassical trajectory, while standard perturbation theory around the vacuum state fails. We will also comment on the intriguing analogy between the simple problem that we address and the unsolved issue concerning the production rate of a large number of particles in massive theories.

At the end of each part of this thesis, we provide conclusions and a detailed outlook of future prospects. Appendices contain additional details and technical derivations.

Summary of conventions: Lorentz indices $\mu, \nu, \ldots$ go from 0 to $d-1$ and we use mostly minus metric signature $\text{sgn}(g_{\mu\nu}) = \{1, -1, \ldots, -1\}$. Spatial indices are labelled via $i, j, \ldots = 1, 2, \ldots, d-1$ and are raised and lowered with a positive metric $|g_{ij}|$. We use the notation $\dot{f} = \partial_0 f$ for time derivatives. Bold characters denote spatial vectors in flat space $\boldsymbol{v} = (v^1, \ldots, v^{d-1})$.

Part I

Aspects of spontaneous symmetry breaking at finite density

Spontaneously broken symmetries have far reaching consequences in the study of physical systems. That is mainly because of the existence of Nambu-Goldstone bosons [7,8], whose low-energy dynamics is largely dictated by symmetry, independently of other details of the microscopic physics [26–28]. As a result, the experimental study of the dynamics of Goldstone bosons at low energies and long distances allows to robustly infer the nature of fundamental symmetries and the pattern of their spontaneous breaking.

In a standard Lorentz invariant setup there are as many Goldstones as broken generators, they are all massless and move at the speed of light. However, Nature is pervaded with systems that spontaneously break spacetime symmetries as well, in which case Goldstone theorem allows for a much richer set of possibilities [29–32]. In this part of the thesis we discuss those systems that are at finite density for a certain spontaneously broken charge. This scenario is ubiquitous in physics [33] and, in particular, it is relevant for the description of operators with large internal quantum numbers in conformal field theories [34,35], which will be discussed in parts II, III and IV of this thesis.

More precisely, we consider relativistic systems that are at finite density for a given charge Q and whose time evolution is governed by a Hamiltonian H. In this case, the ground state of the system can be found as the state with lowest eigenvalue with respect to the modified Hamiltonian (see for instance [33])

$$\bar{H} = H + \mu Q \,, \tag{I.1}$$

where μ is the chemical potential. We focus on systems of this sort that break boost invariance (like all condensed matter states [22]), time translations generated by H, the internal charge Q, as well as another set of internal charges Q_i. The modified Hamiltonian $\bar{H}$ is not broken by construction. This is the symmetry breaking pattern defining a zero-temperature (possibly non-Abelian) superfluid phase [23].

In chapter 1 we will review the general properties of the spectrum which follow from the spontaneous breaking of symmetries in finite density states, focusing on the differences with systems in the vacuum. Most strikingly, we will see that the non-relativistic Goldstone theorem in this setup implies not only the existence of gapless modes, but also of gapped ones, whose gap is fixed nonperturbatively by the algebra and is proportional to the chemical potential of the system, the so-called *gapped Goldstones* [36–40]. Intuitively, these arise whenever some of the broken generators Q_i's do not commute with the charge Q which enters the definition of the unbroken Hamiltonian (I.1).

One expects the low-energy dynamics of Goldstones to be effectively describable in terms of symmetries, and through a systematic derivative expansion [26, 27]. In this respect, the mass gap $\omega(\boldsymbol{k} = 0) \propto \mu$ of the gapped Goldstones poses a conceptual and technical difficulty. Indeed, on the one hand, these modes are needed in order to construct an effective field theory (EFT) invariant under the full symmetry group. On the other hand, in many cases of interest, such as QCD at large Isospin density [41–44] and the large charge sector of conformal field theories invariant under non-Abelian symmetries [34, 35], the chemical potential itself represents the cut-off of the EFT, paradoxically suggesting that gapped Goldstones cannot be part of the latter.

The resolution of this paradox will be the topic of chapter 2. Focussing on the illustrative example of a fully broken $SU(2)$ group, we will demonstrate that such an EFT can be constructed by *zooming* on the Goldstones, gapless and gapped, at small 3-momentum. The rules governing the EFT, where the gapless Goldstones are *soft* while the gapped ones are *slow*, are the same as in standard non-relativistic EFTs, like for instance the one describing positronium. In particular, the EFT lagrangian formally preserves gapped Goldstone number, and processes where such number is not conserved are described inclusively by allowing for imaginary parts in the Wilson coefficients. Thus, while symmetry is manifestly realized in the EFT, unitarity is not.

Some of the concepts discussed in this part of the thesis will appear repeatedly in the following chapters, devoted to the large charge expansion in conformal field theories. In particular, the construction of chapter 2 will be applied in the discussion of conformal field theories invariant under non-Abelian symmetry groups in chapter 4. However, as already remarked, the superfluid scenario which we discuss here can be relevant in different contexts as well, including the description of the low energy physics of some condensed matter systems [32] or QCD at finite density [45]. We will henceforth keep the discussion general. For the sake of definiteness, we will work in four-dimensional theories, but all the results can be straightforwardly generalized to arbitrary spacetime dimensions.

1 Goldstone bosons at finite density

In this chapter we review some relevant results on the spectrum of Goldstone bosons at finite density. Most importantly, we present the non-perturbative Goldstone theorem for gapless and gapped Goldstones in sec. 1.1. Our main argument will be a simple modification of that of [38], which we follow closely in the rest of the presentation. We will then exemplify these general results in sec. 1.2, where we review the standard Abelian superfluid low energy theory and we discuss two simple renormalizable models. One of these features an additional light *pseudo-Goldstone* mode, which, as we will review, is a typical feature of systems in which the symmetry breaking scale is parametrically larger than the chemical potential [39].

1.1 Goldstone theorem at finite density

1.1.1 Setup and summary of results

We consider a relativistic system with an internal symmetry G, whose continuous component is a compact Lie group generated by the charges Q_1, $Q_2\,, \dots Q_N$. We call $|\mu\rangle$ the state of minimal energy for given average charge density of an internal generator, which, with no loss of generality, we take to be $Q \equiv Q_1$. Such a state clearly breaks spontaneously boost invariance, while we assume the system to be homogeneous and isotropic so that rotations and translations are unbroken. This state minimizes the modified Hamiltonian $\bar{H} = H + \mu Q$, where μ is the chemical potential [1]

$$\bar{H}\,|\mu\rangle = (H + \mu Q)\,|\mu\rangle = 0\,. \tag{1.1}$$

Eq. (1.1) can then be satisfied in two qualitatively different ways.

---

[1] In general, the ground state will satisfy $\bar{H}|\mu\rangle = \lambda|\mu\rangle$, with minimum λ. In the absence of dynamical gravity, one can always add a cosmological constant term to the Hamiltonian to set $\lambda = 0$, with no physical consequences.

The first possibility, apparently the simplest one, is that the state $|\mu\rangle$ is an eigenstate of H and Q simultaneously, in which case none of them would be broken. This situation is realized in nature in Fermi liquids [46,47], where the internal symmetry group is $G = U(1)$, corresponding to the particle number in the non-relativistic limit. We will not discuss this scenario in this thesis and we refer the reader to [48–50] for recent works on the Goldstone phenomenon associated with the breaking of boost invariance in this setup.

The second possibility is that the state $|\mu\rangle$ breaks spontaneously both H and Q, while being an eigenstate of $\bar{H}$. This situation provides a field-theoretical definition of a zero-temperature superfluid phase [22]. Perhaps surprisingly, this is the most common scenario in nature [33] and it is the one we will focus on in this chapter (and effectively in all of this thesis). Furthermore, when the internal symmetry group G is non-Abelian other internal generators may be broken as well, which we take to be Q_2, $Q_3, \ldots, Q_n$ with $n < N$; in particular, it is easy to see that the generators which do not commute with the finite density charge Q *must* be broken. [2] This means that there exists some order parameter $A_I(x)$, transforming in a non-trivial representation of the group G with components labelled by I, such that [3]

$$i\kappa_{aI} \equiv \langle\mu|[Q_a, A_I(0)]|\mu\rangle \neq 0\,, \qquad a = 1, \ldots, n\,. \tag{1.2}$$

A similar eq. holds for the fundamental Hamiltonian H. In this case, it is not possible to classify the states of the system as eigenstates of H. We instead consider the spectrum of the unbroken combination $\bar{H} = H + \mu Q$. [4] According to eq. (1.1) the state $|\mu\rangle$ is the ground state, while excitations of the system–including the Goldstone bosons–correspond to higher eigenstates.

In this setup, the breaking of symmetry generators commuting with Q, and hence the modified Hamiltonian $\bar{H}$, implies the existence of massless excitations [29]. Differently from the relativistic case, these are as many as the number of commuting generators only provided Goldstones with quadratic dispersion relation in the low momentum limit, $\omega(\boldsymbol{k}) \propto \boldsymbol{k}^2$, are counted *twice* [30]. [5] For a compact Lie group, the generators that do not commute with Q may always be split into pairs $\{Q_a^+, Q_a^-\}$, such that $[Q, Q_a^\pm] = \pm q_a Q_a^\pm$, where the constant $q_a > 0$ depends on the algebra. For each of such pairs, Goldstone theorem predicts the existence of a gapped quasi-particle, whose gap is nonperturbatively fixed to be $\omega(\mathbf{0}) = |\mu| q_a$. The existence of these modes was not discussed in the classical papers [29, 30], where the difference between the modified *non-relativistic* Hamiltonian $\bar{H}$ and the fundamental one was not appreciated. Consequently, all symmetry generators were assumed to commute with $\bar{H}$. We refer the reader to [38] for further discussions of this point.

---

[2] For instance, for a theory invariant under an internal $SU(2)$ group at finite density for the charge $Q = Q_3$, this follows from the relation $\langle\mu|[Q_1, Q_2]|\mu\rangle = i\,\langle\mu|Q_3|\mu\rangle \neq 0$, in obvious notation.

[3] More precisely, the existence of an order parameter, which we assume to be local, with a non-vanishing expectation value *defines* symmetry breaking [32]. Indeed the charge associated with a spontaneously broken symmetry is not a well-defined operator in a local QFT [51] (see also appendix B of [52]) and cannot be diagonalized anyway; however, we can compute its commutators with well defined (local and non-local) operators. Eq. (1.2) then implies that $|\mu\rangle$ is not an eigenstate of the Q_a's.

[4] Equivalently, we can diagonalize a linear combination of $\bar{H}$ and any unbroken generator [39].

[5] More precisely, the number of Goldstones equals the number of broken generators, provided those which have a dispersion $\omega(\boldsymbol{k}) \propto \boldsymbol{k}^n$ with n even in the low momentum limit are counted twice. The nonperturbative proof of this result relies on the assumption of the absence of long-range forces [32]. Counting rules for the number of non-relativistic Goldstones have been recently refined in the literature, mostly using effective field theory methods [31,39,44,53–56].

Finally, we should remark that, as a consequence of the broken boost invariance, strictly speaking nonrelativistic Goldstone theorem requires only the existence of zero-momentum excitations, but does not say anything about their properties at finite momentum. For instance, phonons in superfluids have a finite width, which vanishes in the limit where their momentum goes to zero (see, e.g., [57]).

1.1.2 Proof of the theorem

By definition, the existence of an internal symmetry Lie group corresponds to the existence of N Noether conserved charges Q_a satisfying the group algebra [58]. In all known local relativistic quantum field theories, such charges may be written as the integral of the time component of some conserved currents. In Heisenberg picture, these evolve in time with the original Hamiltonian H and in space with the space momentum P^i: $J_a^\nu(x) = e^{iHt - i\boldsymbol{P}\cdot\boldsymbol{x}} J_a^\nu(0) e^{-iHt + i\boldsymbol{P}\cdot\boldsymbol{x}}$. The existence of these conserved currents, together with the symmetry breaking pattern and the properties of the state $|\mu\rangle$, specified before, are the only assumptions required by the theorem.

Using $Q_a = \int d^3x J_a^0(x)$ and $\bar{H}\,|\mu\rangle = P^i\,|\mu\rangle = 0$, we may write eq. (1.2) in terms of Wightman functions as

$$i\kappa_{aI} = \int d^3x \left[\langle\mu|J_a^0(x) A_I(0)|\mu\rangle - \langle\mu|A_I(0) J_a^0(x)|\mu\rangle\right] . \tag{1.3}$$

With no loss of generality, we take A_I to be Hermitian, but the currents do not need to be written in a real basis. To make the proof of the theorem as similar as possible to the relativistic case [28], it is convenient to derive a spectral decomposition for the Wightman functions. To this aim, let us insert the identity in terms of a complete set of momentum eigenstates $\{|n, \boldsymbol{p}\rangle\}$, where n label additional quantum numbers characterizing them. We further choose these states to be eigenstates of the modified Hamiltonian $\bar{H}$. Doing so for the first element in the parenthesis of eq. (1.3), for instance, we get

$$\begin{aligned}\langle\mu|J_a^0(x) A_I(0)|\mu\rangle &= \langle\mu|e^{-i\mu t Q} J_a^0(0) e^{-iHt + i\boldsymbol{P}\cdot\boldsymbol{x}} \left(\int \frac{d^3p}{(2\pi)^3} \sum_n |n, \boldsymbol{p}\rangle \langle n, \boldsymbol{p}|\right) A_I(0)|\mu\rangle \\ &= \int \frac{d^3p}{(2\pi)^3} \sum_n e^{-iE_n(\boldsymbol{p})t} e^{i\boldsymbol{p}\cdot\boldsymbol{x}} \langle\mu|e^{-i\mu t Q} J_a^0(0) e^{i\mu t Q} |n, \boldsymbol{p}\rangle \langle n, \boldsymbol{p}| A_I(0)|\mu\rangle .\end{aligned} \tag{1.4}$$

To proceed, we use that the algebra fixes the commutator of the charge and the current in the form: [6]

$$[Q_a, J_b^0(x)] = i f_{ab}^c J_c^0(x) \tag{1.5}$$

where f_{ab}^c are the structure constants of the group. From this and from the identification $Q = Q_1$, it follows that $e^{-i\mu t Q} J_a^0(0) e^{i\mu t Q} = \left[e^{\mu t f_1}\right]_a^{\ b} J_b^0(0)$, where the matrix f_{1a}^b is the adjoint representation of the generator Q_1. We then recast eq. (1.4) as

$$\langle\mu|J_a^0(x)A_I(0)|\mu\rangle = \int \frac{d^3p\, d\omega}{(2\pi)^4} \frac{e^{-i\omega t + i\boldsymbol{x}\cdot\boldsymbol{p}}}{2\omega} \sum_b \left[e^{\mu t f_1}\right]_a^{\ b} \rho_{J_b^0, A_I}(\omega, \boldsymbol{p})\,, \tag{1.6}$$

where we defined the spectral density for two operators $\mathcal{O}_A$ and $\mathcal{O}_B$ as [50] [7]

$$\rho_{\mathcal{O}_A,\mathcal{O}_B}(\omega,\boldsymbol{p}) = 2\omega \sum_n \langle\mu|\mathcal{O}_A(0)|n,\boldsymbol{p}\rangle \langle n,\boldsymbol{p}|\mathcal{O}_B(0)|\mu\rangle \times (2\pi)\delta\left(\omega - E_n(\boldsymbol{p})\right)\,. \tag{1.7}$$

Applying similar steps to the second term in eq. (1.3) and performing the integral over space, we arrive at [8]

$$i\kappa_{aI} = \int \frac{d\omega}{2\pi} e^{-i\omega t} \sum_b \left[e^{\mu t f_1}\right]_a^{\ b} \lim_{\boldsymbol{k}\to 0} \left\{ \frac{1}{2\omega} \left[\rho_{J_b^0, A_I}(\omega, \boldsymbol{k}) - \rho_{A_I, J_b^0}(-\omega, -\boldsymbol{k})\right]\right\} = \text{const.}\,, \tag{1.9}$$

where in the last equality we stressed that κ_{aI} is constant (and non-zero) due to the conservation of Q_a in eq. (1.2). Let us consider the consequences of this fact, separately, on broken generators commuting and non-commuting with $Q = Q_1$.

Consider first a broken generator Q_a which commutes with Q. With no loss of generality, we may take Q_a, and hence $J_a^\mu(x)$, Hermitian. In this case $\left[e^{\mu t f_1}\right]_a^{\ b} = \delta_a^b$ and thus, for eq. (1.9) to be satisfied, we must have

$$\lim_{\boldsymbol{p}\to 0} \frac{1}{2\omega} \left[\rho_{J_a^0, A_I}(\omega, \boldsymbol{p}) - \rho^*_{J_a^0, A_I}(-\omega, -\boldsymbol{p})\right] = (2\pi)\delta(\omega) i\kappa_{aI}\,. \tag{1.10}$$

This is the classical result of [29]. It implies the existence of a Goldstone state $|\pi, \boldsymbol{p}\rangle$,

---

[6] In the presence of 't Hooft anomalies, contact terms may modify this relation, but these are irrelevant in the limit $\boldsymbol{p} \to 0$ which we will use in our argument.

[7] With this normalization, the spectral density of a free real and canonically normalized relativistic scalar field reads $\rho_{\phi,\phi}(\omega,\boldsymbol{p}) = 2\pi\delta\left(\omega - E(\boldsymbol{p})\right)$ with $E(\boldsymbol{p}) = \sqrt{m^2 + \boldsymbol{p}^2}$; this definition is related to the standard relativistic spectral density $\rho^{rel}_{\mathcal{O}_A,\mathcal{O}_B}(p^\nu)$ of [59] as $\rho_{\mathcal{O}_A,\mathcal{O}_B}(\omega,\boldsymbol{p}) = 2\omega(2\pi)\rho^{rel}_{\mathcal{O}_A,\mathcal{O}_B}(p^\nu)$.

[8] To understand the origin of the limit for $\boldsymbol{k} \to 0$ in this formula, we observe that the charge associated with a spontaneously broken symmetry is not a well-defined operator in a local QFT (see footnote 3). Concretely, this means that the integral of a single Wightman function in eq. (1.3) is not convergent [32] and we cannot commute sum and integration. To remedy this, we rewrite eq. (1.3) as

$$i\kappa_{aI} = \lim_{\boldsymbol{k}\to 0} \int d^3x\, e^{-i\boldsymbol{k}\cdot\boldsymbol{x}} \left[\langle\mu|J_a^0(x)A_I(0)|\mu\rangle - \langle\mu|A_I(0)J_a^0(x)|\mu\rangle\right]\,. \tag{1.8}$$

We can now compute the space integral of the two contributions separately before taking the limit and we arrive at eq. (1.9).

different than $|\mu\rangle$, such that in the zero-momentum limit it is an exact eigenstate of $\bar{H}$ with vanishing energy: $E_\pi(\mathbf{0}) = 0$. From eq. (1.7), we see that both the current and the order parameter must have a non zero matrix element with such state.

The presence of both the spectral density and its conjugate, evaluated at opposite momentum, on the left hand side of eq. (1.10) does not allow to conclude that there exists a Goldstone state for each broken generator as in the relativistic case. Indeed, we will comment below eq. (1.12) that, in some cases, Goldstone theorem may be satisfied with a single Goldstone state for each pair of broken generators. This is the origin of the mismatch in the counting of Goldstone states and broken generators mentioned before. We refer the reader to the original work [30] and the recent reviews [31, 32] for details.

Since we take G to be a compact group, we can always organize the generators which do not commute with Q in (non-Hermitian) pairs such that $[Q, Q_a^\pm] = q_a Q_a^\pm$ [60]; this is equivalent to diagonalizing the adjoint matrix f^a_{1b}. Let us call, with obvious notation, $J^\nu_{a_\pm}$ the associated currents. In this basis $\left[e^{\mu t f_1}\right]_{a_\pm}^{\;b_\pm} = e^{\mp i\mu q_a t}\delta_a^b$ and $\left[e^{\mu t f_1}\right]_{a_\pm}^{\;b_\mp} = 0$. Then, taking for instance $a = a_-$, eq. (1.9) reads

$$i\kappa_{a_- I} = \int \frac{d\omega}{2\pi}\, e^{-i(\omega-\mu q_a)t} \lim_{\boldsymbol{k}\to 0}\left\{\frac{1}{2\omega}\left[\rho_{J^0_{a_-},A_I}(\omega,\boldsymbol{k}) - \rho^*_{J^0_{a_+},A_I}(-\omega,-\boldsymbol{k})\right]\right\} = \text{const.}\,, \tag{1.11}$$

where we used $(J^\nu_{a_\pm})^\dagger = J^\nu_{a_\mp}$. Assuming for definiteness $\mu q_a > 0$ and using that the positivity of the spectrum implies that the spectral function vanishes for negative frequencies, hence $\rho_{J^0_{a_+},A_I}(\omega,\boldsymbol{k}) = 0$ for $\omega < 0$, eq. (1.11) can be satisfied only if

$$\lim_{\boldsymbol{p}\to 0}\frac{1}{2\omega}\rho_{J^0_{a_-},A_I}(\omega,\boldsymbol{p}) = (2\pi)\delta(\omega-\mu q_a)i\kappa_{a_- I} \qquad \text{and} \qquad \lim_{\boldsymbol{p}\to 0}\frac{1}{2\omega}\rho_{J^0_{a_+},A_I}(\omega,\boldsymbol{p}) = 0\,. \tag{1.12}$$

The first condition implies that for each pair $\{Q_a^+, Q_a^-\}$ there must be a *gapped* Goldstone state $|\pi_\mu, \boldsymbol{p}\rangle$, such that at zero-momentum it is an eigenstate of the *modified* Hamiltonian $\bar{H}$ with energy

$$E_{\pi_\mu}(\mathbf{0}) = \mu q_a. \tag{1.13}$$

Furthermore, eq. (1.10) implies that both $\langle\mu|J^0_{a_-}(0)|\pi_\mu,\boldsymbol{p}\rangle$ and $\langle\mu|A_I(0)|\pi_\mu,\boldsymbol{p}\rangle$ are non-zero, while the matrix element of the plus component of the current with this state vanishes in the zero momentum limit: $\lim_{\boldsymbol{p}\to 0}\langle\mu|J^0_{a_+}(0)|\pi_\mu,\boldsymbol{p}\rangle = 0$. This completes the proof of the theorem.

Notice that eq. (1.11) holds also for $q_a = 0$, corresponding to a complex pair of generators $\{Q_a^+, Q_a^-\}$ that commutes with the charge at finite density Q. In that case eq. (1.12), which requires the existence of a single Goldstone state, provides a possible (but not the only) solution to the latter. As anticipated above, we see that a single Goldstone state may account for the breaking of two generators, even when these commute with Q.

1.1.3 Unbroken, explicitly broken and spontaneously broken Lorentz invariance

As we already pointed out, without further assumptions, Goldstone theorem provides a constraint on spectral functions only in the zero-momentum limit. The stronger relativistic Goldstone theorem may be recovered from eq. (1.10) for $\mu = 0$, in which case $\bar{H} = H$, using the additional constraints imposed by the unbroken Lorentz invariance. To see this, notice that eq. (1.10) implies the following constraint for the relativistic spectral density $\rho^{rel}_{J^0_a,A_I}(p^\nu) = \rho_{J^0_a,A_I}(\omega,\boldsymbol{p})/(4\pi\omega)$ (see footnote 7):

$$\lim_{\boldsymbol{p}\to 0}\left\{\rho^{rel}_{J^0_a,A_I}(p^\nu) - \left[\rho^{rel}_{J^0_a,A_I}(-p^\nu)\right]^*\right\} = \delta(p_0)i\kappa_{aI}\,, \tag{1.14}$$

where $p^\nu = (\omega,\boldsymbol{p})$. To proceed, consider the following identity:

$$\delta(p_0) = \lim_{m^2\to 0^+} p_0\delta(p_0^2 - m^2)\left[\theta(p_0) - \theta(-p_0)\right]\,, \tag{1.15}$$

where we stressed the limit $m^2 \to 0^+$ since the change of variables from p_0 to p_0^2 is singular at $p_0 = 0$. When boosts are unbroken, Lorentz invariance implies $\rho^{rel}_{J^0_a,A_I}(p^\nu) = ip_0\rho^{rel}_{J_a,A_I}(p^2)\theta(p_0)$, with $\rho^{rel}_{J_a,A_I}(p^2) \in \mathbb{R}$ [28]. Therefore plugging the identity (1.15) in eq. (1.14), factoring out the overall p^0 and taking the limits, we conclude:

$$\rho^{rel}_{J_a,A_I}(p^2) = \delta(p^2)\kappa_{aI}\,. \tag{1.16}$$

This implies the existence of a massless particle for each broken generator in the spectrum [59], which is the statement of the relativistic Goldstone theorem [8].

Conversely, the underlying Lorentz invariance of the theory, if conceptually useful in understanding the origin of the modified Hamiltonian, strictly speaking, does not play any role in the proof of eq.s (1.10) and (1.12). Indeed these assume only (unbroken) translational and rotational symmetry [40]. Consequently, these results apply also in those systems in which the breaking of boost invariance happens, via a different mechanism, at much higher scales than the breaking of the internal symmetries under considerations. Relevant examples of this kind include ferromagnets and anti-ferromagnets [30, 61], and certain kinds of superconductors [62].

One may then wonder whether the spontaneous breaking of Lorentz symmetry provides additional constraints on the spectrum. This is not the case, as we will see explicitly in the examples of the next section. Technically, this is because the Goldstone theorem for broken boosts, which may be derived analogously to eq. (1.10), does not require additional states to be satisfied [50]. A more intuitive justification is based on the semiclassical picture of Goldstone fields as describing fluctuations of the order parameter. When spacetime symmetries are broken, it may happen that the same physical fluctuation can be described as the action of different generators [63]. In particular, if the order parameter is a scalar, as in the examples of the next section, a small fluctuation generated by a boost can be obtained via the action of the internal generator Q appearing in the modified Hamiltonian (1.1) as well [39]. Therefore, the field fluctuations associated to the action of boosts are not independent from the ones parametrized by the other fields and, consequently, no independent boost Goldstone states exist. [9]

1.2 Examples

1.2.1 Abelian superfluids

Let us first consider the simplest scenario, a relativistic superfluid with an Abelian $U(1)$ symmetry generated by Q [23]. The minimal field content to realize the breaking pattern we are interested in is provided by a compact Lorentz scalar $\chi(x) \sim \chi(x) + 2\pi$ invariant under a shift symmetry $\chi(x) \to \chi(x) - \text{const.}$. This is expanded around a background configuration of the form $\langle \chi(x) \rangle = \mu t + \text{const.}$. More precisely, since only functions of χ which are invariant under periodic shifts of 2π are well defined operators, we have

$$\langle \mu | e^{i\chi(x)} | \mu \rangle = e^{i(\mu t + \text{const.})} \,. \tag{1.17}$$

The most general low energy effective action can be written in a derivative expansion as

$$S = \int d^4x \left\{ F_1(X) + \partial^\mu\chi\partial^\nu\chi\partial_\mu\partial_\nu\chi F_2(X) + \ldots \right\} , \tag{1.18}$$

where $X \equiv (\partial\chi) = \sqrt{\partial_\mu\chi\partial^\mu\chi}$ and F_1, F_2 are arbitrary functions. [10] To leading order in derivatives, the energy momentum tensor and the $U(1)$ current are given by:

$$T_{\mu\nu} = F_1'(X)X\, u_\mu u_\nu - \eta_{\mu\nu} F_1(X) \,, \qquad J_\mu = F_1'(X) u_\mu \,, \tag{1.19}$$

where $u_\mu = \partial_\mu\chi/(\partial\chi)$ is the superfluid four-velocity. The background (1.17) provides a non-zero charge density $J^0 = F_1'(\mu) \equiv n$ and we can obtain the energy density ρ and the pressure P as a function of μ inverting $T^{\mu\nu} = (\rho + P)u_\mu u_\nu + P\eta_{\mu\nu}$ [65]; doing so on the background we recover the zero temperature thermodynamic identity $\rho + P = n\mu$ [66].

---

[9] Strictly speaking, this argument only explains why, for certain order parameters, independent Goldstone *fields* are absent. In finite density systems, it may happen that the number of Goldstone fields is larger than that of Goldstone states, defined as those modes whose existence is *nonperturbatively* predicted by the theorem. For instance, this is what happens in relativistic type-II superfluids [22] where, in the simplest scenario, the order parameter is an $SO(3)$ triplet of complex Lorentz vectors [22]. In that case the Goldstone fields for boosts are independent of the ones associated with the broken internal generators, but they interpolate modes whose properties and existence do not follow from Goldstone theorem, with a gap naturally of order μ which cannot be determined solely by symmetry considerations [64].

[10] The properties of the derivative expansion depend on the precise form of these functions; the simplest scenario, in which the chemical potential itself sets the cutoff of the low energy description, corresponds to the following scaling for the derivatives of F_1 and F_2: $F_1^{(n)}(\mu) \sim \mu^{-n} F_1(\mu)$ and $F_2^{(n)}(\mu) \sim \mu^{-4-n} F_1(\mu)$.

The action (1.18) is clearly Poincaré invariant, while the background breaks spontaneously boosts, time translations generated by H and the $U(1)$ shift symmetry generated by Q, leaving unbroken the combination (1.1). Defining $\pi(x) = \chi(x) - \mu t$, the action to leading order in derivatives and to quadratic order in fluctuation reads

$$S \simeq \frac{n}{\mu c_s^2} \int d^4x \frac{1}{2} \left[\dot{\pi}^2 - c_s^2 \left(\boldsymbol{\nabla} \pi \right)^2 \right] , \qquad c_s^2 = \frac{F_1'(\mu)}{\mu F_1''(\mu)} . \tag{1.20}$$

In agreement with the general theorem, the field $\pi(x)$ describes a massless excitation with a linear dispersion relation $\omega(\boldsymbol{k}) = c_s|\boldsymbol{k}| + \mathcal{O}\left(|\boldsymbol{k}|^3\right)$, the superfluid phonon [57]. Due to the shift symmetry, the field is derivatively coupled and phonons are free when they are *soft*, as it happens with relativistic Goldstones [28].

Notice that, despite the absence of additional Goldstone fields for boosts, Lorentz invariance constrains the general form of the action (1.18). For instance, without it the leading order action would be an arbitrary function of $\dot{\pi}$ and $(\boldsymbol{\nabla}\pi)^2$, while in eq. (1.18) they only appear through the combination $X = \sqrt{(\mu + \dot{\pi})^2 - (\boldsymbol{\nabla}\pi)^2}$.

Finally let us mention the obvious generalization to an Abelian fully broken $U(1)^N$ symmetry. Calling Q_a the associated generators, the most general form for the modified Hamiltonian (1.1) reads

$$\bar{H} = H + \sum_a \mu_a Q_a . \tag{1.21}$$

The general low energy theory is formulated in terms of N shift invariant scalars expanded around a background solution analogous to eq. (1.17):

$$\chi_a(x) = \mu_a t + \pi_a(x) . \tag{1.22}$$

The most general effective action to leading order in derivatives reads

$$S = \int d^4x \, F(X_{ab}) , \qquad X_{ab} \equiv \sqrt{\partial_\mu \chi_a \partial^\mu \chi_b} . \tag{1.23}$$

Expanding to quadratic order in fluctuations, we find that the spectrum consists of N massless phonons with linear dispersion relation: $\omega(\boldsymbol{k}) \propto |\boldsymbol{k}|$.

1.2.2 The linear triplet

As a next example, consider the following renormalizable Lagrangian for an $O(3)$ triplet $\boldsymbol{\Phi}$ in four spacetime dimensions:

$$\mathcal{L} = \frac{1}{2}(\partial \boldsymbol{\Phi})^2 - \frac{m^2}{2} \boldsymbol{\Phi}^2 - \frac{\lambda}{4} \boldsymbol{\Phi}^4 , \tag{1.24}$$

where $\lambda > 0$, and we do not make any assumptions on the sign of m^2. The classical field configuration that realizes the desired symmetry breaking pattern is

$$\mathbf{\Phi}_0 = e^{-i\mu t Q_3} \begin{pmatrix} \phi_0 \\ 0 \\ 0 \end{pmatrix} , \qquad \phi_0^2 = \frac{\mu^2 - m^2}{\lambda} > 0 \, , \tag{1.25}$$

where $(Q_i)_{jk} = -i\epsilon_{ijk}$ are the generators in the defining representation of $SO(3)$. If $m^2 > 0$ then spontaneous symmetry breaking happens only for $\mu^2 > m^2$. The state described by this configuration is indeed at finite density for the charge Q_3, as one can check by computing the corresponding Noether's current. Moreover, since it depends explicitly on time, this vacuum expectation value (vev) breaks both boosts and time translations. On top of that, it also breaks the internal $O(3)$ symmetry to $\mathbb{Z}_2$ of $\Phi_3 \to -\Phi_3$ but preserves the combination $\bar{H} = H - \mu Q_3$. This is then precisely the setup when the charge at finite density does not commute with other broken charges. We thus expect the existence of a gapped Goldstone mode.

Before studying the full spectrum, let us give an intuitive *semiclassical* argument in favor of the existence of a gapped Goldstone. Starting from the configuration (1.25) and performing, say, a rotation generated by Q_1, one obtains a nontrivial configuration for the third component of the triplet, $\delta\Phi_3(x) = -\phi_0 \sin \mu t$, which oscillates with precisely frequency μ. The existence of a mode that has energy μ when it is at rest is, therefore, necessary for consistency with the non-Abelian symmetry. This is parallel to what happens with a rotation generated by Q_3, which instead ensures the existence of a gapless mode. At the same time, this suggests that, similarly to soft massless Goldstones, gapped Goldstones are free when they are at rest [67]: their zero-mode corresponds to nothing but a global transformation. [11]

The fluctuations around equilibrium can be conveniently parametrized in terms of three real fields, $\psi(x)$, $\theta(x)$ and $h(x)$:

$$\mathbf{\Phi}(x) = e^{-i(\mu t + \psi(x)/\phi_0) Q_3} \begin{pmatrix} \phi_0 + h(x) \\ 0 \\ \theta(x) \end{pmatrix} . \tag{1.26}$$

The unbroken $\mathbb{Z}_2$ acts as $\theta \mapsto -\theta$. The Lagrangian then reads

$$\begin{aligned} \mathcal{L} = {} & \frac{1}{2}(\partial\theta)^2 - \frac{\mu^2}{2}\theta^2 + \frac{1}{2}(\partial\psi)^2 + \frac{1}{2}(\partial h)^2 + 2\mu h \dot{\psi} - \lambda \phi_0^2 h^2 \\ & - \lambda \phi_0 h \left(h^2 + \theta^2\right) - \frac{\lambda}{4}\left(h^4 + \theta^4 + 2h^2\theta^2\right) + \frac{\mu}{\phi_0} h^2 \dot{\psi} + \frac{1}{\phi_0} h (\partial\psi)^2 + \frac{1}{2\phi_0^2} h^2 (\partial\psi)^2 \, . \end{aligned} \tag{1.27}$$

---

[11] Note that, as remarked in footnote 8, at infinite volume the global charges are not well defined, and consequently neither is the zero-mode. More precisely, one should work at finite volume, and add an infinitesimal perturbation explicitly breaking the symmetry before taking the infinite volume limit [28,32].

Extracting the propagator from (1.27), one finds that, as expected, the spectrum of the theory consists of

- A gapless Goldstone, π_3, with dispersion relation

$$\begin{aligned}\omega^2(\boldsymbol{k}) &= \boldsymbol{k}^2 + 3\mu^2 - m^2 - \sqrt{(3\mu^2-m^2)^2 + 4\boldsymbol{k}^2\mu^2} \\ &= \frac{\mu^2-m^2}{3\mu^2-m^2}\boldsymbol{k}^2 + \mathcal{O}\left(\frac{\boldsymbol{k}^4}{\mu^2}\right) .\end{aligned} \tag{1.28}$$

- A gapped Goldstone, θ, with gap μ:

$$\omega^2(\boldsymbol{k}) = \boldsymbol{k}^2 + \mu^2 . \tag{1.29}$$

- A radial mode, ρ, with gap $m_\rho^2 = 6\mu^2 - 2m^2$ and dispersion relation:

$$\begin{aligned}\omega^2(\boldsymbol{k}) &= \boldsymbol{k}^2 + 3\mu^2 - m^2 + \sqrt{(3\mu^2-m^2)^2 + 4\boldsymbol{k}^2\mu^2} \\ &= 6\mu^2 - 2m^2 + \frac{5\mu^2-m^2}{3\mu^2-m^2}\boldsymbol{k}^2 + \mathcal{O}\left(\frac{\boldsymbol{k}^4}{\mu^2}\right) .\end{aligned} \tag{1.30}$$

Due to the mixing term in (1.27), the radial mode and the gapless one are interpolated both by ψ and h—which decouple only for $\mu = 0$. In this limit, for $m^2 < 0$, the $U(1)$ symmetry generated by Q_1 is restored, and the two Goldstones are just the standard relativistic massless particles associated to the breaking of Q_2 and Q_3.

Finally note that if chemical potential is large enough, $\mu^2 \gtrsim |m^2|$, the gap of the radial mode and that of the gapped Goldstone can be of the same order, $m_\rho \sim \mu$. At low energies, m_ρ sets the cutoff of the standard *quasi-relativistic* effective theory for the Goldstone bosons [39]. In the setup we are considering, the gapped Goldstones might hence lie outside the regime of validity of such EFT. We will study in detail this scenario in the next chapter, starting from the analysis of scattering amplitudes of massive Goldstones in this model.

1.2.3 Complex doublets at small density and *pseudo*-Goldstone modes

As a final example, we consider the theory of two complex (Lorentz scalar) doublets Ψ_1, $\Psi_2 \in \mathbb{C}^2$ with Lagrangian given by

$$\mathcal{L} = |\partial\Psi_1|^2 + |\partial\Psi_2|^2 - \frac{\lambda_1}{4}\left(v_1^2 - |\Psi_1|^2\right)^2 - \frac{\lambda_2}{4}\left(v_2^2 - |\Psi_2|^2\right)^2 - \frac{\lambda_{12}}{2}|\Psi_2|^2|\Psi_1|^2 - \frac{\kappa}{2}|\Psi_2^\dagger\Psi_1|^2 . \tag{1.31}$$

This is the most general renormalizable Lagrangian invariant under the group $G = U(1)^2 \times SU(2)$, where the two $U(1)$'s act independently on the two fields. We call $Q_{1/2/3}$ and $J^\mu_{1/2/3}$ the generators and the currents of the $SU(2)$ component of G, while we use a tilde for those of the $U(1)^2$, $\tilde{Q}_{1/2}$ and $\tilde{J}^{\mu}_{1/2}$. We take $\lambda_1, \lambda_2, \kappa > 0$ and $\lambda_{12} > -\sqrt{\lambda_1\lambda_2}$, ensuring that the potential is bounded from below. When not specified otherwise, we assume all couplings to be of the same order and similarly $v_1^2 \sim v_2^2$ [68].

We assume $v_1^2, v_2^2 > 0$, implying that the theory spontaneously breaks the internal symmetry also in the vacuum. The term proportional to κ forces the two fields to acquire a nonvanishing vev in orthogonal directions. We will study the spectrum around the following classical field configuration:

$$\langle\Psi_1\rangle = \begin{pmatrix} e^{i\mu_1 t}c_1 \\ 0 \end{pmatrix}, \qquad \langle\Psi_2\rangle = \begin{pmatrix} 0 \\ e^{i\mu_2 t}c_2 \end{pmatrix}, \tag{1.32}$$

where c_1 and c_2 are real positive constants given by

$$c_1^2 = \frac{\lambda_2(\lambda_1 v_1^2 + 2\mu_1^2) - \lambda_{12}(\lambda_2 v_2^2 + 2\mu_2^2)}{\lambda_1\lambda_2 - \lambda_{12}^2}, \tag{1.33}$$

$$c_2^2 = \frac{\lambda_1(\lambda_2 v_2^2 + 2\mu_2^2) - \lambda_{12}(\lambda_1 v_1^2 + 2\mu_1^2)}{\lambda_1\lambda_2 - \lambda_{12}^2}. \tag{1.34}$$

This solution is a local minimum of the effective potential provided the following two conditions are met [12]

$$\begin{cases} \lambda_{12} < \min\left\{\sqrt{\lambda_1\lambda_2},\, \lambda_1\dfrac{\lambda_2 v_2^2 + 2\mu_2^2}{\lambda_1 v_1^2 + 2\mu_1^2},\, \lambda_2\dfrac{\lambda_1 v_1^2 + 2\mu_1^2}{\lambda_2 v_2^2 + 2\mu_2^2}\right\}, \\ 0 \le \mu_1^2 - \mu_2^2 \le \dfrac{\kappa}{2}(c_1^2 - c_2^2) \qquad \text{or} \qquad 0 \le \mu_2^2 - \mu_1^2 \le \dfrac{\kappa}{2}(c_2^2 - c_1^2). \end{cases} \tag{1.36}$$

The charge densities have a nonvanishing expectation value given by

$$\langle J_1^0\rangle = \langle J_2^0\rangle = 0, \qquad \langle J_3^0\rangle = \mu_1 c_1^2 - \mu_2 c_2^2, \qquad \langle\tilde{J}_1^0\rangle = \mu_1 c_1^2, \qquad \langle\tilde{J}_2^0\rangle = \mu_2 c_2^2. \tag{1.37}$$

Even for $\mu_1 = \mu_2 = 0$, the configuration (1.32) breaks G spontaneously to the $U(1)$ group generated by $\tilde{Q}_1 - \tilde{Q}_2 - Q_3$. For μ_1, $\mu_2 \neq 0$ it further breaks boosts and time translations, preserving the linear combination

$$\begin{aligned} \bar{H} &= H + \mu_1\left(\frac{\tilde{Q}_1 + \tilde{Q}_2}{2} + Q_3\right) + \mu_2\left(\frac{\tilde{Q}_1 + \tilde{Q}_2}{2} - Q_3\right) \\ &= H + (\mu_1 + \mu_2)\,\frac{\tilde{Q}_1 + \tilde{Q}_2}{2} + (\mu_1 - \mu_2)\,Q_3\,. \end{aligned} \tag{1.38}$$

---

[12] Though we were not able to reduce the second inequality to a more transparent form, we checked that these conditions are compatible. For instance, taking $\mu_2^2 > \mu_1^2$, for $\lambda_{12} = 0$ they reduce to

$$v_2^2 - v_1^2 > 2\left(\frac{1}{\kappa} - \frac{1}{\lambda_2}\right)\mu_2^2 - 2\left(\frac{1}{\kappa} - \frac{1}{\lambda_1}\right)\mu_1^2, \tag{1.35}$$

which is satisfied for large enough v_2^2.

Two of the four spontaneously broken internal generators do not commute with $\bar{H}$, implying the existence of a gapped Goldstone with gap $|\mu_1 - \mu_2|$.

To study the spectrum, we parametrize the fluctuations around equilibrium using four real fields, $\pi_1(x)$, $\pi_2(x)$, $r_1(x)$, $r_2(x)$, and two complex fields, $\psi_1(x)$ and $\psi_2^*(x)$:

$$\Psi_1(x) = \begin{pmatrix} e^{i\chi_1(x)}\left(c_1 + \frac{r_1(x)}{\sqrt{2}}\right) \\ e^{i\chi_2(x)}\psi_1(x) \end{pmatrix} , \qquad \Psi_2 = \begin{pmatrix} e^{i\chi_1(x)}\psi_2^*(x) \\ e^{i\chi_2(x)}\left(c_2 + \frac{r_2(x)}{\sqrt{2}}\right) \end{pmatrix} , \tag{1.39}$$

where we defined for shortness $\chi_{1/2}(x) = \mu_{1/2}t + \pi_{1/2}(x)/(\sqrt{2}c_{1/2})$. In this parametrization, all fields transform as scalars under the time translations (1.38) and, thanks to the conjugate on ψ_2 in eq. (1.39), the unbroken $U(1)$ group acts as $\psi_{1/2} \to e^{i\alpha}\psi_{1/2}$. The expansion to quadratic order of the Lagrangian eq. (1.31) reads, neglecting total derivatives,

$$\begin{aligned} \mathcal{L} \simeq & \sum_{a=1}^{2}\left[\frac{1}{2}(\partial r_a)^2 + \frac{1}{2}(\partial \pi_a)^2 + 2\mu_a r_a \dot{\pi}_a\right] - \frac{1}{2}\sum_{a,b=1}^{2}(m_r^2)_{ab} r_a r_b \\ & + \sum_{a=1}^{2}|\partial\psi_a|^2 - i\mu_2\left(\psi_1^*\dot{\psi}_1 - c.c.\right) + i\mu_1\left(\psi_2^*\dot{\psi}_2 - c.c.\right) - \sum_{a,b=1}^{2}(m_\psi^2)_{ab}\psi_a^*\psi_b \, , \end{aligned} \tag{1.40}$$

where we defined the following matrices

$$m_r^2 = \begin{pmatrix} \lambda_1 c_1^2 & \lambda_{12}c_1c_2 \\ \lambda_{12}c_1c_2 & \lambda_2 c_2^2 \end{pmatrix} , \qquad m_\psi^2 = \begin{pmatrix} \frac{\kappa}{2}c_2^2 + \mu_1^2 - \mu_2^2 & \frac{\kappa}{2}c_1c_2 \\ \frac{\kappa}{2}c_1c_2 & \frac{\kappa}{2}c_1^2 + \mu_2^2 - \mu_1^2 \end{pmatrix} . \tag{1.41}$$

From eq. (1.40), we can extract the spectrum. For simplicity, we shall study it in the limit in which the chemical potentials μ_1 and μ_2 are much smaller than the mass scale $\sim \sqrt{\lambda}\, v_{1/2}$, where λ is of the order of any of the quartic couplings. For ease of presentation, we shall introduce a set of dimensionless coefficients $\gamma^{(\phi)}$'s, naturally of order one, whose precise value in terms of the Lagrangian couplings and chemical potentials is given in appendix A.1. Extracting the propagator for the fields $\pi_{1/2}$ and $r_{1/2}$ from the first line of the Lagrangian (1.40), we find

- Two gapless Goldstones π_1 and π_2, with linear dispersion relations given by

$$\omega_{1/2}^2(\boldsymbol{k}) = \left[1 - \frac{\mu_1\mu_2}{\sqrt{\lambda_1\lambda_2}\, v_1 v_2}\gamma_{1/2}^{(\pi)} + \mathcal{O}\left(\frac{\mu_{1/2}^4}{\lambda^2 v_{1/2}^4}\right)\right]\boldsymbol{k}^2 \, , \tag{1.42}$$

  where $\gamma_{1/2}^{(\pi)}$ are dimensionless coefficents which depend on the couplings and the ratio μ_1^2/μ_2^2. Consistently with subluminality, we find $\mu_1\mu_2\gamma_{1/2}^{(\pi)} > 0$.

- Two radial modes r_1 and r_2, whose masses are given by
$$\omega^2_{1/2}(\mathbf{0}) = \lambda_{1/2} v^2_{1/2} \gamma^{(r)}_{1/2} + \mathcal{O}\left(\frac{\mu^2_{1/2}}{\lambda v^2_{1/2}}\right) ; \tag{1.43}$$
as before, $\gamma^{(r)}_{1/2}$ are dimensionless coefficents, which reduce to one for $\lambda_{12} = 0$ and in general depend on the couplings, but not on the ratio μ_1^2/μ_2^2.

As before, the Goldstone and the radial modes are interpolated by both $\pi_{1/2}$ and $r_{1/2}$, which decouple only for $\mu_1 = \mu_2 = 0$. Nonetheless, with an abuse of notation, we called $\pi_{1/2}$ and $r_{1/2}$ the corresponding modes. Assuming $\mu_2 > \mu_1$ with no loss of generality, from the propagator for ψ_1 and ψ_2 we instead infer the existence of the following four excitations in the spectrum:

- A gapped Goldstone π_μ, positively charged under the unbroken $U(1)$, with gap $(\mu_2 - \mu_1)$. Its dispersion relation at very small momentum, but arbitrary chemical potentials, is given by
$$\omega(\boldsymbol{k}) = (\mu_2 - \mu_1) + \gamma^{(\pi_\mu)} \frac{\boldsymbol{k}^2}{(\mu_2 + \mu_1)} + \mathcal{O}\left(\frac{\boldsymbol{k}^4}{\mu^3_{1/2}}\right) , \tag{1.44}$$
in terms of a dimensionless coefficient $\gamma^{(\pi_\mu)}$. In the limiting case $\mu_1 = \mu_2$, this mode becomes a gapless Goldstone with quadratic dispersion relation, which contributes twice to the counting of Goldstones according to the discussion in sec. 1.1 [30].

- A light mode $\tilde{\pi}_\mu$, negatively charged under the unbroken $U(1)$, whose gap is proportional to $\mu_1 + \mu_2$:
$$\omega(\mathbf{0}) = (\mu_1 + \mu_2) \gamma^{(\tilde{\pi}_\mu)} + \mathcal{O}\left(\frac{\mu^3_{1/2}}{\lambda v^2_{1/2}}\right) , \tag{1.45}$$
where the coefficient $\gamma^{(\tilde{\pi}_\mu)}$ depends on the couplings but not on the ratio μ_1^2/μ_2^2. The existence of this quasi-particle is not predicted by the Goldstone theorem at finite density. However, in the limit $\mu_{1/2} \to 0$, this mode becomes a massless Goldstone, as required by the relativistic version of the theorem [8].

- Two radial modes $\psi_\pm$, oppositely charges under the unbroken $U(1)$, with masses given by
$$\omega_\pm(\mathbf{0}) = \sqrt{\kappa v_1 v_2} \gamma^{(\psi)}_0 \pm (\mu_1 + \mu_2) \gamma^{(\psi)}_1 + \mathcal{O}\left(\frac{\mu^2_{1/2}}{\sqrt{\lambda}\, v_{1/2}}\right) , \tag{1.46}$$
where $\gamma^{(\psi)}_0$ and $\gamma^{(\psi)}_1$ depend on the couplings and the ratio μ_1/μ_2.

In the limit of vanishing densities the charge conjugation symmetry, broken by the chemical potentials, is restored and the four charged modes become degenerate in pairs.

This system provides a further illustration of the general theorem. Its spectrum includes three Goldstone bosons, whose dispersion relation is given in eq.s (1.42) and (1.44). One of them is generically gapped and accounts for two broken generators. At the special point $\mu_2 = \mu_1$ it becomes a gapless mode, with quadratic dispersion relation, which, as explained in sec. 1.1, still accounts for two broken generators. In the limit of small charge densities, the spectrum also contains an additional light quasi-particle, whose gap is proportional to the chemical potential but it is not fixed by the symmetry breaking pattern. Its existence is easily understood since for $\mu_1 = \mu_2 = 0$ the relativistic Goldstone theorem requires four massless particles. For small but non-zero chemical potentials, we can thus think of this mode as a *pseudo*-Goldstone, analogously to the pions in QCD. We can compare this situation with the triplet model studied in sec. 1.2.2. There, for m^2 large and negative only two generators are broken in the vacuum; therefore there is no additional light mode besides the two Goldstones for small chemical potential. Notice also that for $\mu_{1/2}^2 \sim \lambda v^2$ the mode in eq. (1.45) behaves like the other radial modes, whose gap is not fixed by symmetry considerations.

The existence of additional light *pseudo*-Goldstone modes when the symmetry breaking scale is much larger than the chemical potential is a generic feature of relativistic systems [39]. As the discussion of this and the previous section suggest, their existence is tied to the details of the symmetry breaking pattern at vanishing charge densities. Consider indeed a system which in the vacuum breaks an internal symmetry group G down to H, with, respectively, n_G and n_H Lie generators. At energies $E \ll \lambda v^2$, where v is the symmetry breaking scale and λ is a coupling, possibly of order $(4\pi)^2$ for strongly coupled theories [69, 70], one can study the theory through the low energy action for the Goldstone fields parametrizing the coset G/H [26, 27]. These are as many as the broken generators $n_G - n_H$. The same action allows studying the system at small charge density, which is equivalent to turning on a small chemical potential $\mu \ll \sqrt{\lambda} v$ for one of the broken charges Q; this may further break the group down to $H_\mu \subseteq H$, as in the example of the triplet. By continuity with the description in the vacuum, the spectrum still consists of $n_G - n_H$ quasi-particles; however, the non-relativistic Goldstone theorem generically guarantees the existence of a fewer number of modes. In particular, for each pair of generators non-commuting with Q a single Goldstone exists; thus, if the system in the vacuum breaks both the generators forming the pair, the spectrum will *unavoidably* contain an additional pseudo-Goldstone mode with gap of order μ, similar to the one of eq. (1.45). For a detailed and more general analysis of pseudo-Goldstone modes of this kind in relativistic systems at small charge density we refer the reader to [39].

We remark however that, when the symmetry breaking scale coincides with the chemical potential, there seems to be nothing special about these additional modes. On the one hand, as we have seen in the example of this section, even in a weakly coupled theory when $\mu^2 \gtrsim \lambda v^2$ they behave like the other radial modes. On the other hand, when the chemical potential itself sets the strong coupling scale of the system, it is not even clear if these modes should exist at all. Indeed, we argued that their presence is guaranteed only when there exists a *quasi-relativistic* weakly coupled description valid up to scales $E \gg \mu$, which may not be there in general situations. As in this thesis we will mostly focus on the setup in which μ and the strong coupling scale coincide, it is important for us to distinguish between the *true* Goldstone states, whose existence is guaranteed non-perturbatively by the Goldstone theorem, and the pseudo-Goldstone modes, whose presence in the spectrum follows from symmetry considerations only when the system is weakly coupled at scales much larger than the chemical potential.

2 Non-Abelian superfluids: gapped Goldstones at the cutoff scale

Independently of the presence of a gap, all Goldstone modes share a defining property: their scattering amplitudes vanish with their 3-momentum—the so-called Adler's zeros [67].[1] In other words, all Goldstone bosons are free when their 3-momentum vanishes. An effective field theory (EFT) description of their dynamics should then focus on the regime of small 3-momentum. For gapless modes this coincides with the regime of low *energy*, while for the gapped ones it instead coincides with the regime of low *kinetic energy* or, equivalently, low velocity.

The presence of both gapless and gapped modes, however, makes the piecing together of an EFT approach not straightforward. This is immediately appreciated by considering the process of annihilation of two gapped modes into two gapless ones; a process that is generically allowed. Even if the spatial momentum of the incoming states approaches zero, their total energy is of order μ, and so are the momenta of the final state quanta. Now, when the underlying microscopic dynamics is strong, the gap scale μ should coincide, by simple dimensional analysis, with the momentum scale where the gapless modes become strongly coupled.[2] In that case, while the amplitude is still suppressed at small initial momenta, the emission and exchange of additional gapless modes will contribute $\mathcal{O}(1)$ relative corrections to the total rate, thus making it practically incalculable. In other words, the interaction among slow gapped modes can lead to the production of very energetic gapless ones, beyond the reach of the ordinary EFT description of their dynamics.

The question is then how to properly describe this state of affairs. On the one hand, the gapped Goldstones are free at zero momentum/velocity, as dictated by symmetry, while on the other, at arbitrarily small velocity, the processes involving them do not seem calculable. Integrating out the gapped modes in favor of an ordinary EFT for the gapless ones, while certainly doable, does not seem satisfactory, as it would preclude describing those aspects of the dynamics that are dictated by symmetry (like the relation between the gap and the chemical potential or the freedom of gapped modes at zero velocity). Relatedly that would make the underlying symmetry breaking pattern not visible in the EFT.[3] In this chapter we address the problem by constructing a proper EFT that allows for a more limited but systematic description of the gapped Goldstone dynamics. The construction is fully analogous to the nonrelativistic EFT (NREFT) used, for instance, to describe positronium [71]. Like in the positronium case, the price to pay is the existence of absorbitive (imaginary) terms in the effective action [72, 73]. Within this NREFT approach, we shall illustrate how to describe the dynamics in a systematic small momentum expansion.

---

[1] Note that the presence of Adler's zeros for gapless Goldstones is not always guaranteed due to possible kinematic singularities, cf. [28]. On the other hand, the gap of the gapped Goldstones precludes these singularities, and Adler's zeros for them are always present [67].

[2] That is, for instance, the case in QCD, where the ρ mass parametrically coincides with the scale where π interactions become strong

Besides the above mentioned conceptual issues, understanding the consequences of a spontaneously broken non-Abelian symmetry at finite density is also a question of phenomenological relevance. Indeed gapped Goldstones appear in many different contexts [40], ranging from condensed matter systems [61, 74, 75], to QCD at finite isospin density in the chiral limit [41–44]. Furthermore, they are also relevant in conformal field theories, where one can use the state/operator correspondence to map operators with large internal quantum numbers to finite density states [34, 35]. As such gapped Goldstones appear in the description of the spectrum of deformations of critical points in statistical physics.

In this chapter we illustrate our ideas by focusing on a simple system with an $SU(2)$ symmetry fully broken by the finite density of one of its charges. The resulting spectrum features a gapless and a gapped Goldstone, whose gap is precisely μ. In section 2.1 we study a simple model that exhibits this symmetry breaking pattern, namely the linear triplet introduced in sec. 1.2.2, and verify the presence of Adler's zero in the amplitudes for the gapped Goldstones. This will be our benchmark for the rest of the chapter. In section 2.2 we construct a nonrelativistic effective field theory for gapless and gapped Goldstones at small 3-momentum, showing how their interactions are constrained by the full symmetry group. Remarkably, such a construction is applicable for any value of the chemical potential, even when it is of the same order as the UV cutoff of the theory. In order to account for the gapped Goldstone's decay or annihilation, we argue that the NREFT must contain imaginary coefficients, which makes it non-unitary. The lack of unitarity is simply due to the limited class of degrees of freedom that make up our EFT, and is of course not a fundamental property. Power counting and interactions in such a theory are analyzed in detail. Finally, in section 2.3 we discuss the reasons why there is no remnant of the non-Abelian part of the broken symmetry at energies much smaller than the chemical potential.

---

[3] For instance in the case of a fully broken non-Abelian group G the gapless modes are purely described by the spontaneous breaking of the Cartan subgroup of G [35], with seemingly no visible low-energy remnant of the non-Abelian nature of the original group.

2.1 Interactions of slow gapped Goldstones in the linear triplet

In this section we examine the amplitudes for the scattering and annihilation in the regime when the gapped Goldstones' velocities are small for the linear triplet model discussed in sec. 1.2.2. The model is weakly coupled and renormalizable, and hence all observables can be computed perturbatively. Because of that, we will use it as the main example to match the effective theory developed in the rest of the chapter.

First we recall that, expanding the triplet around the finite density solution (1.25) we obtained the Lagrangian (1.27). The latter consists consists of three fields: h, ψ and θ. The first two interpolate, both, a gapless Goldstone state π_3 and a radial mode ρ, whose dispersion relations are given in eq.s (1.28) and (1.30). The field θ corresponds instead to the gapped Goldstone, with mass μ (1.29).

Given the action (1.27) we can now compute the amplitudes for the two processes involving the gapped Goldstone on the external legs: the $\theta\theta \to \theta\theta$ scattering and the $\theta\theta \to \pi_3\pi_3$ annihilation. We examine the amplitudes in the limit when the gapped Goldstones are slow. The reason for doing that is twofold. First, we verify the existence of Adler's zero in the amplitudes when one of the gapped Goldstones is at rest. Note that the interaction strength is not manifestly controlled by the gapped Goldstone's 3-momentum. Consequently, when the latter vanishes, the amplitude does not vanish diagram by diagram, but only once all of them are taken into account. Second, we will use these results as our reference point to match the NREFT we will build in the next sections. In particular, the second process does not preserve the number of gapped Goldstones and, as anticipated in the Introduction, will be included in the NREFT through an imaginary part for some of the effective coefficients.

Note that, because of the kinetic mixing between h and ψ, the calculation of the scattering amplitude is rather tedious (but straightforward). We spare the reader the details.

Consider first the elastic scattering, $\theta(\boldsymbol{p}_a) + \theta(\boldsymbol{p}_b) \to \theta(\boldsymbol{p}_c) + \theta(\boldsymbol{p}_d)$, in the limit where the gapped Goldstones are slow. In the presence of a slow massive particle, it is customary to power-count interactions in terms of its velocity, $v \ll 1$ [76], which is related to its momentum and kinetic energy by $\boldsymbol{p} = \mu \boldsymbol{v}$ and $\epsilon = \omega - \mu \sim \mu v^2$. We then expand the tree-level matrix element for the scattering in powers of velocity:

$$\mathcal{M} = \mathcal{M}^{(1)} + \mathcal{M}^{(2)} + \dots , \qquad \text{with} \qquad \mathcal{M}^{(n)} \sim \mathcal{O}(\boldsymbol{p}^{2n}/\mu^{2n}) \,. \tag{2.1}$$

The leading order contribution is $\mathcal{O}(v^2)$ and is given by

$$\mathcal{M}^{(1)} = \frac{\lambda}{\mu^2 - m^2}\left[\frac{(\boldsymbol{p}_a^2 - \boldsymbol{p}_c^2)^2}{(\boldsymbol{p}_a - \boldsymbol{p}_c)^2} + \frac{(\boldsymbol{p}_a^2 - \boldsymbol{p}_d^2)^2}{(\boldsymbol{p}_a - \boldsymbol{p}_d)^2} - (\boldsymbol{p}_a + \boldsymbol{p}_b)^2\right] . \tag{2.2}$$

Setting one of the momenta to zero, say $\boldsymbol{p}_a = 0$, this amplitude vanishes by conservation of energy, which implies $\boldsymbol{p}_b^2 = \boldsymbol{p}_c^2 + \boldsymbol{p}_d^2$ at the lowest order in velocity. Notice also that the amplitude is bounded albeit discontinuous in the collinear limits, $\boldsymbol{p}_a \to \boldsymbol{p}_c$ or $\boldsymbol{p}_a \to \boldsymbol{p}_d$.

For the purpose of matching with the NREFT it is also instructive to compute the next order amplitude, which reads

$$\begin{aligned}
\mathcal{M}^{(2)} = \frac{\lambda}{\mu^2(\mu^2-m^2)} \Bigg\{ & \frac{\mu^2}{\mu^2-m^2}\left(\boldsymbol{p}_a^2\boldsymbol{p}_b^2 + \boldsymbol{p}_c^2\boldsymbol{p}_d^2\right) - \frac{\mu^2+m^2}{4(\mu^2-m^2)}(\boldsymbol{p}_a^2+\boldsymbol{p}_b^2)^2 \\
&+ \frac{7\mu^2+m^2}{\mu^2-m^2}(\boldsymbol{p}_a\cdot\boldsymbol{p}_b)^2 + \frac{2\mu^2}{\mu^2-m^2}\left[(\boldsymbol{p}_a\cdot\boldsymbol{p}_c)(\boldsymbol{p}_b\cdot\boldsymbol{p}_d) + (\boldsymbol{p}_a\cdot\boldsymbol{p}_d)(\boldsymbol{p}_b\cdot\boldsymbol{p}_c)\right] \\
&- \frac{2\mu^2}{\mu^2-m^2}(\boldsymbol{p}_a^2+\boldsymbol{p}_b^2)(\boldsymbol{p}_a\cdot\boldsymbol{p}_b) \qquad\qquad\qquad\qquad (2.3) \\
&+ \frac{(\boldsymbol{p}_a^2-\boldsymbol{p}_c^2)^2}{(\boldsymbol{p}_a-\boldsymbol{p}_c)^2}\left[\frac{3\mu^2-m^2}{4(\mu^2-m^2)}\frac{(\boldsymbol{p}_a^2-\boldsymbol{p}_c^2)^2}{(\boldsymbol{p}_a-\boldsymbol{p}_c)^2} - \frac{1}{2}(\boldsymbol{p}_a^2+\boldsymbol{p}_b^2) + \frac{1}{2}\frac{\boldsymbol{p}_a^2\boldsymbol{p}_b^2-\boldsymbol{p}_c^2\boldsymbol{p}_d^2}{(\boldsymbol{p}_a^2-\boldsymbol{p}_c^2)}\right] \\
&+ \frac{(\boldsymbol{p}_a^2-\boldsymbol{p}_d^2)^2}{(\boldsymbol{p}_a-\boldsymbol{p}_d)^2}\left[\frac{3\mu^2-m^2}{4(\mu^2-m^2)}\frac{(\boldsymbol{p}_a^2-\boldsymbol{p}_d^2)^2}{(\boldsymbol{p}_a-\boldsymbol{p}_d)^2} - \frac{1}{2}(\boldsymbol{p}_a^2+\boldsymbol{p}_b^2) + \frac{1}{2}\frac{\boldsymbol{p}_a^2\boldsymbol{p}_b^2-\boldsymbol{p}_c^2\boldsymbol{p}_d^2}{(\boldsymbol{p}_a^2-\boldsymbol{p}_d^2)}\right]\Bigg\} .
\end{aligned}$$

Again one can check the existence of the Adler's zero when one of the three-momenta vanishes. Note also that s-channel exchange of the radial mode ρ gives terms whose expansion in velocity is controlled by $\frac{\boldsymbol{p}^2}{m_\rho^2-4\mu^2} \propto \frac{\boldsymbol{p}^2}{\mu^2-m^2}$. The expansion therefore breaks down at the ρ production threshold, which also coincides with the limit $\mu^2 \to m^2$ where the expectation value $\phi_0^2 \propto (\mu^2-m^2) \to 0$ and the symmetry is restored.

Again one can check the existence of Adler's zero when one of the 3-momenta vanishes. Note also that s-channel exchange of the radial mode ρ gives terms whose expansion in momenta is controlled by $\frac{\boldsymbol{p}^2}{m_\rho^2-4\mu^2} \propto \frac{\boldsymbol{p}^2}{\mu^2-m^2}$. The expansion therefore breaks down at the ρ production threshold $\boldsymbol{p} \sim (\mu^2-m^2)/\mu$ or, alternatively, in the limit $\mu^2 \to m^2$ where the expectation value $\phi_0^2 \propto (\mu^2-m^2)$ vanishes and the symmetry is restored.

Since the internal symmetry group is fully broken, there is no symmetry left to protect the number of gapped Goldstones. Indeed, two of them may annihilate into two gapless Goldstones via the process $\theta(\boldsymbol{p}_a)+\theta(\boldsymbol{p}_b) \to \pi_3(\boldsymbol{k}_a)+\pi_3(\boldsymbol{k}_b)$. Since the gapped Goldstones have energies $\geq \mu$, the final products of this annihilation have momenta and energies $\geq \mu$. Consequently, in the regime $\mu \sim m_\rho$, this process is beyond the regime of applicability of an ordinary low-energy EFT.

At the leading order in the gapped Goldstones' velocities the annihilation amplitude reads

$$\mathcal{M} = \frac{\lambda}{\mu^2-m^2}\left[\alpha\,(\boldsymbol{p}_a\cdot\boldsymbol{p}_b) + \beta\,\frac{(\boldsymbol{p}_a\cdot\boldsymbol{k})(\boldsymbol{p}_b\cdot\boldsymbol{k})}{\mu^2}\right] + \mathcal{O}\left(\frac{\boldsymbol{p}^2(\boldsymbol{p}\cdot\boldsymbol{k})}{\mu^4}\right), \tag{2.4}$$

where at the lowest order $\boldsymbol{k}_a = -\boldsymbol{k}_b \equiv \boldsymbol{k}$, with $|\boldsymbol{k}| = \mu$, and the dimensionless coefficients α and β can be found in appendix A.2.1. Once again the amplitude vanishes when either initial three-momenta is set to zero. The leading order total annihilation cross section reads

$$\sigma_{\text{ann}} \simeq \frac{1}{2\mu|\boldsymbol{p}_a - \boldsymbol{p}_b|}\left[(\gamma+\delta)\,\frac{(\boldsymbol{p}_a \cdot \boldsymbol{p}_b)^2}{\mu^4} + \delta\,\frac{\boldsymbol{p}_a^2\boldsymbol{p}_b^2}{\mu^4}\right], \tag{2.5}$$

where γ and δ are dimensionless coefficients again given in appendix A.2.1.

Notice that θ is odd under the unbroken $\mathbb{Z}_2$ symmetry. Processes with an odd number of θ legs are thus forbidden, and θ is stable. The $\mathbb{Z}_2$ symmetry is an accident of the simple model under consideration and not a structural property of gapped Goldstones. That is appreciated, for instance, by showing that the addition of a new field allows to write $\mathbb{Z}_2$-breaking terms and induce θ-decay—see appendix A.2.2 for an explicit construction using a complex $U(2)$ doublet. One finds that the decay amplitude vanishes when the 3-momentum of θ approaches zero. The total decay rate for a gapped Goldstone with momentum $\boldsymbol{p}$ to leading order in velocity reads

$$\Gamma = c\,\frac{\boldsymbol{p}^2}{\mu}, \tag{2.6}$$

where c is a dimensionless coefficient which depends on the couplings.

In summary, just like for standard Goldstones, the interaction strength of gapped Goldstones is set by their spatial momentum. This is due to the fact that the zero mode of θ is not dynamical, but corresponds to a symmetry transformation of the vacuum. More precisely, one can prove the existence of Adler's zeros [28] for the matrix elements of gapped Goldstones at rest [67]. Lastly, since no symmetry protects the number of gapped Goldstones, they may decay and/or annihilate into final states with energies of order μ. When $\mu \sim m_\rho$ such final states cannot be described within any low-energy EFT, which is valid at energies much smaller than m_ρ itself. However, in this very situation, the decay and annihilation processes happen within a short distance scale. As we shall see, that allows to consistently describe these effects via local operators in the NREFT. These operators are however non-Hermitian, which makes the NREFT non-unitary.

2.2 The Nonrelativistic EFT: the universal description of slowly moving gapped Goldstones

In the presence of spontaneous symmetry breaking one expects the low-energy dynamics to be effectively describable in terms of symmetries, and through a systematic derivative expansion. Such a construction (also known in jargon as coset or CCWZ construction) is expected to apply universally, i.e. purely on the basis of the symmetry breaking pattern and independently of the details of the underlying microscopic physics. In the known examples, it applies equally well to cases that purely involve the breaking of internal symmetries [26, 27], and to cases that involve the breaking of the spacetime ones (see, e.g., [39, 64, 77]).

In the presence of gapped Goldstone bosons the situation can however be more involved. That depends on the existence of two in principle distinguished scales: the chemical potential μ, which controls the gap of some of the Goldstones, and the scale Λ which controls the gap of non-Goldstone degrees of freedom, as well as the derivative expansion.[4] The existence of a hierarchy, $\mu \ll \Lambda$, should generically correspond to the existence and smoothness of the limit $\mu \to 0$, where the charge density goes to zero, Lorentz invariance is recovered and the Goldstone bosons are the only light modes. An example of this situation is given by the linear σ-model of the previous section for the choice $m^2 < 0$, where the symmetry is broken already at $\mu = 0$, where the density vanishes. Generically, $\mu \ll \Lambda$ thus corresponds to the situation where the internal symmetry is partially broken already at zero density, and where the state with finite charge density (and the corresponding Lorentz breaking) is fully described as a particular solution of the original relativistic Goldstone EFT. Previous studies of the finite density systems based on the EFT methods [39, 40, 67] have all focused on this case. In this setup the construction of the effective Lagrangian for the Goldstones proceeds in a way similar to the Lorentz invariant case, where there is a well defined derivative expansion, whose strength is controlled by Λ itself. For $\mu \ll \Lambda$, besides the counting of Goldstone degrees of freedom, there are no major structural novelties with respect to the standard relativistic CCWZ construction.

The novelties appear when there is basically a single mass scale, $\mu \sim \Lambda$, which is indeed a minimal option for a system at finite density. Again, intuitively this regime corresponds to the situation where all symmetry breaking is fully dominated by the presence of finite density. The limit $\mu \to 0$ cannot therefore be smooth. An example of this situation is given by the linear σ-model in the regime $\mu^2 \gg m^2 > 0$, where μ controls both the gap of the Goldstones and the gap of the radial non-Goldstone mode ρ. In fact, this situation is unavoidably realized whenever the system is (approximately) scale invariant with μ representing the dominant *spontaneous* source of breaking of scale invariance. This class of systems includes the physically relevant cases of conformal field theories (CFTs) in the large charge regime [34, 35, 78, 79], and finite density QCD with large isospin chemical potential $\mu_I \gtrsim \Lambda_{\text{QCD}}$ [41–44].

The goal of this section is to present general, systematic and self-consistent rules for constructing the effective Lagrangian. The relevant degrees of freedom will be the small 3-momentum modes: *soft* gapless and *slow* gapped. The first step will be to show explicitly how to organize the derivative expansion, which involves of course both time and space derivatives, as an expansion in the 3-momentum. Secondly, we will have to properly interpret the result according to the rules of nonrelativistic EFTs. In particular, the conservation of the number of gapped Goldstones will emerge as a formal symmetry of the effective action. Processes where the gapped Goldstone number is not conserved will then be described consistently, but in an inclusive manner only, by allowing for absorbitive imaginary coefficients in the effective Lagrangian.

---

[4] We are working under the simplifying assumption that the typical speed of the excitations around the cut of scale Λ are $\mathcal{O}(1)$ so that there is no need to distinguish energy and momentum cutoffs.

We shall focus on the general class of models where a global $SU(2)$ is nonlinearly realized at finite chemical potential μ. The triplet model discussed in the previous section is a particular weakly coupled renormalizable example. It will serve as template and test case for our results. Our discussion wants to be general, and applies in particular to the case $\mu \sim \Lambda$. In fact, our EFT construction will even apply to the case where non-Goldstone degrees of freedom with gap $\Lambda \ll \mu$ have been integrated out. However for economy of thought we shall mostly stick to the case $\mu \sim \Lambda$ when picturing our scenario. Under our assumptions, any process where the number of gapped Goldstones is not conserved necessarily leads to the production of states with momentum $\sim \mu$ (either gapless Goldstones or non-Goldstone states with gap less than μ) that lie outside the domain of validity of the EFT. Our effective Lagrangian must thus necessarily be endowed with an effectively conserved gapped Goldstone number. We will concretely see how this happens.

As specified in the Introduction, we are interested in systems which spontaneously break an $SU(2)$ internal symmetry, as well as time translations and boosts, leaving unbroken the combination $\bar{H} = H + \mu Q_3$. In general we could parametrize the degrees of freedom of our EFT using the coset construction generalized to include spacetime symmetries [39, 64, 77]. This construction is illustrated in appendix A.3. We however find it more convenient to employ an equivalent approach: we define our fields in terms of the Lorentz-preserving $SU(2)$ coset which involves three Goldstone fields, and then consider a generic time-dependent solution which further breaks spacetime symmetries down to spatial rotations, spatial translations and the modified time translation $\bar{H} = H + \mu Q_3$.

Our dynamical variable just corresponds to a general $SU(2)$ matrix, $\Omega(x)$, on which the group acts on the left:

$$\Omega(x) \to g\Omega(x) , \qquad\qquad g \in SU(2) . \tag{2.7}$$

We can now choose local Lie parameters, the Goldstone fields, to parametrize Ω. We will work with two different parametrizations, each showing advantages and disadvantages. The first parametrization, which we will name “Left”, is

$$\Omega(\chi, \alpha) = e^{i\chi Q_3} e^{i\alpha \frac{Q_+}{2} + i\alpha^* \frac{Q_-}{2}} \equiv e^{i\chi Q_3}\, \Omega_L(\alpha) , \tag{2.8}$$

where χ and $\alpha \equiv \alpha_1 + i\alpha_2$, represent the three real Goldstone scalars, and $Q_\pm \equiv Q_1 \pm iQ_2$.

Notice that Ω_L parametrizes the coset $SU(2)/U_3(1)$, with obvious notation. The other parametrization, which we dub as “Right”, is instead

$$\Omega(\chi,\pi) = e^{i\pi\frac{Q_+}{2}+i\pi^*\frac{Q_-}{2}}\, e^{i\chi Q_3} \equiv \Omega_R(\pi)\, e^{i\chi Q_3}\,, \tag{2.9}$$

with similar comments. The mapping between Left and Right parametrization is simply given by $\pi = e^{i\chi}\alpha$.

2.2.1 Building the EFT with the Left parametrization

The CCWZ prescription [26,27] allows to construct an $SU(2)$ invariant Lagrangian for the Goldstone fields χ and α. Explicitly, the Maurer-Cartan one-form defines the covariant derivatives of the Goldstones [64] as

$$\begin{aligned}\Omega^{-1}\partial_\mu\Omega &= i\partial_\mu\chi\,\Omega_L^{-1}Q_3\Omega_L + \Omega_L^{-1}\partial_\mu\Omega_L \\ &\equiv iD_\mu\chi Q_3 + iD_\mu\alpha\frac{Q_+}{2} + iD_\mu\alpha^*\frac{Q_-}{2}\,,\end{aligned} \tag{2.10}$$

where

$$D_\mu\chi = \partial_\mu\chi\cos\left(|\alpha|\right) + \frac{i\alpha^*\partial_\mu\alpha - i\alpha\partial_\mu\alpha^*}{|\alpha|^2}\sin^2\left(|\alpha|/2\right)\,, \tag{2.11}$$

$$D_\mu\alpha = i\partial_\mu\chi\,\alpha\frac{\sin\left(|\alpha|\right)}{|\alpha|} + \frac{1}{2}\partial_\mu\alpha\left(1+\frac{\sin|\alpha|}{|\alpha|}\right) + \frac{\alpha}{2\alpha^*}\partial_\mu\alpha^*\left(1-\frac{\sin|\alpha|}{|\alpha|}\right)\,. \tag{2.12}$$

Then the most general $SU(2)$ invariant Lagrangian for χ and α is an arbitrary function of the covariant derivatives in (2.10) and ∂_μ:

$$\mathcal{L} = F\left[D_\mu\chi, D_\mu\alpha, D_\mu\alpha^*, \partial_\mu\right]\,, \tag{2.13}$$

with spacetime indices contracted in a Lorentz invariant way.

We are interested in a setup where spacetime symmetries are spontaneously broken as well. To this aim, we notice that the equations of motion deriving from (2.13) generically admit a solution of the form

$$\chi = \mu t\,, \qquad \alpha = v\,, \tag{2.14}$$

where v is a constant whose value depends on μ. This is particularly easy to show using the Left parametrization (2.8). Indeed, the Euler-Lagrange equation for the field χ takes the form

$$-\partial_\mu\frac{\partial\mathcal{L}}{\partial(\partial_\mu\chi)} + \partial_\mu\partial_\nu\frac{\partial\mathcal{L}}{\partial(\partial_\mu\partial_\nu\chi)} + \ldots = 0\,, \tag{2.15}$$

which is automatically satisfied since the Lagrangian and its derivatives do not depend on x on the ansatz (2.14). Similarly, the only nontrivial contribution from the equation for α is

$$\frac{\partial\mathcal{L}}{\partial\alpha} = \mu\left\{-\frac{v^*\sin(|v|)}{2|v|}\frac{\partial F}{\partial D_0\chi} + \frac{1}{2}\left[\cos(|v|) + \frac{\sin(|v|)}{|v|}\right]\frac{\partial F}{\partial D_0\alpha} \right. \\ \left. + \frac{v^*}{2v}\left[\cos(|v|) - \frac{\sin(|v|)}{|v|}\right]\frac{\partial F}{\partial D_0\alpha^*}\right\} = 0\,, \quad (2.16)$$

where the derivatives of the Lagrangian are evaluated on the ansatz. This is an algebraic equation determining the complex value of $v \equiv v(\mu)$.

It is convenient to work in a field parametrization for which α vanishes on the background. For this parametrization to be independent of the specific value of the chemical potential, we *formally* define:

$$\tilde{v} \equiv v\left(\sqrt{(D\chi)^2 + |D\alpha|^2}\right)\,, \quad (2.17)$$

where the function $v(\mu)$ is determined solving (2.16) for arbitrary values of μ. Notice that on the solution (2.14) $\sqrt{(D\chi)^2 + |D\alpha|^2} = \mu$. We then perform the following field redefinition

$$\Omega(\chi,\alpha) = \Omega(\chi',\alpha')\exp\left[i\tilde{v}\frac{Q_+}{2} + i\tilde{v}^*\frac{Q_-}{2}\right]\,, \quad (2.18)$$

which brings the solution (2.14) to the form

$$\chi' = \mu t\,, \qquad \alpha' = 0\,. \quad (2.19)$$

With the field redefinition (2.18) and defining $R \equiv \exp\left[i\tilde{v}\frac{Q_+}{2} + i\tilde{v}^*\frac{Q_-}{2}\right]$, the covariant derivatives in (2.10) now read

$$iD_\mu\chi Q_3 + iD_\mu\alpha\frac{Q_+}{2} + iD_\mu\alpha^*\frac{Q_-}{2} = \\ R^{-1}\left[iD_\mu\chi' Q_3 + iD_\mu\alpha'\frac{Q_+}{2} + iD_\mu\alpha'^*\frac{Q_-}{2}\right]R + R^{-1}\partial_\mu R\,. \quad (2.20)$$

By construction, all the components of the matrix R are $SU(2)$ invariant (as they are functions of invariants). Then, since the left hand side of (2.20) is also $SU(2)$ invariant, $D_\mu\chi'$, $D_\mu\alpha'$ and $D_\mu\alpha'^*$, the covariant derivatives of χ' and α', must be invariant as well. Hence, by redefining its coefficients, the Lagrangian (2.13) takes an analogous form in terms of the fields χ' and α', and we can work equivalently with the primed fields. In the following we drop the prime supscript.

The solution (2.19) spontaneously breaks time translations and boosts while being invariant under the action of $\bar{H}$. Therefore, to explicitly realize a symmetry breaking pattern of the desired form it is enough to expand the generic Lagrangian in (2.13) around the background (2.19).

Notice that in this way of proceeding we did not need to introduce Goldstone fields for the broken boost generators. It is indeed known that, in order to realize spacetime symmetries nonlinearly, one normally needs less Goldstones than the number of broken generators [63]. In the procedure detailed in appendix A.3, where one introduces a coset parametrizing the full spacetime symmetry group [39, 64, 77], the boost Goldstone bosons are eliminated via an inverse Higgs constraint [80]. The final result is equivalent to the simple construction presented above.

The field parametrization in eq. (2.8), expanded around the background (2.19), makes clear the origin of the gap for the massive Goldstone. Indeed, as a consequence of the $SU(2)$ symmetry, the Goldstone fields admit a solution where $\chi(x) = \mu t$ and the π field oscillate in time with frequency μ. To see this, it is enough to show that such a configuration is generated by a symmetry transformation of the background (2.19). Acting with a rotation generated by, say, Q_1 on the coset element one gets

$$\begin{aligned} e^{i\xi Q_1}\Omega(\chi,\alpha) &= e^{i\chi Q_3}\left(e^{-i\chi Q_3}e^{i\xi Q_1}e^{i\chi Q_3}\right)\Omega_L(\alpha) \\ &= e^{i\chi Q_3}e^{i\xi\left(e^{-i\chi}\frac{Q_+}{2}+e^{i\chi}\frac{Q_-}{2}\right)}\Omega_L(\alpha) \equiv e^{i\tilde{\chi}Q_3}\Omega_L(\tilde{\alpha})\,. \end{aligned} \tag{2.21}$$

When one acts on the background $\chi = \mu t$ and $\alpha = 0$, the transformed field, $\tilde{\alpha} = e^{-i\mu t}\xi$, is oscillating with frequency μ.

When spacetime symmetries are unbroken, the Goldstone fields transform with a constant shift under an infinitesimal group transformation of the background. Standard relativistic EFTs describe the dynamics of slowly varying fields, corresponding to those configurations which are indistinguishable from a symmetry transformation at short distances. The situation is quite different when considering a background of the form (2.19). Indeed, we saw in eq. (2.21) that an $SU(2)$ rotation can generate a configuration oscillating in time with a frequency of the order of the cutoff of the theory. This is the main disadvantage of the Left parametrization. Then, to proceed formulating the EFT, it is more convenient to use the alternative field parametrization (2.9), for which the group action takes a different form.

2.2.2 Building the EFT with the Right parametrization

In the field parametrization (2.9), the background solution reads as in (2.19):

$$\chi = \mu t + \pi_3\,, \qquad \pi_3 = \pi = 0\,. \tag{2.22}$$

However, the group action takes now a different form. As a result, a generic infinitesimal $SU(2)$ transformation acting on the background provides a solution of the form $\pi_3 =$

constant and π = constant, precisely like in a Poincarè invariant coset. In analogy with that case the EFT will thus be limited to the slowly varying field configurations, $\partial\pi \ll \mu\pi\,,\ \partial\pi_3 \ll \mu\pi_3$, in the Right parametrization (2.9).

Notice that, despite π = constant being a solution, the field π describes a gapped mode with frequency μ. To see this, recall that the gap is measured by the action of the unbroken generator of time translations: $\bar{H} = H + \mu Q_3$. It is then possible to verify that under the action of $\bar{H}$, the field acquires a phase proportional to μ: $\pi(t,\boldsymbol{x}) \to e^{-i\mu\delta t}\pi(t+\delta t,\boldsymbol{x})$. Thus, in this parametrization, low frequency modes for the field π are associated with *slowly moving* gapped Goldstones. The EFT thus consists of modes with small 3-momentum, and with eigenvalues of $\bar{H} = H + \mu Q_3$ around respectively 0 for π_3 and μ for π. Modes that do not satisfy these requirements should be thought as having been integrated out.

Because of the unusual transformation property of the field π under the unbroken time translations, the Lagrangian (2.13), written in the the Right parametrization, is correspondingly unusual: it is explicitly time dependent when expanded in fluctuations around (2.19). To see this explicitly, let us compute the Maurer-Cartan one-form. Using (2.9), we write it as follows

$$\begin{aligned}\Omega^{-1}\partial_\mu\Omega &= e^{-i\chi Q_3}\Omega_R^{-1}\partial_\mu\Omega_R e^{i\chi Q_3} + i\partial_\mu\chi Q_3\\ &= e^{-i\chi Q_3}\left(id_\mu\pi\frac{Q_+}{2} + id_\mu\pi^*\frac{Q_-}{2} + iA_\mu Q_3\right)e^{i\chi Q_3} + i\partial_\mu\chi Q_3\\ &= i\left(e^{-i\chi}d_\mu\pi\frac{Q_+}{2} + e^{i\chi}d_\mu\pi^*\frac{Q_-}{2} + D_\mu\chi Q_3\right)\,. \qquad (2.23)\end{aligned}$$

Here $d_\mu\pi$ and A_μ are the covariant derivative and the connection for the $SU(2)/U_3(1)$ coset, given by

$$d_\mu\pi = \pi\frac{\pi^*\partial_\mu\pi - \pi\partial_\mu\pi^*}{2|\pi|^3}\sin\Big(|\pi|\Big) + \pi\frac{\pi^*\partial_\mu\pi + \pi\partial_\mu\pi^*}{2|\pi|^2}\,, \qquad (2.24)$$

$$A_\mu = i\frac{\pi^*\partial_\mu\pi - \pi\partial_\mu\pi^*}{|\pi|^2}\sin^2\Big(|\pi|/2\Big)\,. \qquad (2.25)$$

The full $SU(2)$ covariant derivatives (2.10) are written in terms of these as

$$D_\mu\alpha = e^{-i\chi}d_\mu\pi\,, \qquad D_\mu\chi = \partial_\mu\chi + A_\mu\,. \qquad (2.26)$$

By Eqs. (2.23)-(2.26) a generic invariant Lagrangian, through the factor $e^{i\chi}$, contains terms that explicitly depend on time on the background. This seems a rather unpleasant property. However one must keep in mind that our EFT only contains low frequency/low momentum modes ($\partial\pi \ll \mu\pi\,,\ \partial\pi_3 \ll \mu\pi_3$). Then, by simple Fourier analysis, Lagrangian terms involving a non-trivial power of $e^{i\chi}$ integrate to zero in the action, as its fast oscillation cannot be compensated by any finite combination of EFT modes. Only terms featuring no power of $e^{i\chi}$ survive. These are invariant under an emergent $U(1)$ symmetry,

$U_\pi(1)$, acting as $d_\mu\pi \to e^{i\xi}d_\mu\pi$,[5] which is nothing but the particle number conservation of nonrelativistic theories (see e.g. [81]). As typical of a nonrelativistic limit, this property emerges naturally after factoring out the mass contribution from the time evolution of the gapped fields, as we did switching from the Left to the Right parametrization.

The emergence of this $U(1)$ symmetry does not allow to describe processes where the number of gapped Goldstones is changed, such as decay or annihilation. Physically this is because they necessarily feature modes with momentum $\sim \mu$ in the final state, outside the regime of validity of the effective theory. As a consequence the resulting nonrelativistic EFT cannot be unitary. Indeed, through the optical theorem, these processes give rise to imaginary parts in the gapped Goldstone propagators and matrix elements, which can only be matched in the nonrelativistic EFT by allowing for imaginary parts in the Wilson coefficients [73]. We will discuss this matching in some detail for the linear triplet model in the following sections.

We would now like to expand the Lagrangian (2.13) in a series of higher derivative terms. In order to power count, it is useful to indicate by $\partial_s \ll \mu$ the *small* derivatives of our EFT modes. More precisely, the spacial part $\boldsymbol{\partial}$ obviously represents the small momentum for both π_3 and π, while ∂_t, represents respectively energy and kinetic energy for π_3 and π. Remember indeed that in the Right parametrization we have in practice subtracted μ from the oscillation frequency of π excitations.

The parametrization (2.9) shows that the naïve derivative expansion must be reorganized when working around the typical background we are interested in. Consider, in fact, the derivative of the Maurer-Cartan form:

$$\begin{aligned}\partial_\mu\left[\Omega^{-1}\partial_\nu\Omega\right] = {} & -i\partial_\mu\chi\left[Q_3,\Omega^{-1}\partial_\nu\Omega\right] + e^{-i\chi Q_3}\partial_\mu\left(\Omega_R^{-1}\partial_\nu\Omega_R\right)e^{i\chi Q_3} \\ & + i\partial_\mu\partial_\nu\chi Q_3\,.\end{aligned} \tag{2.27}$$

The last two terms are genuinely suppressed by two EFT derivatives, $\mathcal{O}(\partial_s^2)$. However, around the background $\chi = \mu t$, the first term counts as a one-derivative term, $\mathcal{O}(\mu\partial_s)$, unsuppressed with respect to $\mu\,\Omega^{-1}\partial_\nu\Omega$. This shows that some reorganization of terms is needed in order to write the Lagrangian in a manifest expansion in powers of ∂_s. Notice for that purpose that the first term in (2.27) is not a new independent object; instead, it is proportional to the commutator of Q_3 with the Maurer Cartan form (2.10). This indicates how to proceed: one can simply subtract the first term on the right hand side of eq. (2.27), so that the remaining terms are $\mathcal{O}(\partial_s^2)$. Although this term is not $SU(2)$ invariant, there is a simple $SU(2)$ invariant Lorentz vector that is proportional to $\partial_\mu\chi$ at linear order, i.e. $D_\mu\chi$. We therefore can define a *nonrelativistic derivative* in the following way:

$$\hat{\partial}_\mu \equiv \partial_\mu + iD_\mu\chi\Big[Q_3,\cdot\Big]\,, \tag{2.28}$$

---

[5] This coincides with the $U(1)$ generated by the action of Q_3 on the right of the coset.

where by $\Big[Q_3, \cdot\Big]$ we mean the action of the commutator and the derivative is meant to act on the Maurer-Cartan form.[6] By its definition, the action of any power of $\hat{\partial}$ on the Maurer-Cartan form is suppressed by the corresponding power of ∂_s:

$$\hat{\partial}_{\mu_1} \cdots \hat{\partial}_{\mu_n} \left[\Omega^{-1}\partial_\nu\Omega\right] \ll \mu\, \hat{\partial}_{\mu_1} \cdots \hat{\partial}_{\mu_{n-1}} \left[\Omega^{-1}\partial_\nu\Omega\right] . \tag{2.29}$$

The action on the covariant derivatives of (2.26) reads:

$$\hat{\partial}_\mu D_\nu\chi = \partial_\mu D_\nu\chi \,, \qquad \hat{\partial}_\mu D_\nu\alpha = (\partial_\mu + iD_\mu\chi)D_\nu\alpha = e^{-i\chi}\left(\partial_\mu + iA_\mu\right) d_\nu\pi . \tag{2.30}$$

Since the second term in eq. (2.28) is not a new object, formulating the EFT in terms of $\hat{\partial}$ just amounts to rearranging the terms in the action so as to make the expansion in powers of ∂_s manifest. The new derivative allows us to define a consistent power counting in the small spatial momentum for both the gapless and gapped Goldstones.

We remark that eq. (2.28) is not the only possible choice for the definition of the *nonrelativistic* derivative. For instance, it is possible to multiply $D_\mu\chi$ by an arbitrary function of $\sqrt{D_\mu\chi D^\mu\chi}/\mu$ without affecting the property (2.29).

In summary, to construct an effective action for the Goldstones that is invariant under the full symmetry group $SU(2)$ × Poincarè, and that has a consistent expansion in the limit of slow gapped Goldstones one needs to (*i*) use the coset construction to build terms that are manifestly invariant under the unbroken group, (*ii*) consider only operators that are invariant under an additional $U_\pi(1)$ particle conservation symmetry, and (*iii*) construct higher derivative terms using the nonrelativistic covariant derivative (2.28). This recipe can be generalized to different symmetry breaking patterns.

At the lowest derivative order, one finds three invariants under Lorentz and $U_\pi(1)$: $D_\mu\chi D^\mu\chi$, $\Big|D_\mu\chi D^\mu\alpha\Big|^2$ and $D_\mu\alpha D^\mu\alpha^*$. It is convenient to organize them in terms of operators whose expectation value vanishes on the background (2.19). To match to the spacetime coset construction reported in appendix A.3, we reorganize them in the following way:

$$\begin{gathered}
\nabla_0\pi_3 \equiv \sqrt{D_\mu\chi D^\mu\chi} - \mu\,, \qquad \Big|\nabla_0\alpha\Big|^2 \equiv \frac{\Big|D_\mu\chi\, D^\mu\alpha\Big|^2}{D_\nu\chi D^\nu\chi} = \frac{\Big|D_\mu\chi\, d^\mu\pi\Big|^2}{D_\nu\chi D^\nu\chi}\,, \\
\Big|\nabla_i\alpha\Big|^2 \equiv \frac{\Big|D_\mu\chi\, D^\mu\alpha\Big|^2}{D_\nu\chi D^\nu\chi} - D_\mu\alpha\, D^\mu\alpha^* = \frac{\Big|D_\mu\chi\, d^\mu\pi\Big|^2}{D_\nu\chi D^\nu\chi} - d_\mu\pi\, d^\mu\pi^* .
\end{gathered} \tag{2.31}$$

At the leading order in derivatives, the effective nonrelativistic Lagrangian then takes the form:

---

[6] Formally, eq. (2.28) corresponds to the covariant derivative for an $SU(2)$ gauge group acting *on the right* of the coset (2.9), with a gauge connection given by $A^I_\mu = \delta^I_3 D_\mu\chi$.

$$\mathcal{L}_{\text{eff}} = c^{(1)}\mu^3\nabla_0\pi_3, +c_1^{(2)}\mu^2(\nabla_0\pi_3)^2 + c_2^{(2)}\mu^2|\nabla_0\alpha|^2 - c_3^{(2)}\mu^2|\nabla_i\alpha|^2 + \mathcal{O}\left(\mu\hat{\partial}^3\right)\,. \tag{2.32}$$

The action up to the fourth order in derivatives is given in appendix A.4.1. In the next sections we discuss the degrees of freedom in this EFT and illustrate the power counting by calculating several sample processes.

2.2.3 The NREFT to quadratic order

Let us expand the Lagrangian (2.32) to quadratic order in the fields:

$$\begin{aligned}\mathcal{L}_{\text{eff}} \supset & c_1^{(2)}\mu^2(\partial_0\pi_3)^2 - \frac{1}{2}c^{(1)}\mu^2(\boldsymbol{\nabla}\pi_3)^2 + \frac{1}{4}c^{(1)}\mu^3\left[i\pi^*\partial_0\pi + \text{c.c.}\right] \\ & - c_3^{(2)}\mu^2|\boldsymbol{\nabla}\pi|^2 + c_2^{(2)}\mu^2\left|\partial_0\pi\right|^2 .\end{aligned} \tag{2.33}$$

We focus on configurations with small derivatives. From eq. (2.33) one finds that π_3 interpolates a gapless mode with dispersion relation

$$\omega_k^2 = c_s^2\boldsymbol{k}^2 + \mathcal{O}\left(\boldsymbol{k}^4/\mu^2\right)\,, \qquad c_s^2 \equiv \frac{c^{(1)}}{2c_1^{(2)}}\,. \tag{2.34}$$

The quantization of π_3 then proceeds as usual, i.e.

$$\pi_3(x) = \frac{c_s}{\mu\sqrt{c^{(1)}}}\int\frac{d^3k}{(2\pi)^3\sqrt{2\omega_k}}a_{\boldsymbol{k}}e^{-i\omega_k t + i\boldsymbol{k}\cdot\boldsymbol{x}} + \text{h.c.}\,, \quad [a_{\boldsymbol{k}}, a_{\boldsymbol{p}}^\dagger] = (2\pi)^3\delta^3(\boldsymbol{k}-\boldsymbol{p})\,. \tag{2.35}$$

To quantize the π field, we notice that the last term in (2.33) contains two time derivatives and can be treated as a higher derivative perturbation of the third one, which contains only one. Indeed, π has the kinetic term of a nonrelativistic field and is quantized as

$$\pi(x) = \sqrt{\frac{2}{c^{(1)}\mu^3}}\int\frac{d^3p}{(2\pi)^3}b_{\boldsymbol{p}}e^{-i\epsilon_p t + i\boldsymbol{p}\cdot\boldsymbol{x}}\,, \qquad [b_{\boldsymbol{p}}, b_{\boldsymbol{k}}^\dagger] = (2\pi)^3\delta^3(\boldsymbol{p}-\boldsymbol{k})\,, \tag{2.36}$$

with dispersion relation given by:

$$\epsilon_p = c_m\frac{\boldsymbol{p}^2}{2\mu} + \mathcal{O}\left(\boldsymbol{p}^4/\mu^3\right)\,, \qquad c_m \equiv \frac{4c_3^{(2)}}{c^{(1)}}\,. \tag{2.37}$$

As commented before, due to its transformation properties under $\bar{H}$, π really is a gapped field. The ladder operator $b_{\boldsymbol{p}}^\dagger$ then creates a gapped Goldstone state with energy $E_p = \mu + \epsilon_p$.[7]

---

[7] For the sake of the discussion, we are momentarily considering a theory in which the gapped Goldstone cannot decay.

The nonrelativistic complex field π only contains annihilation operators (and π^* contains only creation ones) and thus propagates one degree of freedom.[8] As anticipated, the present effective theory describes a gapless mode and a nonrelativistic gapped mode. As a consistency check, one can see that including higher derivative corrections, such as the last term in (2.33) or terms constructed with (2.28), generates both new poles as well as correction to the dispersion relation (2.37). The new poles generically appear for frequency or momenta of order μ and are outside the regime of validity of our EFT; they should therefore be discarded. The corrections to the dispersion relation are instead higher order in the low-momentum expansion, showing that these additional terms can consistently be considered as perturbations in the EFT.

2.2.4 Gapped Goldstone number conservation and non unitarity

The NREFT enjoys a $U_\pi(1)$ invariance, $\pi \to e^{i\xi}\pi$, corresponding to particle number conservation for the gapped Goldstones. As already remarked, this does not correspond to a symmetry of the microscopic theory, but it is rather a consequence of the small momentum and energy window which characterizes the degrees of freedom of our EFT. In particular the EFT does not contain degrees of freedom with energy and momentum such that the π can decay or annihilate into them [81]. Hence the conservation of π-number. On the other hand, in the full theory these processes will in general exist, with final states involving π_3 modes with momentum $\sim \mu$, and also, possibly, other non-Goldstone degrees of freedom with gap $\sim \mu$.

The EFT cannot describe the π decay or annihilation processes *exclusively*, since the final states have short wavelengths. It can however describe them *inclusively*. Indeed, by the optical theorem, these processes give rise to imaginary parts in the π propagator and matrix elements, which can be matched in the NREFT by assigning proper imaginary parts to the Wilson coefficients. For instance, an imaginary part for the "kinetic energy coefficient" c_m corresponds to a decay width of the gapped Goldstone:

$$\Gamma_p = -2\,\mathrm{Im}\,[E_p] = -\mathrm{Im}\,[c_m]\,\frac{\boldsymbol{p}^2}{\mu}\,. \tag{2.38}$$

Notice that the above momentum dependence matches the explicit result we found in eq. (2.6). The resulting theory is therefore non-unitary and is sometimes called a complex NREFT [73].

---

[8] Alternatively one could use the equations of motion to eliminate one of the two real components of the field $\alpha = \alpha_1 + i\alpha_2$ of the Right parametrization (2.8) in terms of the other. Doing so would change the description of the gapped Goldstone mode from a complex field with one time derivative kinetic term to a two derivatives real scalar field. To leading order in derivatives, this procedure *formally* coincides with imposing an extra inverse Higgs constraint of the form $\mathrm{Re}[\nabla_0\alpha] = 0$. The same inverse Higgs constraint, but with a different physical interpretation, was discussed in [39] for the case in which the EFT cutoff is much larger than the chemical potential, $\Lambda \gg \mu$. We provide a more detailed discussion in appendix A.3.1.

Physically, annihilation and decay can be matched by means of local terms since these processes are determined by short distance dynamics. More precisely, to match the imaginary parts of the propagator or scattering amplitudes for a slow π of the full theory via local terms in the NREFT, requires the latter to be analytical in the spatial momentum. This is expected to be true as long as the relevant kinematic region is separated by a finite gap from any excitation which was not included in the NREFT.

Notice also that since the zero gapped Goldstone sector, $\pi = 0$, of the theory reduces to an EFT of a single gapless superfluid Goldstone, which should be unitary, the effective coefficients that multiply operators which do not contain $D_\mu\pi$ should always be real. Consistently, we will see that this is the case when we will match our EFT to the linear triplet in the next section.

2.2.5 Interactions and power counting

In this section we describe some interaction processes arising in the NREFT we built. In particular, we focus on two peculiar aspects: power counting and non-unitarity. The techniques described here are heavily inspired by nonrelativistic QED (NRQED) [71] and nonrelativistic QCD (NRQCD) [82], which describe the interactions of heavy fermions in the presence of light gauge fields. Like in those theories, we will find convenient to power count amplitudes in powers of the velocity $\boldsymbol{v} \sim \boldsymbol{p}/\mu$ of the heavy field.

Consider first the expansion of the covariant derivatives (2.26),

$$\begin{aligned} D_\mu\pi_3 &= \partial_\mu\pi_3 + \frac{i\pi^*\partial_\mu\pi - i\pi\partial_\mu\pi^*}{4} - |\pi|^2\frac{i\pi^*\partial_\mu\pi - i\pi\partial_\mu\pi^*}{48} + \mathcal{O}(\pi^6)\,, \\ D_\mu\pi &= e^{-i\chi}\left[\partial_\mu\pi + i\pi\frac{i\pi^*\partial_\mu\pi - i\pi\partial_\mu\pi^*}{12} + \mathcal{O}(\pi^5)\right]\,. \end{aligned} \tag{2.39}$$

We see that all terms in the action display derivatives acting on all the fields, making manifest the vanishing of the interaction strength with the 3-momentum, or equivalently with the gapped Goldstone velocity, in agreement with the results in section 2.1.

In deriving the dispersion relation (2.37), we realized that time and space derivatives of the on-shell gapped Goldstone field scale differently—namely $\boldsymbol{\nabla}\pi \sim \mu v$ and $\partial_0\pi \sim \mu v^2$—and some care is thus required in power counting.[9] Indeed, even after subtracting the mass contribution, a simple power counting in derivatives ∂/μ does not distinguish between v and v^2, retaining more terms than needed at a fixed order in v. As in NRQED and NRQCD, the power counting in velocity is complicated by the presence of states with two different forms of dispersion relation [83, 84].

We will now match the results of our NREFT to those of the model presented in section 2.1.

---

[9] For processes involving only the gapless mode the power counting is similar to the relativistic case.

In particular, this means the gapped Goldstone is stable and its dispersion relation real, which allows us to put its external legs on-shell.

To facilitate power counting it is convenient to split each field in components with support on different regions of phase space [76, 83, 84]. In particular, we write $\pi_3 = \pi_3^{\mathrm{s}} + \pi_3^{\mathrm{p}} + \pi_3^{\mathrm{us}}$ and $\pi = \pi^{\mathrm{s}} + \pi^{\mathrm{p}} + \pi^{\mathrm{us}}$, where the labels stand respectively for soft, potential and ultrasoft. These components have energy and momentum (i.e. time and space derivatives) scaling as[10]

$$\begin{aligned} \text{soft:} \quad & (\omega, \boldsymbol{k}) \sim (\mu v, \mu v)\,, \\ \text{potential:} \quad & (\omega, \boldsymbol{k}) \sim (\mu v^2, \mu v)\,, \\ \text{ultrasoft:} \quad & (\omega, \boldsymbol{k}) \sim (\mu v^2, \mu v^2)\,. \end{aligned} \tag{2.40}$$

Note that on-shell gapless Goldstones are contained in both π_3^{s} and π_3^{us}, while on-shell gapped Goldstones are contained in π^{p}. The rules are now the following: for each process under consideration one has to determine which field is participating in the different parts of the diagrams, perform the expansion of π and π_3 mentioned above, and determine what are the relevant interaction terms at the given order in velocity.

For leading order applications, it might still be useful in practice to first extract Feynman rules in a ∂/μ expansion and perform v counting only afterwards. In appendix A.4.2 we provide a list of Feynman rules to leading order in ∂/μ.

Let us start discussing the $\pi(\boldsymbol{p}_a) + \pi(\boldsymbol{p}_b) \to \pi(\boldsymbol{p}_c) + \pi(\boldsymbol{p}_d)$ scattering at tree-level. In the NREFT only contact interactions and π_3 exchange diagrams contribute to this process, as in figure 2.1. By momentum conservation, the exchanged π_3 is an off-shell potential field. Given that, the leading $\mathcal{O}(v^2)$ amplitude is fully determined by the vertices of the leading Lagrangian (2.32) in the derivative expansion:

$$\begin{aligned} \mathcal{L}_{\text{eff}} \supset & -\frac{i c_s}{2\mu^2\sqrt{c^{(1)}}}\left(\pi^{\mathrm{p}\,*}\boldsymbol{\nabla}\pi^{\mathrm{p}} - \pi^{\mathrm{p}}\boldsymbol{\nabla}\pi^{\mathrm{p}\,*}\right)\cdot\boldsymbol{\nabla}\pi_3^{\mathrm{p}} \\ & + \frac{(2c_m-3)}{24c^{(1)}\mu^4}\left(\pi^{\mathrm{p}\,*}\boldsymbol{\nabla}\pi^{\mathrm{p}} - \pi^{\mathrm{p}}\boldsymbol{\nabla}\pi^{\mathrm{p}\,*}\right)^2 - \frac{|\pi^{\mathrm{p}}|^2}{12c^{(1)}\mu^3}\left(\pi^{\mathrm{p}\,*}\dot{\pi}^{\mathrm{p}} - \pi^{\mathrm{p}}\dot{\pi}^{\mathrm{p}\,*}\right)\,, \end{aligned} \tag{2.41}$$

where we canonically normalized fields as $\pi_3 \to \frac{c_s}{\mu\sqrt{c^{(1)}}}\pi_3$ and $\pi \to \sqrt{\frac{2}{c^{(1)}\mu^3}}\pi$. To order

---

[10] Note that for off-shell Goldstones there is a fourth possibility, namely $(\omega, \boldsymbol{k}) \sim (\mu v, \mu v^2)$; this never appears in scattering processes [84], but might be relevant in other contexts. For example, when an external probe coupled to the system releases finite energy but almost vanishing spatial momentum [85].

$\mathcal{O}(v^2)$ the corresponding matrix element reads

$$\mathcal{M}_{\rm NR}^{(1)} = \frac{1}{4c^{(1)}\mu^4}\left[\frac{(\boldsymbol{p}_a^2-\boldsymbol{p}_c^2)^2}{(\boldsymbol{p}_a-\boldsymbol{p}_c)^2}+\frac{(\boldsymbol{p}_a^2-\boldsymbol{p}_d^2)^2}{(\boldsymbol{p}_a-\boldsymbol{p}_d)^2}+(2c_m-3)\,(\boldsymbol{p}_a+\boldsymbol{p}_b)^2\right.$$
$$\left.+\,2(1-c_m)\left(\boldsymbol{p}_a^2+\boldsymbol{p}_b^2\right)\right]. \tag{2.42}$$

Once the coefficient c_m is fixed by the dispersion relation (2.37), this only depends on the overall coefficient $c^{(1)}$. Below we will match its value to the linear triplet model. Eq. (2.42) correctly vanishes in the limit where any of the gapped Goldstones is at rest, again in agreement with [67]. One can similarly compute the $\mathcal{O}(v^4)$ correction. To this end one has to consider the action up to the fourth order in covariant derivatives, which is presented in appendix A.4.1. The resulting correction to the amplitude reads:

$$\begin{aligned}\mathcal{M}_{\rm NR}^{(2)} = \frac{1}{\mu^6[c^{(1)}]^2}\Bigg\{&\left(b_1-\frac{c^{(1)}c_m^2}{16c_s^2}\right)(\boldsymbol{p}_a^2+\boldsymbol{p}_b^2)^2+\frac{c^{(1)}}{8}\left(\frac{c_m^2}{c_s^2}-c_m^{(2)}\right)\left(\boldsymbol{p}_a^2\boldsymbol{p}_b^2+\boldsymbol{p}_c^2\boldsymbol{p}_d^2\right)\\
&+b_2(\boldsymbol{p}_a^2+\boldsymbol{p}_b^2)\boldsymbol{p}_a\cdot\boldsymbol{p}_b+b_3(\boldsymbol{p}_a\cdot\boldsymbol{p}_b)^2+b_4\left[(\boldsymbol{p}_a\cdot\boldsymbol{p}_c)(\boldsymbol{p}_b\cdot\boldsymbol{p}_d)+(\boldsymbol{p}_a\cdot\boldsymbol{p}_d)(\boldsymbol{p}_b\cdot\boldsymbol{p}_c)\right]\\
&+\frac{(\boldsymbol{p}_a^2-\boldsymbol{p}_c^2)^2}{(\boldsymbol{p}_a-\boldsymbol{p}_c)^2}\left[\frac{c^{(1)}c_m^2}{16c_s^2}\frac{(\boldsymbol{p}_a^2-\boldsymbol{p}_c^2)^2}{(\boldsymbol{p}_a-\boldsymbol{p}_c)^2}-b_1(\boldsymbol{p}_a^2+\boldsymbol{p}_b^2)+\frac{c^{(1)}c_m^{(2)}}{8c_m}\frac{\boldsymbol{p}_a^2\boldsymbol{p}_b^2-\boldsymbol{p}_c^2\boldsymbol{p}_d^2}{(\boldsymbol{p}_a^2-\boldsymbol{p}_c^2)}\right]\\
&+\frac{(\boldsymbol{p}_a^2-\boldsymbol{p}_d^2)^2}{(\boldsymbol{p}_a-\boldsymbol{p}_d)^2}\left[\frac{c^{(1)}c_m^2}{16c_s^2}\frac{(\boldsymbol{p}_a^2-\boldsymbol{p}_d^2)^2}{(\boldsymbol{p}_a-\boldsymbol{p}_d)^2}-b_1(\boldsymbol{p}_a^2+\boldsymbol{p}_b^2)+\frac{c^{(1)}c_m^{(2)}}{8c_m}\frac{\boldsymbol{p}_a^2\boldsymbol{p}_b^2-\boldsymbol{p}_c^2\boldsymbol{p}_d^2}{(\boldsymbol{p}_a^2-\boldsymbol{p}_d^2)}\right]\Bigg\}.\end{aligned} \tag{2.43}$$

Here c_s^2 is defined in (2.34) and $c_m^{(2)}$ is defined by the gapped Goldstone dispersion relation at subleading order (2.37)

$$\epsilon_p = c_m\frac{\boldsymbol{p}^2}{2\mu}-c_m^{(2)}\frac{\boldsymbol{p}^4}{8\mu^3}+\mathcal{O}\left(\boldsymbol{p}^6/\mu^5\right)\,. \tag{2.44}$$

We also introduced four independent coefficients, b_1, b_2, b_3 and b_4, given in terms of the Lagrangian parameters in appendix A.4.3. One can show that loop corrections do not contribute to the matrix element at this order—see appendix A.4.4.

A non-trivial check of our NREFT construction is obtained by comparing the above results to those obtained in section 2.1 for the benchmark model. Eqs. (1.29), (2.2) and (2.3) should match respectively Eqs. (2.44), (2.42) and (2.43). The matching beautifully

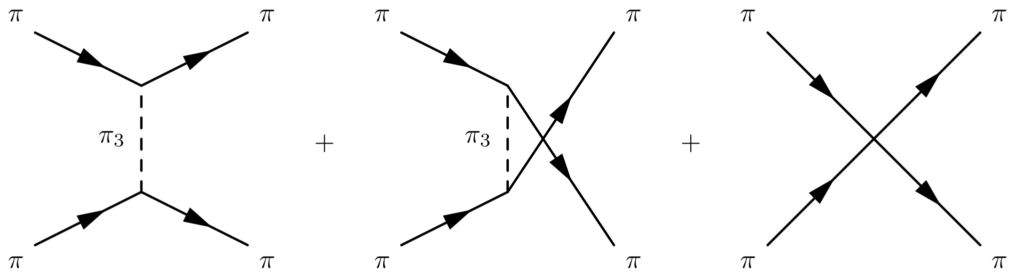

Figure 2.1 – Diagrams contributing to $\pi\pi \to \pi\pi$ at tree-level.

works, fixing[11]

$$\frac{1}{c^{(1)}} = \frac{\lambda\mu^2}{\mu^2 - m^2}\,, \qquad c_m = c_m^{(2)} = 1\,, \qquad c_s^2 = \frac{\mu^2 - m^2}{3\mu^2 - m^2}\,, \tag{2.45}$$
$$\frac{b_1}{c^{(1)}} = \frac{1}{4}\,, \quad \frac{b_2}{c^{(1)}} = \frac{m^2+\mu^2}{4(m^2-\mu^2)}\,, \quad \frac{\mathrm{Re}[b_3]}{c^{(1)}} = \frac{7\mu^2+m^2}{4(\mu^2-m^2)}\,, \quad \frac{\mathrm{Re}[b_4]}{c^{(1)}} = \frac{\mu^2}{2(\mu^2-m^2)}\,.$$

Notice in particular that the dispersion relation fixes $c_m = 1$ at lowest order, which immediately gives eq. (2.42) the same momentum dependence as (2.2).

This is however not the end of the story. As already discussed, our benchmark model allows for the process in which two gapped Goldstones annihilate into two gapless ones. Although this process is outside the regime of applicability of the NREFT, it will give rise to an imaginary part in the scattering amplitude via the Cutkosky rules.[12] That can be matched by assigning an imaginary part to the Wilson coefficients, as we now show in detail. Notice first that unitarity of the theory at $\pi = 0$ implies that the coefficient $c^{(1)}$ and the sound speed c_s^2 of the gapless Goldstone are real—see eq. (2.33). Furthermore, the accidental $\mathbb{Z}_2$ symmetry, which forbids gapped Goldstone decay in the linear triplet model, implies that the coefficients of the dispersion relation (2.44) and, more in general, of all the operators contributing to amplitudes with only one (slow) gapped Goldstone and an arbitrary number of (soft) gapless modes in the initial and final states must be real.[13] From inspection of Eqs. (A.42), (A.53) and (A.54), this implies that c_m, $c_m^{(2)}$, b_1 and b_2 are real as well. Overall, we find that the scattering amplitude must be real at leading order in velocity, while at the subleading order we can use only the imaginary parts of the coefficients b_3 and b_4 to match the annihilation contribution. To check that

---

[11] In the matching one must consider that in the triplet model we used the relativistic normalization of states, while in the NREFT (see (2.36)) we used the nonrelativistic one which differs by a velocity dependent factor: $|\boldsymbol{p},\mu\rangle_{\text{triplet}} = \sqrt{2E_p}\,|\boldsymbol{p},\mu\rangle_{\text{NREFT}}$.

[12] The imaginary part induced by elastic scattering itself can be computed within the NREFT and it is of higher order in the velocity.

[13] This is because, in the linear triplet, the only possible intermediate states contributing to all possible cuts of such amplitudes are those included in the NREFT.

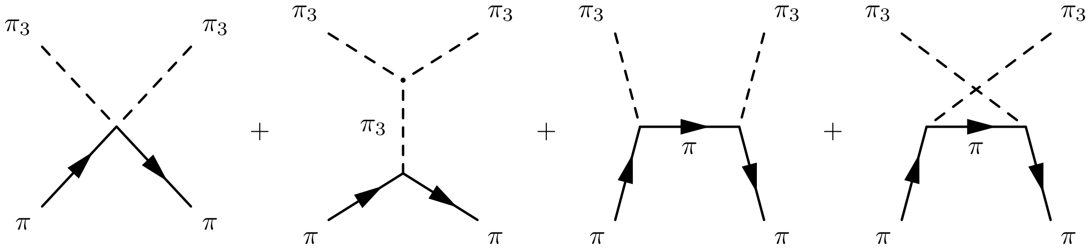

Figure 2.2 – Diagrams contributing to $\pi_3\pi \to \pi_3\pi$ at tree-level.

is enough, notice that from the annihilation cross section (2.5) of the UV theory one finds

$$\mathrm{Im}\left[\mathcal{M}_{\text{elastic}}\right] \simeq \gamma \frac{(\boldsymbol{p}_a \cdot \boldsymbol{p}_b)^2}{\mu^4} + \delta \frac{(\boldsymbol{p}_a \cdot \boldsymbol{p}_c)(\boldsymbol{p}_b \cdot \boldsymbol{p}_d) + (\boldsymbol{p}_a \cdot \boldsymbol{p}_d)(\boldsymbol{p}_b \cdot \boldsymbol{p}_c)}{\mu^4} \,. \tag{2.46}$$

Non-trivially, this contribution is local and it precisely has the structure to be matched in the NREFT via an imaginary part for b_3 and b_4:

$$\frac{\mathrm{Im}[b_3]}{[c^{(1)}]^2} = \frac{\gamma}{4}\,, \qquad \frac{\mathrm{Im}[b_4]}{[c^{(1)}]^2} = \frac{\delta}{4}\,. \tag{2.47}$$

As one last example, to further clarify the procedure of power counting in velocity, consider the scattering $\pi(\boldsymbol{p}_a) + \pi_3(\boldsymbol{k}_1) \to \pi(\boldsymbol{p}_b) + \pi_3(\boldsymbol{k}_2)$. The relevant diagrams are presented in figure 2.2. As before, we take all external 3-momenta of order $\mathcal{O}(\mu v)$. One can see that momentum conservation requires the intermediate π_3 of the second diagram to be a potential mode, and the intermediate π of the last two to be soft. One then needs to isolate the relevant interaction terms in the effective Lagrangian, after which it is straightforward to extract the Feynman rules and compute the matrix elements.

One finds that the leading order result is $\mathcal{O}(v^3)$ and receives contribution from all diagrams in figure 2.2 but the second, which starts contributing at $\mathcal{O}(v^4)$. The matrix element reads[14]

$$\begin{aligned}\mathcal{M} = \frac{1}{2\mu^4 c^{(1)}} \frac{1}{c_s|\boldsymbol{k}_1|} \Big\{ &(c_s^2 - 1)c_s^2 \boldsymbol{k}_1^2 (\boldsymbol{k}_1 + \boldsymbol{k}_2) \cdot (\boldsymbol{p}_a + \boldsymbol{p}_b) \\ &+ 2c_s^2 \left[(\boldsymbol{p}_a \cdot \boldsymbol{k}_2)(\boldsymbol{p}_b \cdot \boldsymbol{k}_1) - (\boldsymbol{p}_a \cdot \boldsymbol{k}_1)(\boldsymbol{p}_b \cdot \boldsymbol{k}_2)\right] \Big\} + \mathcal{O}\left(v^4\right).\end{aligned} \tag{2.48}$$

This expression vanishes when any of the momenta approaches zero.

A final comment concerns the calculation and power counting of loop diagrams. As well-known from NRQCD, the formulation of the NREFT at the quantum level is more subtle than in the standard relativistic case, even when using a mass independent regulator, like dimensional regularization. A consistent treatment, first given in [86, 87] and refined in [88], relies crucially on the splitting into soft, potential and ultrasoft modes performed in (2.40). The prescription explained there applies straightforwardly to our case. We review some details and provide few examples in appendix A.4.4.

---

[14] Notice that to leading order in v energy conservation implies $|\boldsymbol{k}_1| = |\boldsymbol{k}_2|$.

2.3 Integrating out the gapped Goldstone: a less effective field theory

As we already discussed in the Introduction, in quantum field theory with unbroken Poincaré symmetry, the presence of Goldstone modes in the IR has very nontrivial consequences. In particular, Goldstones associated to a coset G/H signals the existence of a symmetry group $G \times G'$ in the UV. G is spontaneously broken, and G' is any other distinct group which either is trivial or such that all the states charged under it are heavy and absent in the G/H effective theory. This is for instance the case in QCD, where $G = SU(N_f)_L \times SU(N_f)_R$, with N_f the number of light quarks, is broken down to the isospin group $H = SU(N_f)_V$, and the corresponding Goldstones are the light mesons. In this case G' is the baryon number, $U(1)_B$, which is unbroken and whose lightest charged state is the proton.

One might then wonder what happens to our finite density system when the involved energies, as measured by the unbroken Hamiltonian $\bar{H} = H + \mu Q_3$, are much smaller than the chemical potential μ. One could be tempted to treat the gapped Goldstones just like protons in QCD. However, while, on the one hand, they can be integrated out in the EFT at energies $E \ll \mu$, on the other they are needed to non-linearly realize the full non-Abelian symmetry. Is there any hint left of the original symmetry once we have integrated them out? In other words, is the information about the non-Abelian nature of the group lost at low energies, similarly like for $U(1)_B$ in QCD?

It is easy to show that in the zero-π sector ($\pi = 0$ in the action), the invariants built out of the coset construction reduce to those of a simple Abelian $U(1)$ group, i.e. $D_\mu \pi = 0$ and $D_\mu \chi = \partial_\mu \chi$. It cannot be otherwise, since the internal $SU(2)$ algebra cannot be nontrivially realized on a single field. Physically, when we integrate out the gapped Goldstone we specify boundary conditions for it to vanish at infinity. In our case that clearly breaks the non-Abelian symmetry since, as argued in section 1.2.2, symmetry transformations produce a fast oscillating mode that does not decay at infinity.

That is also evident in the linear triplet model (1.27). At low energies one can, in fact, integrate out explicitly the heavy fields $h(x)$ and $\theta(x)$. At tree level the resulting effective Lagrangian is

$$\mathcal{L}_{\text{eff}} = \frac{1}{2}\left(1 + \frac{2\mu^2}{\lambda\phi_0^2}\right)\dot{\psi}^2 - \frac{1}{2}(\boldsymbol{\nabla}\psi)^2 + \frac{\mu}{\lambda\phi_0^3}\,\dot{\psi}(\partial\psi)^2 + \mathcal{O}\left(\partial^4/\mu^4\right) , \qquad (2.49)$$

which is a Lagrangian for the Goldstone boson of an ordinary (Abelian) relativistic superfluid, but no other symmetry is manifest.[15]

To clarify this situation, it is helpful to think in terms of the Hilbert space of the low-energy EFT for the gapless Goldstone only. The latter is obtained by restricting the Hilbert space $\mathcal{H}$ of the full theory to the subspace $\mathcal{H}_{\text{EFT}}$ specified by the condition:

$$|\psi\rangle \in \mathcal{H}_{\text{EFT}} \qquad \Longleftrightarrow \qquad \langle\psi|\bar{H}|\psi\rangle = \langle\psi|H+\mu Q_3|\psi\rangle \ll \mu \,. \tag{2.50}$$

Despite the theory being $SU(2)$ invariant, the presence of Q_3 in the modified Hamiltonian that we use to specify the configurations that are part of the EFT explicitly breaks the symmetry. As a concrete illustration, consider a free quantum mechanical particle living on a sphere, with Lagrangian $L = \frac{I}{2}\left(\dot{\theta}^2 + \sin^2\theta\,\dot{\phi}^2\right)$, where I is the moment of inertia. The states of the theory are organized in $SO(3)$ multiplets, $|\ell, m\rangle$, with energy $E_\ell = \ell(\ell+1)/2I$. The quantum number ℓ specifies the representation and m is the value of the angular momentum along the z-axis: $-\ell \leq m \leq \ell$. If we take m to be fixed, negative and large, the state with minimum energy is $|\ell, m=-\ell\rangle$ and the chemical potential is $\mu = \partial E_{\ell=-m}/\partial m \approx m/I$ [35]; any other state in the same $SO(3)$ multiplet has a gap of at least $|\mu| \approx |m|/I$ as measured by $\bar{H}$. Thus, for every fixed value of the third component of the angular momentum, the low-energy EFT is made of the single state $|\ell, m=-\ell\rangle$, which is not invariant under the full rotation group. At the Lagrangian level, the restriction to such states corresponds to “integrating out" the polar angle, θ, considering an effective theory for the azimuthal angle, ϕ, spinning around the z-axis. Indeed, a single excitation of θ describes a state with total angular momentum increased by a unity, $\ell+1$, but with the same projection along the z-axis, $m=-\ell$. This corresponds to a state with gap $|\mu|$ at large angular momentum [35]. This is analogous to the gapped Goldstone, providing a simple illustration of its key role in the nonlinear realization of the full symmetry group.[16]

The condition in eq. (2.50) implies that the theory without the gapped Goldstone can only be used to compute correlators whose long-distance behaviour is determined by intermediate states with small energy under $\bar{H}$. However, since time evolution is still controlled by the Hamiltonian H, not all correlation functions having a non-trivial long-distance limit satisfy this property. In other words, the operators corresponding to such correlation function cannot be matched in the low-energy EFT for the gapless Goldstone only, and they would simply be lost. In contrast, if one employs the NREFT we described so far, the previous correlators can be consistently reproduced within its regime of applicability. As an illustration, consider the time component of the Noether currents for the Q_+ and Q_- generators of $SU(2)$. It is clear that, in an EFT that only contains the gapless Goldstones, such operators cannot be matched. Indeed, in such a theory, only the Abelian subgroup of $SU(2)$ is realized nontrivially, and the Noether currents associated to $Q_\pm$ cannot be computed. On the other hand, working in the NREFT, in which the full non-Abelian symmetry group is realized, it is straightforward to compute them from Noether theorem and, at leading order in fields and derivatives, we find

---

[15] In fact, due to the $\mathbb{Z}_2$ symmetry, integrating out θ at tree level accounts to setting it to zero in the Lagrangian (1.27), which turns it into an $O(2)$ doublet theory.

[16] In field theory (at infinite volume) the action of the spontaneously broken charges on the Hilbert space of the theory is not well-defined and we cannot classify state according to representation of the broken group; this however does not invalidate our main point, that the restriction (2.50) *explicitly* breaks the symmetry.

$$J^0_+(t,\boldsymbol{x}) \simeq -ic^{(1)}\mu^3\pi(t,\boldsymbol{x})\,, \qquad J^0_-(t,\boldsymbol{x}) \simeq ic^{(1)}\mu^3\pi^*(t,\boldsymbol{x})\,. \tag{2.51}$$

As it could have been expected from the conservation of the global charges, these are written purely in terms of the *slow* field π of the Right parametrization (2.9). We can now compute their correlators at large time separation and spatial distance. For instance, the spatial Fourier transform of the two-point function of these currents can be computed from the gapped Goldstone propagator and reads

$$\int d^3x\, e^{-i\boldsymbol{p}\cdot\boldsymbol{x}}\, \langle\mu| T\left\{J^0_+(t,\boldsymbol{x})J^0_-(0,\boldsymbol{0})\right\}|\mu\rangle = 2c^{(1)}\mu^3\theta(t)e^{-i\epsilon_p t}\,, \tag{2.52}$$

where T is the time-ordered product and ϵ_p is the (possibly complex) kinetic energy of the gapped Goldstone, given by eq. (2.37) at leading order in 3-momentum. For long wavelengths, $|\boldsymbol{p}| \ll \mu$, the correlator (2.52) oscillates slowly in time—i.e. it has nontrivial long time tails. Nonetheless, it cannot be computed from the low-energy EFT without the gapped Goldstone, as already anticipated.[17] This is clear when the gapped Goldstone is stable and ϵ_p is real, in which case the result in eq. (2.52) is interpreted as the free evolution in time of a single π mode. Such a simple interpretation does not exist in more general cases, but this does not affect the main picture presented above. [18]

In summary, in the low-energy EFT specified by eq. (2.50) no signature of the non-Abelian nature of the symmetry is present. To obtain a fully $SU(2)$ covariant description one should work within the NREFT presented in this work, which reduces to the Abelian superfluid in the zero gapped Goldstone sector. In particular, our construction shows that the non-Abelian structure of the group constrains the dynamics at small *spatial* momenta, similarly to the relativistic case, but around non-zero frequencies which are multiples of the chemical potential. The NREFT further provides access to certain non-trivial correlation functions at large spacetime separations, which cannot be matched without the gapped Goldstone due to the difference between the fundamental Hamiltonian H and $\bar{H}$. We illustrated that point by discussing the two-point function of the $SU(2)$ Noether current; we leave a systematic analysis of operator matching in the NREFT for future work. These considerations, we believe, clarify previous works [35,78,89,90], which, at large chemical potential, restricted their attention to the Abelian component of the spontaneously broken internal symmetry. We conclude this section marking the differences between the present case and the relativistic case, i.e. a broken internal symmetry with unbroken Poincarè invariance.

---

[17] That this result cannot be obtained by somehow matching the currents in the low-energy theory is also manifest from the fact that the correlator oscillates with frequency $\epsilon_p \sim \boldsymbol{p}^2/\mu$, while no state with such dispersion relation is present in the EFT for the gapless Goldstone only.

[18] Equivalently, one could look at the operator $\bar{J}^0_\pm(t,\boldsymbol{x}) \equiv e^{i\bar{H}t}J^0_\pm(0,\boldsymbol{x})e^{-i\bar{H}t}$, which instead evolves with $\bar{H}$. It is simple to show that the two-point correlator for this (non-conserved) current oscillates with frequency μ. Consequently, it can never be obtained from the EFT for the gapless Goldstones only, which has support only on frequencies $\ll \mu$, as measured by $\bar{H}$.

In the relativistic case symmetry constrains all the Goldstone bosons to have 4-momentum on the lightcone. Then, given a coset G/H, the gapless Goldstone bosons carry all the information about the symmetry breaking and, as made evident by the CCWZ construction, all degrees of freedom falling into gapped H-multiplets can be integrated out preserving the full G symmetry. As concerns instead the role of an additional unbroken G' factor in the fundamental symmetry, if all the states charged over G' are gapped, then the corresponding Noether currents do not have low frequency components. In view of that in no way the low energy modes can match them, and the information about G' is lost in the EFT. Similarly, gapped Goldstones cannot be integrated out while still preserving the full G symmetry. However, in this case, the currents that interpolate them do have low frequency components—see eq. (2.52)—and there must therefore exist a way to recover that information via an EFT construction, ours indeed.

Conclusions to Part I

The breaking of internal symmetries has qualitatively different implications on low-energy physics, depending on whether or not it is accompanied by the breaking of spacetime symmetries. One crucial difference arises for the spectrum of excitations. With unbroken Poincarè invariance, Goldstone theorem dictates the presence of one stable particle with light-like dispersion relation, $E(\boldsymbol{k}) = |\boldsymbol{k}|$, for each spontaneously broken symmetry generator. With the spontaneous breaking of the Poincarè group, Goldstone theorem leaves instead space for a greater variety of options, as concerns the counting of modes, their dispersion relations and their stability. A particularly interesting case is offered by non-Abelian superfluids, which are characterized by chemical potentials μ_I for the Cartan charges Q_I. In chapter 1 we reviewed the corresponding Goldstone theorem, which implies the presence of a set of modes, labeled by $a = 1, \ldots, N$, whose energy satisfies $E_a(\boldsymbol{k} = 0) = c_{aI}\mu_I$, with c_{aI} real coefficients that are fully dictated by group theory [38]. Generically one then has both gapless modes, $E_a(\boldsymbol{0}) = 0$ and gapped ones $E_a(\boldsymbol{0}) \neq 0$. Moreover one has variety in the functional dependence of $E_a(\boldsymbol{k})$ on $\boldsymbol{k}$, including the possibility for imaginary parts, associated, when allowed, with the decay of the modes at $\boldsymbol{k} \neq 0$.

Symmetry controls not only the spectrum, but also the interaction of the Goldstone bosons. In the Poincaré invariant case, this results in a low-energy EFT whose main features are *universal* and rather independent of the details of the microphysics. In finite density systems constraints on the structure of the interactions are expected, and, to some extent, have been studied. However, with gapped Goldstones, the EFT construction also raises issues of technical and conceptual nature. One concerns universality, and stems from the generic possibility of other, non-Goldstone degrees of freedom in the range of energies and momenta $\mathcal{O}(\mu)$. Those are, for instance, expected in systems like CFTs, where μ is the main dimensionful parameter. In that situation creation and destruction of gapped Goldstones, even slow moving ones, entails momenta $\sim \mu$ evading a universal EFT description. Another issue concerns the possibility of reconstructing the pattern of symmetry breaking by pure consideration of the dynamics at the lowest possible energies. That is possible in the relativistic case, but seems impossible at finite density, as the gapped Goldstones are integrated out at $E \ll \mu$.[19]

In chapter 2 we have clarified the above questions. We have shown that the EFT that universally implements the information on the symmetry breaking pattern has degrees of freedom given by the Goldstone modes, all of them, at low 3-momentum, $\boldsymbol{k}$. In particular the gapped Goldstones are limited to small velocity, which also manifestly controls the strength of their interactions, in agreement with [67]. Such EFT cannot produce amplitudes that violate gapped Goldstone number (GGN), as these necessarily involve external legs with large 3-momentum $\sim \mu$. Consequently GGN is an "emergent" symmetry of the EFT where time evolution proceeds without transitions between Hilbert spaces with different GGN. This bars the calculability of physical processes where the GGN is not conserved. The latter are nonetheless consistently described in an *inclusive* form through the optical theorem, by allowing for imaginary parts in the local coefficients of operators in the EFT. The price to pay is that the unitarity of the original theory is not manifest in the EFT. The fact that GGN non-conservation involves short modes however allows to describe it via local operators in the EFT. The resulting picture is fully analogous to that of non-relativistic EFTs (NREFTs), like for instance non-relativistic QCD [82,88] or the EFT for nucleon-nucleon scattering [91,92], which have indeed almost completely guided our construction. We have illustrated our ideas by focussing on an $SU(2)$ superfluid, where we also checked that the results of the EFT construction match those of an explicit renormalizable model. We expect our results to be easily generalizable to arbitrary symmetry breaking patterns, as well as to allow the inclusion of other possible relevant matter fields in the action via standard techniques [28].

With the above picture in place it is evident that the complete information about symmetry breaking in the microscopic theory is encoded in the full set of NREFTs Hilbert spaces with all possible GGN. The subspace with zero GGN, which purely involves the soft gapless modes, is only part of the picture and does not encode the complete information about symmetry breaking. In particular it does not contain information about the spectrum of gapped modes. This subspace also happens to correspond to the EFT describing the lowest lying modes of the unbroken time translation generator $\bar{H} = H + \mu_I Q_I$ of the superfluid. This Hamiltonian is only invariant under a subgroup of the original internal symmetry, which makes it clear why such lowest energy EFT cannot describe the full pattern of symmetry breaking. A more detailed discussion of this is given in section 2.3.

The analysis of this part of the thesis was mainly motivated by its applications in the study of operators with large quantum numbers in strongly coupled conformal field theories [34,35]. The relation of that problem with superfluids will be the main topic of part II of this thesis. In particular, the NREFT discussed in chapter 2, when specialized to the cylinder, will be used to make predictions for the large charge sector of CFTs invariant under non-Abelian symmetry groups in chapter 4. However, our ideas might prove useful in different contexts as well. Before closing, therefore, we would like to mention other possible applications of the gapped Goldstone NREFT.

---

[19] An interesting question regards whether gapped Goldstones can be excited by some light external probe charged under the internal symmetry. We leave this investigation for future work.

As remarked in the introduction, gapped Goldstones appear in different physical systems [40]. An interesting example is given by QCD at finite density, as it is for instance found in the interior of neutron stars [41–44]. Depending on the parameters, in particular baryon density, it is conceivable that the system relaxes to a superfluid phase for the non-Abelian isospin symmetry. One concrete possibility is represented by Kaon condensation [41]. The resulting scenario, given the approximate nature of the isospin symmetry, broken by the small quark masses, would be approximated by the physical situation described in this part of the thesis: there would be pseudo-Goldstone bosons, whose gap and interactions are controlled by symmetry breaking, spontaneous and explicit, very much like in the QCD chiral Lagrangian around the vacuum. In particular in the regime where the chemical potential is of the order of the strong interaction scale, our NREFT would capture, amid a hardly calculable strong dynamics, the universal features of the gapped pseudo-Goldstones dynamics.

The underlying Lorentz invariance of the theory, if conceptually useful in understanding the origin of the modified Hamiltonian $\bar{H}$, is not necessary for the existence of both gapless and gapped Goldstone bosons [40]. Indeed, our construction may be straightforwardly applied to systems where either only the Galilean limit of Lorentz transformations is considered, or boost invariance is not present from the beginning.[20] Possibly relevant examples of this kind include ferromagnets, anti-ferromagnets [61], electron gases [74] and vortex lattices [93, 94] where spin or angular momentum play the role of the non-Abelian charges, while the role of the chemical potential is played by either a uniform magnetic field [40] or by an externally induced angular velocity. In these examples the role of the gapped Goldstones is played respectively by the magnons for spin systems and by the Kohn mode for electron gases and vortex lattices. It would be interesting to investigate the possibility to apply our NREFT methodology to such systems, searching in particular for situations where the Goldstone gap is comparable to or larger than the energy of other potentially strongly coupled modes. Our methodology would allow to zoom on the universal properties of otherwise hardly tractable strongly coupled systems.

---

[20] Physically, this means that boost invariance is broken by some more microscopic dynamics, typically due to the presence of a lattice or some other fluid, whose associated hydrodynamics modes can be neglected in first approximation.

Part II

Superfluids and the large charge sector of strongly coupled CFTs

Many interesting physical theories do not possess a small coupling, allowing for a systematic perturbative expansion of observables. However, even in such cases, a weakly coupled description may *effectively* emerge in some sectors of the theory. This is for instance the case in QCD, which, at energies E much smaller than the hadron scale $\Lambda_{QCD} = 4\pi f_\pi \approx 1\,\text{GeV}$, can be studied via the chiral Lagrangian in terms of Goldstone degrees of freedom. The existence of a perturbative description is related to a large separation between the relevant mass scales, whose ratio E/Λ_{QCD} provides the small expansion parameter.

A particularly relevant class of strongly coupled theories is given by those invariant under an extended spacetime symmetry: conformal transformations. These are called conformal field theories (CFTs) and play a key role in particle and condensed matter physics. First, as fixed points of the renormalization group flow, they act as landmarks in the space of quantum field theories (QFTs). Furthermore, through the AdS/CFT correspondence, they promise to shed light on quantum gravity [95, 96]. Finally, they also describe critical points for second order phase transitions. Recently, the bootstrap program [25, 97], aiming at constraining (and possibly solving) strongly coupled CFTs by imposing self-consistency relations, achieved much progress in their study, mostly through numerical techniques [98].

Despite the absence of an intrinsic mass scale, a simplification similar to the one at hand in low energy QCD occurs in CFTs when studying operators with large quantum numbers under an internal symmetry group G. This was first pointed out in [34] and it is based on the following picture. As a consequence of the state/operator correspondence, a scalar operator with charge Q under a certain generator of the group G corresponds to a state with charge density $\rho \sim Q/R^{d-1}$ for the theory compactified on the cylinder $\mathbb{R} \times S^{d-1}$ with radius R. For $Q \gg 1$ the mass scale associated to the charge density $\rho^{\frac{1}{d-1}} \sim Q^{\frac{1}{d-1}}/R$ is parametrically larger than the compactification scale $1/R$. In between these scales, the CFT state and its excitations are expectedly associated with a certain *condensed matter* finite density phase, the simplest option being that of a generalized superfluid of the kind analyzed in part I of this thesis. Assuming the theory to be in a superfluid phase, we may associate the charged states with excitations of the corresponding hydrodynamic Goldstone modes, whose property are largely constrained by the symmetry independently of other details of the theory. Similarly to the chiral Lagrangian in QCD, accurate predictions are obtained by mean of an effective field theory (EFT) description, in which the derivative and the loop expansion are controlled by the ratio between the IR and the UV scale, $R^{-1}/\rho^{\frac{1}{d-1}} \sim 1/Q^{\frac{1}{d-1}}$. The non-universal features associated with any specific CFT are instead encoded in a finite number of Wilson coefficients at each order in the $1/Q$ expansion. This framework is sometimes referred to as the *large charge expansion* in CFTs.

In this part of the thesis, we will study the large charge expansion for CFTs in $d > 2$ dimensions. In what follows, we shall first elucidate our approach presenting in more detail the simple example discussed in the introduction to this thesis: the hydrogen atom at large angular momentum. We will then study the case of a $U(1)$-invariant CFT in chapter 3. We will finally discuss CFTs invariant under more general internal symmetry groups in chapter 4, relying on the construction presented in chapter 2 of this thesis. We review some basic properties of CFTs in appendix B.1, where we also specify our conventions for the normalization of operators.

Invitation: the hydrogen atom at large angular momentum

The following example was already presented in [99,100] and it is inspired by the analogous discussion of the rigid rotor in [35]. We consider a non-relativistic point particle of mass M in a Coulomb potential, whose Lagrangian in spherical coordinates reads

$$L = \frac{M}{2}\left(\dot{r}^2 + r^2\dot{\theta}^2 + r^2\sin^2\theta\,\dot{\phi}^2\right) + \frac{\alpha}{r}\,. \tag{II.1}$$

As well known, this system is invariant under an $SO(4)$ symmetry. The $SO(3)$ component corresponding to physical rotations is generated by the angular momentum $\boldsymbol{J} = \boldsymbol{r}\times\boldsymbol{p}$, where $\boldsymbol{p} = M\dot{\boldsymbol{r}}$ is the classical momentum. The remaining three generators are proportional to the Laplace-Runge-Lenz vector $\boldsymbol{A} = \frac{1}{2}\left(\boldsymbol{p}\times\boldsymbol{J} - \boldsymbol{J}\times\boldsymbol{p}\right) - \alpha\,\boldsymbol{r}/r$. The bound states of the system have energy $E_n = -\frac{M\alpha}{2n^2}$ and are labeled by three integer quantum numbers n, ℓ, and m. [1] We have $n \geq \ell + 1$, and ℓ and m specify, respectively, the angular momentum $\boldsymbol{J}^2 = \ell(\ell+1)$ and its projection $J_3 = m$ on the third axis. We will now discuss how we can obtain this result semiclassically for large angular momentum, by expanding the path integral around a configuration with fixed angular momentum J_3. Notice that for fixed $J_3 = m$, the minimum energy state is obtained for $n - 1 = \ell = m$, corresponding to the following value for the energy:

$$E_0(m) = -\frac{M\alpha}{2(m+1)^2} = -\frac{M\alpha}{2m^2}\left(1 - \frac{2}{m} + \frac{3}{m^2} + \dots\right)\,. \tag{II.2}$$

The basic idea of the calculation is to consider the matrix element of the Euclidean evolution operator e^{-TH} in between two states with angular momentum $J_3 = m$ and fixed arbitrary values for r and θ; taking then the $T \to \infty$ limit we project onto the lowest energy state $|\Psi_0, m\rangle$ with fixed angular momentum:

---

[1] For every fixed n, labeling states with ℓ and m corresponds to the decomposition of the $(\frac{n-1}{2}, \frac{n-1}{2})$ representation of $SO(4) \simeq SU(2)\times SU(2)$ in irrep.s of the diagonal $SU(2)$.

$$\langle r_f, \theta_f, m|e^{-TH}|r_i, \theta_i, m\rangle \overset{T\to\infty}{\longrightarrow} \langle r_f, \theta_f, m|\Psi_0, m\rangle \, \langle \Psi_0, m|r_i, \theta_i, m\rangle \, e^{-E_0(m)T} \, , \qquad \text{(II.3)}$$

where subleading corrections are exponentially suppressed in T. Using that ϕ and J_3 are conjugated variables, we write the matrix element in (II.3) as the following path-integral:

$$\langle r_f, \theta_f, m|e^{-TH}|r_i, \theta_i, m\rangle = \iint \frac{d\phi_i d\phi_f}{2\pi} e^{-im(\phi_f-\phi_i)} \int_{(r_i,\theta_i,\phi_i)}^{(r_f,\theta_f,\phi_f)} \mathcal{D}r\mathcal{D}\theta\mathcal{D}\phi \, e^{-\int_{-T/2}^{T/2} d\tau L_E} \, , \qquad \text{(II.4)}$$

where L_E is the Euclidean version of the Lagrangian:

$$L_E = \frac{M}{2}\left(\dot{r}^2 + r^2\dot{\theta}^2 + r^2 \sin^2\theta \, \dot{\phi}^2\right) - \frac{\alpha}{r} \, . \qquad \text{(II.5)}$$

The wave-functions $e^{im\phi_i}$ and $e^{-im\phi_f}$ ensure that the initial and final state have the right value for the angular momentum J_3. The crucial observation is that for $m \gg 1$ the path-integral (II.4) can be computed systematically in a saddle-point approximation. Including the variation of the boundary terms, the stationarity conditions deriving from eq. (II.4) read

$$\ddot{r} = r\dot{\theta}^2 + r\sin^2\theta\dot{\phi}^2 + \frac{\alpha}{Mr^2} \, , \qquad \ddot{\theta} = \sin\theta\cos\theta\dot{\phi}^2 \, , \qquad Mr^2\sin^2\theta\dot{\phi} = -im \, . \qquad \text{(II.6)}$$

Choosing for simplicity $r_i = r_f = \frac{m^2}{M\alpha}$ and $\theta_i = \theta_f = \pi/2$, we find the following solution

$$r = \frac{m^2}{M\alpha} \equiv r_0 \, , \qquad \theta = \frac{\pi}{2} \, , \qquad \phi = -i\frac{m}{Mr_0^2}\tau + \phi_0 \, , \qquad \text{(II.7)}$$

where ϕ_0 is an integration constant. Recalling the identification $\tau = it$ between Euclidean and Lorentzian time, we recognize eq. (II.7) a superfluid solution of the kind discussed in part I of this thesis. At a classical level, such solution breaks spontaneously time translations and the $SO(4)$ symmetry to the subgroup generated by $\bar{H} = H - \mu J_3$ and the third component of the Laplace-Runge-Lenz vector A_3, [2] where the chemical potential is given by $\mu(m) = m/Mr_0^2$; we shall see below that the spectrum of fluctuations matches the expectation for this symmetry breaking pattern. Computing the classical action on the solution (II.7), we recover the leading order value for the energy at large m:

$$\int_{-T/2}^{T/2} d\tau L_E + im(\phi_f - \phi_i) = \frac{M\alpha}{2m^2}T = E_0^{(0)}T \, . \qquad \text{(II.8)}$$

It is also possible to check that the contribution of the classical solution to the stationary action which grows with T is independent of the choice of the initial and final values of θ and r, in agreement with eq. (II.3).

---

[2] To see this, recall that the Laplace-Runge-Lenz vector A_j generates the transformation $\delta r_i = M\left(2\dot{r}_i r_j - r_i\dot{r}_j - \delta_{ij}\,\boldsymbol{r}\cdot\dot{\boldsymbol{r}}\right)$, under which the Lagrangian shifts by a total derivative.

Subleading corrections in $1/m$ correspond to higher orders in the loop expansion. Let us see this explicitly. We introduce (dimensionless) fluctuations over the classical solution:

$$\delta\rho = \frac{r - r_0}{r}\,, \qquad \delta\theta = \theta - \frac{\pi}{2}\,, \qquad \delta\phi = \phi + i\frac{m}{Mr_0^2}\tau - \phi_0\,. \tag{II.9}$$

We then rewrite the path-integral (II.4) as

$$\langle r_f, \theta_f, m | e^{-TH} | r_i, \theta_i, m\rangle = e^{-\frac{M\alpha}{2m^2}T}\int \mathcal{D}\delta\rho\mathcal{D}\delta\theta\mathcal{D}\delta\phi\, e^{-\int_{-T/2}^{T/2} d\tau\, L_E'}\,, \tag{II.10}$$

where

$$L_E' = \frac{Mr_0^2}{2}\left[\delta\dot{\rho}^2 + \frac{m^2}{M^2r_0^4}\delta\rho^2 + \delta\dot{\theta}^2 + \frac{m^2}{M^2r_0^4}\delta\theta^2 + \left(\delta\dot{\phi} - \frac{2im}{Mr_0^2}\delta\rho\right)^2\right] + \ldots\,. \tag{II.11}$$

Such Lagrangian describes a gapless excitation and two gapped excitations with proper frequency $\omega = \mu$, classically corresponding to a massless and two massive Goldstones. Upon rescaling time as $\tau = \tilde{\tau}\frac{Mr_0^2}{m}$, we can recast

$$\int d\tau L_E' = m\int d\tilde{\tau}\tilde{L}_E'\,, \tag{II.12}$$

where $\tilde{L}_E'$ is equal to L_E' with $m/Mr_0^2 = 1$ and thus it is written, to all nonlinear orders in the fields, purely in terms of order one numerical coefficients. Then, we manifestly see that $1/m$ plays the role of loop counting parameter in the path integral, showing that the expansion in eq. (II.2) coincides indeed with a loop expansion. To make this remark concrete, let us consider the lowest order correction to the energy $E_0(m)$. This arises from the one-loop fluctuation determinant and reads

$$E_0^{(1)} = \frac{1}{2}\int d\omega\left[2\log\left(\omega^2 + \frac{m^2}{M^2r_0^4}\right) + \log\omega^2\right] = \Lambda_{UV} + \frac{M\alpha}{m^3}\,, \tag{II.13}$$

where Λ_{UV} is a divergent constant contribution, generically allowed by the symmetries of the problem and whose precise value depends upon the regularization scheme. This result matches the expansion of the exact expression in eq. (II.2).

The semiclassical description is not limited to the ground state at fixed charge. At the lowest order, this can be seen considering excited states of the frequency $\mu(m)$ harmonic oscillators described by the Lagrangian (II.11). These correspond to states with $J_3 = m$ and energy given by

$$E_k(m) = E_0(m) + k\frac{M\alpha}{m^3} + \mathcal{O}\left(\frac{1}{m^4}\right) = -\frac{M\alpha}{2(m+k+1)^2}\left[1 + \mathcal{O}\left(\frac{1}{m^2}\right)\right]\,. \tag{II.14}$$

Each energy level is $k+1$-times degenerate and corresponds to states with $n-1 = m+k \geq \ell \geq m$.

A final comment concerns the zero-mode integration constant ϕ_0 in eq. (II.7). The latter does not contribute to the calculation of the energy E_0, as the action depends only on $\dot{\phi}$. However, the integration over ϕ_0 is relevant in the calculation of correlation functions involving ϕ. In particular, considering the operators $\psi_q(\tau) = e^{iq\phi(\tau)}$ with $J_3 = q$, we have

$$\langle r_f, \theta_f, m; T/2|\psi_{q_n}(\tau_n)\dots\psi_{q_1}(\tau_1)|r_i, \theta_i, m; -T/2\rangle \propto \int_0^{2\pi} \frac{d\phi_0}{2\pi} e^{i\sum_i q_i \phi_0} = \delta\Big(\sum_i q_i\Big)\,, \tag{II.15}$$

where obviously here $\delta(\dots)$ stands for a Kronecker delta. Eq. (II.15) is consistent with angular momentum conservation; in particular, no charged operator acquires a vacuum expectation value. Therefore, while the stationary profile (II.7) may be characterized as a classical superfluid configuration, integration over the zero-mode implies that no symmetry breaking truly occurs in the theory, as it is generically[3] expected in one-dimensional quantum-mechanical systems.

---

[3] See e.g. the appendix of [101] for an example of spontaneous symmetry breaking in a quantum-mechanical system.

3 The large charge expansion in $U(1)$-invariant CFTs

This chapter begins the exploration of the large charge expansion in CFTs. Following [35], in sec. 3.1 we will present the general strategy for studying CFTs at large internal charge using the path-integral formulation. We will then specialize to the case of a $U(1)$-invariant CFT. The results for the spectrum of the theory will be presented in sec. 3.2. We will address the study of n-point functions and OPE coefficients in sec. 3.3. In this chapter we will work in generic $d > 2$ spacetime dimensions, so that our discussion will apply to both the physically interesting case $d = 3$ and $d = 4$. Some results hold also in $d = 2$, but we will not discuss that case explicitly.

3.1 Path-integral at fixed charge

Here we generalize the strategy discussed in the invitation to the case of a d-dimensional CFT invariant under an internal symmetry group G. Let us call $\mathcal{O}_{\vec{Q}}(x)$ the operator of minimal scaling dimension for fixed values of the charges $\vec{Q} = (Q_1, \dots, Q_N)$ associated to the Cartan generators $\widehat{Q}_I$ of the group. Working in Euclidean space $\mathbb{R}^d$, we consider correlation functions of the form

$$\langle \mathcal{O}^\dagger_{\vec{Q}}(x_{out}) \mathcal{O}_m(x_m) \dots \mathcal{O}_1(x_1) \mathcal{O}_{\vec{Q}}(x_{in}) \rangle \,, \tag{3.1}$$

where $\mathcal{O}^\dagger_{\vec{Q}}(x)$ is the conjugate operator of $\mathcal{O}_{\vec{Q}}(x)$, carrying charge $-\vec{Q}$, and $\mathcal{O}_i$ are additional operators carrying finite quantum numbers, such as the energy momentum tensor or the Noether currents.

By the state-operator correspondence, in the limit $x_{in} \to 0$ and $x_{out} \to \infty$ the action of $\mathcal{O}_{\vec{Q}}$ and $\mathcal{O}^\dagger_{\vec{Q}}$ on the vacuum creates a primary state $|\vec{Q}\rangle$ for the theory on $\mathbb{R} \times S^{d-1}$, with sphere radius R. Then, exploiting the Weyl invariance of the theory, the vacuum-correlator in eq. (3.1) is equal, up to a trivial rescaling (see eq. (B.21)), to the following matrix element for the theory quantized on the cylinder:

$$\langle\vec{Q},\tau_{out}|\mathcal{O}_m(\tau_m,\hat{n}_m)\dots\mathcal{O}_1(\tau_1,\hat{n}_1)|\vec{Q},\tau_{in}\rangle\ , \tag{3.2}$$

where $\tau = R\log(|x|/R)$ denotes Euclidean time on the cylinder, $\hat{n}^\mu = x^\mu/|x|$ specify the coordinates on the sphere and the states are defined in Schrödinger picture:

$$|\vec{Q},\tau_{in}\rangle\equiv e^{H\tau_{in}}\,|\vec{Q}\rangle = e^{E_{\vec{Q}}\tau_{in}}\,|\vec{Q}\rangle\ ,\qquad \langle\vec{Q},\tau_{out}|\equiv\langle\vec{Q}|\,e^{-H\tau_{out}}=\langle\vec{Q}|\,e^{-E_{\vec{Q}}\tau_{out}}\,. \tag{3.3}$$

We recall that the energy of the state on the cylinder is related to the scaling dimension $\Delta_{\vec{Q}}$ of the corresponding operator as $E_{\vec{Q}} = \Delta_{\vec{Q}}/R$.

Eq. (3.2) is analogous to the setup that we studied for the hydrogen atom. We therefore expect that, for sufficiently large Q_I's, the path integral corresponding to the matrix element in eq. (3.2) will be dominated by a semiclassical trajectory specifying a definite symmetry breaking pattern. Operator insertions and states with higher energy will be characterized as excitations over the classical configuration associated with the ground state $|\vec{Q}\rangle$. The symmetries of the leading trajectory may be inferred considering the insertion of the operator $\mathcal{O}_{\vec{Q}}$ at, respectively, $x_{in}=0$ and $x_{out}=\infty$, which set the boundary conditions for the path-integral. These break, respectively, translations P_μ and special conformal transformation K_μ. The fate of the rotation group $SO(d)$ depends on whether the operator $\mathcal{O}_{\vec{Q}}$ carries spin. Here we assume the simplest and most plausible option in which $\mathcal{O}_{\vec{Q}}$ is a scalar, implying that $|\vec{Q}\rangle$ describes a state with homogeneous charge density. [1] It remains to specify what happens to the dilatation generator D, corresponding to the Hamiltonian on the cylinder, and the internal group G. Since the origin and the point at infinity are stable under dilatations, the generator D may or may not be broken. As we argued in chapter 1, the most natural option is provided by a superfluid phase, in which case both the dilatation generator and G are broken, leaving unbroken a linear combination of D and the Cartan generators:

$$\bar{D} = D + \mu_I\widehat{Q}_I\,. \tag{3.4}$$

This was indeed the case for the hydrogen atom (see the discussion below (II.7)). Overall, we expect that the symmetry breaking pattern characterizing the leading semiclassical trajectory generically reads, in obvious notation,

$$SO(d+1,1)\times G\longrightarrow SO(d)\times\bar{D}\times G'\,, \tag{3.5}$$

where $G'\subset G$ denotes the internal unbroken subgroup, which, as we will discuss in more detail in chapter 4, is expected to be trivial for generic choices of the charges Q_I. Therefore, the properties of the ground state and its fluctuations will be characterized by the Goldstone excitations corresponding to the pattern in eq. (3.5). When not implied differently by additional symmetries, such as supersymmetry [102], additional degrees of freedom are expected to be separated by a finite gap from the Goldstones and may be integrated out. We can therefore *effectively* compute the path-integral (3.2) using a low energy action for the Goldstones, whose most general form is largely constrained by the nonlinear realization of the symmetry.

---

[1] Interestingly, also in the case of charged operators carrying macroscopic spin, analyzed in part III of this thesis, the leading trajectory in the path-integral may be characterized by similar arguments, see appendix C.1.

Let us consider for illustration the path-integral corresponding to the free-evolution in Euclidean time of the ground state at fixed charges Q_I, corresponding to eq. (3.2) with no insertions. Calling $S[\chi,\pi]$ the most general action for the Goldstones compatible with the symmetry breaking pattern (3.5), and denoting χ^I the Goldstone fields associated to the Cartan charges, the matrix element takes the form

$$\begin{aligned}&\langle\vec{Q}|e^{-HT}|\vec{Q}\rangle=\\ &\int d^N\chi_i d^N\chi_f\int_{\chi_i,\pi_i}^{\chi_f,\pi_f}\mathcal{D}\chi\mathcal{D}\pi\exp\left\{-S[\chi,\pi]-\frac{i}{\Omega_{d-1}}\int_{-T/2}^{T/2}d\tau\int d\Omega_{d-1}\dot{\chi}^I Q_I\right\},\end{aligned}\tag{3.6}$$

where $\Omega_{d-1}=\frac{2\pi^{d/2}}{\Gamma(d/2)}$ is the volume of the $d-1$-dimensional sphere. As in the case of the hydrogen atom, the last term in the action is a boundary term which fixes the charge of the initial and final state, while the precise value of the boundary conditions for the additional Goldstones π_i is irrelevant in the $T\to\infty$ limit, similarly to r and θ in the hydrogen atom. For large Q_I, this integral can be computed by the saddle-point method.

Notice that the characterization of the leading trajectory in the path-integral in terms of the symmetry breaking pattern in eq. (3.5), does not imply that the state $|\vec{Q}\rangle$ truly breaks the symmetry; indeed, it does not, as it is an eigenstate of both the $\widehat{Q}^I$'s and the dilatation D. Nonetheless, the existence of such a semiclassical trajectory dominating the path-integral justifies the description of the system in terms of a low energy action for the Goldstone fields associated to the corresponding breaking pattern. As in the case of the hydrogen atom, integration over the corresponding zero modes ensures charge conservation in correlation functions. This situation is to be contrasted with symmetry breaking in infinite volume systems, in which case the zero-modes are not normalizable and the boundary conditions of the path-integral fix their value. We will provide further insights on this point in the next section, when discussing the canonical quantization of the $U(1)$ conformal superfluid.

A final comment concerns the possibility that the leading trajectory in the path-integral does not break the dilatation operator. As we mentioned at the beginning of chapter 1, this situation is expectedly associated to a Fermi liquid phase, which involves fermionic excitations and whose characterization in terms of Goldstone degrees of freedom is less clear than for a superfluid phase. While certainly a viable and interesting option, we will not consider this possibility in what follows.

3.2 The spectrum of $U(1)$-invariant CFTs at large global charge

We now specialize our analysis to the case of an internal symmetry group $G = U(1)$. Besides providing the simplest case in which our analysis applies, CFTs with $U(1)$ symmetry are of theoretical and phenomenological relevance. For instance, our analysis will expectedly apply to the critical $O(2)$ model in $d = 3$, which describes phase transitions in many physical systems, such as the Curie point in easy-plane ferromagnets and antiferromagnets, and the superfluid transition in liquid Helium [98, 103]. Another example of theories for which we expect our claims to hold is provided by bosonic gauge theories with Monopole operators [104], the $U(1)$ symmetry being generated by the associated topological charge.

3.2.1 The action and the semiclassical analysis

Under the assumption of a superfluid phase, the symmetry breaking pattern for the leading trajectory in the path integral reads

$$SO(d+1,1)\times U(1)\longrightarrow SO(d)\times\bar{D}\,,\qquad \bar{D}=D+\mu\widehat{Q}\,,\tag{3.7}$$

where $\widehat{Q}$ denotes the $U(1)$ generator. The most general action nonlinearly realizing the symmetry according to eq. (3.7) can be systematically constructed using the CCWZ approach [26, 27] for broken spacetime symmetries [64]. The latter in particular provides a systematic way to obtain all the terms up to given order in the derivative expansion. We detail this procedure in appendix B.2. Here we provide a more direct, but less systematic, construction.

First, we remark that we work under the assumption that the theory is invariant under Weyl rescaling of the metric $g_{\mu\nu}\to\Omega^2(x)g_{\mu\nu}$. Therefore, we will construct the Goldstone action demanding this property. In fact, this is necessary to map the theory to the cylinder and all unitary CFTs are believed to be Weyl invariant (up to the anomaly) [105]. Notice that this is not trivial since, while Weyl invariance implies conformal symmetry, the converse is not necessarily true without additional assumptions [106].

As for the case of broken boosts discussed in chapters 1 and 2, the pattern (3.7) may be realized without introducing Goldstones for the broken translations and special conformal transformation. It is enough to consider a single shift-invariant superfluid Goldstone $\chi(x) = -i\mu\tau + \pi(x)$, associated to the breaking of the $U(1)$ symmetry, where the chemical potential μ will be determined eventually by the charge Q. The leading order action may be easily obtained specializing the Abelian superfluid action in eq. (1.18) to $\mathbb{R}\times S^{d-1}$

and demanding Weyl invariance

$$S[\chi] = -c_1 \int d^dx\sqrt{g}(-\partial_\mu\chi\partial^\mu\chi)^d + \dots\,, \tag{3.8}$$

where $g_{\mu\nu}$ is the cylinder metric, c_1 is a Wilson coefficient and we work in Euclidean signature. We can also easily construct operators with more than one derivative acting on χ. To this aim, it is useful to notice that the following *modified metric* $\hat{g}_{\mu\nu} = g_{\mu\nu}(\partial\chi)^2$, where $(\partial\chi) = (-\partial_\mu\chi\, g^{\mu\nu}\partial_\nu\chi)^{1/2}$, is invariant under Weyl transformations. We can then build invariant operators considering diffeomorphism invariant contractions of $\partial_\mu\chi$, $\hat{g}_{\mu\nu}$ and the covariant derivative $\hat{\nabla}_\mu$ compatible with the modified metric. For instance, the leading order Lagrangian reads just $\sqrt{g}\mathcal{L} = -c_1\sqrt{\hat{g}}$ in this notation. Including terms with up to two *modified covariant derivatives* $\hat{\nabla}_\mu$ and calling $\hat{\mathcal{R}}^{\rho}{}_{\mu\sigma\nu}$ the Riemann tensor obtained from $\hat{g}_{\mu\nu}$, we find [2]

$$\begin{aligned}
S[\chi] =& -\int d^dx\sqrt{\hat{g}}\left\{c_1 - c_2\hat{\mathcal{R}} + c_3\hat{\mathcal{R}}^{\mu\nu}\partial_\mu\chi\partial_\nu\chi + \mathcal{O}\left(\hat{\nabla}^4\right)\right\} \\
=& - c_1 \int d^dx\sqrt{g}(\partial\chi)^d \\
&+ c_2 \int d^dx\sqrt{g}(\partial\chi)^d\left\{\frac{\mathcal{R}}{(\partial\chi)^2} + (d-1)(d-2)\frac{[\nabla_\mu(\partial\chi)]^2}{(\partial\chi)^4}\right\} \\
&- c_3 \int d^dx\sqrt{g}(\partial\chi)^d\left\{\mathcal{R}_{\mu\nu}\frac{\partial^\mu\chi\partial^\nu\chi}{(\partial\chi)^4} + (d-1)(d-2)\frac{[\partial^\mu\chi\nabla_\mu(\partial\chi)]^2}{(\partial\chi)^6}\right. \\
&\qquad\qquad \left. +(d-2)\nabla_\mu\left[\frac{\partial^\mu\chi\partial^\nu\chi}{(\partial\chi)^2}\right]\frac{\nabla_\nu(\partial\chi)}{(\partial\chi)^3}\right\} + \mathcal{O}\left((\partial\chi)^d\frac{\nabla^4}{(\partial\chi)^4}\right)\,,
\end{aligned} \tag{3.9}$$

where we expanded the action in terms of the standard covariant derivative ∇_μ and Riemann tensor $\mathcal{R}^{\rho}{}_{\mu\sigma\nu}$ deriving from cylinder metric $g_{\mu\nu}$, discarding total derivatives. To obtain the first line of eq. (3.9) we neglected terms which vanish on the equation of motion of the leading order action[3] (3.8) [28]. The c_i's are Wilson coefficients, whose value is determined by the specific underlying CFT. The derivative expansion in the action is controlled by these and the chemical potential $\mu = \langle(\partial\chi)\rangle$. In the simplest scenario, corresponding to an underlying strongly couple theory, the c_i's are given by inverse powers of 4π's according to generalized dimensional analysis [69, 70] and the system becomes strongly coupled at energies $E \sim \mu$. Weakly coupled theories correspond instead to non-generic sizes for the Wilson coefficients. For instance, the Wilson-Fisher fixed points in the ε-expansion have $c_i \sim 1/\lambda \gg 1$, where $\lambda \sim \varepsilon$ is the perturbatively small coupling of the theory. We will discuss these theories in more detail in part IV of this thesis

Using this action, we can extract the scaling dimension of the lightest operator with fixed

---

[2] The term proportional to c_3 here corrects the typos in eq.s (5.14) and (5.15) of [35].

[3] This is conveniently written as $\hat{\nabla}^\mu\partial_\mu\chi = 0$.

$Q \gg 1$ from the path-integral expression (3.6), which in this case reads:

$$\langle Q|e^{-HT}|Q\rangle = \int \mathcal{D}\chi \exp\left\{-\int_{-T/2}^{T/2} d\tau \int d^{d-1}x\sqrt{g}\left[\mathcal{L} + i\frac{Q}{R^{d-1}\Omega_{d-1}}\dot{\chi}\right]\right\} , \tag{3.10}$$

We can compute this path-integral semiclassically around the saddle-point solution

$$\chi = -i\mu\tau + \pi_0 \,. \tag{3.11}$$

Notice that on the solution the term proportional to c_3 in the action (3.9) vanishes, since $\mathcal{R}_{00} = 0$ on $\mathbb{R} \times S^{d-1}$. Recalling that rotations on $\mathbb{R} \times S^{d-1}$ play a role analogous to that of translations in flat space, one can check that the solution (3.11) realizes precisely the symmetry breaking pattern in eq. (3.7) in terms of a single field,[4] as anticipated. As in eq. (II.7), π_0 is an integration constant and the field is analytically continued away from the real axis. The variation of the field at the boundary fixes the chemical potential μ in terms of the charge Q as

$$\frac{Q}{R^{d-1}\Omega_{d-1}} = J_0 = i\frac{\partial\mathcal{L}}{\partial\dot{\chi}} = c_1 d\mu^{d-1} - c_2(d-2)\mu^{d-3}\mathcal{R} + \mathcal{O}\left(\mu^{d-5}\right) , \tag{3.12}$$

where we called J_μ the $U(1)$ Noether current. Using $\mathcal{R} = (d-1)(d-2)/R^2$, this equation can be solved perturbatively for large Q:

$$R\mu = \left(\frac{Q}{c_1 d\,\Omega_{d-1}}\right)^{\frac{1}{d-1}}\left[1 + \frac{c_2(d-2)^2}{c_1 d}\left(\frac{Q}{c_1 d\,\Omega_{d-1}}\right)^{-\frac{2}{d-1}} + \mathcal{O}\left(\left(\frac{Q}{c_1 d\,\Omega_{d-1}}\right)^{-\frac{4}{d-1}}\right)\right] . \tag{3.13}$$

For $Q \gg 1$ we thus have $\mu \propto Q^{\frac{1}{d-1}}$, with subleading corrections suppressed by powers of $Q^{-2/(d-1)}$.[5] Computing the action on this solution, we find the energy of the state as

$$\Delta_Q = \alpha_1 Q^{\frac{d}{d-1}} + \alpha_2 Q^{\frac{d-2}{d-1}} + \mathcal{O}\left(Q^{\frac{d-4}{d-1}}\right) , \tag{3.14}$$

where the α_i's are combination of the Wilson coefficients:

$$\alpha_1 = \frac{c_1(d-1)\Omega_{d-1}}{(c_1 d\,\Omega_{d-1})^{\frac{d}{d-1}}} , \qquad \alpha_2 = \frac{c_2(d-1)(d-2)\Omega_{d-1}}{(c_1 d\,\Omega_{d-1})^{\frac{d-2}{d-1}}} . \tag{3.15}$$

The scaling with Q of the leading term in eq. (3.14) could have been inferred on dimensional grounds [34]. Indeed, for a scale invariant theory in the semiclassical regime the charge density J_0 and the energy density ε are expected to obey a local relation of the form $\varepsilon \propto J_0^{\frac{d}{d-1}}$. Subleading terms are suppressed by the ratio of the cutoff and the compactification scale $(R^{-1}/\mu)^2 \sim Q^{-\frac{2}{d-1}}$; this structure follows from the existence of an

---

[4] This is most easily realized noticing that eq. (3.11) reads $\chi = -i\mu \log|x| + \text{const.}$ in flat space.

[5] Notice however that for $c_1 \ll 1$, as it is expected in weakly coupled theories, the chemical potential may be parametrically smaller than $Q^{\frac{1}{d-1}}$.

EFT description, in which curvature invariants appear analytically in the Lagrangian.

As in the case of the Hydrogen atom, we may further consider quantum corrections to eq. (3.14). To this aim, we define $\chi(x) = -i\mu\tau + \pi(x)$ and we expand the leading low energy action (3.8) to quadratic order in the fluctuations:

$$S^{(2)} \simeq \frac{d(d-1)}{2} c_1 \mu^{d-2} \int d^d x \sqrt{g} \left[\dot{\pi}^2 + \frac{1}{d-1} (\partial_i \pi)^2 + \mathcal{O}\left(\nabla^4/\mu^2\right) \right] \tag{3.16}$$

This action describes a phonon with speed of sound $c_s^2 = \frac{d\rho}{dP} = \frac{1}{d-1}$, as it is mandated by tracelesness of the energy momentum tensor (see the comments below eq. (1.19)). We will study in detail the spectrum of fluctuations in the next section. For the purposes of computing the energy of the lowest energy state, we just notice that the the one-loop contribution to the energy is given by the fluctuation determinant arising from the Gaussian integration of eq. (3.16):

$$\begin{aligned} \frac{T}{R} \delta\Delta_Q^{(1)} &= \frac{1}{2} \log\det \left[-\partial_\tau^2 - \frac{1}{d-1} \Delta^{(S^{(d-1)})} + \mathcal{O}\left(\nabla^4/\mu^2\right) \right] &(3.17)\\ &= \frac{T}{R} \left[\beta_0 + \beta_1 Q^{-\frac{2}{d-1}} + \mathcal{O}\left(Q^{-\frac{4}{d-1}} \right) \right] , &(3.18) \end{aligned}$$

where $|g^{ij}|\nabla_i\nabla_j = \Delta^{(S^{(d-1)})}$ is the Laplacian on the $d-1$-dimensional sphere. We wrote the result in a large Q expansion in terms of dimensionless coefficients β_i's, whose specific value depends on the number of dimensions d. Notice that β_0 cannot depend on the c_i's, because the sound-speed in eq. (3.16) is fixed by conformal invariance at leading order in Q. Summing the quantum corrections to the classical result (3.14) we find

$$\Delta_Q = Q^{\frac{d}{d-1}} \left[\alpha_1 + \alpha_2 Q^{-\frac{2}{d-1}} + \alpha_3 Q^{-\frac{4}{d-1}} + \ldots \right] + Q^0 \left[\beta_0 + \beta_1 Q^{-\frac{2}{d-1}} + \ldots \right] . \tag{3.19}$$

The contribution from the classical solution, associated to the coefficients α_i, does not contain any term scaling as Q^0 for non-even d. This implies that, in odd spacetime dimensions, the one-loop correction (3.17) cannot be renormalized by any local counterterm and it is hence finite and calculable. In particular, the Q^0 contribution takes the same *universal* value for all three-dimensional $U(1)$-invariant CFTs whose large charge sector is described by a superfluid phase. The explicit result in $d = 3$ reads

$$\beta_0 = -0.0937255\,, \qquad \beta_1 = (c_2 + c_3) \times 1.21666\,, \qquad \text{for } d = 3. \tag{3.20}$$

Details on the calculation are reported in appendix B.3.

Conversely, in $d = 4$ the β_0 term in eq. (3.19) can be renormalized by the classical contribution proportional to α_3, and it is hence divergent. In this case, while the Q^0 term is not universally predicted by the EFT, upon renormalization one finds a $\log Q$ term whose coefficient depends only on the divergent part of β_0 and is hence calculable. This is analogous to the logarithm of the sliding scale in standard perturbative calculations [107].

In appendix B.3, we show that the final result reads:

$$\begin{aligned}\Delta_Q\big|_{d=4} &= \alpha_1 Q^{\frac{4}{3}} + \alpha_2 Q^{\frac{2}{3}} - \frac{1}{48\sqrt{3}}\log Q + \alpha_3 \\ &+ \frac{7\pi^{4/3}(2c_2+c_3)}{144\sqrt{3}c_1^{1/3}} Q^{-\frac{2}{3}}\log Q + \alpha_4 Q^{-\frac{2}{3}} + \mathcal{O}\left(Q^{-\frac{4}{3}}\right).\end{aligned} \tag{3.21}$$

We neglected logarithms in the estimate of the corrections.

3.2.2 Canonical quanization and the spectrum of phonons

In the previous sections we have seen how to project onto the desired state using the Euclidean path-integral. As discussed in sec. 3.1, this viewpoint justifies the expectation of a semiclassical description in terms of Goldstone degrees of freedom. Nonetheless, in the following chapters we shall often find convenient an alternative, if almost equivalent, approach, in which we simply assume the EFT description and then quantize its Hamiltonian, while always remaining in Lorentzian spacetime. It is thus instructive to work out the quantization of the phonon field in this perspective. In the process, we will also comment on the structure of the low energy spectrum.

Consider for simplicity the leading order Lagrangian in eq. (3.8) in Lorentzian signature

$$\mathcal{L}/\sqrt{g} = c_1(\partial\chi)^d\,, \tag{3.22}$$

where in real time $t=-i\tau$ we have $(\partial\chi) = (\partial_\mu\chi\partial^\mu\chi)^{1/2}$. The canonical momentum coincides with the time component of the $U(1)$ current $P_\chi = J_0$. Upon expanding $\chi(x) = \mu t + \pi(x) \implies P_\chi \simeq c_1 d\mu^{d-1} + c_1 d(d-1)\mu^{d-2}\dot{\pi}$, to leading order in the field expansion we obtain the following decomposition for the field:

$$\begin{aligned}\pi(t,\hat{n}) =& \frac{1}{\sqrt{c_1 d(d-1)}\,\mu^{\frac{d-2}{2}}}\sum_{\ell=1}^{\infty}\sum_m \left[e^{-i\omega_\ell t}Y^\ell_m(\hat{n})\frac{a_{\ell m}}{\sqrt{2\omega_\ell R^{d-1}}} + h.c.\right] \\ &+ x_0 + \frac{p_0 t}{\Omega_{d-1}R^{d-1}c_1 d(d-1)\,\mu^{d-2}}\,,\end{aligned} \tag{3.23}$$

where $Y^\ell_m(\hat{n})$ are the hyperspherical harmonics [108], with m collectively denoting their labels. The mode operators satisfy the following algebra:

$$[a_{\ell m}, a^\dagger_{\ell' m'}] = \delta_{\ell\,\ell'}\delta_{m\,m'}\,, \qquad [x_0, p_0] = i\,. \tag{3.24}$$

The frequencies are given by

$$\begin{aligned}\omega_\ell = {} & \frac{1}{\sqrt{d-1}}J_\ell \\ & -\frac{(d-2)\left[c_2(d-2)+c_3\right]}{c_1 d\sqrt{d-1}}\frac{J_\ell}{\mu^2R^2}+\frac{(d-2)\left[c_2(d-2)+c_3\right]}{c_1 d(d-1)^{3/2}}\frac{J_\ell^3}{\mu^2} \\ & +\mathcal{O}\left(\frac{J_\ell^5}{\mu^4}\right),\end{aligned} \tag{3.25}$$

where $J_\ell^2=\ell(\ell+d-2)/R^2$ are the eigenvalues of the Laplacian on the sphere. As already remarked, to leading order the sound speed is fully fixed by conformal invariance, so that ω_ℓ is independent of the Wilson coefficients. Eq. (3.25) holds for angular momenta parametrically smaller than the EFT cutoff: $\ell \lesssim R\mu \sim Q^{\frac{1}{d-1}}$.

As usual in QFT the vacuum state satisfies $a_{\ell m}\left|Q\right\rangle=0$. The action of the zero-mode on the vacuum is specified by the requirement that the state $\left|Q\right\rangle$ be an eigenstate of the $U(1)$ charge generator $\widehat{Q}$:

$$\widehat{Q}\left|Q\right\rangle = R^{d-1}\int d\Omega_{d-1}P_\chi\left|Q\right\rangle = Q\left|Q\right\rangle \quad\Longrightarrow\quad p_0\left|Q\right\rangle = 0\,, \tag{3.26}$$

where we used that $\widehat{Q}\simeq Q+p_0$ from eq.s (3.13) and (3.23).

We may now use eq. (3.23) in the Hamiltonian. Restoring subleading terms in the derivative expansion, we find the following result to leading order in fluctuations

$$\begin{aligned} RH &= R^d\int d\Omega_{d-1}\left(P_\chi\dot{\chi}-\mathcal{L}\right) \\ &= \Delta_Q+\frac{\partial\Delta_Q}{\partial Q}p_0+\sum_{\ell,m}R\omega_\ell\, a^\dagger_{\ell m}a_{\ell m}+\dots\,, \end{aligned} \tag{3.27}$$

where Δ_Q is given by eq. (3.19). Eq. (3.27) makes clear the structure of the spectrum. The action of the zero-mode relates different charge sectors as $e^{iqx_0}\left|Q\right\rangle = \left|Q+q\right\rangle$; [6] the presence of p_0 in eq. (3.27) ensures that these states have the expected energy $\Delta_{Q+q}=\Delta_Q+q\partial\Delta_Q/\partial Q+\dots$. The Fock space of the $\ell\geq 1$ modes instead describes excited states with the same value of the $U(1)$ charge, corresponding to operators with scaling dimension given by

$$\Delta = \Delta_Q+\sum_\ell n_\ell R\omega_\ell\,. \tag{3.28}$$

The $\ell=1$ mode has $\omega_1=1/R$ exactly and creates descendant states, as it can be checked from an explicit computation of the Noether current associated with the generator of translations. The $\ell\geq 2$ states correspond to additional charge Q primary states of the theory; we shall refer to them as *phonon* primaries, in light of the superfluid picture.

---

[6] Notice that x_0 is a periodic variable, hence only the action of operators e^{iqx_0} with $q\in\mathbb{Z}$ is defined.

It is instructive to compare the quantization of the theory on the cylinder with the usual one at infinite volume. In that case, differently from eq. (3.23), the mode decomposition of the field does not contain the zero-modes x_0 and p_0, which are not normalizable. Similarly the broken charge $\widehat{Q}$ is not defined, since the integral of the current over volume is now divergent, and eq. (3.26) cannot be satisfied. We remark again that at finite volume, instead, the ground state is truly an eigenstate of the charge operator and no symmetry breaking occurs, even if the symmetry group is realized non-linearly in the effective Lagrangian (3.22). Correspondingly, no truly gapless state exists in theory. Nonetheless, the symmetry guarantees that the gap of the phonon states does not grow with the chemical potential; they are hence parametrically lighter than all the other states which have been integrated out from the EFT. For this reason, we shall still refer, somewhat improperly, to the mode interpolated by π as a Goldstone mode.

3.3 Correlation functions from EFT in $U(1)$-invariant CFTs

The CFT data defining a theory are not limited to the spectrum of scaling dimensions, which fully fixes only the two-point functions of local operators, but they also include the three-point couplings. It is then natural to ask what can be said about them using the EFT description. In this section we address this question, showing how the previous analysis may be applied in the evaluation of n-point functions on the cylinder. We shall focus on insertions of light operators in between two large charge operators $\mathcal{O}_Q$, corresponding to matrix elements of the form in eq. (3.2) on the cylinder [35].

3.3.1 Operator matching and three-point functions

Three-point function with an insertion of the Noether current

The simplest observable one can compute is given by the three-point function with an insertion of the Noether current J_μ. Though this is fully fixed by the Ward identities (see the discussion above eq. (B.13) in appendix B.1), it is instructive to see how we can evaluate it using the EFT. As already noticed, from the Lagrangian (3.9) we can express the current operator in terms of the Goldstone field as

$$\begin{aligned} J_\mu = i\frac{\partial\mathcal{L}}{\partial\partial^\mu\chi} &= i\, c_1 d\, \partial_\mu\chi(\partial\chi)^{d-2} + i\, c_2(d-2)\mathcal{R}\partial_\mu\chi(\partial\chi)^{d-4} + \dots \\ &= \frac{Q}{R^{d-1}\Omega_{d-1}}\delta^0_\mu + i\, c_1 d(d-1)\mu^{d-2}\dot{\pi}\,\delta^0_\mu + i\, c_1 d\mu^{d-2}\partial_i\pi\,\delta^i_\mu + \dots\,, \end{aligned} \tag{3.29}$$

where, working in Euclidean signature, we expanded the expression to linear order in fluctuations. Following [35], the correlator of interest corresponds to the expectation value of the current for the theory quantized on the cylinder:

$$\langle Q,\tau_{out}|J_\mu(\tau,\hat{n})|Q,\tau_{in}\rangle = e^{-\Delta_Q(\tau_{out}-\tau_{in})/R}\frac{Q}{R^{d-1}\Omega_{d-1}}\delta^0_\mu\,. \tag{3.30}$$

This result is exact, since the charge Q is not renormalized. We can also map it to the plane using eq. (B.21). Recalling $|Q\rangle = \mathcal{O}_Q(0)\,|0\rangle$ and that the current has scaling dimensions $\Delta_J = d-1$, we obtain

$$\langle\mathcal{O}_{-Q}(x_{out})J_\mu(x)\mathcal{O}_Q(x_{in})\rangle \underset{x_{out}\to\infty}{\overset{x_{in}\to 0}{=}} \frac{Q}{\Omega_{d-1}}\frac{x_\mu}{x^d x_{out}^{2\Delta_Q}}\,, \tag{3.31}$$

where we denoted with $\mathcal{O}_{-Q}(x_{out})$ the Hermitian conjugate of $\mathcal{O}_Q$ in the Minkowskian continuation, which differs by they usual CFT definition, reviewed in appendix B.1, by the absence of the Jacobian factors associated with the inversion. Eq. (3.31) agrees with eq. (B.13) of the appendix in the same limit.

Three-point function with a scalar insertion

A more interesting application concerns correlators with the insertion of light scalars with small $U(1)$ charge q. More precisely, suppose that in the CFT under consideration there exists a scalar primary operator with scaling dimension $\delta \ll \Delta_Q$ and charge $q \ll Q$. We can reconstruct this operator in the EFT by matching its quantum numbers in terms of the Goldstone field. Demanding $U(1)$ charge q and Weyl weight δ we immediately find $\mathcal{O}_q^{(\delta)}(x) \propto e^{iq\chi}(\partial\chi)^\delta$ at leading order. Higher orders in the derivative expansion are obtained multiplying this expression by Weyl invariant operators constructed with the procedure explained above eq. (3.9). Overall, we find

$$\mathcal{O}_q^{(\delta)} = C^{(1)}_{\delta,q}(\partial\chi)^\delta e^{iq\chi} - C^{(2)}_{\delta,q}(\partial\chi)^{\delta-2}\left[\mathcal{R}+\ldots\right]e^{iq\chi}+\ldots\,, \tag{3.32}$$

where the dots stand for both the terms which are needed to complete $\mathcal{R}/(\partial\chi)^2$ in a Weyl invariant tensor and for other terms which are second order in derivatives, but whose contribution vanishes on the background solution (3.11). As in the Lagrangian (3.9), $C^{(1)}_{\delta,q}$ and $C^{(2)}_{\delta,q}$ are Q-independent Wilson coefficients whose value is not predicted by the EFT.

We can use the expression (3.32) to compute the three-point function with a scalar insertion, $\langle\mathcal{O}_{-Q-q}(x_{out})\mathcal{O}_q^{(\delta)}(x_c)\mathcal{O}_Q(x_{in})\rangle$, which on the cylinder corresponds to

$$\langle Q+q,\tau_{out}|\mathcal{O}_q^{(\delta)}(\tau_c,\hat{n}_c)|Q,\tau_{in}\rangle = \frac{\lambda^{(\delta)}_{(Q+q),q,Q}}{R^\delta}e^{-\Delta_{Q+q}(\tau_{out}-\tau_c)/R-\Delta_Q(\tau_c-\tau_{in})/R}\,. \tag{3.33}$$

On the right hand side we wrote the general structure for the matrix element, which depends on a single dimensionless *OPE coefficient* $\lambda^{(\delta)}_{(Q+q),q,Q}$.

We now proceed to show how to recover the structure (3.33) and determine the corresponding OPE coefficient in the EFT. To this aim, consider the Euclidean path-integral corresponding to eq. (3.33):

$$\langle Q+q,\tau_{out}|\mathcal{O}_q^{(\delta)}(\tau_c,\hat{n}_c)|Q,\tau_{in}\rangle = \int \mathcal{D}\chi \left[C_{\delta,q}^{(1)}\left(\partial\chi\right)^{\delta}+\ldots\right]\exp\left\{-S_{mod}[\chi]\right\} , \tag{3.34}$$

where we included the $e^{iq\chi}$ contribution from the operator insertion in the definition of the following modified action

$$S_{mod}[\chi] = S[\chi] + i\frac{Q+q}{\Omega_{d-1}}\int d\Omega_{d-1}\chi_f - iq\chi(\tau_c,\hat{n}_c) - i\frac{Q}{\Omega_{d-1}}\int d\Omega_{d-1}\chi_i\,. \tag{3.35}$$

To compute the path-integral in a saddle-point approximation, we look for a solution of the equations of motion deriving from S_{mod}:

$$\nabla_\mu J^\mu(x) = q\frac{\delta(\tau-\tau_c)\delta^{d-1}(\hat{n}-\hat{n}_c)}{\sqrt{g}}\,, \tag{3.36}$$

where the current is given in eq. (3.29) and in the limit $\tau_{in/out}\to\mp\infty$ the boundary conditions read

$$J^\mu(x) \xrightarrow{\tau\to-\infty} \delta_0^\mu\frac{Q}{R^{d-1}\Omega_{d-1}}\,, \qquad J^\mu(x) \xrightarrow{\tau\to+\infty} \delta_0^\mu\frac{Q+q}{R^{d-1}\Omega_{d-1}}\,. \tag{3.37}$$

Physically, we can think of equation (3.36) as a non-linear version of the electrostatic Gauss-law (where the current is not an exact form), the scalar operator acting as a point-like source with charge q, slightly deforming the path-integral [99]. For sufficiently small q, we may solve this equation expanding the field around the solution in eq. (3.11). To leading order the solution is unmodified, $\chi=-i\mu\tau$, and we find

$$\langle Q+q,\tau_{out}|\mathcal{O}_q^{(\delta)}(\tau_c,\hat{n}_c)|Q,\tau_{in}\rangle = C_{\delta,q}^{(1)}\mu^\delta e^{-\Delta_Q(\tau_{out}-\tau_{in})-q\mu(\tau_{out}-\tau_c)}\,. \tag{3.38}$$

Eq. (3.38) can be seen to agree with the structure (3.33) using

$$R\mu = \frac{\partial\Delta_Q}{\partial Q} \approx \Delta_{Q+1}-\Delta_Q\,. \tag{3.39}$$

Furthermore, using (3.13) we find that the EFT structure predicts the following scaling law for the OPE coefficient:

$$\lambda_{(Q+q),q,Q}^{(\delta)} \propto Q^{\frac{\delta}{d-1}}\,. \tag{3.40}$$

We can also easily extend the analysis to the next order by expanding the solution in fluctuations $\pi(x)=\chi(x)+i\mu\tau-\pi_0$. We provide the details in appendix B.4.1. One finds that the first correction in the small field expansion is proportional to $q/Q^{\frac{d-2}{d-1}}$. Similarly to the discussion below eq. (3.19), this scale coincides with some integer power of the one controlling the derivative expansion, given by $Q^{-\frac{2}{d-1}}$, only in even dimensions. Therefore, as in sec. 3.2.1, it is convenient to discuss the cases $d = 3$ and $d = 4$ separately.

Consider first $d = 3$. In this case, the first subleading correction to eq. (3.40) cannot be renormalized by the operator-dependent coefficients of the matching (3.32). It is hence finite and calculable. Absorbing all the anyway unknown constants in a new Wilson parameter $\eta^{(1)}_{(\delta,q)}$, the OPE coefficient reads

$$\lambda^{(\delta)}_{(Q+q),q,Q}\Big|_{d=3} = Q^{\delta/2}\left[\eta^{(1)}_{(\delta,q)}\left(1 + 0.10102 \times \frac{q^2}{\sqrt{c_1 Q}}\right) + \mathcal{O}\left(Q^{-1}\right)\right]. \tag{3.41}$$

The second term in round brackets provides the first correction to the leading order result, and it is entirely fixed in terms the same parameter c_1 controlling the scaling dimension Δ_Q at leading order (see eq.s (3.14) and (3.15)). [7] This arises from the first non-trivial correction to the saddle-point solution. Notice that eq. (3.41) holds also for $q = 0$, in which case the $1/\sqrt{Q}$ correction vanishes.

This situation is to be contrasted with $d = 4$, in which case the corrections arising from the modification of the profile (3.11) are renormalized from the first subleading term in the operator matching in (3.32), proportional to $C^{(2)}_{(\delta,q)}$. Accordingly, in appendix B.4.1 we show that this correction is divergent. As in eq. (3.21), upon renormalization this implies that there exists a calculable logarithmic correction which is independent of $C^{(2)}_{(\delta,q)}$. The final result reads

$$\lambda^{(\delta)}_{(Q+q),q,Q}\Big|_{d=4} = Q^{\delta/3}\left[\eta^{(1)}_{(\delta,q)}\left(1 - \frac{q^2 Q^{-2/3}}{24\sqrt{3}\pi^{2/3}c_1^{1/3}}\log Q\right) + \eta^{(2)}_{(\delta,q)}Q^{-2/3} + \mathcal{O}\left(Q^{-4/3}\right)\right], \tag{3.42}$$

where $\eta^{(2)}_{(\delta,q)}$ is an independent Wilson coefficient. As before, the logarithmic term in round brackets is independent of the specific operator under consideration.

Three-point function with a spinning operator insertion

Correlation functions involving an insertion of an operator in a spin ℓ traceless-symmetric representation can be evaluated similarly. Here we provide some details. A spin ℓ primary, with scaling dimension δ and charge q, can be matched in the low energy EFT as

$$\mathcal{O}^{(\delta)}_{q\,\mu_1\ldots\mu_\ell} = C^{(1)}_{\delta,\ell,q}\Pi^{\nu_1\ldots\nu_\ell}_{\mu_1\ldots\mu_\ell}\partial_{\nu_1}\chi\partial_{\nu_2}\chi\ldots\partial_{\nu_\ell}\chi(\partial\chi)^{\delta-\ell}e^{i\chi q} + \ldots, \tag{3.43}$$

where $\Pi^{\nu_1\ldots\nu_\ell}_{\mu_1\ldots\mu_\ell}$ is the projector onto traceless symmetric tensors and again $C^{(1)}_{\delta,\ell,q}$ is a coefficient which depends on the underlying theory and operator. Analogously to eq. (3.38), we then find the three-point function to leading order as:

$$\langle Q+q, \tau_{out}|\mathcal{O}^{(\delta)}_{q\,\mu_1\ldots\mu_\ell}(\tau_c, \hat{n}_c)|Q, \tau_{in}\rangle \propto \mu^\delta \delta^0_{\mu_1}\ldots\delta^0_{\mu_\ell}e^{-\Delta_Q(\tau_{out}-\tau_{in})-q\mu(\tau_{out}-\tau_c)}. \tag{3.44}$$

---

[7] This contribution was not considered in previous analysis of the same three-point function [35, 109].

When mapped to flat space this results is in agreement with the general structure for a conformal correlator (B.7). Including subleading correction as before, the EFT then predicts the following scaling law for the OPE coefficient:

$$\lambda^{(\delta,\ell)}_{(Q+q),q,Q} \propto \begin{cases} Q^{\delta/2}\left[1+0.10102\times\frac{q^2}{\sqrt{c_1 Q}}+\mathcal{O}\left(Q^{-1}\right)\right] & d=3\,, \\ Q^{\delta/3}\left[1-\frac{q^2}{24\sqrt{3}\pi^{2/3}c^{1/3}}Q^{-2/3}\log Q+\eta^{(2)}_{(\delta,q)}Q^{-2/3}+\mathcal{O}\left(Q^{-4/3}\right)\right] & d=4\,. \end{cases} \tag{3.45}$$

3.3.2 Four-point functions

Here we finally discuss four-point functions, focusing on their operator product expansion (OPE) decomposition. [8] This will allow for the calculation of the OPE coefficients of light operators in between the ground state at fixed charge and its phonon excitations, whose spectrum we discussed in sec. 3.2.2.

Four-point function with two insertions of the Noether current

Let us consider the four-point function with two insertions of the time component of the Noether current, aka the charge density. Using the expression (3.29), on the cylinder this corresponds to the following matrix element:

$$\begin{aligned} G_{J_0,J_0} &= \langle Q,\tau_{out}|J_0(\tau_2,\hat{n}_2)J_0(\tau_1,\hat{n}_1)|Q,\tau_{in}\rangle \\ &= e^{-\Delta_Q(\tau_{out}-\tau_{in})/R}\left(\frac{Q}{R^{d-1}\Omega_{d-1}}\right)^2\left[1-\frac{(d-1)^2}{\mu^2}\langle\dot{\pi}_2\dot{\pi}_1\rangle+\dots\right]\,, \end{aligned} \tag{3.46}$$

where $\pi_i\equiv\pi(\tau_i,\hat{n}_i)$. The propagator for the Goldstone field may be computed from the action (3.16) and it can be written as a sum over the phonon modes: [9]

$$\langle\pi(\tau,\hat{n}_2)\pi(0,\hat{n}_1)\rangle=\frac{(R^{d-1}\Omega_{d-1})^{-1}}{c_1 d(d-1)\mu^{d-2}}\left[-\frac{1}{2}|\tau|+\sum_{\ell=1}^{\infty}\frac{2\ell+d-2}{d-2}\frac{e^{-\omega_\ell|\tau|}}{2\omega_\ell}C_\ell^{\left(\frac{d}{2}-1\right)}(\hat{n}_2\cdot\hat{n}_1)\right]\,. \tag{3.47}$$

In this expression $C_\ell^{\left(\frac{d}{2}-1\right)}(x)$ stand for the Gegenbauer polynomials, which reduce to the usual Legendre polynomials in $d=3$. For future reference, we report their expression for $\ell=0$ and $\ell=1$:

$$C_0^{\left(\frac{d}{2}-1\right)}(x)=1\,,\qquad C_1^{\left(\frac{d}{2}-1\right)}(x)=(d-2)x\,. \tag{3.48}$$

---

[8] We review the OPE in appendix B.1 and we derive the conformal block decomposition for a four-point function in appendix B.4.2.

[9] More precisely, the propagator is defined up to the addition of an arbitrary constant, since the action of the zero mode on the vacuum is not defined (see the footnote 6); in practice, this constant always cancels in calculations and we neglected it for simplicity in eq. (3.47). One may indeed check that a careful treatment of the zero mode, e.g. using the decomposition (3.23) in canonical formalism, reproduces all the results that we will discuss in the following.

We can now use the propagator in eq. (3.46) to get:

$$\begin{aligned} G_{J_0,J_0} = e^{-\Delta_Q(\tau_{out}-\tau_{in})/R}\left(\frac{Q}{R^{d-1}\Omega_{d-1}}\right)^2 \Bigg[1+\frac{(d-1)^2}{2\Delta_Q(d-2)}e^{-|\tau_2-\tau_1|/R}C_1^{\left(\frac{d}{2}-1\right)}(\hat{n}_2\cdot\hat{n}_1) \\ +\sum_{\ell=2}^{\infty}\frac{R\omega_\ell(d-1)(2\ell+d-2)}{2c_1 d(d-2)(R\mu)^d\Omega_{d-1}}e^{-\omega_\ell|\tau_2-\tau_1|}C_\ell^{\left(\frac{d}{2}-1\right)}(\hat{n}_2\cdot\hat{n}_1)+\mathcal{O}\left(\frac{1}{(R\mu)^{d+2}}\right)\Bigg]\,, \end{aligned} \tag{3.49}$$

where we used eq. (3.13) and we separated the $\ell=1$ term from the rest of the sum for reasons which shall become clear in a moment.

The EFT reliably predicts the correlator (3.46) when the two insertions are separated by a distance larger than the inverse EFT cutoff μ^{-1}. In this regime, we may match our result with the decomposition of the four-point function obtained using the s-channel OPE $J_0\times\mathcal{O}_Q\sim\sum_{\Delta,\ell}\mathcal{O}_Q^{(\Delta,\ell)}$. We provide details on the derivation of this decomposition in appendix B.4.2. This is written as a sum of the three-point function coefficients squared multiplied by the *conformal blocks* $g_{\Delta,\ell}^{\mathcal{O}_Q,J_0}(\tau,\hat{n}_2\cdot\hat{n}_1)$. The form of the conformal blocks is fixed by conformal invariance in terms of the quantum numbers under the conformal group of the primary operators $\mathcal{O}_Q^{(\Delta,\ell)}$, $\mathcal{O}_q^{(\delta)}$ and $\mathcal{O}_Q$. Crucially, in appendix B.4.2 we also show that the conformal blocks admit a simple expansion when the scaling dimension Δ of the exchanged operator is much larger than the difference $\Delta-\Delta_Q$. This property, first noticed in [109], allows to easily match the four-point function (3.46) with such a decomposition. We find

$$\begin{aligned} G_{J_0J_0} = e^{-\Delta_Q(\tau_{out}-\tau_{in})/R}R^{-2(d-1)}\left(\frac{Q}{\Omega_{d-1}}\right)^2 g_{\Delta_Q,0}^{\mathcal{O}_Q,J_0}(\tau_2-\tau_1,\hat{n}_2\cdot\hat{n}_1) \\ +e^{-\Delta_Q(\tau_{out}-\tau_{in})/R}R^{-2(d-1)}\sum_{\ell=2}^{\infty}\left[\lambda_{Q,J_0,Q}^{[\ell]}\right]^2 g_{\Delta_{Q,\ell},\ell}^{\mathcal{O}_Q,J_0}(\tau_2-\tau_1,\hat{n}_2\cdot\hat{n}_1)+\ldots\,. \end{aligned} \tag{3.50}$$

In the first line we singled out the contribution associated to the exchange of the operator $\mathcal{O}_Q$ itself, whose OPE coefficient was computed in eq. (3.30). The associated conformal block reads

$$g_{\Delta_Q,0}^{\mathcal{O}_Q,J_0}(\tau,x)=1+e^{-\tau/R}\frac{(d-1)^2}{2\Delta_Q}x+\mathcal{O}\left(\Delta_Q^{-2}\right)\,, \tag{3.51}$$

where the first (trivial) term is the contribution from the primary state, the second term is suppressed by $1/\Delta_Q\sim Q^{-\frac{d}{d-1}}$ and corresponds to the contribution from the first descendant and similarly higher level descendants are suppressed by additional powers of Δ_Q^{-1}. Using $C_1^{\left(\frac{d}{2}-1\right)}(\hat{n}_2\cdot\hat{n}_1)=(d-2)\hat{n}_2\cdot\hat{n}_1$, we indeed recognize the contribution of the conformal block (3.51) in the first two terms of the parenthesis of the EFT result (3.49). The second line of eq. (3.50) corresponds instead to the exchange of the charge Q phonon primary states discussed in sec. 3.2.2, as it may be seen from the expression of the conformal block:

$$g^{\mathcal{O}_Q,J_0}_{\Delta_{Q,\ell},\ell}(\tau,x) = e^{-(\Delta_{Q,\ell}-\Delta_Q)\tau/R} C_\ell^{(\frac{d}{2}-1)}(x) + \mathcal{O}\left(\frac{\Delta_{Q,\ell}-\Delta_Q}{\Delta_Q}\right), \qquad \Delta_{Q,\ell} = \Delta_Q + R\omega_\ell\,. \tag{3.52}$$

By matching this expression with the EFT result (3.49) we may also compute the OPE coefficient for the current J_0 in between a single phonon primary with $\ell \geq 2$ and $\mathcal{O}_Q$ as:

$$\left[\lambda^{[\ell]}_{Q,J_0,Q}\right]^2 = \left(\frac{Q}{\Omega_{d-1}}\right)^{\frac{d-2}{d-1}} \frac{R\omega_\ell(d-1)(2\ell+d-2)}{2(d-2)\Omega_{d-1}(c_1 d)^{-\frac{1}{d-1}}}\left[1+\mathcal{O}\left(\frac{\ell^2}{Q^{\frac{2}{d-1}}}\right)\right]. \tag{3.53}$$

Remarkably, since $R\omega_\ell = J_\ell/\sqrt{d-1}$ to leading order, this expression is fully determined in terms of the same coefficient c_1 controlling the scaling dimension Δ_Q. Notice that the modes with angular momentum $\ell \gtrsim R\mu \sim Q^{\frac{1}{d-1}}$ describe correlations at lengths shorter than the cutoff and therefore their OPE coefficients cannot be computed within the EFT.

Four-point function with two scalar insertions

We conclude this chapter with a last example, the four-point function with two insertions of a scalar operator:

$$F^{\delta,\delta}_{q,-q} = \langle Q,\tau_{out}|\mathcal{O}^{(\delta)}_{-q}(\tau_2,\hat{n}_2)\mathcal{O}^{(\delta)}_{q}(\tau_1,\hat{n}_1)|Q,\tau_{in}\rangle\,, \qquad \tau_2 > \tau_1\,, \tag{3.54}$$

where $\left[\mathcal{O}^{(\delta)}_{-q}(\tau,\hat{n})\right]^\dagger = \mathcal{O}^{(\delta)}_{q}(-\tau,\hat{n})$. Using the expression (3.32) for the scalar operator, we may write this as:

$$F^{\delta,\delta}_{q,-q} = e^{-\Delta_Q(\tau_{out}-\tau_{in})/R} e^{-\mu q(\tau_2-\tau_1)} R^{-2\delta}\left|\lambda^{(\delta)}_{(Q+q),q,Q}\right|^2\left[1+q^2\langle\pi_2\pi_1\rangle+\dots\right], \tag{3.55}$$

where the OPE coefficient for the correlator $\langle\mathcal{O}_{-Q-q}\mathcal{O}^{(\delta)}_q\mathcal{O}_Q\rangle$ was computed before in eq. (3.38). [10] We may use the propagator (3.47) to write the second term in square parenthesis as

$$\begin{aligned} q^2\langle\pi_2\pi_1\rangle = &-\frac{q^2}{2}\frac{\partial^2\Delta_Q}{\partial Q^2}\frac{|\tau_2-\tau_1|}{R} + \frac{q^2}{2\Delta_Q}\left(\frac{\partial\Delta_Q}{\partial Q}\right)^2 e^{-|\tau_2-\tau_1|/R}\,\hat{n}_2\cdot\hat{n}_1 \\ &+ q^2\sum_{\ell=2}^{\infty}\frac{(2\ell+d-2)[d(d-1)R\omega_\ell]^{-1}}{2c_1(d-2)(R\mu)^{d-2}\Omega_{d-1}} e^{-\omega_\ell|\tau_2-\tau_1|} C_\ell^{(\frac{d}{2}-1)}\left(\hat{n}_2\cdot\hat{n}_1\right). \end{aligned} \tag{3.56}$$

Proceeding as in the previous section, eq. (3.55) can be matched to the s-channel conformal block decomposition, obtained considering the OPE $\mathcal{O}^{(\delta)}_q \times \mathcal{O}_Q \sim \sum_{\Delta,\ell}\mathcal{O}^{(\Delta,\ell)}_{Q+q}$, in terms of the exchange of the operator $\mathcal{O}_{Q+q}$ and the charge $Q+q$ phonon primaries:

---

[10] We included the corrections from subleading terms and contractions of fields at the same point, which provide the subleading contributions to the OPE coefficient discussed before.

$$\begin{aligned} F^{\delta,\delta}_{q,-q} &= e^{-\Delta_Q(\tau_{out}-\tau_{in})/R} R^{-2\delta} \left|\lambda^{(\delta)}_{(Q+q),q,Q}\right|^2 g^{\mathcal{O}_Q,\mathcal{O}_q^{(\delta)}}_{\Delta_{Q+q},\ell}\left(\tau,\hat{n}_2\cdot\hat{n}_1\right) \\ &+ e^{-\Delta_Q(\tau_{out}-\tau_{in})/R} R^{-2\delta} \sum_{\ell=2}^{\infty} \left|\lambda^{[\ell],(\delta)}_{(Q+q),q,Q}\right|^2 g^{\mathcal{O}_Q,\mathcal{O}_q^{(\delta)}}_{\Delta_{Q+q,\ell},\ell}(\tau,\hat{n}_2\cdot\hat{n}_1) + \dots . \end{aligned} \tag{3.57}$$

The exchange of the operator $\mathcal{O}_{Q+q}$ provides the leading contribution to (3.55), as it can be seen comparing (3.55) with the expression of the corresponding conformal block

$$\begin{aligned} g^{\mathcal{O}_Q,\mathcal{O}_q^{(\delta)}}_{\Delta_Q,\ell}\left(\tau,\hat{n}_2\cdot\hat{n}_1\right) &= e^{-(\Delta_{Q+q}-\Delta_Q)\tau/R}\left[1+\frac{(\Delta_{Q+q}-\Delta_Q+\delta)^2}{2\Delta_{Q+q}}e^{-\tau/R}\hat{n}_2\cdot\hat{n}_1+\dots\right] \\ &\simeq e^{-(\Delta_{Q+q}-\Delta_Q)\tau/R}\left[1+\frac{q^2}{2\Delta_Q}\left(\frac{\partial\Delta_Q}{\partial Q}\right)^2 e^{-\tau/R}\hat{n}_2\cdot\hat{n}_1+\mathcal{O}\left(Q^{-1}\right)\right] , \end{aligned} \tag{3.58}$$

and using eq. (3.39) together with $\Delta_{Q+q}-\Delta_Q \approx q\frac{\partial\Delta_Q}{\partial Q}$. The contributions from the $\ell=0$ and $\ell=1$ modes in eq. (3.56) precisely match the first subleading contribution in eq. (3.58), arising from the expansion of the exponential in a Taylor series around $q=0$ and from the second term in parenthesis. Indeed, one can check that the sum of all the higher order corrections corresponding to additional exchanges of the zero-mode sum to give the exponential $\exp\left[-q\frac{\partial\Delta_Q}{\partial Q}\tau/R\right]$. Finally, as in eq. (3.49), the second line of (3.56) is matched to the exchange of charge $Q+q$ phonon primary states, whose corresponding conformal block is just given by

$$g^{\mathcal{O}_Q,\mathcal{O}_q^{(\delta)}}_{\Delta_{Q+q,\ell},\ell}(\tau,x) = e^{-(\Delta_{Q+q,\ell}-\Delta_Q)\tau/R} C_\ell^{\left(\frac{d}{2}-1\right)}(x) + \mathcal{O}\left(Q^{-\frac{d-2}{d-1}}\right) , \qquad \Delta_{Q+q,\ell} = \Delta_{Q+q} + R\omega_\ell . \tag{3.59}$$

The EFT then predicts the OPE coefficient $\lambda^{[\ell],(\delta)}_{(Q+q),q,Q}$ for the matrix element of $\mathcal{O}_q^{(\delta)}$ in between the ground state and a charge $Q+q$ spin ℓ excited phonon primary as

$$\left|\frac{\lambda^{[\ell],(\delta)}_{(Q+q),q,Q}}{\lambda^{(\delta)}_{(Q+q),q,Q}}\right|^2 = Q^{-\frac{d-2}{d-1}} \times \frac{q^2/(R\omega_\ell)(2\ell+d-2)}{2(d-2)(d-1)(c_1 d\Omega_{d-1})^{\frac{1}{d-1}}}\left[1+\mathcal{O}\left(Q^{-\frac{1}{d-1}}\right)\right] . \tag{3.60}$$

We provide a detailed analysis of the four-point function (3.54) to subleading orders in the appendix B.4.3, where we compute the first correction to (3.60), as well as the OPE coefficient for a scalar insertion in between the ground state and the operator corresponding to the creation of two phonons. It is clearly straightforward to generalize this analysis to other correlators. For instance, one finds the following scaling law for the OPE coefficient of $\mathcal{O}_q^{(\delta)}$ in between the ground state and a state with k phonons:

$$\left|\lambda^{[k-\text{phonons}](\delta)}_{(Q+q),q,Q}\right|^2 \propto \left|\lambda^{(\delta)}_{(Q+q),q,Q}\right|^2 \times q^{2k} Q^{-k\frac{d-2}{d-1}} \propto q^{2k} Q^{\frac{2\delta-k(d-2)}{d-1}} . \tag{3.61}$$

4 The large charge expansion in CFTs: general symmetry groups

In the previous chapter we have studied the large charge expansion for CFTs invariant under a $U(1)$ internal symmetry. However, many theories of interest possess larger internal symmetry groups. Relevant examples in three dimensions include the critical $O(N)$ models [103], the multifield $SO(N) \times SO(M)$ Landau-Ginzburg models [110] and the projective CP^{N-1} models [111] (which enjoy $SU(N)$ symmetry [98]); another interesting example is provided by the Banks-Zaks fixed points for four-dimensional gauge theories [112]. We expect the large charge sector of these theories to admit an effective semiclassical description. The analysis of the large charge expansion for CFTs invariant under general symmetry groups is the topic of this chapter.

With respect to the case of a $U(1)$ symmetry, some structural novelties are expected to emerge for non-Abelian symmetry groups. In this case, as explained in part I of this thesis, the spontaneous breakdown of symmetries generically implies the existence of both gapless and gapped modes in the spectrum of the superfluid phase. The natural framework to describe this state of affairs is the non-relativistic EFT (NREFT) presented in chapter 2, which allows for a systematic description of all the Goldstone modes at long spatial wavelengths. Interestingly, the specialization of the NREFT to the cylinder poses some questions on its interpretation. On the one hand, states made purely of gapless modes may be analyzed as in the previous chapter; on the other hand, for gapped Goldstones things are generically made more involved by the mixing with states made of lighter modes, but outside the validity of the NREFT. As argued in [35], this generically implies that the spectrum of the lowest dimension operators at fixed charge for a rank N group coincides with the one for a $U(1)^N$ symmetry. We review these considerations in sec. 4.1.

A notable exception to the above discussion occurs when the quantum numbers of the gapped Goldstones ensure the absence of such mixings for certain states. [1] This is expected to happen in the specific but physically interesting case of the three-dimensional $O(N)$ models, which we discuss in sec. 4.2. There, certain states made of gapped Goldstone quanta may be associated with the lowest dimension operators in mixed symmetric representations of the internal group. Correspondingly, they cannot mix with states made of modes outside the validity of the NREFT and we can compute their scaling dimensions. These predictions might be verified in the near future by Monte-Carlo simulations.

---

[1] Here we are implicitly neglecting the possibility that light modes with the same quantum numbers of

Irrespectively of the presence of mixings for the gapped Goldstone states, we expect the NREFT to provide non-trivial information on CFTs invariant under non-Abelian symmetry groups. Indeed, these mixings correspond to the decay and annihilation of the gapped Goldstone states in the infinite volume limit. Therefore the NREFT approach should allow the description of the resulting inclusive features, encoded in the spectral distribution of certain correlators. Relatedly, the NREFT allows to match operators transforming in non-trivial representations of the internal symmetry group in terms of Goldstone fields, in a certain kinematic regime. We will begin the exploration of these ideas in sec. 4.3, focusing on correlators of the non-Abelian current in a generic theory with $SU(2)$ symmetry.

For the sake of simplicity, in this chapter we shall only consider CFTs in three dimensions, the generalization of our results to arbitrary spacetime dimensions being straightforward. Furthermore, in order to apply the NREFT construction of chapter 2, it will be convenient to work in Lorentzian signature for the cylinder time coordinate.

4.1 Operators with lowest dimensions at large charge

4.1.1 The case of a fully broken group

Let us discuss how to generalize the results of the previous chapter for the lightest operators at fixed charge. Consider first the example of a CFT with an internal non-Abelian $SU(2)$ symmetry group. In this case, the leading semiclassical trajectory for the path-integral in between two charged states is expected to induce the following symmetry breaking pattern:

$$SO(4,1)\times SU(2)\longrightarrow SO(3)\times\bar{D}\,,\qquad \bar{D}=D+\mu\widehat{Q}_3\,. \tag{4.1}$$

The corresponding Goldstone excitations are given by a gapless and a gapped mode, with mass μ. These can be described by the NREFT presented in chapter 2, whose Lagrangian can be found specializing that construction to the cylinder and imposing Weyl invariance. We shall construct the action explicitly in sec. 4.2. For the moment, we content ourselves with noticing that the gapped mode does not play any role in the determination of the spectrum of light operators. Formally, this follows from the considerations in sec. 2.3,

---

the gapped Goldstones exist, in which case the corresponding states would generically mix with them.

where we also showed that the NREFT reduces to a standard Abelian superfluid in the zero gapped Goldstone sector. As a consequence, the results in sec. 3.2 immediately apply to $SU(2)$-invariant CFTs as well. In particular, the superfluid ground state corresponds to the component of maximal eigenvalue for the $\widehat{Q}_3$ generator of a $2Q_3+1$-dimensional $SU(2)$ representation. The EFT then predicts the scaling dimension of the corresponding operator in a large charge expansion as

$$\Delta_{Q_3} = \alpha_1 Q_3^{3/2} + \alpha_2 Q_3^{1/2} - 0.0937256 + \alpha_3 Q_3^{-1/2} + \mathcal{O}\left(Q^{-1}\right) . \tag{4.2}$$

Similarly, the lightest excitations on the ground state are given by the phonon states, whose spectrum we described in sec. 3.2.2.

As already remarked, the EFT for the gapless mode only describe the lowest energy highest weight states in a given $SU(2)$ representation. What about the other states in the same $SU(2)$ multiplet? We shall see in the next section that, upon quantization, the zero mode of the gapped Goldstone is proportional to the charges $\widehat{Q}_\pm$. Therefore it cannot mix with states outside the NREFT and it allows to reconstruct all the $(2Q_3+1)$ states of the multiplet. The creation and annihilation operators of the $\ell \geq 1$ modes instead commute with all the $SU(2)$ generators, and therefore describe gapped states in the same representation of the superfluid ground state. These are generically expected to mix with other states outside the NREFT.

These considerations admit an immediate generalization to higher rank groups. Consider for instance a CFT invariant under an $SU(3)$ internal symmetry, with generators $\widehat{Q}_1,\ldots,\widehat{Q}_8$. [2] The lowest energy state at fixed values Q_3 and Q_8 of the Cartan generators will generically be given by the highest weight state of a certain $SU(3)$ multiplet. According to the discussion in sec. 3.1, we expect this state to be in a superfluid phase for which the cylinder Hamiltonian $H_{cyl} = D/R$ and the Cartan generators $\widehat{Q}_3$ and $\widehat{Q}_8$ are classically broken; the unbroken time translations are generated by a linear combination of the form

$$\bar{D} = D + \mu_3 \widehat{Q}_3 + \mu_8 \widehat{Q}_8 \,. \tag{4.3}$$

For generic values of the charges, and hence of the chemical potentials $\mu_{3/8}$, the modified Hamiltonian (4.3) does not commute with any of the other generators of the internal group, which, therefore, must be fully broken. For the same reason, the Goldstone modes associated with these generators are gapped for generic values of the charges and do not contribute to the spectrum of low energy states. Thus, in the zero-gapped Goldstone sector the EFT reduces to the one of a $U(1)^2$ superfluid and it is formulated in terms of two shift-invariant Goldstone fields $\chi_{3/8} = \mu_{3/8} t + \pi_{3/8}$. At leading order, the action is given by

$$S = \int d^3x \sqrt{g} (\partial\chi_3)^{3/2} (\partial\chi_8)^{3/2} P\left(X, Y\right) , \tag{4.4}$$

---

[2] In the fundamental representations these are given by the Gell-Mann matrices: $\widehat{Q}_a = \lambda_a/2$ [60].

where P is an arbitrary function and, following [35], we defined

$$X=\frac{\partial_\mu\chi_3\partial^\mu\chi_8}{(\partial\chi_3)(\partial\chi_8)}\,,\qquad\qquad Y=\frac{(\partial\chi_8)}{(\partial\chi_3)}\,. \tag{4.5}$$

The function P and all its derivatives are smooth for generic values of the charges; singular points are expectedly associated with phases in which the symmetry is, at least partially, restored and the EFT description breaks down. Higher order terms can be constructed similarly to eq. (3.9) noticing that any combination of the form $g_{\mu\nu}(\partial\chi_{3/8})^2F(X,Y)$ is Weyl invariant, where F is an arbitrary function.

We may study the consequences of the EFT (4.4) for the CFT spectrum as in section 3.2. First notice that the charges on the classical solution are given by

$$\frac{Q_3}{4\pi R^2}=\frac{3}{2}\mu^2Y^{\frac{1}{2}}P\left(1-\frac{2}{3}Y\frac{P_Y}{P}\right),\qquad \frac{Q_8}{4\pi R^2}=\frac{3}{2}\mu^2Y^{-\frac{1}{2}}P\left(1+\frac{2}{3}Y\frac{P_Y}{P}\right), \tag{4.6}$$

where $\mu^2=\mu_3\mu_8$, and the subscripts on P denote differentiation with respect to the corresponding argument. All quantities are evaluated on the background solution with $X=1$, $Y=\mu_8/\mu_3$. At a generic point in the space of the charges we have $\mu_3\sim\mu_8\sim\sqrt{Q_3}\sim\sqrt{Q_8}$. The EFT then generically describes highest weight states corresponding to a vertex of a hexagonal shaped representation in the (Q_3,Q_8) plane [60]. However, depending on the form of the function P, the semiclassical description (4.4) might apply as well when one of the two charges vanishes [35]. In particular, a state with $Q_3=0$ corresponds to a vertex of a triangle shaped representation, obtained from the generic hexagonal one contracting two edges to a point. [3] Due to the nonlinear relation (4.6) between the charges and the chemical potential, we generically expect $\mu_3\sim\mu_8\gg 1/R$ in this case as well. Finally, as in the $SU(2)$ case, quantizing the full NREFT the zero mode of the gapped Goldstones allows to match the non-Abelian charges as well, and therefore to explicitly reconstruct the full structure of the representation from the single highest weight state we are considering here.

Calling $Q=\sqrt{Q_3Q_8}$, from the energy momentum tensor we find that the classical energy of the ground state takes the following form:

$$\Delta_{Q_3,Q_8}=\alpha_1\left(r\right)Q^{3/2}+\alpha_2\left(r\right)Q^{1/2}+\dots\,,\qquad r\equiv Q_8/Q_3\,, \tag{4.7}$$

With respect to eq. (3.19), now the α_i's are function of the ratio of the charges Q_8/Q_3. Furthermore, by expanding the Lagrangian (4.4) we find

$$S^{(2)}\simeq\int d^3x\sqrt{g}\left\{\frac{N_+}{2}\left[(\dot\pi_+)^2-\frac{1}{2}(\partial_i\pi_+)^2\right]+\frac{N_-}{2}\left[(\dot\pi_+)^2-c_-^2(\partial_i\pi_+)^2\right]\right\}, \tag{4.8}$$

---

[3] This is because $\widehat{Q}_1$ and $\widehat{Q}_2$ commute with $\widehat{Q}_8$, hence a pair of ladder operators acts trivially on all states of a triangle shaped representation.

where fluctuations are parametrized as

$$\pi_+ = \frac{1}{2}\left(\frac{\pi_3}{\mu_3}+\frac{\pi_8}{\mu_8}\right) - \frac{1}{3}Y\frac{P_Y}{P}\left(\frac{\pi_3}{\mu_3}-\frac{\pi_8}{\mu_8}\right)\,, \qquad \pi_- = \frac{1}{2}\left(\frac{\pi_3}{\mu_3}-\frac{\pi_8}{\mu_8}\right)\,, \tag{4.9}$$

and we defined

$$N_+ = 6\mu^3 P\,, \qquad N_- = -3\mu^3 P + 4Y\mu^3 P_Y + 4Y^2\mu^3 P_{YY} - \frac{8}{3}Y^2\mu^3\frac{P_Y^2}{P}\,,$$
$$c_-^2 = \frac{\mu^3}{N_-}\left(3P - 4P_X - \frac{4}{3}Y^2\frac{P_Y^2}{P}\right)\,. \tag{4.10}$$

From eq. (4.4) we see that the speed of sound of π_+ is fully determined by Weyl invariance, $c_+ = 1/\sqrt{2}$; the main novelty with respect to the case of a rank one group is the presence of an additional mode, whose sound speed is not fixed by conformal invariance only. Stability and subluminality of small fluctuations require $N_\pm > 0$ and $0 < c_-^2 \leq 1$, imposing constraints on the function P.

The Casimir energy of the fluctuations provide a Q^0 correction to eq. (4.7), fully analogous to eq. (3.17), whose value depends on the speed of sound c_- of the second mode as well. By straightforwardly generalizing the calculation in appendix B.3, the result for the ground state energy reads

$$\Delta_{Q_3,Q_8} = \alpha_1(r)\,Q^{3/2} + \alpha_2(r)\,Q^{1/2} - \left(1+\sqrt{2}c_-\right)\times 0.0937256 + \alpha_3(r)\,Q^{-1/2} + \mathcal{O}\left(Q^{-1}\right)\,. \tag{4.11}$$

Notice that subluminality implies that the coefficient β_0 of the Q^0 term lies in the range $-0.0937256 \times \left(1+\sqrt{2}\right) \leq \beta_0 \leq -0.0937256$.

Finally, the spectrum of *phonon* excitations is given by the Fock space of the two modes:

$$\Delta = \Delta_{Q_3,Q_8} + \sum_\ell n_\ell^+ R\omega_\ell^+ + \sum_\ell n_\ell^- R\omega_\ell^-\,,$$
$$\omega_\ell^+ = \frac{1}{\sqrt{2}}J_\ell + \mathcal{O}\left(J_\ell^3/\mu^2\right)\,, \qquad \omega_\ell^- = c_- J_\ell + \mathcal{O}\left(J_\ell^3/\mu^2\right)\,. \tag{4.12}$$

As before, the operators of eq. (4.12) have the same charge of the ground state and the $\ell = 1$ mode of π^+ corresponds to the creation of a descendant state.

For a CFT invariant under a non-Abelian group G of rank N the situation will be similar. In the simplest case, a large charge state will be associated with a superfluid phase in which G is fully broken. Correspondingly, the only gapless mode will be the Goldstones associated with the Cartan generators. In this case certain quantities, such as the dimensions of the lightest operators at fixed charge, will be independent of the specific choice of the group and will coincide with the ones for the $U(1)^N$ case.

Finally we remark that, while gapped Goldstones generically do not provide informations concerning the spectrum of lightest operators at fixed charge, [4] they play an important role in the matching of operators in the IR onto expressions in terms of the Goldstone fields. We shall illustrate this point in sec. 4.3, focusing on the non-Abelian current for a theory with $SU(2)$ symmetry.

4.1.2 The case of a partially unbroken group

Though the situation described in the previous section is the simplest one, it might happen that, given a specific CFT, the lowest energy state for certain values of the Cartan charges is not in a superfluid state. For instance, such state might be inhomogeneous and carry non-zero angular momentum. In general, this does not imply that the CFT does not admit a superfluid phase, but rather that such phase describes the theory for a smaller (measure zero) subset of all the possible values of the charges. In the case of an internal $SU(3)$ symmetry, a non-generic scenario of this kind might be realized in two qualitatively different ways, which we illustrate below.

Consider first the case in which the conformal superfluid describes only states with $Q_8 = 0$. For this situation to be different from the one we discussed before the generator $\widehat{Q}_8$ must be unbroken, with the modified time translations generated by $\bar{D} = D + \mu\widehat{Q}_3$. Since $\widehat{Q}_3$ does not commute with any of the other generators of $SU(3)$, there is a single gapless mode and the analysis proceeds as in the case of a $U(1)$-invariant CFT. In particular the phonon spectrum describes only the lightest operators with $Q_8 = 0$, corresponding to a hexagonal shaped representation in the (Q_3, Q_8) plane. The lowest energy states charged under Q_8 (and which are not in the same representations of the phonon states) are expected to have a gap of order μ with respect to the ground state, but the precise value of their energy or spin cannot be determined within the EFT. [5] A similar scenario is expected to be realized in the CP^2 projective model [89] (see also [90] for a similar analysis of the CP^N models with $N \geq 3$).

A qualitatively different case might occur when the homogeneous superfluid describes only states with $Q_3 = 0$, corresponding to the vertex of a triangle shaped representation in the plane of the Cartan charges. For this situation to be distinguished from the ones discussed before, $\widehat{Q}_3$ must be unbroken and the modified Hamiltonian reads $\bar{D} = D + \mu\widehat{Q}_8$. However, this information is not enough to fully specify the symmetry breaking pattern. Indeed, the generators $\widehat{Q}_1$ and $\widehat{Q}_2$ commute with $\widehat{Q}_8$ and their fate depends on the specific theory under consideration. If they are unbroken, this situation is analogous to the one described above for $Q_8 = 0$. More interestingly, if $\widehat{Q}_1$ and $\widehat{Q}_2$ are broken, the EFT spectrum contains two additional light Goldstone modes. In this case, the zero-gapped Goldstone sector of the EFT is described by the three Goldstone fields parametrizing the coset $U_8(1) \times SU(2)/U_3(1)$, in obvious notation. As before one finds that the ground state energy is given in a large Q_8 expansion, $\Delta_{Q_8} \propto Q_8^{3/2}$, but now the spectrum of light excitations includes two additional gapless modes with frequency $\omega_\ell \propto J_\ell$. The corresponding states are charged under Q_3 and describe (highest weight)[6] states with charges $Q_8 \gg Q_3 > 0$, corresponding to the vertices of hexagonal shaped representations in which two edges are much shorter than the other four.

---

[4] Because of this, some works [78, 89, 90] (mistakenly) referred to the breaking of the generators not commuting with the modified Hamiltonian as *explicit*, rather than *spontaneous*.

[5] Naively, one might conclude that these coincide with the non-zero modes of the gapped Goldstones, which are charged under the unbroken $\widehat{Q}_8$; however, as already remarked, without further assumptions these generically mix with other charged states not included in the NREFT and we cannot determine the precise properties of the true eigenstates of the Hamiltonian in the effective theory.

4.2 Charged operators in the critical $O(N)$ models

The three-dimensional $O(N)$ models, arguably, provide the simplest example of strongly interacting fixed points in quantum field theory [103]. They have been thoroughly studied in the literature and detailed informations on the spectrum of low dimension operators are known from many sources, including the ε-expansion [113], Monte-Carlo simulations [114, 115] and the conformal bootstrap [116, 117]. Recently, some refinements of the Monte-Carlo algorithms for lattice simulations paved the way for the study of charged operators [118, 119], which are usually harder to access by other means. In the near future these developments might allow for extensive comparisons with the predictions of the large charge expansion. This motivates a detailed investigation of these models.

The simplest observable which can be accessed by numerical simulations is the scaling dimensions of the lightest operator at fixed values for the charges. While in the $O(2)$ and $O(3)$ models this is expected to obey a scaling law of the form (3.19), the additional charges for $N \geq 4$ allow for a richer variety of behaviors, depending on whether the internal group is fully broken or not in the superfluid phase.

In [78] it was observed that all the homogeneous finite density classical configurations in the linear weakly coupled $O(N)$-models preserve a subgroup $O(N-2)$. We indeed analyzed the $O(3)$ model in sec. 1.2.2 and we found that the superfluid state leaves unbroken the subgroup $O(1) \simeq \mathbb{Z}_2$. Since the linear sigma models describe the Wilson-Fisher fixed points in the ε-expansion, it is natural to expect the large charge sector of the related 3d CFT to undergo the same symmetry breaking pattern. In this scenario, gapped Goldstones are charged under the unbroken group; therefore, the lowest energy states carrying non-trivial charge under the unbroken group correspond to their excitations and cannot mix with states made of degrees of freedom not included in the NREFT. For instance, the unbroken $\mathbb{Z}_2$ in the linear triplet analyzed in sec. 2.1 ensured the stability of the single gapped Goldstone state. As in that case, the energy of these states must, therefore, be calculable in a large charge expansion within the NREFT.

---

[6] As we will see in the next section for gapped Goldstones, only the $\ell \geq 1$ modes interpolate independent highest wight states, while the $\ell = 0$ ones correspond to the action of the broken charges $\widehat{Q}_{1/2}$.

In this section, we construct the NREFT which describes these models and show how to obtain predictions for the spectrum of the theory. As a byproduct of our analysis, we will also elucidate some general properties of the gapped Goldstone states at finite volume.

4.2.1 Constructing the action

Consider a linear sigma model for a scalar field ϕ_A, $A = 1, \dots, N$, with potential $V(\phi_A\phi_A)$, such as the one described in sec. 1.2.2 for $N = 3$. As well known from celestial mechanics, every homogeneous classical solution of the equations of motion is constrained to move in the plane of the $\mathbb{R}^N$ field space specified by the two vectors giving the initial conditions: $\phi_A(t = 0)$ and $\dot{\phi}_A(t = 0)$. As a consequence, all homogeneous finite density solutions of the equations of motion are obtained considering rotations of the following configuration:

$$\vec{\phi} = \begin{pmatrix} v \cos \mu t \\ v \sin \mu t \\ 0 \\ \vdots \\ 0 \end{pmatrix} , \tag{4.13}$$

where v depends on μ through the potential. For $N = 3$ this solution reduces to eq. (1.25). Calling $\widehat{T}_{AB}$ the generator exchanging the A and B components of the field, such solution is at finite density for the charge associated with $\widehat{T}_{12}$, all other Noether charges being zero. The subgroup $O(N - 2)$ rotating the last components of the field is clearly preserved by eq. (4.13). More general configurations of the charges necessarily require an inhomogeneous field solution.

Qualitatively, we expect the strongly interacting $O(N)$ models to have properties similar to the ones of the linear sigma models. Therefore, from the solution (4.13), we assume that the large charge sector of the $O(N)$ 3d CFTs undergoes the following symmetry breaking pattern:

$$SO(4, 1) \times O(N) \longrightarrow SO(3) \times \bar{D} \times O(N - 2) , \qquad \bar{D} = D + \mu \widehat{T}_{12} . \tag{4.14}$$

In particular, introducing internal indices $I, J = 3, \dots, N$, the broken internal generators are given by the set $\{\widehat{T}_{12}, \widehat{T}_{1I}, \widehat{T}_{2I}\}$, while the unbroken ones are given by the $\{\widehat{T}_{IJ}\}$. It is also convenient to relabel the broken generators as

$$\widehat{Q}_3 \equiv \widehat{T}_{12} , \qquad \widehat{Q}_1^I = \widehat{T}_{2I} , \qquad \widehat{Q}_2^I = -\widehat{T}_{1I} . \tag{4.15}$$

It is easily verified that, for each I, $\{\widehat{Q}_1^I, \widehat{Q}_2^I, \widehat{Q}_3\}$ form an $SU(2)$ subalgebra. [7] This implies that the spectrum of the theory contains a gapless Goldstone associated to the breaking of $\widehat{Q}_3$ and $N-2$ gapped ones, with gap μ, one for each pair $\{\widehat{Q}_1^I, \widehat{Q}_2^I\}$.

---

[7] In our conventions, the algebra reads $\left[\widehat{T}_{AB}, \widehat{T}_{CD}\right] = i \left(\widehat{T}_{AC}\delta_{BD} - \widehat{T}_{AD}\delta_{BC} - \widehat{T}_{BC}\delta_{AD} + \widehat{T}_{BD}\delta_{AC}\right)$.

To build the NREFT, we proceed as in section 2.2. Namely we introduce a coset representative for $O(N)/O(N-2)$ in terms of a real field and $N-2$ complex ones:

$$\Omega = e^{i\chi\widehat{Q}_3} e^{i\alpha_I\frac{\widehat{Q}_+^I}{2} + i\alpha_I^*\frac{\widehat{Q}_-^I}{2}} = e^{i\pi_I\frac{\widehat{Q}_+^I}{2} + i\pi_I^*\frac{\widehat{Q}_-^I}{2}} e^{i\chi\widehat{Q}_3}\,, \qquad \chi = \mu t + \pi\,, \tag{4.16}$$

where $\widehat{Q}_\pm^I \equiv \widehat{Q}_1^I \pm i\widehat{Q}_2^I$ and, analogously to eq.s (2.8) and (2.9), we have introduced two different parametrizations for the Goldstone fields, related as $\alpha_I = e^{-i\chi}\pi_I$. The NREFT describes soft fields in the second parametrization: $\partial\pi \ll \mu\pi$, $\partial\pi_I \ll \mu\pi_I$. Notice that, in both parametrizations, the gapped Goldstone fields transform in the fundamental representation of the unbroken $O(N-2)$ group, while χ is neutral under the latter. However, the action of $\widehat{T}_{12}$ differs in the two parametrizations: in the first it simply provides a shift of χ, $\chi \to \chi + \alpha$, while in the second it further acts as $\pi_I \to e^{i\alpha}\pi_I$. To build invariants under $O(N)$ we consider the Maurer-Cartan one form

$$\Omega^{-1}\partial_\mu\Omega = i\left(D_\mu\chi\widehat{Q}_3 + D_\mu\alpha_I\frac{\widehat{Q}_+^I}{2} + D_\mu\alpha_I^*\frac{\widehat{Q}_-^I}{2} + A_\mu^{IJ}\frac{\widehat{T}_{IJ}}{2}\right)\,, \tag{4.17}$$

where $D_\mu\chi$ and $D_\mu\alpha_I$ are given by eq.s (2.26) for $N=3$ and in general they can be easily computed in a small field expansion:

$$D_\mu\chi = \partial_\mu\chi + \frac{i}{4}\left(\pi_I^*\partial_\mu\pi_I - c.c.\right) + \mathcal{O}\left(|\pi_I|^4\right)\,, \tag{4.18}$$

$$D_\mu\alpha_I = \partial_\mu\alpha_I + i(\partial_\mu\chi)\alpha_I + \ldots = e^{-i\chi}\left[\partial_\mu\pi_I + \mathcal{O}\left(|\pi_I|^2\pi_I\right)\right]\,. \tag{4.19}$$

The expression for the connection A_μ^{IJ} will not be needed for what follows. To build invariants under the full group we need to construct $O(N-2)$-invariant contractions of the covariant derivatives $D_\mu\chi$ and $D_\mu\alpha_I$. These transform, respectively, as a singlet and as a vector under the unbroken group. Furthermore, from eq. (4.19) we see that, on a configuration such that $\partial\pi_I \ll \mu\pi_I$, $D_\mu\alpha_I$ is fastly oscillating with frequency $\sim \mu$. According to the discussion below (2.26), this implies the existence of an emergent $U(1)_\pi$ symmetry in the NREFT, acting as

$$\pi_I \to e^{i\alpha}\pi_I\,, \tag{4.20}$$

which corresponds to the the particle number conservation for the gapped Goldstones.

It is finally straightforward to build the NREFT. Let us define the following quantities

$$n_\mu = \frac{D_\mu\chi}{D\chi}\,, \qquad P_{\mu\nu} = n_\mu n_\nu - g_{\mu\nu}\,, \tag{4.21}$$

which project, respectively, onto the direction of the superfluid velocity and orthogonally to it. Then, to leading order in derivatives, the action reads

$$S=\int d^3x\sqrt{g}(D\chi)\left\{c_1(D\chi)^2+c_{1,2}n^\mu n^\nu D_\mu\alpha_I^* D_\nu\alpha_I+c_{1,3}D_\mu\alpha_I^* P^{\mu\nu}D_\nu\alpha_I+\ldots\right\}. \tag{4.22}$$

The action is manifestly Weyl invariant. Higher order terms may be constructed similarly to eq. (3.9). As already remarked in the introduction to this chapter, we work in Lorentzian signature. Indeed, the NREFT describes the gapped Goldstone fields α_I only for frequencies $|\omega-\mu|\ll\mu$, a condition which clearly cannot be satisfied for Euclidean values, $i\omega\in\mathbb{R}$. [8] We shall discuss in the next section the precise meaning of this gap for the theory quantized on the cylinder.

4.2.2 The spectrum

The ground state of the theory (4.22) describes a highest weight state with non-zero charge $T_{12}=Q$ for the $\widehat{T}_{12}$ generator and its energy Δ_Q reads as in eq. (3.14). The quantization of the field π proceeds as in sec. 3.2.2 and its mode expansions in terms of phonons reads as in eq. (3.23). To quantize the gapped Goldstone field, we consider the expansion of the action (4.22) to quadratic order in π_I and leading order in derivatives:

$$S\simeq\frac{3}{2}c_1\mu^2\int d^3x\sqrt{g}\left[i\pi_I^*\dot{\pi}_I-\frac{c_{1,3}}{6c_1\mu}|\partial_i\pi_I|^2\right], \tag{4.23}$$

from which we immediately infer the mode expansion

$$\pi_I(t,\hat{n})=\sqrt{\frac{2}{3c_1}\frac{1}{\mu}}\sum_{\ell=0}^{\infty}\sum_{m=-\ell}^{\ell}Y_m^\ell(\hat{n})e^{-i\epsilon_\ell t}b_{I;\ell m}\,,\qquad [b_{I;\ell m},b^\dagger_{J;\ell' m'}]=\delta_{IJ}\delta_{\ell\ell'}\delta_{mm'}\,; \tag{4.24}$$

here the frequency is given by

$$\epsilon_\ell=\frac{c_m}{2\mu}J_\ell^2+\mathcal{O}\left(\frac{J_\ell^4}{\mu^3}\right),\qquad c_m\equiv\frac{c_{1,3}}{3c_1}. \tag{4.25}$$

The modes $b^\dagger_{I,\ell m}$, besides transforming as vectors under $O(N-2)$, are negatively charged under the action of $\widehat{T}_{12}$. To linear order in the field expansion, the Noether charges associated to the generators $\widehat{Q}^I_\pm$ coincide with the zero mode of the Gapped Goldstones:

$$\widehat{Q}^I_+=i\sqrt{2Q}\,b_{I,0}\,,\qquad \widehat{Q}^I_-=-i\sqrt{2Q}\,b^\dagger_{I,0}\,. \tag{4.26}$$

Therefore, these zero modes correspond to the other states in the $O(N)$-multiplet of the ground state. As a consequence, their energy coincides, non-perturbatively, with that of the ground state Δ_Q. Notice that the form of the generators (4.26) receives correction at non-linear orders and it is exact only in the strict $Q \to \infty$ limit. These corrections become important when considering the matrix elements of states in the multiplet with charge $T_{12} \ll Q$. For instance, the exact quantization of the action (4.22) should make manifest that, upon acting Q-times with $\widehat{Q}^I_-$, we eventually get a lowest weight state, and that by acting again with $\widehat{Q}^I_-$ we annihilate it.

---

[8] In direct space, this implies that we consider configurations $\pi_I\sim e^{-i\mu t}$ and $\pi_I^*\sim e^{i\mu t}$; in Euclidean time $t=-i\tau$ this means that we can describe only field configurations analytically continued away from the original contour $\pi_I\pi_I^*\in\mathbb{R}$ of the Euclidean path-integral.

When considering the subspace of the Hilbert space with fixed value of the charge associated with $\widehat{T}_{12}$, the zero-mode of the gapped Goldstone, being negatively charged under $\widehat{T}_{12}$, can be thought of as having a gap $\Delta_Q - \Delta_{Q-1} \approx R\mu + \mathcal{O}\left(\mu^{-1}\right)$ with respect to the lowest energy state with $T_{12} = Q - 1$. The locality of the NREFT implies the existence of the $\ell \geq 1$ modes as well in the decomposition of the gapped Goldstone (4.24), these also having a gap $\Delta_Q - \Delta_{Q-1} \approx R\mu$ with respect to the lowest energy state with $T_{12} = Q - 1$. These states are not part of the same multiplet of the ground state. In a generic theory we would expect them to mix with other states not included in the NREFT, in which case the detailed structure of the spectrum is not calculable. Nonetheless, since these mixings correspond to decay and annihilation processes in the infinite volume limit, the NREFT should be able to encode certain inclusive features of the latter via complex Wilson coefficients. In the next section we will make this remark concrete studying an observable which is calculable within the NREFT. However, for the present case of the $O(N)$ models, we can (partially) overcome these complications by identifying a subclass of states for which these mixings are absent, in which case we can directly compute their energy.

To see this, let us first recall that the $O(N)$ representations are labeled by the maximal allowed values for the Cartan generators $\widehat{T}_{12}$, $\widehat{T}_{34}$, ... The superfluid ground state has charge $T_{12} = Q \gg 1$ and vanishing value for all the other generators, corresponding to the highest weight state in a traceless symmetric representation. We may easily construct highest weight states corresponding to different representations acting with the operators $b^\dagger_{I,\ell m}$, $\ell \geq 1$, on the vacuum $|Q\rangle$. For instance, acting on it with the combination $(b^\dagger_{3,\ell m} + i b^\dagger_{4,\ell m})$ we obtain a highest weight state with non-vanishing charges given by $T_{12} = Q - 1$ and $T_{34} = 1$, spin ℓ and energy

$$\Delta = \Delta_Q + R\epsilon_\ell \,, \tag{4.27}$$

where $\Delta_Q = \alpha_1 Q^{3/2} + \alpha_2 Q^{1/2} - 0.0937256 + \ldots$. In the weakly coupled description of the $O(N)$ models, such as at large N or in the ε-expansion, there is a single non-Goldstone degree of freedom in the superfluid phase, a neutral and heavy radial mode, which clearly cannot mix with states charged under the unbroken $O(N-2)$ subgroup. Assuming that a similar property holds for arbitrary values of N in the three dimensional $O(N)$ model, namely that the the only modes charged under the unbroken group are the gapped Goldstones, we conclude that the non-trivial quantum numbers of the single gapped Goldstone state ensure the absence of mixings with states not included in the NREFT.

This observation is crucial for our analysis and it is equivalent to the absence of decay channels for the gapped Goldstone in the infinite volume limit. Correspondingly ϵ_ℓ is real to all orders and eq. (4.27) is a reliable prediction for the CFT spectrum. In particular, eq. (4.27) implies that the lowest energy state in the corresponding mixed symmetric representation has spin $\ell = 1$. This result is reminiscent of the known fact that, in the ε-expansion, the lowest dimension operator in a mixed symmetric representation of $O(N)$ has unit spin.

To generalize the discussion, let us define $n = \max T_{34} + \max T_{56} + \ldots$ for every irreducible representation of $O(N)$. The lowest energy states transforming in an irreducible representation labeled by n correspond to states made of n gapped Goldstones, whose properties may be reliably computed within the NREFT by the same considerations above. In particular, the minimal energy state is given by n modes with $\ell = 1$. The energy and the other quantum numbers of the associated CFT primary operator are

$$\begin{gathered}\max T_{12} = Q - n\,, \qquad \max T_{34} + \max T_{56} + \ldots = n\,, \\ \Delta = \Delta_Q + n\frac{2c_m}{3\alpha_1\sqrt{Q}} + \mathcal{O}\left(\frac{n}{\sqrt{Q}} \times \frac{n}{Q}\right)\,, \qquad \ell \subset \underbrace{1 \otimes 1 \ldots \otimes 1}_{n-times}\,,\end{gathered} \tag{4.28}$$

where we schematically stressed that the spin should be contained in the decomposition of the product of n spin one states, properly symmetrized when it contains identical modes. Corrections are estimated considering the effect of the first non linear term in the expansion of eq. (4.22) and imply that eq. (4.28) is applicable only for $n \ll Q$. Notice that, to this order, such state is generically degenerate. Eq. (4.28) is the main result of this section.

We remark that there exist also states made of $k \geq 2$ gapped Goldstones which, for instance, transform in the same $O(N)$ representation of the ground state. Differently from the case in which the number of modes k coincides with $n = \max T_{34} + \max T_{56} + \ldots$, these may mix with states outside the NREFT and we cannot make a prediction similar to eq. (4.28) for them.

This observation is particularly relevant for the $O(3)$ model, where only one Cartan generator is present. In this case the unbroken group is discrete, given by $\mathbb{Z}_2$, and only states made of a single gapped Goldstone particle do not mix with other modes outside the NREFT. These states correspond to the lowest dimension operators in a $2Q+1$-dimensional representation which is odd under the internal $\mathbb{Z}_2$. Their energy is given by eq. (4.27). States made out of two or more gapped modes transform either in the same representation of the ground state or that of the single gapped Goldstone, and therefore may mix with modes outside of the control of the NREFT. For example, we saw in chapter 2 that a state made of two gapped Goldstones may annihilate, in the infinite volume limit, into a pair of gapless phonons.

Eq. (4.28) may be straightforwardly applied to the $O(4)$ model, in which case representations are labeled by the two Cartan generators, $\max T_{12} = Q - n$ and $\max T_{34} = n$, as $\left(\frac{Q}{2} - n, \frac{Q}{2}\right)$. Previous analysis of these operators in the $O(4)$ models appeared in [79,120] and in [119]. However, these works failed in identifying the most general EFT describing the system; furthermore, the relation between the gapped Goldstone modes and the operators of interest was not appreciated in these previous studies. Therefore, we believe that our treatment clarifies and supersedes these previous analyses. We conclude mentioning that numerical simulations might soon verify (or perhaps disprove) the prediction (4.28) for $n = 1$ in the $O(4)$ model [121].

4.3 CFT data from a gapped Goldstone resonance

In this section we finally address the effects of the mixing between the gapped Goldstones and states outside the NREFT for the large charge expansion in CFTs invariant under non-Abelian symmetry groups. We shall illustrate our ideas focusing on a generic CFT with $SU(2)$ symmetry, leaving a more general investigation for future work.

Let us first present the issue we are confronted with. Consider for concreteness the action (4.22) for $N = 3$, in which case a single gapped Goldstone field π_1 exists. We have seen in chapter 2 that the decay and annihilation of the gapped Goldstone force its action to be complex; for instance, in general, when there is no unbroken $\mathbb{Z}_2$, the coefficient c_m in eq. (4.25) has an imaginary part, which we interpreted as a decay rate–see eq. (2.38). However, such a simple interpretation is not possible for the theory quantized on the cylinder. To appreciate this, we recall that a decay process may be understood as the mixing between a discrete eigenstate of an approximate free Hamiltonian and the states in the continuum part of the energy spectrum of the theory [122]; this leads to an exponentially decreasing amplitude for the free propagation of the state: $\langle \pi_1 | e^{-iHt} | \pi_1 \rangle \sim e^{-iEt} e^{-\frac{\Gamma}{2} t}$. Instead, the spectrum of the theory quantized at finite volume is discrete and, by the quantum-mechanical superposition principle, the mixing cannot lead to the aforementioned exponential behaviour. In other words, the absorbitive effects which we expect in the NREFT do not seem to be compatible with the discreteness of the spectrum of the CFT.

In this respect, the following observation plays a crucial role. The spectrum of the CFT, while certainly discrete, becomes increasingly dense when considering states whose energy is much larger than that of the ground state at fixed charge. Therefore, observables that do not resolve the typical spacing between energy levels should behave similarly to infinite volume quantities and we expect them to be calculable within the NREFT.

In the following we present the basic ideas that allow making this remark concrete reviewing the treatment of [123], where the authors considered the mixing between the Higgs and the discrete Kaluza-Klein graviton modes in theories with large extra dimensions. Inspired by that, we will then study a specific observable in CFT: the four-point function with two insertions of the non-Abelian current on the ground state.

4.3.1 Invitation: discrete versus continuum in theories with large extra dimensions

Suppose the full spacetime is given by $\mathbb{R}^{d-1,1} \times T_\delta$, where T_δ is a δ-dimensional torus of radius R and volume $V_\delta = (2\pi R)^\delta$. Let us parametrize coordinates as (x^μ, y^a), where x^μ are the Minkowski coordinates and $\vec{y}$ parametrizes the position on T_δ. The basic idea of [123] can be illustrated considering a toy model consisting of a massive scalar h, living on a brane at $y^a = 0$, interacting with a $d+\delta$-dimensional field H. We shall refer to h as the "Higgs". The quadratic action is given by

$$S = \int d^d x d^\delta y \frac{1}{2}(\partial H)^2 + \int d^d x \left[\frac{1}{2}(\partial h)^2 - \frac{m_h^2}{2}h^2 - m_{mix}^{2-\delta/2} h\, H(x, y=0)\right] , \tag{4.29}$$

where m_h is the mass of h and m_{mix} parametrizes the mixing between the Higgs and H on the brane. We assume large extra dimensions, $R \gg m_h^{-1}$, and small mixing $m_{mix}^2 \ll m_h^2$.

We would like to study the physical effects of the mixing between the field h and the $d+\delta$-dimensional field H. To this aim, let us decompose the field into Kaluza-Klein modes:

$$H(x,y) = \sum_{\vec{n}} \frac{e^{i\vec{n}\cdot\vec{y}/R}}{\sqrt{V_\delta}} H^{(\vec{n})}(x) , \tag{4.30}$$

where the sum runs over all $\vec{n} \in \mathbb{Z}^\delta$. Then the action (4.29) becomes

$$\begin{aligned} S = \int d^d x \Bigg[&-\frac{1}{2}\sum_{\vec{n}} H^{(-\vec{n})} \left(\partial_\mu \partial^\mu + m_n^2\right) H^{(\vec{n})} \\ &+ \frac{1}{2}(\partial h)^2 - \frac{m_h^2}{2}h^2 - \frac{m_{mix}^{2-\delta/2}}{\sqrt{V_\delta}} h \sum_{\vec{n}} H^{(\vec{n})}(x) \Bigg] , \end{aligned} \tag{4.31}$$

where $m_n^2 = \vec{n}^{\,2}/R^2$. Eq. (4.31) coincides with the action describing the mixing between the Higgs field and the graviscalar Kaluza-Klein modes discussed in [124].

In light of the mixing term, a Higgs state, defined as the state created by the action of the field $h(x)$ on the vacuum, is a linear combination of the true mass eigenstates of the theory. Working for notational simplicity in the rest frame $p = (m_h, 0)$ with a nonrelativistic normalization, we can write

$$|h\rangle = \sum_a U_a \,|a\rangle \tag{4.32}$$

where U_a and m_a are the mixing angles and the eigenmasses. Their value determines the physical evolution of the Higgs state. For instance, the spatial integral of the Higgs propagator measures the transition amplitude from $|h\rangle$ to $|h\rangle$ in time t:

$$A(t) = \langle h, t|h, 0\rangle = 2m_h \int d^{d-1}x \langle h(\vec{x}, t) h(\vec{0}, 0)\rangle = \sum_a |U_a|^2 e^{-im_a|t|}. \tag{4.33}$$

It is convenient to consider the Fourier transform of the amplitude for $\omega \simeq m_h$:

$$\widehat{A}(\omega) = \int_{-\infty}^{\infty} dt\, e^{i\omega t} A(t) \simeq \sum_a \frac{i|U_a|^2}{\omega - m_a + i\varepsilon} . \tag{4.34}$$

In practice, due to the large number of Kaluza-Klein levels, to compute the precise values of the U_a's and the m_a's is a hard task. Furthermore, some of the eigenmasses m_a will be very close to m_h and perturbation theory does not apply for them. These technical difficulties are concretely appreciated formally extracting the Higgs propagator from the action (4.31) and using it to compute (4.34):

$$\widehat{A}(\omega) \simeq \frac{i}{\omega - m_h + \frac{1}{2m_h}\Sigma(\omega^2) + i\varepsilon} , \tag{4.35}$$

where we used that the sum is dominated by states with $m_a \simeq m_h$ in the limit of small mixing, $\Sigma(p^2)$ is obtained from the resummation of infinite insertions of the mixing terms and it has poles at each value of $\vec{n}^2/R^2$:

$$\Sigma(p^2) = -\frac{m_{mix}^{4-\delta}}{V_\delta} \sum_{\vec{n}} \frac{1}{p^2 - \vec{n}^2/R^2 + i\varepsilon} . \tag{4.36}$$

Clearly this is a badly behaved function on the real axis. Fortunately, as we argue below, its detailed structure is not needed to determine the amplitude $A(t)$ for sufficiently short times, such that we do not resolve the individual oscillations in eq. (4.33).

The crucial technical remark is the following. While the sum in eq. (4.36) has a highly singular behaviour on the real axis, it may be approximated by a regular function in the complex plane as long as $\mathrm{Im}[p^2] \gg 1/n_p$, where $n_p = dn/dp^2 \sim p^{\delta-2} V_\delta$ is the density of Kaluza-Klein states with mass $m^2 = p^2$. Indeed, in this case we expect the effects of the individual poles to average out and produce a smooth behaviour. Concretely, this means that replacing the infinitesimal ε with a finite $\bar{\varepsilon} \gg 1/n_p$ in eq. (4.36) we can approximate the sum with an integral as follows:

$$\begin{aligned} \sum_{\vec{n}} \frac{1}{p^2 - \vec{n}^2/R^2 + i\bar{\varepsilon}} &= \int d^\delta n \frac{1}{p^2 - \vec{n}^2/R^2 + i\bar{\varepsilon}} + \mathcal{O}\left(\frac{1}{\bar{\varepsilon}}\right) \\ &= R^\delta \int d^\delta q_\perp \frac{1}{p^2 - q_\perp^2 + i\bar{\varepsilon}} \left[1 + \mathcal{O}\left(\frac{1}{n_p \bar{\varepsilon}}\right)\right] . \end{aligned} \tag{4.37}$$

In the limit $V_\delta \to \infty$, we can always choose $\bar{\varepsilon}$ much bigger than $1/n_p \sim 1/V_\delta$ and much smaller than any other laboratory energy or inverse time. With this choice, we can compute the imaginary part of Σ treating $\bar{\varepsilon}$ as infinitesimal

$$\mathrm{Im}\left[\Sigma(p^2 + i\bar{\varepsilon})\right] \simeq \frac{\pi}{2}\frac{\Omega_{\delta-1}}{(2\pi)^\delta} m_{mix}^{4-\delta} p^{\delta-2} \,. \tag{4.38}$$

Rescaling $\bar{\varepsilon} \to \bar{\varepsilon}\, m_h$ and defining $n'_\omega = dn/d\omega|_{\boldsymbol{p}=0} \sim \omega^{\delta-1} V_\delta$, we find that $\widehat{A}(\omega + i\bar{\varepsilon})$ takes the following form

$$\widehat{A}(\omega + i\bar{\varepsilon}) \simeq \frac{i}{\omega + i\bar{\varepsilon} - m_h - i\frac{\Gamma_h}{2}}\left[1 + \mathcal{O}\left(\frac{1}{\bar{\varepsilon} n'_\omega}\right)\right] , \tag{4.39}$$

where we defined the *width* for the Higgs as

$$\Gamma_h = \frac{1}{m_h}\mathrm{Im}\left[\Sigma(m_h^2 + i\bar{\varepsilon})\right] \simeq \frac{\pi}{2}\frac{\Omega_{\delta-1}}{(2\pi)^\delta}\frac{m_{mix}^{4-\delta}}{m_h^{3-\delta}} \,. \tag{4.40}$$

Notice that the width is well defined in the infinite volume limit. We assume $m_{mix} \ll m_h$ so that the width can be treated as a perturbative correction to the mass for $\delta \leq 3$, $\Gamma_h \ll m_h$. [9] To appreciate the physical significance of this formula, notice that we can compute the inverse transform of eq. (4.34) integrating on a contour with $\mathrm{Im}\,[\omega] = \bar{\varepsilon}$. This gives

$$A(t) = \int_{-\infty}^{\infty} d\omega\, \widehat{A}\,(\omega + i\bar{\varepsilon})\, e^{-i(\omega + i\bar{\varepsilon})t} \simeq e^{-im_h t - \frac{\Gamma_h}{2}t}\left[1 + \mathcal{O}\left(\frac{e^{\bar{\varepsilon}t}}{\bar{\varepsilon} n'_{m_h}}\right)\right] , \tag{4.41}$$

where we used (4.39) to compute the right hand side. As we anticipated, for sufficiently short times, $t \ll 1/\bar{\varepsilon} \ll n'_{m_h}$, the various oscillations in eq. (4.33) sum up to give an exponential decay $\sim e^{-\Gamma_h t/2}$. Intuitively, this means that the Higgs excite the single-particle modes of the higher-dimensional fields, which escape in the large extra-dimension and come back only after a large time $\Delta t \sim n'_{m_h} \sim m_h^{\delta-1} V_\delta$. Notice that to actually observe this decaying behaviour we need $n'^{-1}_{m_h} \ll \Gamma_h$, so that we can choose $\bar{\varepsilon}$ small enough. We also remark that we can think of the limit of large extra dimensions as that of an heavy Higgs, $m_h = 1/r_h \gg R^{-1}$, where r_h is the Compton wavelength of h.

It is useful to present a complementary viewpoint. Physically, in the limit of large extra dimensions the spectrum of the theory becomes increasingly dense and it can be approximated by a continuum; therefore, for an experimental apparatus which is not able to resolve the single modes, the mixing between the physical Higgs and the quasi-continuum of Kaluza-Klein modes effectively results in a width for the Higgs. We can make this remark concrete modeling the detector with a Lorentzian function with center ω_0 and width L:

---

[9] Notice that this is a natural condition since m_{mix} is the only parameter breaking the shift symmetry of H (or, more precisely, of its zero mode $H^{(\vec{n}=0)}$).

$$f_{\omega_0}^{(L)}(\omega) = \frac{L/\pi}{(\omega-\omega_0)^2+L^2} = f_{\omega}^{(L)}(\omega_0)\,. \tag{4.42}$$

The width L provides the resolution of the experiment. A physical measurement corresponds to the convolution of eq. (4.42) with the amplitude in Fourier space:

$$\widehat{A}_{mes}(\omega_0) = \int_{-\infty}^{\infty} d\omega\, f_{\omega_0}^{(L)}(\omega)\widehat{A}(\omega)\,. \tag{4.43}$$

Expressing $\widehat{A}(\omega)$ as a sum via eq. (4.34) and using the identity

$$\int_{-\infty}^{\infty} d\omega\, f_{\omega_0}^{(L)}(\omega)\frac{i}{\omega-m+i\varepsilon} = \frac{i}{\omega_0-m+iL}\,, \tag{4.44}$$

we conclude that the outcome of the measurement (4.43) coincides with the Fourier amplitude evaluated at $\mathrm{Im}[\omega]=L>0$:

$$\widehat{A}_{mes}(\omega_0) = \widehat{A}(\omega_0+iL)\,. \tag{4.45}$$

In particular, if the resolution of the physical apparatus is much larger than the level separation $L\gg 1/n'_{m_h}$, we can use the continuum approximation discussed before and the result of the measurement coincides with eq. (4.39).

4.3.2 Correlators of the non-Abelian current in $SU(2)$-invariant CFTs

Consider a CFT invariant under an internal $SU(2)$ group. The most general NREFT describing its large charge sector is given by eq. (4.22) for $N=3$. The gapped Goldstone allows to match in the NREFT operators transforming in non-trivial representations of the internal group. Notably, from the action (4.22) we may compute the Noether currents for the internal generators. The Noether current for $\widehat{Q}_3=\widehat{T}_{12}$ reads exactly as in the $U(1)$ case (3.29) to linear order in fluctuations. Its long distance correlators are determined by exchanges of the gapless Goldstone only and the same results of sec. 3.3 hold in this case as well. More interestingly, we can compute the currents for the non-Abelian generators $\widehat{Q}_\pm=\widehat{T}_{23}\pm i\widehat{T}_{31}$. Focusing on the time components as in sec. 2.3, to leading order in fields and derivatives these are proportional to the gapped Goldstone field:

$$J_+^0(t,\hat{n}) \simeq -3ic_1\mu^2\pi_1(t,\hat{n})\,,\qquad J_-^0(t,\hat{n}) \simeq 3ic_1\mu^2\pi_1^*(t,\hat{n})\,. \tag{4.46}$$

In this section we will analyze the four-point function with two insertions of these currents. In the NREFT this corresponds to the two-point function in the superfluid background:

$$G_{J_+J_-}(t,\hat{n}_2\cdot\hat{n}_1) \equiv \langle Q|T\left\{J_+^0(t,\hat{n}_2)J_-^0(0,\hat{n}_1)\right\}|Q\rangle\,. \tag{4.47}$$

As we explained in sec. 2.3, the correlator (4.47) has a non-trivial long-distance limit, corresponding to the exchange of a single gapped Goldstone mode. Since this is in general a resonant mode, we expect the NREFT to provide predictions only for sufficiently short times, analogously to eq. (4.41).

Before presenting the NREFT result, it is useful to analyze the OPE decomposition of the correlator (4.47). This will allow us quantitatively identifying the regime for which the NREFT predictions will apply.

The s-channel conformal block expansion for the correlator (4.47) in Lorentzian time reads:

$$\begin{aligned} G_{J_+J_-}(t,\hat{n}_2\cdot\hat{n}_1) = \theta(t)&\left[\frac{Q}{8\pi^2R^4}+\sum_{\ell=1}^{\infty}\sum_{\phi_A^{(\ell)}}\left|\lambda^{(\ell)}_{A,J_-,Q}\right|^2 e^{-i(\Delta_A-\Delta_Q)t}P_\ell(\hat{n}_2\cdot\hat{n}_1)\right] \\ &+\theta(-t)\sum_{\ell=1}^{\infty}\sum_{\bar{\phi}_A^{(\ell)}}\left|\lambda^{(\ell)}_{\bar{A},J_+,Q}\right|^2 e^{i(\bar{\Delta}_A-\Delta_Q)t}P_\ell(\hat{n}_2\cdot\hat{n}_1)+\dots\,, \end{aligned} \tag{4.48}$$

where $P_\ell(x)=C_\ell^{(1/2)}(x)$ are the Legendre polynomials. Here we used the leading order expression (3.52) for the conformal blocks and separated the sum over exchanged operators according to their spin. The contribution which is constant in space is fixed by the internal symmetry; indeed, using $\widehat{Q}_+\left|Q\right\rangle=0$, the $SU(2)$ algebra implies

$$\langle Q|\widehat{Q}_+\widehat{Q}_-|Q\rangle=\langle Q|[\widehat{Q}_+,\widehat{Q}_-]|Q\rangle=2Q\,,\qquad \widehat{Q}_\pm=R^2\int d\Omega\, J^0_\pm\,. \tag{4.49}$$

From the point of view of the OPE $J^0_-\times\mathcal{O}_Q$, this corresponds to the exchange of the component with $Q_3=Q-1$ of the operator $\mathcal{O}_Q$. The sum in the first line of eq. (4.48) runs over the operators ϕ's contained in the OPE $\mathcal{O}_Q\times J^0_-$, which have charge $Q_3=Q-1$; in the second line we sum over the operators $\bar{\phi}$'s included in the OPE $\mathcal{O}_Q\times J_+$, which instead have $Q_3=Q+1$. This implies that the scaling dimensions of the operators $\bar{\phi}$'s satisfy $\bar{\Delta}_A\geq\Delta_{Q+1}\approx\Delta_Q+R\mu$.

For times $t\gg 1/(R\mu)$, at which we expect to have an EFT description, we can neglect fastly oscillating terms. Since $\bar{\Delta}_A-\Delta_Q\gtrsim R\mu$ for all the operators contained in the OPE $\mathcal{O}_Q\times J_+$, we can neglect the second line in eq. (4.48). The only non-trivial contribution then comes from the exchange of primaries $\phi_A^{(\ell)}\subset J^0_-\times\mathcal{O}_Q$ with energy $\Delta_A\approx\Delta_Q\approx\Delta_{Q-1}+R\mu$, corresponding to (highest weight) gapped states from the point of view of the subspace of the Hilbert space at fixed $Q_3=Q-1$. This can also be seen considering the Fourier components of eq. (4.48) (neglecting the second line):

$$\begin{aligned}\widetilde{G}^{(\ell)}_{J_+J_-}(\omega) &= \int_{-\infty}^{\infty} dt\, e^{i\omega t} \int_0^1 dx P_\ell(x) G_{J_+J_-}(t,x) \\ &= \frac{i}{2\ell+1} \sum_{\phi_A^{(\ell)}} \frac{\left|\lambda^{(\ell)}_{A,J_-,Q}\right|^2}{\omega - (\Delta_A - \Delta_Q)/R + i\varepsilon}\end{aligned} \tag{4.50}$$

For $\omega^2 \ll \mu^2$, eq. (4.50) has poles on the real axis determined by states with energy Δ_A such that $|\Delta_A - \Delta_Q| \ll R\mu$.

Eq. (4.50) is analogous to the Higgs propagator (4.39) in the previous example. As in that case, we expect the effects of the individual poles to average out for sufficiently large $\text{Im}[\omega]$. In other words, we expect that replacing ε with a finite $\bar{\varepsilon}$ in eq. (4.50) we can approximate the sum with an integral over a continuous spectrum:

$$\widetilde{G}^{(\ell)}_{J_+J_-}(\omega + i\bar{\varepsilon}) = \frac{i}{2\ell+1} \int_{\Delta_{Q-1}}^{\infty} d\Delta \frac{\rho^{reg\,(\ell)}_{J_-,Q}(\Delta)}{\omega - (\Delta - \Delta_Q)/R + i\bar{\varepsilon}} \left[1 + \mathcal{O}\left(\frac{1}{\bar{\varepsilon}\, n^{(\ell)}_{\Delta_Q}}\right)\right], \tag{4.51}$$

where $n^{(\ell)}_{\Delta}$ is the density of states with energy Δ and spin ℓ exchanged by the $J_- \times \mathcal{O}_Q$ OPE, whose precise value we shall discuss later, and $\rho^{reg\,(\ell)}_{J_-,Q}(\Delta)$ is a suitable continuous approximation of the spectral density

$$\rho^{reg\,(\ell)}_{J_-,Q}(\Delta) \approx \rho^{(\ell)}_{J_-,Q}(\Delta) = \sum_{\phi_A^{(\ell)}} \left|\lambda^{(\ell)}_{A,J_-,Q}\right|^2 \delta\left(\Delta - \Delta_A\right). \tag{4.52}$$

The approximate equality $\approx$ here means that the two expressions behave similarly as distributions, i.e. when integrated against a sufficiently smooth function $f(\Delta)$ they produce the same result up to corrections of order $1/n^{(\ell)}_{\Delta_Q}$. Eq. (4.51) behaves as if it had a branch cut on the real axis, corresponding to an approximate continuum of states. Henceforth, for $\bar{\varepsilon} \gg 1/n^{(\ell)}_{\Delta_Q}$, the correlator (4.50) can be treated as a standard two-point function for a theory at infinite volume, and we expect the NREFT construction of chapter 2 to capture its behaviour. In particular, the mixing of the gapped Goldstone with states in the approximate continuum outside the NREFT implies the existence of a width for it.

The accuracy of the continuum approximation $\rho^{(\ell)}_{J_-,Q}(\Delta) \to \rho^{reg\,(\ell)}_{J_-,Q}(\Delta)$ depends on the spacing between the energy levels of the exchanged states in the correlator and the regularity of the OPE coefficient as a function of the scaling dimension Δ_A. In this respect, we expect the existence of two extreme situations, corresponding to the case of a weakly coupled CFT and of a strongly coupled one.

In a weakly coupled theory, to leading order in the coupling generically the gapped

Goldstone mixes only with two-particle states, as it happens in the deformation of the linear sigma model discussed in appendix A.2.2. Let us suppose that the gapped Goldstone mixes only with states made by two identical particles with gap much smaller than the cutoff, $m \ll R\mu$; for instance this would be the case in a theory in which the gapped Goldstone can decay into a pair of massless Goldstones, but the discussion applies also in the presence of a finite gap $m = cR\mu$ with $c < 1$. Recalling the rule for the tensor product of two identical $SU(2)$ representations $\ell_1 \otimes \ell_2 = |\ell_1 - \ell_2| \oplus (|\ell_1 - \ell_2| + 2) \oplus \ldots \oplus (\ell_1 + \ell_2)$, one easily estimates that the density of two-particle states with spin ℓ and gap $E \gtrsim \mu$ above the ground state grows linearly with the spin for $1 \ll \ell \ll R\mu$:

$$n_{\Delta_Q}^{(\ell)} \sim \ell \,. \tag{4.53}$$

In this case one also expects the matrix element for the gapped Goldstone field with the two-particle state to be a regular function of the angular momentum of the particles, and hence of the energy inverting the dispersion relations. [10] This situation is analogous to the discussion of the Higgs propagator in the previous section, and thus we expect that the continuum approximation in eq. (4.51) applies for $\bar{\varepsilon} \gg 1/\ell$. That the validity region of eq. (4.51) increases with ℓ could have been intuitively expected from the fact that the NREFT holds exactly in the infinite volume limit, and therefore should apply at sufficiently short distances.

Let us also speculate on the case of a strongly coupled theory. In this case the general expectation is that all states, and not only those made of two particles, contribute at the same order in the sum in eq. (4.50). In appendix B.5 we argue that the density of (all) states with fixed charge $Q_3 = Q - 1$ obeys the following exponential behaviour:

$$n_\Delta \propto \exp\left[b\left(\Delta - \Delta_{Q-1}\right)^{2/3}\right] , \tag{4.54}$$

where b is a positive number, of order one for a strongly coupled theory. In particular, when $\Delta - \Delta_{Q-1}$ is of the order of the mass of the gapped Goldstone, $\approx R\mu$, the typical spacing between energy levels is exponentially small in the EFT expansion parameter $1/R\mu$. Assuming a similar behaviour for the density of states at fixed spin ℓ, we expect that NREFT describes the correlator up to very small values of $\bar{\varepsilon}$, as long as $\bar{\varepsilon} \gg 1/n_{\Delta_Q}^{(\ell)} \sim e^{-b(R\mu)^{2/3}}$. [11]

---

[10] For instance, by rotational invariance the matrix element between the ℓ mode of π_1 and a state made of two particles with spin ℓ_1 and ℓ_2 is proportional to a three-j symbol, which admits a regular analytic expression for $|\ell_1 - \ell_2| \leq \ell \leq \ell_1 + \ell_2$.

[11] For a strongly coupled theory, however, we do not expect the OPE coefficients to be a smooth function of the energy of the exchanged operator; therefore the estimate of the error in eq. (4.51) might not be accurate. As an illustration, in appendix B.5 we show that, assuming the OPE coefficients to be described by an ansatz analogous to the eigenstate thermalization hypothesis [125], the corrections to the continuum approximation scale like $1/\sqrt{\bar{\varepsilon}\, n_{\Delta_Q}^{(\ell)}}$. Though a different ansatz might produce a different result, in practice $1/n_{\Delta_Q}^{(\ell)} \sim e^{-b(R\mu)^{2/3}}$ is non-perturbatively small in the EFT expansion parameter $1/R\mu$ and corrections are irrelevant as long as they scale with some negative power of $\bar{\varepsilon}\, n_{\Delta_Q}^{(\ell)}$.

After having identified the validity regime of the continuum approximation, and hence of the NREFT, it is straightforward to obtain the corresponding predictions. Extracting the propagator of the gapped Goldstone from the action (4.22), we find that the Fourier components of the correlator (4.47) are given by

$$\widetilde{G}^{(\ell)\,EFT}_{J_+J_-}(\omega+i\bar{\varepsilon})=\frac{Q}{8\pi^2R^4}\frac{i}{\omega+i\bar{\varepsilon}-(\epsilon^R_\ell-i\Gamma_\ell/2)}\left[1+\mathcal{O}\left(\frac{\omega^2}{\mu^2},\frac{J_\ell^2}{\mu^2}\right)\right], \tag{4.55}$$

where we estimated the corrections and separated explicitly the real and the imaginary part of ϵ_ℓ as

$$\epsilon_\ell=\epsilon^R_\ell-i\Gamma_\ell/2\,,\qquad \epsilon^R_\ell=\frac{\mathrm{Re}[c_m]}{2\mu}J_\ell^2\geq 0\,,\qquad \Gamma_\ell=-\frac{\mathrm{Im}[c_m]}{\mu}J_\ell^2\geq 0\,. \tag{4.56}$$

Then, according to eq. (4.51) we have

$$\widetilde{G}^{(\ell)}_{J_+J_-}(\omega+i\bar{\varepsilon})=\widetilde{G}^{(\ell)\,EFT}_{J_+J_-}(\omega+i\bar{\varepsilon})\left[1+\mathcal{O}\left(\frac{1}{\bar{\varepsilon}\,n^{(\ell)}_{\Delta_Q}}\right)\right]. \tag{4.57}$$

As already anticipated, the main prediction of the NREFT is that existence of a resonant pole in the correlator. In practice, to see the effect of the latter we need to take $\bar{\varepsilon}\ll J_\ell^2/\mu$. In the strongly coupled case we can always do that compatibly with the requirement $\bar{\varepsilon}\gg 1/n^{(\ell)}_{\Delta_Q}\sim e^{-b(R\mu)^{2/3}}$. Instead, in the weakly coupled case $n^{(\ell)}_{\Delta_Q}\sim\ell$ and thus we need $\ell\gg(R\mu)^{1/3}\sim Q^{1/6}$ for the resonant pole in eq. (4.55) to be a reliable prediction.

As in the previous section, upon transforming back to real time, this result implies the following decaying behaviour for the correlator in real time

$$G^{(\ell)}_{J_+J_-}(t)=\int d\omega\, e^{-i\omega t}\widetilde{G}^{(\ell)}_{J_+J_-}(\omega)\simeq\frac{6c_1\mu^2}{4\pi R^2}e^{-i\epsilon^R_\ell t-\frac{\Gamma_\ell}{2}t}\,,\qquad t\ll 1/n^{(\ell)}_{\Delta_Q}\,. \tag{4.58}$$

In other words, the EFT predicts that, for each ℓ, the various oscillations in eq. (4.48) conspire together to provide a decaying behaviour $e^{-\Gamma_\ell t/2}$ for sufficiently short time. Notice that, using (3.13), the EFT result for $\ell=0$ can be written as $\frac{Q}{8\pi R^4}$; this precisely agrees with the first term of eq. (4.48), whose value is fixed by the consistency of the $SU(2)$ algebra as explained above.

Finally, let us show how to use the NREFT to more directly access the CFT data of the theory. These are encoded in the spectral density (4.52) for the observable at hand. Unfortunately, the knowledge of the correlator for $\bar{\varepsilon}\gg 1/n^{(\ell)}_{\Delta_Q}$ is not enough to determine $\rho^{(\ell)}_{J_-,Q}(\Delta)$ precisely. However, we can extract information on an appropriately *smeared* version of the spectral density. It is particularly convenient to consider the following definition

$$\hat{\rho}^{(\ell)}_{J_-,Q}(\Delta)=\int d\tilde{\Delta}\, f^{(L)}_{\Delta}(\tilde{\Delta})\rho^{(\ell)}_{J_-,Q}(\tilde{\Delta})\,, \tag{4.59}$$

where $f^{(L)}_{\Delta}(\tilde{\Delta})$ is a Lorentzian function (4.42), with center Δ and width $L \gg 1/n^{(\ell)}_{\Delta_Q}$. Analogously to eq. (4.43), from the identity (4.44) we find that replacing the *true* spectral density with its smeared version (4.59) in eq. (4.50) is equivalent to considering the correlator at $\text{Im}[\omega] = L/R$:

$$\frac{i}{2\ell+1}\int d\Delta \frac{\hat{\rho}^{(\ell)}_{J_-,Q}(\Delta)}{\omega-(\Delta-\Delta_Q)/R+i\varepsilon} = \tilde{G}^{(\ell)}_{J_+J_-}\left(\omega+iL/R\right) , \tag{4.60}$$

where on the left-hand side the $+i\varepsilon$ just stands for the usual infinitesimal prescription. This equation holds for $\text{Im}[\omega] \geq 0$. In particular it holds also for $\omega \in \mathbb{R}$ and it can be inverted similarly to the Källén-Lehman decomposition in standard relativistic quantum field theory [126]. More precisely, using

$$\frac{1}{x+i\varepsilon} = P\frac{1}{x} - i\pi\delta\left(x\right) , \tag{4.61}$$

where P denotes the principal part, we conclude

$$\hat{\rho}^{(\ell)}_{J_-,Q}(\Delta) = \frac{1}{\pi}\text{Im}\left[i\,\tilde{G}^{(\ell)}_{J_+J_-}\left(\Delta/R-\Delta_Q/R+iL/R\right)\right] , \qquad \Delta \in \mathbb{R} . \tag{4.62}$$

We may now use the NREFT to systematically compute the right hand side of eq. (4.62) and determine the smeared spectral density. Let us consider for simplicity the strongly coupled case, for which we can always take L negligibly small. Then, using (4.55) we straightforwardly conclude that the smeared spectral density is a Lorentzian with width $\Gamma_\ell/2$, as it could have been intuitively expected:

$$\hat{\rho}^{(\ell)}_{J_-,Q}(\Delta) = \frac{Q(2\ell+1)}{8\pi^2R^4}\frac{R\Gamma_\ell/(2\pi)}{(\Delta-\Delta_Q-R\epsilon^R_\ell)^2+R^2\Gamma_\ell^2/4}\left[1+\mathcal{O}\left(\frac{J_\ell^2}{\mu^2},\frac{(\Delta-\Delta_Q)^2}{R^2\mu^2}\right)\right] . \tag{4.63}$$

In the weakly coupled case a similar prediction holds only for $\ell \gg Q^{1/6}$.

Notice that from eq. (4.59) we can also compute other moments of the spectral function. For instance consider the following "squared" Lorentzian with width $2L$:

$$h^{(2L)}_{\Delta}(\tilde{\Delta}) = \frac{16L^3/\pi}{\left[4L^2+(\Delta-\tilde{\Delta})^2\right]^2} , \tag{4.64}$$

Using the identities

$$\int d\Delta' f^{(L)}_{\tilde{\Delta}}(\Delta') f^{(L)}_{\Delta}(\Delta') = f^{(2L)}_{\Delta}(\tilde{\Delta}) , \tag{4.65}$$

$$\int d\Delta' h^{(L)}_{\tilde{\Delta}}(\Delta') f^{(L)}_{\Delta}(\Delta') = \frac{1}{2}f^{(2L)}_{\Delta}(\tilde{\Delta}) + \frac{1}{2}h^{(2L)}_{\Delta}(\tilde{\Delta}) , \tag{4.66}$$

we can compute the corresponding moment from $\hat{\rho}^{(\ell)}_{J_-,Q}(\Delta)$ as

$$\int d\tilde{\Delta}\, h^{(2L)}_{\Delta}(\tilde{\Delta})\rho^{(\ell)}_{J_-,Q}(\tilde{\Delta}) = \int d\tilde{\Delta} \left[2h^{(L)}_{\Delta}(\tilde{\Delta}) - f^{(L)}_{\Delta}(\tilde{\Delta})\right] \hat{\rho}^{(\ell)}_{J_-,Q}(\tilde{\Delta})\,. \tag{4.67}$$

Similar identities allow to compute different moments. This discussion should make clear that eq. (4.63) is independent of the precise function used to perform the smearing in eq. (4.59) as long as we can take the width L negligibly small compatibly with the requirement $L \gg 1/n^{(\ell)}_{\Delta_Q}$.

In summary, we have argued that the NREFT is expected to accurately describe the four-point function with two insertions of the non-Abelian current for sufficiently short times and distances. This statement is equivalent to the integral equation (4.60), which implies that the smeared spectral density (4.59) takes the Lorentzian shape typically associated with resonances. The precise region of validity of the NREFT and its predictions depend on the number of states contributing to the correlator, and may be very different for a weakly coupled and a strongly coupled theory.

Our analysis might be extended in several directions. For instance one could study correlation functions of different operators, e.g. primary scalars in non-trivial representations of $SU(2)$. Perhaps, ideas similar to those used in the Tauberian analyses of [127–130] might clarify the validity conditions of the continuous approximation in eq. (4.51). [12] Most importantly, one should also be able to probe our ideas in specific weakly interacting theories. For instance one could look for a model which can be studied in the ε-expansion, in which the gapped Goldstone decays in the infinite volume limit. Perhaps, one might also be able to study explicitly the strongly coupled case considering holographic theories, possibly along the lines of [132]. We leave these issues for future work.

---

[12] Notice however that, in those works, Tauberian theorems were used to analyze the moments of the distribution (4.52) for $\Delta \to \infty$ [131], while in the EFT we focus on $|\Delta - \Delta_Q| \ll R\mu$.

Conclusions to Part II

Perhaps a way to phrase the main difference between high energy physics and condensed matter physics is that high energy physics mostly occurs in the vacuum while condensed matter physics occurs at finite density. In a conformal field theory, this particular difference disappears: the state-operator correspondence maps finite density states to local operators and therefore maps finite density correlators to vacuum correlators.

This observation entails substantial simplifications in the study of operators with large global charge Q. Indeed, these are mapped to finite density states, for which the theory is generically found in a *condensed matter phase*. A particularly appealing scenario is provided by the possibility that the CFT is found in a superfluid phase. In that case, the parametric separation between the mass scale associated with the charge density and the compactification scale for the theory on the cylinder can be used to study the theory perturbatively, in a $1/Q$ expansion, by means of an EFT description. The structure of such an EFT follows from the requirement that the symmetries of the theory are realized *nonlinearly*, while the information on the specific CFT at hand is instead encapsulated in a finite number of Wilson coefficients at each order in the $1/Q$ expansion. In particular, its spectrum generically consists solely of the *hydrodynamic* Goldstone modes whose existence follows from the spontaneous breaking of the internal symmetries. As a consequence, a significant amount of *universality* is found in the structure of the CFT data of large charge operators.

The simplest case in which such a universal structure emerges is provided by theories with a $U(1)$ global symmetry, which we studied in chapter 3. In that case, the spectrum of lowest dimension operators at fixed charge is given by the Fock space of a single *phonon* mode, associated with the breaking of the $U(1)$ symmetry. Its propagator and interactions also control the structure of n-point functions in the long distance limit. Notably, the simple form of the EFT correlators nicely matches substantial simplifications for the conformal block expansion in the kinematic regime for which the EFT holds.

The same picture underlies the study of CFTs invariant under more general symmetry groups. Nonetheless, some novel interesting structural features are found for non-Abelian symmetry groups. This is mostly due to the existence of gapped Goldstones in non-Abelian superfluids, whose description is naturally phrased within the NREFT framework that we presented in chapter 2. We analyzed the consequences of that construction for CFTs in chapter 4. We have argued that the spectrum of lowest dimension operators at fixed charge is generically determined only by the Goldstone modes associated with the breaking of the Cartan generators of the group. As a notable exception, we studied the spectrum of the three dimensional critical $O(N)$ models, in which case gapped Goldstones are naturally associated with operators transforming in mixed-symmetric representations of the group. Finally, we addressed the complications related to the existence of mixings between the gapped Goldstones and other states outside the NREFT. In particular, focusing on an $SU(2)$ internal group, in sec. 4.3 we showed that the NREFT provides access to certain *inclusive* features of the spectral distribution of the four-point function with two insertions of the non-Abelian current in between the superfluid ground-state. We expect our results to be easily generalizable to different operators, such as scalars in non-trivial representations of $SU(2)$, as well as to allow for the study of different symmetry groups via similar techniques. On a different note, the NREFT construction should also allow to rigorously analyze the *gapped Goldstino* mode which arises in the superfluid phase of superconformal field theories at large R-charge [34].

Our results apply to any CFT whose large charge sector is described by the EFT we presented. To be clear, we have not proved that there actually exists any such CFT. However, what are the possibilities? Given a state with finite charge density, the internal symmetry may or may not be (classically) spontaneously broken. If it is broken, then the state is a superfluid and our results generically apply. If it is not broken, then the state is not a superfluid and our results do not apply. Because superfluids are such a natural possibility, we believe that there exists a large class of CFTs to which our results apply. This question has been framed within the conformal bootstrap in [109].

Clearly, it should be possible to explicitly identify such CFTs. A natural possibility is to explore theories that are amenable to a perturbative treatment. We shall pursue this idea in part IV of this thesis, where, also motivated by the analogy with the problem of multi-particle production in massive QFTs [133], we will study large charge operators in the ε-expansion (see also [134,135] for related works). Other works [136–141] focused on the large N expansion, e.g. for monopole operators in gauge theories [104, 111, 142–147]. Related to large N, large charge states have also been studied via the AdS/CFT correspondence under the name of "holographic superconductors" [132, 148–151]. [13] We also mention that similar ideas have been applied in the context of non-relativistic CFTs [155–157], in which case they might be experimentally testable for the "unitary Fermi gas" system in a harmonic trap.

---

[13] Another candidate for a large charge state at zero temperature in AdS is an extremal Reissner-Nordström black hole [152–154], which however does not break the internal symmetry [132]; it would be interesting to identify the CFT dual of such AdS state.

As already mentioned at the beginning of sec. 4.2, a very promising direction is provided by the possibility of using Monte-Carlo simulations to explore the spectrum of charged operators in the three dimensional $O(N)$ models. The first steps in this direction were taken in [118], where the scaling dimension of the lowest dimension operators with charge $Q = 1, \ldots, 15$ were calculated for the $O(2)$ model. Surprisingly, despite the relatively modest values of Q accessed so far, the results are in remarkable agreement with the prediction for Δ_Q in eq. (3.19), whose first two coefficients α_1 and α_2 were determined by numerical fit. A similar analysis was performed in the $O(4)$ model in [119], for traceless symmetric operators with charge $T_{12} = 1, \ldots, 10$. Future explorations might extend these analyses to larger values of the charges and access other observables, such as OPE coefficients or the scaling dimensions of operators in mixed symmetric representations in the $O(4)$ model [121]. Hopefully, these analyses will provide non-perturbative checks of the universal predictions of the large charge expansion.

In the future, it would also be interesting to further explore the application of bootstrap techniques to the study of operators with large internal quantum numbers, along the lines of [109]. Perhaps, this might allow relating explicitly the Wilson coefficients of the large charge EFT with the CFT data of light operators, whose value is known, in certain cases, through the numerical bootstrap.

In supersymmetric theories, the presence of moduli spaces might imply the existence of additional light degrees of freedom in the superfluid phase. [14] A situation of this kind was studied in detail for $\mathcal{N} = 2$ superconformal gauge theories at large R-charge. In [102, 158–160] a non-relativistic axion-dilaton effective Lagrangian was used to obtain detailed predictions for the correlations functions of operators saturating or *nearly* satisfying the BPS bound. Those results were further confirmed in [161] via localization techniques in a perturbative gauge theory. These studies are reminiscent of previous works on the BMN limit of $\mathcal{N} = 4$ supersymmetric Yang-Mills (SYM) theory [162] (see [163–165] for reviews and [166, 167] for a recent revival of similar ideas), in which case it was proven that the plane-wave limit for the geometry of the dual string theory corresponds to a large R-charge sector for the field theory.

As already remarked, superfluids are not the only possible phase which can describe the large charge sector of a CFT. For instance, a very natural possibility for a fermionic theory is given by a Fermi liquid [46, 47]. Perhaps, future work in this direction might also provide a different perspective on the ideas recently explored in [48–50], concerning the Goldstone phenomenon for the breaking of spacetime symmetries in this phase.

The most universal quantum numbers characterizing the CFT data are the spin and the scaling dimensions themselves. Recently, the analytic bootstrap has been used to study systematically double-trace operators in a large spin expansion [168–172]. Remarkably, these results have been proved to be associated with precise analyticity properties of the

---

[14] This also happens for free massless scalar theories [109].

CFT data as a function of the spin [173–175]. In particular, similarly to the phonon spectrum as a function of the charge, the twist spectrum of the CFT is organized in Regge trajectories as a function of the spin. It should be possible to find a semiclassical description of these results. Motivated by this question, we initiate the study of operators with large charge and large spin in the next part of this thesis.

Relatedly, building on previous studies [127, 128] on the convergence properties of the OPE based on Tauberian theorems [131], a recent work [129] initiated the bootstrap study of neutral operators with large scaling dimensions for CFTs in more than two dimensions (see [130] and references therein for more works in $2d$ CFTs). Somewhat similarly to our analysis in sec. 4.3, focusing on a four-point function of identical scalars, the authors were able to unveil certain universal properties for the integrated moments of the spectral density. Relatedly, a semiclassical description for the OPE coefficients of a light operator in between two generic heavy states has been proposed in [176], based on the eigenstate thermalization hypothesis [125] and the field theoretical formulation of hydrodynamics [177]. Future works, both from the bootstrap and the semiclassical point of view, might provide new interesting results on the universal features of the CFT data of heavy operators.

Part III

Rotating superfluids and spinning charged operators in CFTs

In part II we showed that effective field theory techniques allow studying the CFT data of charged operators in an expansion in inverse powers of the internal charge. In an independent line of research, the conformal bootstrap was used to study the CFT operator spectrum at large spin J [169,170]. Remarkably, from the solution of the crossing equations in the lightcone limit precise analytic results on the spectrum of operators at large spin were obtained, with $1/J$ playing the role of the expansion parameter. This motivates the following question: can large spin operators also be studied using EFT techniques?

In this part of the thesis, we will take some step forward towards answering this question via the following, perhaps obvious, approach: we start with the large charge operators studied in chapter 3 and then proceed by adding increasing amounts of spin to them. This translates to adding angular momentum to the corresponding superfluid. Experimentally, when enough angular momentum is added to a superfluid in the laboratory, vortices develop [178]. We thus expect large spin charged operators to correspond to vortices moving in the superfluid.

Focusing on the illustrative case of a CFT invariant under a $U(1)$ symmetry, in this part of the thesis we will study operators that have large spin as well as large charge. Making use of the recently developed EFT for describing vortices in superfluids [179], we will find that the lowest energy state corresponds to an increasing number of vortices as the spin is varied from the scale set by the charge density to the value of the energy density: $j_0 \sim Q^{\frac{1}{d-1}} \ll J \ll \Delta_0 \sim Q^{\frac{d}{d-1}}$. This range of spins is disjoint from the range in which the lightcone bootstrap results are valid, which apply to operators parametrically close to the unitarity bound. Therefore our results are complementary to the bootstrap ones.

The physics of vortices depends on the number of spacetime dimensions d and, consequently, so does the detailed form of our results. This nicely matches the fact that the irreducible representations of the rotation group, which label CFT operators, depend on d. We will conveniently discuss first the simple case of a $3d$ CFT in chapter 5. We will then extend our results to four dimensions in chapter 6, where we will also briefly comment on $d > 4$.

In this part of the thesis we shall follow the approach reviewed in sec. 3.2.2. We begin by considering a d dimensional CFT on a cylinder $\mathbb{R} \times S^{d-1}$. Next, we assume that a given EFT on this cylinder is a valid description of our CFT. Finally, we apply the state-operator correspondence directly to the states of this EFT. This strategy differs from that of sec. 3.1, which takes the "top-down" approach of projecting onto a desired state using the Euclidean path integral. Instead, we are taking the "bottom-up" approach of simply assuming an EFT and then quantizing its Hamiltonian while always remaining in Lorentzian spacetime.

5 Spinning charged operators and vortices in $3d$ CFTs

As explained in the introduction to this part of the thesis, we expect large charge operators with large spin to correspond to vortices in the superfluid. However, the conformal superfluid EFT [34, 35] discussed in chapter 3 does not incorporate vortices; all angular momentum is carried by phonons alone. This suggests that the EFT would incorrectly describe high angular momentum states. Conveniently, vortices can be included in the EFT as heavy topological defects following the construction of [179] (see also [180–182] for previous works in this direction). In this chapter we will use this EFT to study operators that have large spin as well as large charge in a three dimensional CFT invariant under an internal $U(1)$ symmetry.

5.1 Summary of Results

We calculated the dimension Δ of the lowest dimension operator with charge $Q \gg 1$ and spin J. [1] As J varies from 0 to Δ, the corresponding superfluid state passes through three qualitatively distinct regimes. We will simply state the results now and derive them later. In the following, we use Δ_Q for the energy of the homogeneous ground state

$$\Delta_Q = \alpha_1 Q^{3/2} + \alpha_2 Q^{1/2} - 0.0937 + \dots \; . \tag{5.1}$$

- For $0 \leq J \lesssim \sqrt{Q}$, the lowest energy state has no vortices and consists of a single phonon of angular momentum J. The corresponding operator dimension Δ is given by eq. (3.25) as
$$\Delta = \Delta_Q + \sqrt{\frac{J(J+1)}{2}} + \mathcal{O}\left(\frac{J^3}{Q}\right) \; . \tag{5.2}$$

---

[1] In order to avoid confusion with the spin J, in this part of the thesis we denote the $U(1)$ current with lower case as j_μ.

- For $\sqrt{Q} \lesssim J \leq Q$, the lowest energy state consists of a vortex-antivortex pair whose separation increases with J. The corresponding operator dimension Δ is

$$\Delta = \Delta_Q + \frac{\sqrt{Q}}{3\alpha_1} \log \frac{J}{\sqrt{Q}} + 2\tilde{\gamma}\sqrt{Q} + \mathcal{O}\left(\sqrt{Q} \times \frac{Q}{J^2}\right) , \tag{5.3}$$

  where $\tilde{\gamma}$ is a new Wilson coefficient of the vortex EFT.

- For $Q < J \lesssim Q^{3/2}$, the lowest energy state consists of multiple vortex-antivortex pairs distributed so that the superfluid has the same velocity profile as that of a rotating rigid body [183]. The corresponding operator dimension Δ is

$$\Delta = \Delta_Q + \frac{1}{2\alpha_1} \frac{J^2}{Q^{3/2}} + \mathcal{O}\left(\frac{J^2}{Q^{3/2}} \times \frac{Q}{J}, \frac{J^2}{Q^{3/2}} \times \frac{J^2}{Q^3}\right) . \tag{5.4}$$

As $J \to Q^{3/2} \sim \Delta$, the EFT breaks down and, as mentioned, we are unable to reach the spin of the operators studied by the analytic bootstrap [169–172, 184–190]. Remarkably, the leading correction to Δ_Q due to the presence of the vortices depends on the same parameter α_1 controlling the leading contribution in eq. (5.1).

The rest of the chapter is organized as follows. In sec. 5.2 we provide a simple discussion of a vortex configuration based on the EFT of chapter 3. In sec. 5.3 we formulate the effective theory for vortices, which we use in sec. 5.4 to derive the results. In sec. 5.5 we provide predictions for correlators involving a current insertion between two vortex states. We present some generalizations of our results in sec. 5.6, discussing weakly coupled or large N theories, and extending our predictions to the case in which the vortices carry spin and to a $U(1)^2$-invariant CFT.

5.2 Spinning superfluid: vortices and singularities

Consider the conformal superfluid Lagrangian in $d = 3$. In Lorentzian signature, this is given by:

$$\mathcal{L}/\sqrt{g} = c_1(\partial\chi)^3 + c_2(\partial\chi)\left\{\mathcal{R} + 2\frac{[\partial_\mu(\partial\chi)]^2}{(\partial\chi)^2}\right\} + \dots . \tag{5.5}$$

We are interested in the scaling dimension of the lowest dimension operator as a function of the charge Q and spin J. As a first attempt, we look for such state in the phonon Fock space discussed in sec. 3.2.2. We have two obvious ways to construct states with angular momentum J: one phonon with spin J and n phonons with spin J/n. The energy of the single phonon state is given by eq. (5.2). For $J \gtrsim \sqrt{Q}$ higher derivative terms become unsuppressed and the expression (5.2) cannot be trusted anymore. For the second class of states we have instead

$$\Delta_{n\ phonons} = \Delta_Q + \frac{J}{\sqrt{2}}\sqrt{1+\frac{n}{J}} + \mathcal{O}\left(J \times \frac{J^2/n^2}{Q}, J \times \frac{J/n}{\sqrt{Q}} \times \frac{n}{Q}\right) , \qquad J \ll Q^{3/2} . \tag{5.6}$$

These states can be reliably described within the EFT as long as the phonon density is much smaller than the charge density, $n \ll Q$, and the angular momentum of the single phonons is much smaller than the chemical potential, [2] $J/n \ll \sqrt{Q}$; this provides the upper bound for J in eq. (5.6).

Comparing eq.s (5.2) and (5.6), we conclude that for $J \ll \sqrt{Q}$ the minimal energy state is given by a single phonon. As we increase J the latter exits the validity of the EFT and we might naively expect that for $\sqrt{Q} \ll J \ll Q^{3/2}$ the ground state is provided by the multi-phonon states in eq. (5.6). However, experimental evidence shows that superfluids admit a third kind of spinning excitation: vortices.

From the point of view of the EFT for the superfluid Goldstone, the latter are stationary solutions of the equations of motion with non-zero winding number. This means that there exist a set of points $\{x_p\}$ for which $\oint_{\mathcal{C}(x_p)} dx^i \partial_i \chi = 2\pi n_p$ with $n_p \in \mathbb{Z} \setminus \{0\}$, where $\mathcal{C}(x_p)$ is an arbitrary curve encircling a single point x_p of the set $\{x_p\}$. Notice that the value of n_p, also called the vorticity, is conserved in time, since the winding number is the charge associated to the one-form symmetry generated by the topological current $j_{\mu\nu} = \sqrt{g}\epsilon_{\mu\nu\rho}\partial^\rho \chi$ [58]. Such solutions are unavoidably singular at the points $\{x_p\}$, the positions of the vortex cores, at which the EFT description (5.5) breaks down.

To build an EFT description of vortices, we can treat them as point-defects moving in the superfluid, including their action to the effective theory. This requires the use of a *dual* formulation of the superfluid EFT. We shall detail the procedure in sec. 5.3. However, the basic features of vortex physics may be understood with an intuitive *naive* approach, simply considering the Lagrangian (5.5) equipped with a short-distance cutoff to regularize the singularities close to the vortex cores. Here we illustrate this procedure. The results presented below will be derived again more carefully in sec. 5.4.4.

For the sake of concreteness, let us consider the following solution for χ:

$$\chi = \mu t + \phi \,, \tag{5.7}$$

where ϕ is the azimuthal angle on the sphere. The solution (5.7) is singular at the poles, $\theta = 0$ and $\theta = \pi$, around which χ has a non zero winding number. On the solution (5.7) the charge and the spin density coincide and are given by

$$j_0 = R\, T_{0\phi} = 3c_1\mu^2 \sqrt{1 - \frac{1}{R^2\mu^2\sin^2\theta}} - \frac{2c_2}{R^2}\frac{1}{\sqrt{1-\frac{1}{R^2\mu^2\sin^2\theta}}} + \ldots \,. \tag{5.8}$$

The charge density is approximately given by the one for the superfluid solution $\chi = \mu t$ everywhere, but for θ close to 0 and π, for which the expression (5.8) is singular. Physically, the effective superfluid description breaks at the south and the north poles. To compute the charge and the energy, we regulate spatial integrals introducing a cutoff at distances $R\delta\theta \gtrsim \Lambda_v^{-1}$ from the poles. Physically Λ_v^{-1} parametrizes the size of the vortices, which depends on the UV details of the underlying theory. By dimensional analysis and scale invariance, we expect it to be of order $1/\mu$, hence we can parametrize our ignorance on the latter via the dimensional ratio $x \equiv \Lambda_v/\mu \sim \mathcal{O}(1)$. We then find the charge, the angular momentum and the energy of the state as:

---

[2] This is due to the second kind of corrections in eq. (5.6), arising from interaction terms $\sim (\partial\pi)^4/\mu$.

$$Q = J = 12\pi c_1 R^2\mu^2 - \frac{2c_2}{R^2} - 6c_1\pi\log(R\mu) + f_Q\left(\frac{\Lambda_v}{\mu}\right) + \mathcal{O}\left(\frac{1}{R^2\mu^2}\right) , \tag{5.9}$$

$$E = 8\pi c_1 R^2\mu^3 + \mu\, f_E\left(\frac{\Lambda_v}{\mu}\right) + \mathcal{O}\left(\frac{1}{R\mu}\right) , \tag{5.10}$$

where $f_Q(x)$ and $f_E(x)$ are dimensionless functions; their detailed form will not be relevant in what follows. [3] The first and second term in eq. (5.9), as well as the first one in (5.10), are the contribution of the homogeneous superfluid density and are present also in the absence of vortices. The new pieces represent instead the contribution of the vortices. Their precise value depend on Λ_v, and cannot be fully fixed within the EFT. However, vortices also provide a logarithmically enhanced contribution $\log\Lambda_v \sim \log\mu$ in eq. (5.9), coming from the integration region where θ is close to 0 or π in the charge. As typical in QFT, logarithms of the cutoff scale are well definite predictions of the theory. To see this, let us solve eq. (5.9) for μ and plug the result in the expression for the energy. Using the state-operator correspondence, we then find that the vortex profile in eq. (5.7) correspond to an operator with the following quantum numbers

$$\Delta = \Delta_Q + \frac{\sqrt{Q}}{6\alpha_1}\log Q + 2\tilde{\gamma}\sqrt{Q} + \mathcal{O}\left(\sqrt{Q}\times\frac{Q}{J^2}\right) , \qquad J = Q\,. \tag{5.11}$$

Here $\tilde{\gamma}$ is a numerical coefficient of order one, whose precise value depends on the ratio Λ_v/μ. The second term in (5.11), proportional $\sqrt{Q}\log Q$, provides the leading correction to the ground state energy and, remarkably, does not depend on the precise value of the short distance cutoff Λ_v. Comparing eq.s (5.11) and (5.6), we also see that the vortex state has lower energy than a multi-phonon state with the same angular momentum.

In the next section, we shall discuss how the structure of result (5.11) arises in a more systematic setup. We shall see in particular that the action for the vortices, to leading order, depends on a single dimensionless Wilson coefficient, analogous to the ratio Λ_v/μ in this discussion. The logarithmic term in eq. (5.11) will then be interpreted as a

---

[3] We give them here for completeness; cutting off the integration over the angle θ at a distance $\arcsin[1/(R\Lambda_v)]$ from the poles, with $\Lambda_v < \mu$, we find

$$f_Q(x) = -3\pi c_1\left[\frac{2\sqrt{1-x^2}}{x^2} + 2\log\left(\frac{x}{\sqrt{1-x^2}+1}\right) + 1 + \log(16)\right] ,$$

$$f_E(x) = -6\pi c_1 - 4\pi c_1\frac{\left(1-x^2\right)^{3/2}}{x^2} .$$

renormalization of the latter, due to the self-energy of the vortex core induced by the interaction with the superfluid, which depends only on the vorticity. Throughout this chapter, unless otherwise stated, we shall work at leading order in the derivative and field expansion within EFT.

5.3 Formulation of the EFT

5.3.1 Dual gauge field

We now specialize the construction of [179] to the cylinder $S^2 \times \mathbb{R}$. The latter uses a dynamical gauge field A_μ instead of the more familiar Goldstone field χ. To relate the two descriptions, we dualize χ by formally treating $v_\mu \equiv \partial_\mu \chi$ as an independent variable and using a Lagrange multiplier A_μ to set the curl of v_μ to zero:

$$\mathcal{L} = c_1 v^3 - \frac{1}{2\pi} A_\mu \frac{\epsilon^{\mu\nu\rho}}{\sqrt{g}} \partial_\nu v_\rho, \tag{5.12}$$

where we use the combination $\epsilon^{\mu\nu\lambda}/\sqrt{g}$ to denote the antisymmetric Levi-Civita *tensor*. Integrating out v_μ gives

$$\mathcal{L} = -\kappa F^{3/2}, \tag{5.13}$$

where $F \equiv \sqrt{F_{\mu\nu}F^{\mu\nu}}$ and $F_{\mu\nu} \equiv \partial_\mu A_\nu - \partial_\nu A_\mu$. We dropped a boundary term that came from integrating (5.12) by parts because it is metric independent and thus does not affect the energy momentum tensor. The coefficient κ in (5.13) is related to the coefficient c_1 in (5.5) as $\kappa = \frac{1}{2^{5/4}(3\pi)^{3/2}} \frac{1}{\sqrt{c_1}}$.

The relation between χ and A_μ is given by the expression for the $U(1)$ current j^μ:

$$j^\mu = 3c_1(\partial\chi)\partial^\mu\chi = \frac{1}{4\pi} \frac{\epsilon^{\mu\nu\lambda}}{\sqrt{g}} F_{\nu\lambda}. \tag{5.14}$$

In the vacuum, the charge density is $\langle j^0 \rangle = \frac{Q}{4\pi R^2}$, where Q is the net charge of the superfluid state and R is the radius of the sphere. This translates to a homogeneous magnetic field

$$\langle F_{\theta\phi} \rangle = B \sin\theta \equiv \frac{Q}{2R^2} \sin\theta \tag{5.15}$$

and results in a net magnetic flux of $2\pi Q$ through the sphere; eq. (5.15) can be thought as the field generated by a magnetic monopole at the center of the sphere. Parametrically, the cutoff Λ of the EFT is

$$\Lambda \sim \sqrt{B} \sim \frac{\sqrt{Q}}{R}. \tag{5.16}$$

The action (5.13) describes a propagating degree of freedom, given by the fluctuations of the magnetic field $F_{\theta\phi}$ and which corresponds to the phonon in the original picture, together with a non-propagating Coulomb field A_0, which does not have any local analog in the scalar formulation. As we will see, it is precisely this extra component which provides the leading coupling to the vortices.

5.3.2 Particle-vortex duality

Vortices in the superfluid description correspond to heavy charged particles in the gauge theory description. They are treated in a first-quantized form as 0+1 dimensional worldlines embedded in the 2+1 dimensional spacetime. We will use the terms “vortex” and “charged particle” interchangeably.

To write the effective action for a conformal superfluid with vortices [179], we parametrize the spacetime trajectory of the pth vortex by $X_p^\mu(\tau)$, where τ is an auxilliary time parameter. We further impose Weyl and τ-reparametrization invariance, with the former reducing to conformal invariance in the relevant case of a static metric. The action can be organized as a derivative expansion with the lowest order terms given by [4]

$$S = -\kappa \int d^3x \sqrt{g} F^{3/2} - \sum_p q_p \int A_\mu dX_p^\mu - \sum_p \int d\tau \sqrt{F} \sqrt{g_{\mu\nu} \dot{X}_p^\mu \dot{X}_p^\nu}\, F_p\left(\frac{j_\mu \dot{X}^\mu}{j\dot{X}}\right) + \dots\,, \tag{5.17}$$

The first term is the kinetic term (5.13) for the gauge field. The second term is the minimal coupling between a particle of charge q_p and the gauge field [191]: this cannot be written in a local form in the scalar picture, showing the convenience of the gauge formulation. The charge q_p corresponds to the Goldstone winding number around x_p and is hence quantized: $q_p \in \mathbb{Z}$. The third term is the action for a relativistic point particle in a superfluid[5]; it is multiplied by an arbitrary function of $\frac{j_\mu \dot{X}^\mu}{j\dot{X}}$, since the superfluid velocity breaks spotaneously Lorentz symmetry and allows constructing an alternative *condensed matter metric* [179]. The dots in (5.17) represent terms with at least two derivatives on either A_μ or X_p^μ. As we will now explain, the leading order description of our system is fully determined by the first two terms of (5.17).

To this aim, let us work in physical gauge for the particle worldlines: $X_p^0 = \tau$. Since the gauge field is expanded around the non-trivial background (5.15), the leading kinetic term for the vortex lines is first order in time derivatives and arises from the second term in eq. (5.17). As we will self-consistently see, this implies that vortices move with non-relativistic velocities $|\dot{\vec{X}}| \sim 1/\sqrt{B}$. The terms with two or more time derivatives arising from the expansion of the square root $\sqrt{g_{\mu\nu}\dot{X}_p^\mu \dot{X}_p^\nu} = \sqrt{1 - \dot{\vec{X}}_p^2}$ in (5.17) are then genuine higher derivative corrections. On the one hand, as we explain below, they bring in new states with energy $\sim \sqrt{B}$. On the other, at sufficiently low energy, they can be treated as small perturbations of the leading single derivative term. This is fully analogous to supplementing the 1D Lagrangian $\dot{q}^2$ with the 4-derivative term $\ddot{q}^2/\Lambda^2$: states arise with energy $\sim \Lambda$, but at low-energy, the 4-derivative term can be treated as a perturbation using standard EFT methods.

---

[4] We discuss a derivation of the vortex action from the coset construction in the appendix C.1.

[5] See appendix C.1 for a derivation from the coset construction.

Physically we can understand this point as follows. Each X_p^μ describes the motion of a 2D particle in a magnetic field and consists of two pairs of canonically conjugate variables. These can be further decomposed into one pair that describes the motion of the guiding center and another pair that describes cyclotron motion. Without interparticle interactions, excitations of the first pair are gapless while excitations of the second pair have a gap $\omega = B/m$, where m is the particle mass. The gapped excitations are the Landau levels [6], and the gaplessness of the guiding center variables is the usual degeneracy of Landau levels.

In our system (5.17), $\omega \sim \sqrt{B}$, which coincides with the EFT cutoff (5.16). Thus, within the domain of validity of our EFT, the dynamics of X^μ reduces to that of just the guiding center—the Landau levels are effectively integrated out [192–194]. One well-known fact [195, 196] is that the guiding center can be described by dropping the mass term (the third contribution) from the Lagrangian (5.17). Physically, this is because in the massless limit, the Landau level gap $\omega \to \infty$. Formally, this is because, as commented above, the leading kindetic term in (5.17) is *linear* in the particle velocity. This constrains the two physical coordinates to be canonically conjugate to each other, halving the dimension of phase space. This procedure is sometimes called *lowest Landau level* approximation in the literature [192–196].

Working at leading order, we thus neglect terms with two time derivatives in the vortex coordinate. Furthermore, we shall be interested in configurations for which the electric field represents a small perturbation with respect to the magnetic field background, $|\vec{E}|/B \sim 1/\sqrt{B}$. Combining these two conditions, from the last term in (5.17) we retain only a constant contribution proportional to $\sqrt{B}$ which is interpreted as the vortex mass. In the following we will hence work with the action

$$S \simeq -\kappa \int d^3x \sqrt{g}\, F^{3/2} - \sum_p q_p \int A_\mu dX_p^\mu - \sum_p \gamma_p \sqrt{B} \int d\tau\,, \tag{5.18}$$

where $\gamma_p = 2^{1/4} F_p(1)$. We leave a systematic study of higher order corrections for future work, though we will briefly mention some effects in sec. 5.4.4.

As a final remark, let us notice that we are assuming the simplest possible structure for the vortex cores in writing the action (5.17), which do not carry additional degrees of freedom. While we believe this corresponds to the most generic situation, it is possible to imagine more complicated setups, in which the vortices carry non-zero spin for instance. We will discuss this possibility explicitly in sec. 5.6.2.

5.4 From vortices to spinning charged operators

5.4.1 Classical analysis

We will now compute the classical energy and angular momentum of a state with a given configuration of vortices. By the state-operator correspondence, this gives us the dimension Δ and spin J of the corresponding operator. We will work to leading order in large Q and in large vortex separations. At this order, the equations of motion from (5.18) are

$$\frac{1}{e^2}\nabla_\mu F^{\mu\nu} = \mathcal{J}^\nu\,, \tag{5.19}$$

$$E^i = (\dot{X}_p)_j F^{ji}\,, \tag{5.20}$$

where $E^i \equiv F^{i0}$ is the electric field and $\mathcal{J}^\nu$ is the current due to the point charges. The coupling e^2 is defined as

$$\frac{1}{e^2} \equiv \frac{3\kappa}{2^{1/4}}\frac{1}{\sqrt{B}}. \tag{5.21}$$

Eqs. (5.19) are Maxwell's equations and (5.20) imposes that the particles move on trajectories with vanishing Lorentz force. In other words, as expected, the particles exhibit pure drift velocity motion. This is consistent with cyclotron degrees of freedom being integrated out. As anticipated, the particle velocities are $|\dot{\vec{X}}_p| \sim |\vec{E}|/B \sim 1/\sqrt{Q}$ and can be neglected. Our problem has reduced to the 2D electrostatics of point charges on a sphere in a constant magnetic field.

The stress energy tensor $T_{\mu\nu} = \frac{2}{\sqrt{g}}\frac{\delta S}{\delta g^{\mu\nu}}$ is

$$T_{\mu\nu} \simeq \frac{\kappa}{\sqrt{f}}\left(-3F_{\mu\rho}F_\nu{}^\rho + g_{\mu\nu}F^2\right) + \sum_p \gamma_p\sqrt{B}\int d\tau \frac{(\dot{X}_p)_\mu(\dot{X}_p)_\nu}{\sqrt{g_{\rho\sigma}\dot{X}_p^\rho\dot{X}_p^\sigma}} \tag{5.22}$$

Using this, we calculate the dimension Δ to be

$$\Delta = \frac{Q^{3/2}}{\sqrt{27\pi c}} + \frac{R^3}{2e^2}\int d\theta d\phi \sin\theta \vec{E}^2 + \sum_p \gamma_p\sqrt{B}R^2\,. \tag{5.23}$$

Physically, the first term is the energy stored in the background magnetic field while the second term is the energy stored in the electric field sourced by the particles. The last term is the contribution of the vortex masses.

In Coulomb gauge, $E_i = \partial_i A_0$ where a_0 is the electric potential due to a collection of point charges on a 2-sphere:

$$A_0(\vec{r}) = -\frac{e^2}{4\pi}\sum_p q_p \log(\vec{r} - \vec{R}_p)^2. \tag{5.24}$$

We used embedding coordinates of the sphere in $\mathbb{R}^3$, where $\vec{r} = (\sin\theta\cos\phi, \sin\theta\sin\phi, \cos\theta)$ is a unit 3-vector and analogously for $\vec{R}_p$. The total electric field energy is a sum of pairwise contributions for each charge:

$$\frac{R^3}{2e^2}\int d\theta d\phi \sin\theta \vec{E}^2 = \frac{Re^2}{8\pi}\left[-\sum_{p\neq r} q_p q_r \log(\vec{R}_p - \vec{R}_r)^2 - \sum_p q_p^2 \log 0^2\right]. \tag{5.25}$$

The last term is the familiar divergent self-energy of a point charge. It will be cut off at angular lengths $\sim 1/\sqrt{Q}$ (5.16), analogously to the discussion above (5.9).

Finally, we can also easily restore the subleading terms in the Lagrangian (5.5). Neglecting the fluctuations induced by vortices everywhere but in the leading term, the dimension Δ (5.23) for a state with n vortices is [6]

$$\Delta = \Delta_Q - \frac{\sqrt{Q}}{12\alpha_1}\sum_{p\neq r} q_p q_r \log Q(\vec{R}_p - \vec{R}_r)^2 + n\tilde{\gamma}\sqrt{Q}, \tag{5.26}$$

where $\Delta_Q = \alpha_1 Q^{3/2} + \ldots$ as in eq. (5.1) and $\alpha_1 \equiv 1/\sqrt{27\pi c_1}$. We also used $\sum_p q_p = 0$, which is required by the consistency of Gauss law on the sphere, to combine the logarithms in (5.25) and we assumed all vortices to have the same mass, parametrized by a Wilson coefficient $\tilde{\gamma}$.

The angular momentum $\vec{J}$ can also be calculated from the stress tensor (5.22) and is

$$\vec{J} = \frac{RB}{e^2}\int d\theta d\phi \sin\theta\, \vec{n}^{\,i}\epsilon_{ij}\sin\theta E^j = -\sum_p q_p \frac{Q}{2}\vec{R}_p\,. \tag{5.27}$$

Here $\epsilon_{ij}\sin\theta$ is the two-dimensional Levi-Civita tensor on S^2 and $\vec{n}^{\,i} = \left(n_1^i, n_2^i, n_3^i\right)$, where n_a^i is the Killing vector corresponding to the rotation around the r_a axis of the $\mathbb{R}^3$ embedding of the sphere. We used Gauss law to obtain the right-hand side.

5.4.2 Derivation of results

The results stated at the beginning of this chapter can now be derived. First, note that the self-energy of a particle of charge q is proportional to q^2—this is the second term in (5.25). Because of this, particles with $|q| > 1$ are energetically unfavored.

- As discussed in sec. 5.2, eq. (5.2) is derived using the phonon dispersion relation and using that the energy is lowest at fixed J with a single phonon.
- The lowest energy state for $\sqrt{Q} \ll J \leq Q$ consists of a vortex-antivortex pair rotating on the sphere, at a distance proportional to the spin $|\Delta\vec{R}|/2 = J/Q$ (see

---

[6] Here we correct a typo in eq. (19) of [2].

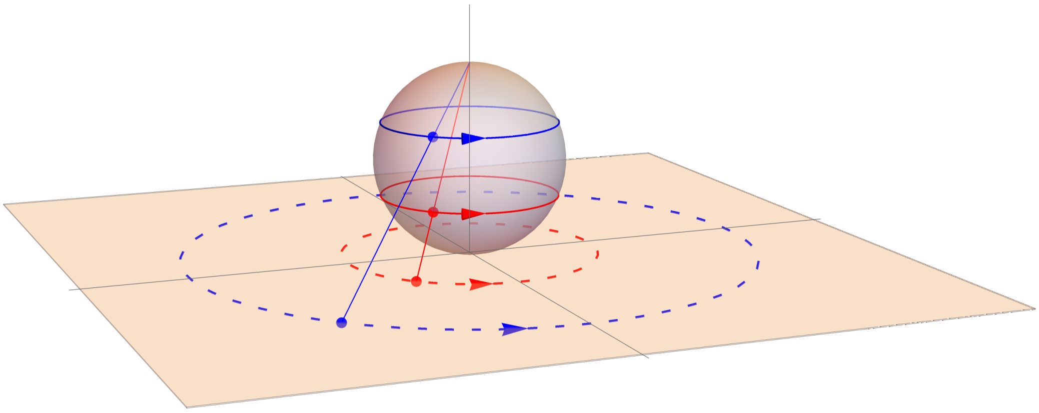

Figure 5.1 – A vortex-antivortex pair moving on the sphere at fixed distance; in the stereographic projection the motion corresponds to two circular orbits.

fig. 5.1). The scaling dimension of the corresponding operator reads

$$\Delta = \Delta_Q + \frac{\sqrt{Q}}{3\alpha_1} \log \frac{J}{\sqrt{Q}} + 2\tilde{\gamma}\sqrt{Q} + \mathcal{O}\left(\sqrt{Q} \times \frac{Q}{J^2}\right). \tag{5.28}$$

The leading correction to the ground state energy arises from the second term as a consequence of the logarithmic divergence of the vortex self-energy. This depends on the same coefficient α_1 appearing in (5.1). The vortex mass contribution, given by the last term in (5.28), depends on a new coefficient and scales as the first subleading term in the ground state energy (5.1). The last term in eq. (5.28) is the contribution of the vortex masses, which scales as the first subleading term in the ground state energy (5.1). Corrections to this formula arise from the particle velocities and the phonon field and will be discussed in sec. 5.4.4. As $J \to \sqrt{Q}$, the vortices become relativistic and the derivative expansion breaks down. Notice that eq. (5.28) for $J = Q$ agrees with eq. (5.11) derived in sec. 5.2.

- For $Q \ll J \ll Q^{3/2}$ the lowest energy state corresponds to a vortex crystal phase [197, 198]. Its energy is found approximating the vortex distribution as a continuous charge distribution $\rho(x)$ and then minimizing Δ (5.26) for fixed J (5.27) using variational techniques. The leading contribution to the energy arises from the electric field $|\vec{E}| \sim e^2|\rho|$ and reads

$$\Delta = \Delta_Q + \frac{1}{2\alpha_1}\frac{J^2}{Q^{3/2}} + \mathcal{O}\left(\frac{J^2}{Q^{3/2}} \times \frac{Q}{J}, \frac{J^2}{Q^{3/2}} \times \frac{J^2}{Q^3}\right), \tag{5.29}$$

corresponding to a vortex distribution ρ of

$$\rho = \frac{3}{2\pi R^2}\frac{J}{Q}\cos\theta \tag{5.30}$$

and results in the superfluid having the same velocity profile as that of a rigid body [183]. The second term in (5.29) is the electrostatic energy of the crystal. The leading corrections arise from the vortex masses and the magnetic field fluctuations. The description holds as long as the electric field is subleading to the homogeneous monopole field B and as long as the particle velocities are negligible. This sets the condition $J \ll Q^{3/2}$. [7]

As $J \to Q^{3/2}$, the electric field $|\vec{E}|$ approaches the magnetic field B and the drift velocities become relativistic. This causes the EFT to break down because the higher order terms neglected in (5.18) become unsupressed. The guiding centers become as energetic as the cyclotron degrees of freedom and anything else at the EFT cutoff (5.16).

5.4.3 Quantization

Since the vortex positions are continuous, some questions may occur: How many distinct states are there? How does the quantization of angular momentum arise? These questions are answered when we quantize our system of charged particles in a magnetic field. Solving for A_0 using (5.24) and ignoring fluctuations of A_i, our effective Lagrangian (5.18) becomes

$$L = \sum_p q_p \vec{A} \cdot \dot{\vec{R}}_p + \frac{e^2}{8\pi} \sum_{p,r} q_p q_r \log(\vec{R}_p - \vec{R}_r)^2, \tag{5.31}$$

where $\vec{A}$ is the potential for a magnetic monopole [199, 200]. We use the gauge in which $A_\phi = \frac{1}{2}Q(1-\cos\theta)$ and $A_\theta = 0$. This system is known as the “fuzzy sphere” [201, 202].

Due to the somewhat complicated form of $\vec{A}$, it is useful to switch to spinor coordinates, defined as [203, 204]:

$$\psi \equiv \begin{pmatrix} \cos\frac{\theta}{2} \\ \sin\frac{\theta}{2} e^{i\phi} \end{pmatrix}, \tag{5.32}$$

where we suppressed the vortex index. In these coordinates, $\vec{R} = \psi^\dagger \vec{\sigma} \psi$ and $\vec{A} \cdot \dot{\vec{R}} = -iQ\psi^\dagger \frac{d}{dt}\psi$. This identifies the canonical momentum corresponding to ψ_p as $-iQq_p\psi_p^\dagger$. The canonical commutation relations are easily understood defining the operator corresponding to the orbital contribution to the angular momentum from a vortex p as

$$\hat{\vec{L}}_p = -\frac{Q}{2} q_p \hat{\vec{R}}_p \,, \qquad \hat{\vec{J}} = \sum_p \hat{\vec{L}}_p \,. \tag{5.33}$$

We use the hat to denote *operators*. The canonincal commutation relations then read $[\hat{L}_p^a, \hat{L}_p^b] = i\epsilon^{abc}\hat{L}_p^c$, which imply that the angular momentum (5.27) commutes with the Hamiltonian and satisfies $[\hat{J}_a, \hat{J}_b] = i\epsilon_{abc}\hat{J}_c$ [201, 202].

---

[7] This is in agreement with the experimental fact that vortex crystals exist when the filling fraction $\nu = j_0/n_v$ is much bigger then one, where $n_v \sim |\rho|$ is the vortex density [93, 94].

For illustration, consider the case of two vortices of unit charge. The Hamiltonian corresponding to (5.31) is then

$$H = \text{const} + \frac{e^2}{4\pi} \log \hat{\vec{J}}^2, \tag{5.34}$$

where "const" involves terms that are independent of the vortex coordinates, and we used (5.27) to express H in terms of $\hat{\vec{J}}$. The spectrum is thus entirely determined by the spectrum of $\hat{\vec{J}}^2$. As is well-known, $\hat{\vec{J}}^2 = J(J+1)$, where J is an integer and for each value of J, there are $2J+1$ degenerate states.

Restoring the constants in (5.34), the dimension of the corresponding operator is

$$\Delta = \Delta_Q + \frac{\sqrt{Q}}{6\alpha_1} \log \frac{J(J+1)}{Q} + 2\tilde{\gamma}\sqrt{Q} + \mathcal{O}\left(\sqrt{Q} \times \frac{Q}{J^2}\right) . \tag{5.35}$$

As in eq. (5.28), we can trust this equation for $\sqrt{Q} \lesssim J \leq Q$. By expanding the logarithm in eq. (5.35), the quantum corrected expression provides an additional contribution of order $\sim \sqrt{Q}/J$ to the classical result (5.28).

5.4.4 Higher order corrections

Corrections arise from higher derivative terms we neglected in (5.18) and are suppressed by powers of the cutoff length scale $l \equiv \Lambda^{-1}$. Here we comment on their form, leaving a systematic study for future work.

The first class of corrections is controlled by the volume of the sphere and scales as $l^2/R^2 \sim 1/Q$. As discussed in part II of this thesis, these correction arises from higher derivative corrections in the superfluid action. They are also present in the absence of vortices and we accounted for them through the inclusion of the subleading terms in (5.1).

Consider now the vortex-antivortex state discussed around eq. (5.28). In this case, a second class of correction exists, controlled by the separation d among vortices and scales as l^2/d^2, where the double power of d is dictated by rotational invariance. Using the relation $J \sim Bd$ (5.27), we have $l^2/d^2 \sim Q/J^2$. This arises from the last term in (5.17). There we find relative corrections to the vortex action proportional to $\vec{E}^2/B^2$ and $\dot{\vec{X}} \wedge \vec{E}/B$. These both scale as $l^2/d^2 \sim Q/J^2$ on our solutions, becoming large at the lower edge $J \sim \sqrt{Q}$ of the two vortex states.

Notice that the second class of corrections is larger than the $\mathcal{O}(1/J)$ quantum correction distinguishing (5.35) from the classical result (5.3). Nonetheless, the quantum correction is functionally distinguished and thus calculable. We also note that the universal $\mathcal{O}(Q^0 J^0)$ contribution from the phonon Casimir energy [34, 35] persists in the presence of vortices because the phonon spectrum is unmodified at leading order.

Consider finally the vortex crystal phase discussed around eq. (5.29). The leading correction in this case arise both from the contribution to the energy from the phonon field, which is proportional to the particle velocities and gives $\delta B^2/|\vec{E}^2| \sim \dot{\vec{X}}^2 \sim \left(J/Q^{3/2}\right)^2$, and from the masses of the particles, which give Q/J corrections using (5.30).

5.5 Correlators

As we have seen in part II of this thesis, the EFT can also be used to compute correlation functions [35]. Let us consider correlators involving the $U(1)$ current j_μ. [8] From (5.14) and Gauss's law, we see that the line integral $\oint j_\mu dx^\mu$ about a closed curve $\mathcal{C}$ at fixed time is simply $\frac{1}{2\pi}$ times the total charge q_{enc} enclosed by $\mathcal{C}$:

$$\langle \text{vortex}| \oint_{\mathcal{C}} j_\mu dx^\mu \, |\text{vortex}\rangle = \frac{e^2 q_{\text{enc}}}{2\pi}, \tag{5.36}$$

where $|\text{vortex}\rangle$ is a generic vortex state. By the state-operator correspondence, this amounts to a prediction about three-point functions. We will now consider two simple examples.

As a first example, we consider a vortex-antivortex pair located at the north and south poles. Then (5.36) becomes

$$\langle \text{vortex}|j_\phi(\theta,\phi)|\text{vortex}\rangle = \frac{e^2}{2\pi R}, \tag{5.37}$$

where now $|\text{vortex}\rangle$ is a state with $J = J_z = Q$ and j_ϕ is the azimuthal component of j_μ. In general, the expectation value of a spin-1 operator j_ϕ in a state $|J, J_z\rangle$ with $J = J_z = Q$ is [205]

$$\langle Q,Q|j_\phi(\theta,\phi)|Q,Q\rangle = R^2 \sum_{m=0}^{Q} a_m \cos^{2m}\theta, \tag{5.38}$$

where a_m are arbitrary (theory-dependent) constants subject to the constraint $\sum_m a_m = 0$. By equating (5.37) to (5.38), we obtain the following predictions for a_m at leading order:

$$a_m = \begin{cases} \frac{\sqrt{Q}}{3\alpha_1}, & \text{if } m = 0; \\ 0, & \text{if } 1 \le m \ll \sqrt{Q}. \end{cases} \tag{5.39}$$

Because of the EFT cutoff (5.16), we can only make predictions for $m \ll \sqrt{Q}$. [9] The constraint $\sum_m a_m = 0$ is thus irrelevant for our discussion.

---

[8] To leading order, scalar insertions read as in the homogeneous phase discussed before.

[9] To appreciate this, it is useful to write $\cos^{2m}\theta \approx \exp\left(-m\,\theta^2\right)$ for $m \gg 1$ and $\theta \ll 1$, which is exponentially suppressed by the cutoff away from the vortex core for $m \gtrsim \sqrt{Q}$.

As a second example, we consider the states described by (5.4). Using (5.30), we find

$$\langle \text{vortex}|j_\phi(\theta,\phi)|\text{vortex}\rangle = \frac{3e^2}{8\pi^2 R}\frac{J}{Q}\sin^2\theta. \tag{5.40}$$

Rewriting (5.38) in the Fourier basis:

$$\langle Q,Q|j_\phi(\theta,\phi)|Q,Q\rangle = R^2\sum_{m=0}^{J} b_m\cos 2m\theta, \tag{5.41}$$

we obtain the following predictions for b_m at leading order:

$$b_m = \begin{cases} \frac{(-1)^m}{8\pi\alpha_1}\frac{J}{\sqrt{Q}}, & \text{if } m=0,1; \\ 0, & \text{if } 2\le m \ll \sqrt{J/Q}. \end{cases} \tag{5.42}$$

Because we used a continuous approximation for the density ρ (5.30), we can only make predictions for $m \ll \sqrt{\rho} \sim \sqrt{J/Q}$.

5.6 Discussion and generalizations

5.6.1 Weak coupling and large N

So far, we assumed that the numerical coefficients in our effective Lagrangian are $\mathcal{O}(1)$, corresponding to an underlying strongly coupled CFT. The case of a weakly coupled or large N theory is quickly illustrated. However, the conclusions depend on whether the weak coupling appears in the χ description (5.5) or in the A_μ description (5.13). We will refer to the χ description as "electric" and to the A_μ one as "magnetic", with couplings $g_e^2 \equiv 1/N_e$ and $g_m^2 \equiv 1/N_m$, respectively.

Consider first a weakly coupled magnetic theory (for example, the large N_m setup discussed in [104, 111, 142–147]). Since $1/\alpha_1 \sim g_m^2$ is small, the "bare" vortex mass ($\sim \tilde{\gamma}\sqrt{Q}$) is no longer subdominant to the electric field energy in (5.23). Therefore, the contribution $n\tilde{\gamma}\sqrt{Q}$ is the dominant one in eq. (5.3) and should be added to eq. (5.4), where $n=2$ for $J\le Q$, and $n = 3J/Q$ for $J \gg Q$. For simplicity, we assumed the same bare mass for all vortices. This gives the dominant spin dependent contribution to Δ for $J \lesssim Q/g_m^2$.

Consider now a weakly coupled electric theory. The essential difference in this case is that the cutoff is naturally identified with $\mu \sim g_e\sqrt{Q}$ [4] instead of with (5.16). Therefore, a single phonon is restricted to $J \lesssim g_e\sqrt{Q}$ and a vortex-antivortex pair to $J \gtrsim Q\mu^{-1} \sim \sqrt{Q}/g_e$. States with J in the gap between the two consist of multiple phonons, approaching a $1/g_e^2$ number of them as $J \to \sqrt{Q}/g_e$. At this point, the lowest energy state shifts from multiple phonons to the vortex-antivortex pair. This consistently reflects the fact that vortices are now heavy solitons and consist of also roughly a $1/g_e^2$

number of elementary quanta. Since $\alpha_1 \sim g_e$, the logarithmic term in (5.3) is indeed the expected result, $\mu/g_e^2 \log \mu d$, for a semiclassical solution with a vortex-antivortex pair split by a distance $d = J/Q$. We will discuss weakly coupled "electric" systems in part IV of this thesis.

5.6.2 Spin and additional degrees of freedom in the vortex cores

In our analysis we assumed the simplest possible structure for the vortex cores, which do not carry any additional degrees of freedom on top. However, it is possible to imagine that the heavy particles have non zero spin. For instance, in the perturbative models studied in [145, 206] we expect that the heavy particles can be identified with certain localized excitations of the fermionic fields coupling to the $U(1)$ gauge field [207], in which case the vortex core would carry half-integer spin. One might then wonder to what extent such an additional structure on the worldline can modify the results discussed so far. In this section we illustrate this point, considering states with a single vortex-antivortex pair with half-integer spin .

To model the effect of spin, we can modify the action of a single vortex in (5.17) following the approach of [208–210]. Recall first that, assuming parity invariance, an half-integer spin particle at rest in $2+1$ dimensions can be in two different states. Such a discrete multiplicity of states is naturally described via a Grassmannian variable living on the worldline, transforming covariantly under the unbroken rotations; [10] concretely, this is achieved by taking a Grassmannian 3-vector $\xi_p^\mu(\tau)$ orthogonal to the particle velocity: $\xi_p^\mu g_{\mu\nu} \dot{X}_p^\nu = 0$. As usual, p labels the different vortices. Neglecting interactions for the moment, the free reparametrization invariant action for one such variable reads:

$$S_\xi^{(p)}\Big|_{free} = -\frac{i}{2}\int d\tau \left[\xi_p^\nu g_{\mu\nu}\left(\frac{D}{D\tau}\xi_p^\mu\right) + \lambda_p\left(\dot{X}_p^\mu g_{\mu\nu}\xi_p^\nu\right)\right], \tag{5.43}$$

where $\frac{D}{D\tau}$ is the covariant derivative on $\mathbb{R}\times S^2$ and λ_p is a Grassmannian Lagrange multiplier.

The Lagrangian in eq. (5.43) was first studied in [208], [11] where it was proven to correctly describe a parity-invariant Dirac particle. We shall not repeat the full analysis here, but it is instructive to look at the non-relativistic limit of (5.43) in flat space. Working in the physical gauge $X_p^0 = t$, the constraint $\xi_p^\mu \eta_{\mu\nu}\dot{X}_p^\nu = 0$ implies $\xi_p^0 \simeq 0$ and we obtain

$$S_\xi^{(p)}\Big|_{free} \simeq \frac{i}{2}\int dt\, \xi_p^i \delta_{ij}\dot{\xi}_p^j = \frac{i}{2}\int dt\, \xi_p^* \dot{\xi}_p\,, \qquad \xi_p = \xi_p^1 + i\xi_p^2\,, \tag{5.44}$$

where in the last equality we have discarded a total derivative. Quantizing the system, the equal time canonical (anti-)commutation relations read:

---

[10] Recall that the worldline action breaks spontaneously boosts, see appendix C.1.

[11] The authors of [208] consider an additional redundant variable ξ_5; eq. (5.43) coincides with their eq. (3.3) in the gauge $\xi_5 = 0$.

$$\{\xi_p^*, \xi_p\} = 2 \qquad \Longleftrightarrow \qquad \{\xi_p^i, \xi_p^j\} = \delta^{ij} \,. \tag{5.45}$$

From these we identify $\xi_p^i = \sigma^i/\sqrt{2}$ ($i = 1, 2$) and the spin is the conserved operator $s_p^{12} = \frac{i}{2}\xi_p^*\xi_p = -\frac{i}{2}[\xi_p^1, \xi_p^2] = \sigma^3/2$. The two eigenstates of s_p^{12} describe the possible spin orientations for a particle at rest.

Let us now consider the possible interactions with the superfluid background which can be introduced in the action (5.43). Considering that the action shoud be quadratic in ξ_p^μ, that classically $\xi_p \cdot \xi_p = 0$ and that we work at leading order in the particle velocities, the leading interaction term is given by

$$S_\xi^{(p)}\Big|_{int.} = \frac{i}{2}\frac{g_p}{\sqrt{2}} \int d\tau \sqrt{\dot{X}_p^\mu g_{\mu\nu} \dot{X}_p^\nu} \frac{F_{\mu\nu}\xi_p^\mu \xi_p^\nu}{\sqrt{F/\sqrt{2}}} \,. \tag{5.46}$$

This term indeed can be interpreted as the relativistic version of the Pauli interaction $\vec{B} \cdot \vec{s}/m$ between the spin and the magnetic monopole field for a particle of mass $m \sim \sqrt{F} \sim \sqrt{B}$ [211]. The powers of F are dictated by Weyl invariance and the dimensionless coupling g_p can be interpreted as the magnetic moment of the particle. We then conclude that, in order to describe fermionic vortices with half-integer spin, we need to add to the action (5.17) the following term

$$\sum_p S_\xi^{(p)} = -\frac{i}{2}\sum_p \int d\tau \left[\xi_p^\nu g_{\mu\nu}\left(\frac{D}{D\tau}\xi_p^\mu\right) + \lambda_p\left(\dot{X}_p^\mu g_{\mu\nu}\xi_p^\nu\right) - \frac{g_p}{\sqrt{2}}\sqrt{\dot{X}_p^\mu g_{\mu\nu}\dot{X}_p^\nu}\frac{F_{\mu\nu}\xi_p^\mu\xi_p^\nu}{\sqrt{F/\sqrt{2}}}\right] . \tag{5.47}$$

To study the model given by (5.17)+(5.47), it is useful to proceed as in sec. 5.4.3. Namely we integrate out the Coulomb field $A_0(x)$ and notice that to leading order in the velocities $\xi_p^0 \simeq 0$. It is further convenient to introduce a Grassmannian vector in the $\mathbb{R}^3$ embedding space as

$$\vec{\xi}_p = \frac{d\vec{R}_p}{dx_p^i}\xi_p^i, \qquad \vec{R}_p \cdot \vec{\xi}_p = 0 \,, \tag{5.48}$$

where $\vec{R}_p$ is the particle position in embedding coordinates. The Lagrangian for n vortices then reads

$$L = \sum_p \vec{A} \cdot \dot{\vec{R}}_p + \frac{e^2}{8\pi}\sum_{p,r} q_p q_r \log\left(\vec{R}_p - \vec{R}_r\right)^2 + \frac{i}{2}\sum_p \left[\vec{\xi}_p \cdot \dot{\vec{\xi}}_p - \frac{g_p}{\sqrt{2}}\sqrt{B}\epsilon_{abc}R_p^a\xi_p^b\xi_p^c\right] , \tag{5.49}$$

which differs from eq. (5.31) by the last term. Here $a, b, c = 1, 2, 3$ are used to label embedding space indices. Due to the new contribution, each particle provides both an orbital and a spin contribution to the angular momentum. Thus eq. (5.33) is generalized to

$$\vec{J}=\sum_p\left(\vec{L}_p+\vec{s}_p\right),\qquad \vec{L}_p=-\frac{Q}{2}q_p\vec{R}_p,\qquad s^a_p=-\frac{i}{2}\epsilon_{abc}\xi^b_p\xi^c_p\,. \tag{5.50}$$

Notice that only $\vec{J}$ is conserved, while the orbital and the spin part alone are not, due to the interaction of the spin with the magnetic monopole field.

We can now quantize the system as in sec. 5.4.3. We find $[\hat{L}^a_p,\hat{L}^b_p]=i\epsilon_{abc}\hat{L}^c_p$ and $[\hat{s}^a_p,\hat{s}^b_p]=i\epsilon_{abc}\hat{s}^c_p$, with $\hat{\vec{s}}_p\cdot\hat{\vec{s}}_p=3/4$, implying the $SU(2)$ algebra for the angular momentum $\hat{\vec{J}}$. Calling $\vec{L}=\sum_p\vec{L}_p$ and dropping the hat from operators, the Hamiltonian is

$$H=\text{const.}+\frac{e^2}{4\pi}\log\vec{L}^2+\sum_p\frac{g_p}{q_p}\frac{\vec{L}_p\cdot\vec{s}_p}{R\sqrt{Q}}\,. \tag{5.51}$$

Consider finally a semiclassical state made of a unit charge vortex-antivortex pair of the kind considered around eq. (5.28). We assume that both vortices have the same magnetic moment $g>0$. For such a state the spin contribution to the angular momentum is negligble: $\vec{J}\simeq\vec{L}=Q\,\Delta\vec{R}$. To compute the energy of this state we can approximate $\langle\vec{L}_p\cdot\vec{s}_p\rangle\simeq\vec{L}^{class.}_p\cdot\langle\vec{s}_p\rangle$, where $\vec{L}^{class.}_p$ is obtained solving the classical equations of motion at fixed angular momentum. Then we can choose the orientation of the particles' spins to minimize the energy and we obtain

$$\Delta=\Delta_Q+\frac{\sqrt{Q}}{3\alpha_1}\log\frac{J}{\sqrt{Q}}+2\tilde{\gamma}\sqrt{Q}-\frac{g}{2}\frac{J}{\sqrt{Q}}+\mathcal{O}\left(\sqrt{Q}\times\frac{Q}{J^2}\right)\qquad\sqrt{Q}\ll J\leq Q\,, \tag{5.52}$$

which differs by the prediction for two spinless vortices in eq. (5.28) only by the last term.

Let us generalize the conclusions of the previous analysis. The leading contribution to the angular momentum, eq. (5.27), is generically unaffected by the presence of additional degrees of freedom characterizing the vortex cores. Similarly, the dominant contribution to the energy from the vortices always arises from the electrostatic interaction (5.24), due to the logarithmic enhancement. Additional degrees of freedom might store energy in the vortex cores, similarly to the vortex masses, and thus may provide new subleading contributions to the energy; this is the case for the last term in eq. (5.52).

5.6.3 Vortices and spinning operators for a rank two symmetry group

The results derived in this chapter for the scaling dimension of spinning charged operators in a CFT invariant under a $U(1)$ symmetry equally apply to a theory with $SU(2)$ symmetry. This is because the non-Abelian structure of the group does not play any role in the determination of the spectrum of operators with lowest dimensions, as we argued in sec. 4.1. Instead, though qualitatively similar, the detailed form of our predictions may change for higher rank groups. Here we discuss in detail the case of a rank two group.

In the simplest scenario, as discussed in sec. 4.1, the EFT determining the low energy spectrum coincides with the one of a $U(1)^2$ Abelian conformal superfluid. [12] The effective Lagrangian is written in terms of two scalar fields $\chi_{1/2} = \mu_{1/2} t + \pi_{1/2}$ as in eq. (4.4):

$$\mathcal{L}/\sqrt{g} = (\partial\chi_1)^{3/2}(\partial\chi_2)^{3/2} P\left(X, Y\right) + \dots\,, \tag{5.53}$$

$$X = \frac{\partial_\mu\chi_1\partial^\mu\chi_2}{(\partial\chi_1)(\partial\chi_2)}\,, \qquad Y = \frac{(\partial\chi_2)}{(\partial\chi_1)}\,. \tag{5.54}$$

The spectrum of fluctuations is given by two gapless modes. The speed of sound of one of them is fixed to be $1/\sqrt{2}$ by conformal invariance, while the sound speed c_- of the other mode depends on the specific theory under consideration. The precise value of the cutoff depends on the function P. For economy of thought, we shall focus on the regime where the charges are comparable, $Q_1 \sim Q_2 \gg 1$, in which case the cutoff is parametrically given by $\Lambda \sim \sqrt{Q_{1/2}}/R$. The scaling dimension of the lowest dimension operator at fixed values of the charges reads

$$\Delta_{Q_1,Q_2} = \alpha_1\left(r\right) Q^{3/2} + \alpha_2\left(r\right) Q^{1/2} - \left(1 + \sqrt{2} c_-\right) \times 0.0937 + \mathcal{O}\left(Q^{-1/2}\right)\,, \tag{5.55}$$

where $Q = \sqrt{Q_1 Q_2}$ and the α_i's are functions of $r = Q_2/Q_1$. The gapless modes describe the Fock space in eq. (4.12). In particular, the lowest energy state for fixed angular momentum $J \ll \sqrt{Q}$ corresponds to a single phonon state with energy

$$\Delta = \Delta_{Q_1,Q_2} + \min\left(\frac{1}{\sqrt{2}}, c_-\right) \times \sqrt{J(J+1)} + \mathcal{O}\left(\frac{J^4}{Q}\right)\,. \tag{5.56}$$

To study states with spin $J \gtrsim \sqrt{Q}$, we need to include vortices in the EFT. As in sec. 5.3, we first consider a dual formulation of the theory in terms of two gauge fields A_μ^m, $m = 1, 2$, related to the scalar fields in eq. (5.53) via the Noether currents j_μ^m:

$$F_m^{\mu\nu} = \frac{1}{4\pi}\frac{\epsilon^{\mu\nu\rho}}{\sqrt{g}} j_\rho^m\,, \qquad m = 1, 2\,. \tag{5.57}$$

As in eq. (5.15), the homogeneous charge densities translate into large monopole magnetic fields $B_m = Q_m/2R^2$. The dual Lagrangian reads

$$\mathcal{L}/\sqrt{g} = -F_1^{3/4} F_2^{3/4} K(\tilde{X}, \tilde{Y})\,, \qquad \tilde{X} = \frac{F_1 \cdot F_2}{F_1\, F_2}\,, \qquad \tilde{Y} = \frac{F_2}{F_1}\,, \tag{5.58}$$

where $F_1 \cdot F_2 = F_1^{\mu\nu} g_{\mu\rho} g_{\nu\sigma} F_2^{\rho\sigma}$ and the function K is given by the Legendre transform of eq. (5.53):

---

[12] As explained in sec. 4.1, this may not be the case for all theories. For instance we argued in sec. 4.2 that in the $O(4)$ and $O(5)$ models the ground state itself, for mixed symmetric representations, is inhomogeneous and may carry non-zero angular momentum. Therefore, the following results do not apply in that case.

$$F_1^{3/4}F_2^{3/4}K(\tilde{X},\tilde{Y}) = \sum_{r=1}^{2} j^r_\mu \partial^\mu \chi_r - (\partial\chi_1)^{3/2}(\partial\chi_2)^{3/2}P\left(X,Y\right) . \tag{5.59}$$

The formulation of the EFT then proceeds as before. Vortices correspond to heavy charged particles, whose spacetime trajectory is parametrized by $X^\mu_p(\tau)$. The full action for the theory reads

$$\begin{aligned} S = &-\int d^3x\sqrt{g}F_1^{3/4}F_2^{3/4}K(\tilde{X},\tilde{Y}) - \sum_p\sum_{m=1}^{2} q_{p,m}\int A^m_\mu dX^\mu_p \\ &-\sum_p \int d\tau\, F_1^{3/4}F_2^{3/4}K_p(\tilde{X},\tilde{Y})\sqrt{g_{\mu\nu}\dot{X}^\mu_p\dot{X}^\nu_p}\,F_p\left(\frac{j^r_\mu\dot{X}^\mu}{j^r\dot{X}}\right) + \dots\,, \end{aligned} \tag{5.60}$$

where the second term in the first line is the minimal coupling between the gauge fields and the vortices, which are generically charged under both the gauge interactions, while the term in the last line generalize the point-particle action of eq. (5.17). The same considerations done before apply in this case. In particular, the EFT describes slowly moving vortices, in which case the last line in eq. (5.60) reduces to a constant *mass* contribution to leading order.

The analysis of the EFT (5.60) then mirrors the one in sec. 5.4.1. From the equations of motion one finds that the vortices source electric fields $E^i_m \equiv F^{0i}_m$ of order $\sim\sqrt{Q}$ and that they move with drift velocity $\dot{\vec{X}} \sim |\vec{E}_m|/B_m \sim 1/\sqrt{Q}$. Assuming a state of n vortices with the same mass, from the energy momentum tensor we find the energy of the system as

$$\Delta = \Delta_{Q_1,Q_2} + \sum_{m,n=1}^{2}\frac{R^3}{2}\left[e^{-2}\right]_{mn}\int d\theta d\phi\sin\theta\vec{E}_m\cdot\vec{E}_n + n\gamma(r)\sqrt{Q}\,, \tag{5.61}$$

where we defined the following matrix

$$\left[e^{-2}\right] = (2B_1B_2)^{3/4}\begin{pmatrix} \frac{3K-4K_X-4K_Y\tilde{Y}}{4B_1^2} & \frac{K_X}{B_1B_2} \\ \frac{K_X}{B_1B_2} & \frac{3K-4K_X+4K_Y\tilde{Y}}{4B_2^2} \end{pmatrix} . \tag{5.62}$$

The subscripts on K denote differentiation with respect to the corresponding argument and all quantities are evaluated on the background solution $\tilde{X}=1$ and $\tilde{Y}=B_2/B_1$. Eq. (5.61) is physically analogous to (5.23). However, now the *gauge coupling* e^2 is a 2×2 matrix and the masses of the vortices depend on $r = Q_2/Q_1$ through the independent function $\gamma(r)$. Stability of the ground state against the formation of vortices requires the matrix (5.62) to be positive definite: $[e^{-2}]\succeq 0$. [13] The components of the matrix $[e^{-2}]$

---

[13] Interestingly, this constraint is independent of the ones mentioned below eq. (4.10); we do not know

cannot be expressed in terms of the ground state energy (5.55) or its derivatives, nor as a function of the unfixed sound speed c_-^2 in eq. (4.10). As we will see below, this implies that the predictions of the EFT will depend on more parameters than in the $U(1)$ case.

Working in Coulomb gauge we may further express the total electric field energy a sum of pairwise contributions for each charge. Cutting off the self-energy of the point charges analogously to eq. (5.25), we find:

$$\sum_{m,n=1}^{2}\frac{R^3}{2}\left[e^{-2}\right]_{mn}\int d\theta d\phi\sin\theta\vec{E}_m\cdot\vec{E}_n=-\frac{R}{8\pi}\sum_{p\neq r}\sum_{m,n=1}^{2}[e^2]_{m,n}q_{p,m}q_{r,n}\log Q(\vec{R}_p-\vec{R}_r)^2\,, \tag{5.63}$$

where $[e^2]$ is the inverse of $[e^{-2}]$. The angular momentum $\vec{J}$ can also be calculated from the stress tensor and its expression is analogous to eq. (5.27):

$$\vec{J}=R\sum_{m,n=1}^{2}B_m\left[e^{-2}\right]_{mn}\int d\theta d\phi\sin\theta\,\vec{n}^{\,i}\epsilon_{ij}\sin\theta E_n^j=-\sum_p\sum_{m=1}^{2}q_{p,m}\frac{Q_m}{2}\vec{R}_p\,. \tag{5.64}$$

We may finally derive the results for the lowest energy state at fixed angular momentum. For $\sqrt{Q}\ll J\lesssim Q$ the ground state is given by a vortex anti-vortex pair, as in fig. 5.1. Assuming $[e^2]_{1,1}\leq[e^2]_{2,2}$ with no loss of generality, from the self-energy contribution to the energy we infer that particles with $q_{p,2}\neq 0$ are energetically unfavored; thus the particles in fig. 5.1 have $q_{p,1}=\pm 1$ and $q_{p,2}=0$. We then find that for $\sqrt{Q}\ll J\leq Q_1$ the scaling dimension of the minimal energy state takes the following functional form

$$\Delta=\Delta_{Q_1,Q_2}+\delta(r)\sqrt{Q}\log\vec{J}^2/Q+\sqrt{Q}\,\tilde{\gamma}(r)+\mathcal{O}\left(\sqrt{Q}\times\frac{Q}{J^2}\right)\,, \tag{5.65}$$

where the functions $\delta(r)$ and $\tilde{\gamma}(r)$ cannot be determined by the EFT only.

As we increase the spin the analysis gets less intuitive. However, according to the previous findings, we expect the CFT to be in a vortex crystal phase in the regime $J\gg Q_1,Q_2$. We can compute the corresponding energy approximating the vortex charge distributions as continuous and minimizing the energy at fixed angular momentum. In this case, the final result does not depend on new parameters with respect to eq. (5.55) and it is analogous to eq. (5.4) for a $U(1)$ symmetry:

$$\Delta=\Delta_{Q_1,Q_2}+\frac{1}{2\alpha_1(r)}\frac{J^2}{Q^{3/2}}+\mathcal{O}\left(\frac{J^2}{Q^{3/2}}\times\frac{Q}{J},\frac{J^2}{Q^{3/2}}\times\frac{J^2}{Q^3}\right)\,,\qquad Q\ll J\ll Q^{3/2}\,, \tag{5.66}$$

where $\alpha_1(r)$ is the coefficient of the leading term in the ground state energy (5.55). As before, for $J\to Q^{3/2}$ the electric fields become comparable to the magnetic ones, the vortex velocities approach the speed of light and the EFT breaks down.

---

any way to derive it directly in the scalar formulation.

6 Spinning charged operators and vortices in four dimensions

In the previous chapter, we have discussed the predictions of the vortex EFT for operators which have large spin as well as large charge. Here we extend those predictions to four-dimensional CFTs invariant under a $U(1)$ internal symmetry. As explained in the introduction to this part of the thesis, this is not an entirely trivial task. Indeed vortices in four dimensions are described as heavy strings moving in the superfluid, whose physics is richer than that of point-particles. We will find that this nicely matches the richer structure of the rotation group in four dimensions.

6.1 Summary of results

Let us first set our conventions for the four dimensional rotation group $SO(4)$. Spinning operators in four dimensions are classified in representations labelled by two positive half-integer quantum numbers $(J, \bar{J})$. These are related to the maximal values allowed for the Cartan generators J_{34} and J_{12} as

$$(J, \bar{J}) = \left(\frac{|J_{34} - J_{12}|}{2}, \frac{|J_{12} + J_{34}|}{2} \right) . \tag{6.1}$$

With no loss of generality, we assume $J_{34} \geq J_{12} \geq 0$.

We consider a CFT invariant under an internal $U(1)$ symmetry. In this case, the prediction (3.21) of the conformal superfluid EFT for the scaling dimension of the lightest scalar operator of charge $Q \gg 1$ in the spectrum is given by [35]

$$\Delta_Q = \alpha_1 Q^{4/3} + \alpha_2 Q^{2/3} + \dots \, . \tag{6.2}$$

In this chapter, we compute the scaling dimension of the lightest operator as the spin is increased. As in chapter 5, the EFT describes the regime where the spin is below the unitarity bound, $J, \bar{J} \ll Q^{4/3}$, and cannot reach the regime analyzed by the analytic bootstrap [169–172, 184–190]. To leading order in the charge and the spin, the results depend on the first coefficient in (6.2) and on an extra Wilson coefficient $\tilde{\gamma}$ parametrizing the vortex tension.

For traceless symmetric operators $J = \bar{J} = J_{34}/2$, the corresponding state passes through three distinct regimes, qualitatively similar to the CFT$_3$ case:

- For $2 \leq J_{34} \ll Q^{1/3}$ the lightest operator corresponds to a phonon wave of angular momentum J in the superfluid. The scaling dimension is given by (3.25), which in $d = 4$ reads:
$$\Delta = \Delta_Q + \sqrt{\frac{J_{34}(J_{34}+2)}{3}} + \mathcal{O}\left(\frac{J_{34}^4}{Q^{2/3}}\right). \tag{6.3}$$
- For $Q^{1/3} \ll J_{34} \leq Q$, the minimal energy state is given by a single vortex ring, whose radius increases with J. Its energy is
$$\Delta = \Delta_Q + \Delta_V(Q, J_{34}), \tag{6.4}$$
  where
$$\begin{aligned}\Delta_V(Q, J) \equiv \frac{3}{8\alpha_1} Q^{1/6} J^{1/2} \log\left(J/Q^{1/3}\right) - \frac{3}{4\alpha_1} Q^{1/6} J^{1/2} \log\left(1 + \sqrt{J/Q}\right) \\ - \frac{3}{2\alpha_1} Q^{2/3} \log\left(1 + \sqrt{J/Q}\right) + \tilde{\gamma} Q^{1/6} J^{1/2} + \mathcal{O}\left(Q^{1/6} J^{1/2} \times \frac{Q^{1/3}}{J}\right).\end{aligned} \tag{6.5}$$
  The leading contribution in (6.5) comes from the first term, because of the logarithmic enhancement. The other terms can be interpreted as finite-size corrections due to the vortex extension and are functionally distinguished from the relative $Q^{1/3}/J$ corrections.
- For $Q \ll J_{34} \ll Q^{4/3}$ the superfluid forms a vortex crystal. The scaling dimension of the corresponding operator is given by
$$\Delta = \Delta_Q + \frac{3}{4\alpha_1} \frac{J_{34}^2}{Q^{4/3}} + \mathcal{O}\left(\frac{J_{34}^2}{Q^{4/3}} \times \frac{Q}{J_{34}}, \frac{J_{34}^2}{Q^{4/3}} \times \left(\frac{J_{34}}{Q^{4/3}}\right)^2\right). \tag{6.6}$$

Mixed symmetric representations are conveniently parametrized in terms of J_{34}, J_{12} in (6.1). We write J_{ab} to generically denote any of them. We find the following results:

- For $2 \leq J_{12} \leq J_{34} \ll Q^{1/3}$ the minimal energy state is given by two phonons propagating on the superfluid, with energy:
$$\Delta = \Delta_Q + \sqrt{\frac{J_{34}(J_{34}+2)}{3}} + \sqrt{\frac{J_{12}(J_{12}+2)}{3}} + \mathcal{O}\left(\frac{J_{ab}^4}{Q^{2/3}}\right). \tag{6.7}$$

- For $1 \leq Q - J_{34} \ll Q$ and $2 \leq J_{12} \ll Q^{1/3}$, the lowest energy state corresponds to a Kelvin wave of spin J_{12} propagating on a large vortex ring. The corresponding operator scaling dimension is given by:

$$\begin{aligned}\Delta = \Delta_Q &+ \Delta_V(Q, J_{34}) \\ &+ \frac{3}{8\alpha_1}\frac{\pi(J_{12}^2-1)}{Q^{1/3}}\left[\log Q^{2/3} - 2\psi\left(\frac{J_{12}+1}{2}\right) - 2\gamma_E - 1 - \log 64\right] \\ &\qquad + \tilde{\gamma}\frac{\pi(J_{12}^2-1)}{Q^{1/3}} + \mathcal{O}\left(\frac{J_{12}^4}{Q}\right). \end{aligned} \tag{6.8}$$

- For $Q^{1/3} \ll J_{12} \leq J_{34} \leq Q$ and $(J_{12}+J_{34}-Q)^2 \gg J_{12}J_{34}/Q^{2/3}$, the minimal energy state is given by two vortex rings. When $1 \leq Q - J_{34} \ll Q^{1/3}$ the energy is given by the sum of the two free contributions

$$\Delta = \Delta_Q + \Delta_V(Q, J_{34}) + \Delta_V(Q, J_{12}), \qquad 1 \leq Q - J_{34} \ll Q^{1/3}. \tag{6.9}$$

  Interactions correct the result in the general case, which takes the same form only to logarithmic accuracy

$$\begin{aligned}\Delta = \Delta_Q + \frac{3}{8\alpha_1}Q^{1/6}\left[J_{34}^{1/2}\log\left(J_{34}/Q^{1/3}\right) + J_{12}^{1/2}\log\left(J_{12}/Q^{1/3}\right)\right] \\ + \mathcal{O}\left(Q^{1/6}J_{ab}^{1/2}\right). \end{aligned} \tag{6.10}$$

- For $Q \ll J_{12} \leq J_{34} \ll Q^{4/3}$ the superfluid arranges in a vortex lattice as in (6.6); the scaling dimension of the corresponding operator is

$$\Delta = \Delta_Q + \frac{3}{4\alpha_1}\frac{J_{34}^2 + J_{12}^2}{Q^{4/3}} + \mathcal{O}\left(\frac{J_{ab}^2}{Q^{4/3}} \times \frac{Q}{J_{ab}}, \frac{J_{ab}^2}{Q^{4/3}} \times \left(\frac{J_{ab}}{Q^{4/3}}\right)^2\right). \tag{6.11}$$

The rest of this chapter is organized as follows. In sec. 6.2 we formulate the effective field theory (EFT) for vortices in $3+1$ dimensions. The results are derived in sec. 6.3. In sec. 6.4 we show how to make predictions for correlators involving a current insertion between two vortex states and in sec. 6.5 we briefly comment on how the results (6.4) and (6.6) change in generic spacetime dimensions. Some details are given in appendix C.

Conventions and coordinates on S^3: We use indices $a, b, \dots$ for the $\mathbb{R}^4$ embedding of S^3, which go from 1 to 4. Embedding coordinates are denoted $X_a = X^a$. Calling $X_a(x)$ the $\mathbb{R}^4$ coordinate corresponding to an S^3 point x, the chordal distance between two points x and x' is given by:

$$\Delta X^2(x, x') = \sum_a \left[X_a(x) - X_a(x')\right]^2. \tag{6.12}$$

A convenient parametrization of S^3 is provided by Hopf coordinates, defined via the embedding:

$$X_1 = R\cos\xi\sin\eta, \quad X_2 = R\sin\xi\sin\eta, \quad X_3 = R\cos\phi\cos\eta, \quad X_4 = R\sin\phi\cos\eta. \tag{6.13}$$

This gives the following metric tensor

$$\frac{ds^2}{R^2} = d\eta^2 + \sin^2\eta d\xi^2 + \cos^2\eta d\phi^2, \qquad \eta \in [0,\pi/2], \quad \xi \in [0,2\pi], \quad \phi \in [0,2\pi]. \tag{6.14}$$

For fixed η different from 0 and $\pi/2$, ξ and ϕ describe an $S^1 \times S^1$ submanifold.

6.2 Formulation of the EFT in four dimensions

6.2.1 Dual gauge field

Let us recall that the leading order conformal superfluid Lagrangian in $d = 4$ reads

$$\mathcal{L} = c_1(\partial\chi)^4 + c_2(\partial\chi)^2 \left\{ \mathcal{R} + 6\frac{[\partial_\mu(\partial\chi)]^2}{(\partial\chi)^2} \right\} + \dots, \tag{6.15}$$

whose cutoff is set by $\Lambda \sim j_0 \sim Q^{1/3}/R$. We assume c_1 and all other Wilson coefficients to be of order one, corresponding to the generic expectation for a strongly coupled system. From this Lagrangian we derive the phonon spectrum $\omega_J = \sqrt{J(J+2)/3}$, as discussed in chapter 3. The results (6.3) and (6.7) then follow as explained in the three-dimensional case in sec. 5.2. Throughout this chapter, unless otherwise stated, we shall work at leading order in the derivative and field expansion within EFT.

As in $2+1$ dimensions, to write a local coupling between vortices and the superfluid we consider a dual description in terms of a gauge field. Following the same steps of sec. 5.3, we rewrite the leading order Lagrangian (6.15) using a two form Lagrange multiplier $A_{\mu\nu} = -A_{\nu\mu}$:

$$\mathcal{L} = cv^4 - \frac{1}{4\pi}A_{\mu\nu}\frac{\epsilon^{\mu\nu\rho\sigma}}{\sqrt{g}}\partial_\rho v_\sigma, \tag{6.16}$$

Integrating out v_μ then gives

$$\mathcal{L} = -\kappa H^{4/3}, \qquad H_{\mu\nu\rho} = \partial_\mu A_{\nu\rho} + \partial_\nu A_{\rho\mu} + \partial_\rho A_{\mu\nu}, \tag{6.17}$$

where $H = \sqrt{-H_{\mu\nu\rho}H^{\mu\nu\rho}}$ and $\kappa = \frac{1}{16\pi^{4/3}}\left(\frac{3}{4c_1}\right)^{1/3}$. The $U(1)$ current provides the relation between χ and $A_{\mu\nu}$:

$$j^\mu = 4c(\partial\chi)^2\partial^\mu\chi = \frac{1}{12\pi}\frac{\epsilon^{\mu\nu\rho\sigma}}{\sqrt{g}}H_{\nu\rho\sigma}. \tag{6.18}$$

Consequently, the homogeneous charge density $\langle j^0 \rangle = \frac{Q}{2\pi^2 R^3}$ in the vacuum translates into a constant background field:

$$\langle H_{\eta\xi\phi}\rangle = -B\sin\eta\cos\eta, \qquad B \equiv \frac{Q}{\pi R^3}. \tag{6.19}$$

The cutoff of the theory is thus set by $B^{1/3}$ in the dual description:

$$\Lambda \sim B^{1/3} \sim \frac{Q^{1/3}}{R}. \tag{6.20}$$

The action (6.17) is often called of Kalb-Ramond type and is invariant under the gauge transformations $A_{\mu\nu} \to A_{\mu\nu} + \partial_\mu\xi_\nu - \partial_\nu\xi_\mu$, for an arbitrary vector ξ_μ. The gauge redundancy allows imposing three gauge fixing conditions, since a gauge transformation generated by a total derivative $\xi_\mu = \partial_\mu\alpha$ acts trivially.

In the following, we shall be interested in fluctuations of the background (6.19). It is thus convenient to expand the gauge field in a background value $\bar{A}_{\mu\nu}$ plus fluctuations:

$$A_{\mu\nu} = \bar{A}_{\mu\nu} + \delta A_{\mu\nu}, \tag{6.21}$$

where a possible choice is

$$\bar{A}_{\eta\xi} = \bar{A}_{\eta\phi} = 0, \qquad \bar{A}_{\xi\phi} = -\frac{B}{2}\left(1-\cos^2\eta\right). \tag{6.22}$$

Fluctuations are conveniently parametrized in terms of two three vectors b^i and a_i defined as:

$$\delta A_{ij} = \sqrt{g}\,\epsilon_{ijk}b^k, \qquad \delta A_{0i} = a_i. \tag{6.23}$$

We partially fix the gauge requiring $\nabla_i A^{ik} = 0$, which sets the curl of b^i to zero. Then the Lagrangian to quadratic order in the fluctuation reads:

$$\mathcal{L} \simeq \frac{1}{4e^2}f^2 + \frac{1}{2e^2}\left[\dot{b}^i\dot{b}_i - \frac{1}{3}\left(\nabla_i b^i\right)^2\right], \tag{6.24}$$

where $e^2 = \frac{(\sqrt{6}B)^{2/3}}{8\kappa}$ and $f^2 = f_{ij}f^{ij}$ with

$$f_{ij} = \partial_i a_j - \partial_j a_i. \tag{6.25}$$

Following the gauge fixing, the field b^i is purely longitudinal and corresponds to the phonon. Instead a_i is a non-propagating degree of freedom, called the *hydrophoton* since the residual $U(1)$ gauge invariance acts as $a_i \to a_i - \partial_i\xi_0$. Analogously to the Coulomb field in eq. (5.13), the hydrophoton does not correspond to a local field in the original description and provides the leading coupling to the vortices.

6.2.2 String-vortex duality

Vortices in the dual description correspond to topological line defects, which are described as $1+1$ dimensional strings embedded in the $3+1$ dimensional spacetime [179–181]. The line element of a vortex p is parametrized by $X_p^\mu(\tau,\sigma)$, where τ and σ are the world-sheet coordinates. We use the words "vortex" and "string" interchangeably. We also assume that no light degrees of freedom, besides the string coordinates, live on the worldsheet.

The Lagrangian is required to be Weyl invariant and reparametrization invariant for both τ and σ and is analogous to (5.17). The lowest order terms are given by

$$S = -\kappa \int d^4x \sqrt{g} H^{4/3} - \sum_p \lambda_p \int d\tau d\sigma A_{\mu\nu} \partial_\tau X_p^\mu \partial_\sigma X_p^\nu \\ - \sum_p \int d\tau d\sigma H^{2/3} \sqrt{|\det(G_{\alpha\beta})|} F_p \left[h_{\alpha\beta} G^{\alpha\beta} \right] + \dots . \tag{6.26}$$

The first term was discussed in the previous section. The second term is the leading coupling between a string of vorticity $\lambda_p \in \mathbb{Z}$ and the gauge field. The last term is the generalized Nambu-Goto (NG) action for the vortex; in appendix C.1 we derive its form via the coset construction. Here, the world-sheet metric is provided by:

$$G_{\alpha\beta} = g_{\mu\nu} \partial_\alpha X_p^\mu \partial_\beta X_p^\nu, \qquad \alpha, \beta = \tau, \sigma. \tag{6.27}$$

Since the superfluid velocity breaks Lorentz invariance, one can construct another independent symmetric world-sheet tensor, which can be chosen as

$$h_{\alpha\beta} = \partial_\alpha X^\mu \partial_\beta X^\nu \frac{j_\mu j_\nu}{j^2}. \tag{6.28}$$

In general the NG action contains an arbitrary function of $G^{\alpha\beta} h_{\alpha\beta}$, where $G^{\alpha\beta}$ is the inverse of $G_{\alpha\beta}$. Weyl invariance further fixes the power of H which multiplies it. Finally dots in (6.26) stands for higher derivative terms.

Consider now the physical gauge $X_p^0 = \tau$ for vortices. Using (6.22), the second term in (6.26) is linear in time derivatives of the vortex line. As we will self-consistently see in the next section, this implies that vortices move with drift velocity $|\dot{\vec{X}}| \sim f/B \sim B^{-1/3}$. Then, similarly to what we argued below (5.17), terms of the kind $\dot{\vec{X}} \cdot \dot{\vec{X}}$ in the NG action can be treated as higher derivatives and we neglect them. The coupling of the phonon field to the strings is also negligible to leading order. In this regime, the action reduces to

$$S \simeq \frac{1}{e^2} \int d^4x \left\{ \frac{1}{4} f^2 + \frac{1}{2} \left[\dot{b}^i \dot{b}_i - \frac{1}{3} \left(\nabla_i b^i \right)^2 \right] \right\} \\ - \sum_p \int d\tau d\sigma \left[\lambda_p \left(\bar{A}_{ij} \partial_\tau X^i \partial_\sigma X^j + a_i \partial_\sigma X_p^i \right) + \gamma_p B^{2/3} (\partial_\sigma X) \right], \tag{6.29}$$

where $\gamma_p = 6^{1/3}F_p(1)$ and we define

$$(\partial_\sigma X) = \sqrt{|g_{ij}|\partial_\sigma X_p^i \partial_\sigma X_p^j}\,. \tag{6.30}$$

From the first line of eq. (6.29), we see that the phonon spectrum to leading order is not affected by the presence of vortices.

6.3 Scaling dimensions from vortices in four dimensions

6.3.1 Classical analysis

From the leading order action (6.29) the following equations of motion for the hydrophoton and the strings are derived

$$-\frac{1}{e^2}\nabla_i f^{ij} = \sum_p \mathcal{J}_p^j \equiv \sum_p \lambda_p \int d\sigma\, \partial_\sigma X_p^j \frac{\delta^3(x^i - X_p^i)}{\sqrt{g}}, \tag{6.31}$$

$$\lambda_p \left(f_{ik} - B\sqrt{g}\epsilon_{ijk}\dot{X}_p^j\right)\partial_\sigma X_p^k = \gamma_p B^{2/3}|g_{ij}|\frac{D}{D\sigma}\left[\frac{\partial_\sigma X^j}{(\partial_\sigma X)}\right]. \tag{6.32}$$

Eq. (6.31) is analogous to Ampère's circuital law in magnetostatic, a vortex acting as an electric current $\mathcal{J}_p^i$ sourcing the field f^{ij}. Eq. (6.32) is the string equation of motion. Notice that it is first order in time derivatives and implies that vortices move with drift velocity $|\dot{\vec{X}}| \sim f/B \sim B^{-1/3}$. The right-hand side arises from the NG action and it is proportional to the covariant derivative of the line element $\frac{D}{D\sigma}\left[\frac{\partial_\sigma X^j}{(\partial_\sigma X)}\right]$; the left-hand side comes from the minimal coupling to the gauge field.

As in sec. 5.4.1 the electrostatic problem required the net charge on the sphere to be zero, the $3+1$ dimensional magnetostatic problem defined by (6.31) and (6.32) requires zero vorticity flux on every closed surface. To this aim, we only consider closed strings. This point is perhaps more easily understood considering a vortex in the scalar description (6.15), simlarly to what we did in sec. 5.2. In that language, a vortex configuration is a field profile where the value of the field changes from $\pi(x) = 0$ to $\pi(x) = 2\pi\lambda$ from below to above of a certain two-dimensional spacelike surface, where $\lambda \in \mathbb{Z}$ ($\lambda \neq 0$) is the vorticity [207]. The vortex is just the boundary of this surface. As S^3 is a compact manifold, the string must form a closed curve. In this picture it is also clear that a closed vortex configuration cannot break into an open string. [1]

The energy and the angular momentum associated to solutions of the EOMs are computed from the stress energy tensor $T_{\mu\nu} = \frac{2}{\sqrt{g}}\frac{\delta S}{\delta g^{\mu\nu}}$:

---

[1] More formally, the surface described above is the object charged under the 2-form symmetry associated with the current $J_{\mu\nu\rho} = \sqrt{g}\epsilon_{\mu\nu\rho\sigma}\partial^\sigma\chi \propto H_{\mu\nu\rho}/H^{2/3}$ [58]; conservation of this current, associated with the winding number of the Goldstone, forbids the breaking of a closed string.

$$\begin{aligned} T_{\mu\nu} = {} & \frac{\kappa}{H^{2/3}}\left(4H_{\mu\sigma\rho}H_{\nu}{}^{\sigma\rho} + g_{\mu\nu}H^2\right) \\ & + \sum_p \gamma_p B^{2/3} \int d\tau d\sigma \frac{\delta^4(x^\mu - X_p^\mu)}{\sqrt{g}} \sqrt{\left|\det(G_{\alpha\beta})\right|}\, G^{\alpha\beta}\, \partial_\alpha X_p^\sigma \partial_\beta X_p^\rho\, g_{\sigma\mu} g_{\rho\nu}. \end{aligned} \tag{6.33}$$

The classical energy of the state is found from

$$E = \frac{\Delta}{R} = \frac{3Q^{4/3}}{8\pi^{2/3} c_1^{1/3} R} + \frac{1}{4e^2}\int d^3x \sqrt{g} f^2 + \sum_p \gamma_p B^{2/3} \int d\sigma (\partial_\sigma X). \tag{6.34}$$

The first term is the energy of the homogenous ground state. The second term is the energy stored in the *magnetostatic* field f_{ij} created by the vortices. Finally, the last term is the contribution from the tension and is proportional to the length of the string L_p.

Eq. (6.31) gives the field a_i in terms of the string current:

$$a_i(x) = e^2 \sum_p \int d^3x' G_{ij}(x, x') \mathcal{J}_p^j(x'), \tag{6.35}$$

where $G_{ij}(x, x')$ is the photon propagator on S^3. In appendix C.2 it is shown that the photon Green function on S^{d-1} takes the form

$$G_{ij'}(x, x') = -\left(\partial_i \partial_{j'} u(x, x')\right) F(u(x, x')), \qquad u = \frac{1}{2}\Delta X^2(x, x') \tag{6.36}$$

where ΔX^2 is the chordal distance between two points in embedding space, and

$$F(u) = \frac{\Gamma(d-3)}{(4\pi)^{\frac{d-1}{2}} \Gamma\left(\frac{d-1}{2}\right) R^{d-3}}\, {}_2F_1\left(1, d-3; \frac{d-1}{2}; 1 - \frac{u}{2R^2}\right). \tag{6.37}$$

Finally, we can also restore the subleading terms in the Lagrangian (6.15). Neglecting the fluctuations induced by vortices everywhere but in the leading term, the scaling dimension of the corresponding operator is written as

$$\Delta = \Delta_Q + \frac{Re^2}{2} \sum_{p,p'} \int d^3x \sqrt{g} \int d^3x' \sqrt{g'} \mathcal{J}_p^j(x) G_{jk'}(x, x') \mathcal{J}_{p'}^{k'}(x') + \sum_p \gamma_p R\, B^{2/3} L_p, \tag{6.38}$$

where $\Delta_Q = \alpha_1 Q^{4/3} + \dots$ as in eq. (6.2) and $\alpha_1 = \frac{3}{8\pi^{2/3} c^{1/3}}$. Notice the analogy with the structure of eq. (5.26).

The angular momentum (in units of $1/R$) of the corresponding state can be computed similarly:

$$J_{ab} = \frac{RB}{2e^2} \int d^3x \sqrt{g}\, n^i_{ab} \epsilon_{ijk} \sqrt{g} f^{jk}, \tag{6.39}$$

where n_{ab} is the Killing vector corresponding to a rotation in the (X_a, X_b) plane. Using Ampère's law (6.31) and Stoke's theorem, we can conveniently rewrite it as

$$\frac{1}{2} J_{ab}\epsilon_{abcd} = -\frac{RB}{2} \sum_p \lambda_p \int d\sigma_p \left[X^p_c(\partial_\sigma X^p_d) - X^p_d(\partial_\sigma X^p_c)\right] = -RB \sum_p \lambda_p \int dX^p_c \wedge dX^p_d, \tag{6.40}$$

where X^p_a are the vortex coordinates in the $\mathbb{R}^4$ embedding of S^3. The last equation on the right-hand side is a formal notation for the area enclosed by the vortex projection in the (X_c, X_d) plane of the $\mathbb{R}^4$ embedding of S^3.

In the following we will study simple specific configurations.

6.3.2 Vortex rings

In nature, vortices often have a ring shape and move with a constant speed inversely proportional to the radius [178]. It is hence natural to look for vortex ring solutions of the EOMs (6.31) and (6.32). As we will see, a vortex ring generalizes the vortex-antivortex configuration in fig. 5.1.

The simplest configuration one can study is a slowly moving vortex ring with unit negative charge $\lambda = -1$. We pick the gauge $\xi = \sigma$ and consider a radius $rR \leq R$ ring in the (X_1, X_2) plane in embedding space. The EOMs implies that the ring rotates with constant drift velocity v in the (X_3, X_4) plane:

$$X_1^2(t,\sigma) + X_2^2(t,\sigma) = R^2 \sin^2 \eta(t,\sigma) = R^2 r^2 = const. \qquad \phi(t,\sigma) = vt + const.\,. \tag{6.41}$$

The precise value of v is fixed by eq. (6.31). From eq. (6.40) it follows that the only nonvanishing component of the angular momentum is given by:

$$J_{34} = Qr^2. \tag{6.42}$$

In figure 6.1 the motion is depicted in stereographic coordinates, defined by the relation $(x, y, z) = \frac{1}{1+X_1}(X_3, X_4, X_2)$. Eq. (6.41) corresponds to a ring orbiting around the z axis; as the angular momentum is increased, the ring size increases and its velocity decreases. For $r \to 1$ the surface embedded by the ring in the stereographic projection extends to cover the whole plane and the vortex lies statically on the geodesic corresponding to the z axis. Fig. 6.1 qualitatively generalizes the $2+1$ dimensional motion depicted in fig. 5.1.

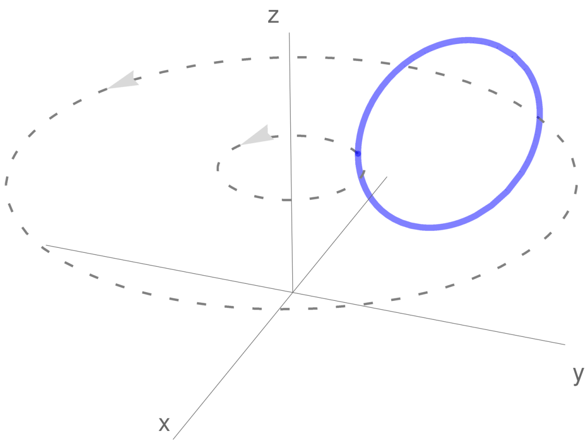

Figure 6.1 – The vortex ring orbit in stereographic coordinates.

Using (6.38) we can calculate the energy of this configuration as:

$$E = \Delta_Q/R + \frac{e^2 R}{2}\iint d\xi d\xi' \mathcal{J}^i(\xi) G_{ij}\left(x(\xi), x(\xi')\right)\mathcal{J}^j(\xi') + \gamma B^{2/3} 2\pi r R, \tag{6.43}$$

The only nontrivial contribution arises from the second term, corresponding to the magnetostatic self-energy of the string. It diverges due to the short distance behaviour of the hydrophoton propagator. We regulate the calculation working in d spacetime dimensions, as explained in appendix C.3; the result is

$$\begin{aligned} E = \Delta_Q/R + e^2\pi R \Bigg\{ & \frac{r}{2\pi(4-d)} + \frac{r\left[\log\left(4\pi r^2 B^{2/3} R^2\right) + \frac{9}{2} + \frac{1}{3}\log 6 - \gamma_E - 2\psi\left(\frac{3}{2}\right)\right]}{4\pi} \\ & - \frac{r}{2\pi}\log(r+1) - \frac{1}{\pi}\log(r+1) \Bigg\} + \gamma B^{2/3} 2\pi r R. \end{aligned} \tag{6.44}$$

Details of the computation are given in appendix C.3.1. There is a divergent piece for $d \to 4$ proportional to the vortex length, which renormalizes the string tension. The contribution logarithmically enhanced by the cutoff $\sim e^2 r \log\left(r^2 B^{2/3}\right)$ can be seen as a consequence of the renormalization group running of γ induced by the hydrophoton [179]. Collecting everything, the scaling dimension (6.38) for a vortex ring state reads

$$\Delta = \Delta_Q + \Delta_V(Q, J_{34}), \tag{6.45}$$

where we isolated the vortex contribution to the energy:

$$\begin{aligned} \Delta_V(Q,J) = \frac{3}{8\alpha_1} Q^{1/6} J^{1/2} \log\left(J/Q^{1/3}\right) - \frac{3}{4\alpha_1} Q^{1/6} J^{1/2} \log\left(1 + \sqrt{J/Q}\right) \\ - \frac{3}{2\alpha_1} Q^{2/3} \log\left(1 + \sqrt{J/Q}\right) + \tilde{\gamma} Q^{1/6} J^{1/2}. \end{aligned} \tag{6.46}$$

Here $\tilde{\gamma}$ is a finite new coupling which absorbs all contributions proportional to r in (6.44). As in (5.28), the leading contribution arises because of the classical running of the tension induced by the magnetostatic self-energy and is given by the first term in (6.46). For $J \ll Q$, the other contributions can be expanded in powers of the vortex length and to leading order effectively scale as $Q^{1/6}J^{1/2}$. Physically, this is understood noticing that the vortex energy *density* is set by $e^2 \sim Q^{2/3}$, hence for short vortices the energy can be estimated as the length times the energy density (neglecting the logarithmic running of the tension): $2\pi rR \times e^{2/3} \sim Q^{1/6}J^{1/2}$. However, as $J \to Q$ the functional dependence of the second and third term in eq. (6.46) deviates from this expectation, as a consequence of the vortex finite size.

As the ring radius is decreased to inverse cutoff length $r \to 1/(\Lambda R)$, corresponding to $J_{34} \to Q^{1/3}$, the magnetostatic field $f \sim e^2/(Rr)$ becomes of the same order of the background field B and the vortex velocity approaches the relativistic regime. Hence subleading contributions to (6.29) become unsuppressed and the EFT breaks down.

Eq. (6.45) can be identified as the minimal energy state at fixed angular momentum in its regime of validity.

We now study states with two vortices, one laying on the (X_1, X_2) plane and the other on the (X_3, X_4) plane in embedding space. Because of (6.40), these configurations are associated to operators in mixed symmetric representations of the $SO(4)$ group.

Consider first a radius R ring in the (X_1, X_2) plane interacting with a ring of arbitrary size in the (X_3, X_4) plane. In this geometry, the interaction does not affect the equations of motion and the solution takes a simple form

$$\begin{array}{llll} \text{vortex 1}: & X_1^2(t,\sigma_1) + X_2^2(t,\sigma_1) = R^2, & & \sigma_1 = \xi_1; \\ \text{vortex 2}: & \cos^2\eta_2(t,\sigma_2) = r_2^2, & \xi_2(t,\sigma_2) = v_2 t, & \sigma_2 = \phi_2. \end{array} \tag{6.47}$$

Focussing on negative unit charge vortices $\lambda_1 = \lambda_2 = -1$, this configuration corresponds to an operator in a mixed symmetric representation with spin given by

$$J_{34} = Q, \qquad J_{12} = Q r_2^2. \tag{6.48}$$

Since the *electric* currents $\mathcal{J}^i$ sourced by the strings are orthogonal, the corresponding scaling dimension is found analogously to (6.45):

$$\Delta = \Delta_Q + \Delta_V(Q, J_{34}) + \Delta_V(Q, J_{12}). \tag{6.49}$$

To leading order, a similar solution exists for $0 \le (1 - r_1^2) \ll (R\Lambda)^{-2}$, hence for $0 \le Q - J_{34} \ll Q^{1/3}$. As before, the consistency of the EFT requires $J_{12} \gg Q^{1/3}$.

In general, the mutual interaction affects non trivially the motion of the two vortex rings. One can, however, identify the logarithmically enhanced contributions analogous to the first term in (6.46) just from the free action. These indeed arise from the running of the tension induced by the hydrophoton contribution to the vortex self-energy. For $Q^{1/3} \ll J_{12}, J_{34} \leq Q$, the leading contribution to the energy reads:

$$\Delta = \Delta_Q + \frac{3}{8\alpha_1} Q^{1/6} \left[J_{34}^{1/2} \log\left(J_{34}/Q^{1/3}\right) + J_{12}^{1/2} \log\left(J_{12}/Q^{1/3}\right)\right]. \tag{6.50}$$

This result holds as long as the minimal distance ΔX_{min} between the two vortices is larger than the inverse of the cutoff:

$$\frac{\Delta X_{min}^2}{R^2} \sim \frac{(J_{12}+J_{34}-Q)^2}{J_{12}J_{34}} \gg \frac{1}{Q^{2/3}}. \tag{6.51}$$

6.3.3 Vortex crystals

Since the magnetostatic self-energy of a single vortex is proportional to λ^2, strings with $|\lambda| \geq 1$ are energetically unfavored. Hence the minimal energy state for values of the angular momentum $J_{34} \gg Q$ is made by $n \gg 1$ vortices. We then approximate the vortex distribution with a continuous current density $\mathcal{J}^i(x)$. The corresponding state is found minimizing the energy (6.34) at fixed angular momentum (6.39), giving the following density profile:

$$\mathcal{J}^\xi = \frac{2}{\pi R^2}\frac{J_{34}}{Q}, \qquad \mathcal{J}^\phi = \mathcal{J}^\eta = 0. \tag{6.52}$$

The leading contribution to the energy comes from the magnetostatic field and reads

$$\Delta = \Delta_Q + \frac{3}{4\alpha_1}\frac{J_{34}^2}{Q^{4/3}}. \tag{6.53}$$

Physically, this state corresponds to a vortex crystal [197, 198]. When $J_{34} \to Q^{4/3}$, the magnetic field f approaches B, vortices become relativistic and the EFT breaks down.

Similarly, the ground state for $Q \ll J_{34}, J_{12} \ll Q^{4/3}$ is provided by a vortex crystal, whose current density and energy are given by

$$\mathcal{J}^\xi = \frac{2}{\pi R^2}\frac{J_{34}}{Q}, \qquad \mathcal{J}^\phi = \frac{2}{\pi R^2}\frac{J_{12}}{Q}, \qquad \mathcal{J}^\eta = 0, \tag{6.54}$$

$$\Delta = \Delta_Q + \frac{3}{4\alpha_1}\frac{J_{34}^2+J_{12}^2}{Q^{4/3}}. \tag{6.55}$$

6.3.4 Quantization and Kelvin waves

Vortices in four dimensions are extended objects and can thus propagate *Kelvin* waves on them [179]. The corresponding states are associated to primary operators in the CFT. To study them, we consider a single string of vorticity $\lambda = -1$. It is convenient to parametrize its coordinates via the following variables:

$$z(t,\sigma) = X_1(t,\sigma) + iX_2(t,\sigma) = R\sin\eta(t,\sigma)e^{i\xi(t,\sigma)}, \tag{6.56}$$

$$w(t,\sigma) = X_3(t,\sigma) + iX_4(t,\sigma) = R\cos\eta(t,\sigma)e^{i\phi(t,\sigma)}. \tag{6.57}$$

These are related through the constraint $|z|^2 + |w|^2 = 1$. We pick the gauge $\xi = \sigma$ and $t = \tau$. Integrating out explicitly the hydrophoton from eq. (6.29), we find the single vortex action as

$$\begin{aligned} S_{1-vortex} = &\int dt d\sigma \left[i\frac{B}{2} w^* \dot{w} - \gamma B^{2/3}\sqrt{|\partial_\sigma z|^2 + |\partial_\sigma w|^2}\right] \\ &+ \frac{e^2}{4}\int dt d\sigma d\sigma' \left(\partial_\sigma \partial_{\sigma'} \Delta X^2(\sigma,\sigma')\right) F\left(\frac{\Delta X^2(\sigma,\sigma')}{2R^2}\right), \end{aligned} \tag{6.58}$$

where F is given in (6.36). Eq. (6.58) can be seen as the (nonlocal) action of a complex field $w(t,\sigma)$ living on $\mathbb{R}\times S^1$. It is manifestly invariant under the action of the unbroken rotation generators J_{34}, corresponding to rotations around the vortex $w \to e^{i\alpha}w$, and J_{12}, corresponding to translations along the string $\sigma \to \sigma + \alpha$.

We expand for small fluctuations around the background $w = 0$, which describes a radius R ring in the (X_1, X_2) plane with $J_{34} = Q$. The action to quadratic order reads:

$$S_{1-vortex} \simeq \int dt d\sigma \left[i\frac{B}{2} w^*\dot{w} - \gamma B^{2/3} - \frac{\gamma B^{2/3}}{2}|\partial_\sigma w|^2 + \frac{\gamma B^{2/3}}{2}|w|^2\right] + S^{(2)}_{non-local}, \tag{6.59}$$

where $S^{(2)}_{non-local}$ is found expanding the second line in (6.58). It follows that the vortex is quantized as a standard non-relativistic field:

$$w(t,\sigma) = \sqrt{\frac{2}{B}}\sum_{n=-\infty}^{\infty}\frac{a_n}{2\pi}e^{-i\omega_n t + in\sigma}, \qquad [a_n, a_m^\dagger] = 2\pi\delta_{nm}. \tag{6.60}$$

As usual the a_n annihilate the vacuum $a_n|0\rangle = 0$, and thus so does $w(t,\sigma)$. The proper frequencies ω_n are computed in appendix C.3.2 and read

$$R\omega_n \equiv \Delta_k(n) = \frac{\pi(n^2-1)}{Q^{1/3}}\left\{\frac{3}{8\alpha}\left[\log Q^{2/3} - 2\psi\left(\frac{n+1}{2}\right) - 2\gamma_E - 1 - \log 64\right] + \tilde{\gamma}\right\}. \tag{6.61}$$

Notice that the $n = 0$ mode decreases the energy, while the $n = \pm 1$ modes have $\omega_{\pm 1} = 0$. This can be understood from the expression of the angular momentum in terms of ladder operators at order $\mathcal{O}(Q^0)$. The rotations generated by J_{12} and J_{34} are linearly realized and their generators are quadratic in terms of ladder operators:

$$J_{34} = Q - \sum_n \frac{a_n^\dagger a_n}{2\pi}, \qquad J_{12} = \sum_n n\frac{a_n^\dagger a_n}{2\pi}. \tag{6.62}$$

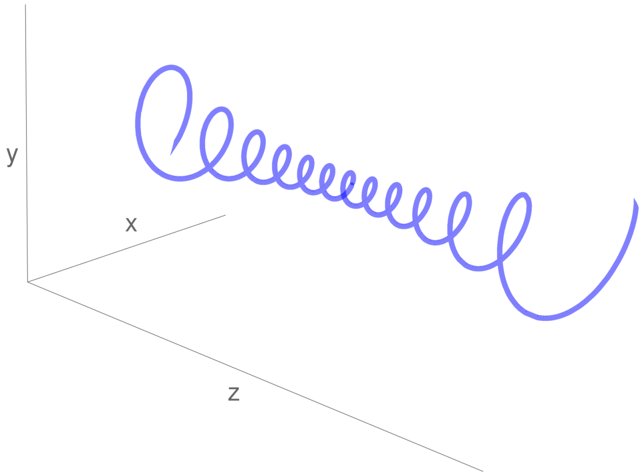

Figure 6.2 – A Kelvin wave in stereographic coordinates $(x, y, z) = \frac{1}{1+X_1}(X_3, X_4, X_2)$.

The string realizes *nonlinearly* the full rotation group. As a consequence, the broken components of the angular momentum are linear in the $n = \pm 1$ annihilation and creation operators:

$$\begin{aligned} J_{23} + J_{14} &= -\sqrt{\frac{Q}{2\pi}}\left(a_{-1} + a_{-1}^{\dagger}\right), & J_{23} - J_{14} &= \sqrt{\frac{Q}{2\pi}}\left(a_{1} + a_{1}^{\dagger}\right), \\ J_{31} + J_{24} &= i\sqrt{\frac{Q}{2\pi}}\left(a_{-1} - a_{-1}^{\dagger}\right), & J_{31} - J_{24} &= i\sqrt{\frac{Q}{2\pi}}\left(a_{1} - a_{1}^{\dagger}\right). \end{aligned} \tag{6.63}$$

From (6.62) we see that the $n = 0$ mode decreases J_{34} (and the radius of the vortex) by one unit, hence it corresponds to the quantization of the classical ring solution discussed in 6.3.2. Eq. (6.63) implies that the $n = \pm 1$ modes do not correspond to new states, but describe rotations of the string orientation and therefore have vanishing frequency. In this sense, their role is analogous to that of the $J = 1$ phonons for the conformal superfluid, which describe descendants of the ground state as explained in sec. 3.2.2.

The modes with $|n| \geq 2$ correspond to new solutions and are interpreted as Kelvin waves propagating on the vortex; in the CFT they correspond to operators with the following quantum numbers [2]

$$J_{34} = Q - 1, \qquad J_{12} = n, \qquad \Delta = \Delta_Q + \Delta_V(Q, Q) + \Delta_k(n). \tag{6.64}$$

As shown in fig. 6.2, a Kelvin wave in stereographic coordinates takes the form of a solenoid, trapping the magnetic field inside. The string undergoes a helical motion analogous to the one of a wine opener.

---

[2] In Δ we neglect a $\sim Q^{-1/3}$ contribution from the vortex Casimir energy; this term does not depend on J_{12} and can be thought as a subleading correction to Δ_V.

Notice that Kelvin waves carry less energy than phonons with the same angular momentum. It follows that a state obtained acting on the vacuum as

$$(a_0^\dagger)^m a_n^\dagger\left|0\right\rangle \equiv \left|J_{34}=Q-m-1, J_{12}=n\right\rangle \tag{6.65}$$

is the minimal energy state for the specified value of the angular momentum.

This description applies in the linear regime $m+1=Q-J_{34}\ll Q$. When $n=J_{12}\to Q^{1/3}$ higher derivative terms become unsuppressed and the EFT breaks.

6.3.5 Higher order corrections

Corrections arise from higher derivative terms we neglected in (6.29) and are suppressed by powers of the cutoff scale (6.20). Here we comment on their form.

The first class of corrections was discussed in chapter 3 and arises considering the effect of curvature terms in the superfluid and vortex action; these corrections are controlled by the sphere radius and hence scale as $1/(\Lambda R)^2\sim 1/Q^{2/3}$. They are also present in the absence of vortices and provide the subleading terms in eq. (6.2).

Focus now on the single vortex state described in sec. 6.3.2. We find corrections controlled by the vortex length $L\sim\sqrt{J_{34}/Q}$, which hence scale as $1/(\Lambda L)^2\sim Q^{1/3}/J_{34}$ (we assume parity invariance, hence they depend only on L^2). They arise from the terms we neglected in the NG action to write (6.26) and are proportional to $(\nabla_i b^i)/B$, f^2/B^2 and $\dot{\vec{X}}^2$. Higher derivatives of the string line element as well as the phonon contribution to the energy (6.17) belong to the same class. Similarly, there are corrections of the form $Q^{1/3}/J_{34}$, $Q^{1/3}/J_{12}$ to eq. (6.49) for a two vortex state. Notice that the subleading $Q^{2/3}$ term in the ground state energy is bigger than the vortex contribution (6.46) for $Q^{1/3}\ll J_{34}\ll Q$. The latter gives instead the leading contribution for $J_{34}\sim Q$. The vortex contribution is anyway functionally distinguished from the ground state energy correction and is thus calculable.

Let us now turn our attention to the Kelvin waves discussed in 6.3.4. The same corrections discussed for a vortex ring exists in this case. Furthermore, for $n\gg 1$ higher derivative corrections to the single vortex action (6.59) become important. As typical for a non-relativistic field, these arise due to terms with two time derivatives, or, equivalently, with four space derivatives (suppressed by an extra $H^{-2/3}$ factor by Weyl invariance) and scale as $n^2/Q^{2/3}=J_{12}^2/Q^{2/3}$. Notice that the relative corrections to the ground state energy of the vortex are bigger than the Kelvin wave energy (6.61) for $J_{12}^2/Q^{1/3}\lesssim Q^{1/2}/J_{34}^{1/2}$; however, these corrections are independent of J_{12}, which enters only through (6.61).

Finally, the leading corrections to the energy of the vortex crystals states discussed in 6.3.3 arise both from the phonon contribution to the energy, which is proportional to $(\nabla_i b^i)^2/f^2\sim\left(J_{ab}/Q^{4/3}\right)^2$, and from the free tension contribution, which gives Q/J

corrections using (6.52) or (6.54). Here J_{ab} stands for both J_{34} and/or J_{12} depending on the state.

6.4 Correlators

We now turn our attention to the study of correlators. As in sec. 5.5, the most natural correlation function[3] which can be studied corresponds to a current insertion within two equal vortex states. In the EFT, this is determined through the following relations:

$$\langle j_0 \rangle = \frac{Q}{2\pi^2 R^3}\,, \qquad \langle j_\phi \rangle = \frac{\sqrt{g}}{2\pi} f^{\eta\xi}\,, \qquad \langle j_\xi \rangle = -\frac{\sqrt{g}}{2\pi} f^{\eta\phi}\,. \tag{6.66}$$

The hydrophoton field is obtained from (6.31), which, in analogy with Ampère's law, can be conveniently rewritten in integral form as

$$\frac{1}{2}\oint_{\mathcal{C}} dx^i \epsilon_{ijk}\sqrt{g} f^{jk} = -e^2 \lambda_{enc}\,, \tag{6.67}$$

where λ_{enc} is the vorticity flux through the surface enclosed by the curve $\mathcal{C}$. Using this relation, eq.s (6.66) can be used to make nontrivial predictions about the OPE coefficients of the theory.

Consider first the traceless symmetric state corresponding to a radius R vortex in the (X_1, X_2) plane, which has $J_{34} = Q$ and $J_{12} = 0$. For this state, eq. (6.66) reads:

$$\langle j_0 \rangle = \frac{Q}{2\pi^2 R^3}\,, \qquad \langle j_\phi \rangle = \frac{e^2}{4\pi^2 R}\,, \qquad \langle j_\xi \rangle = 0\,. \tag{6.68}$$

The expectation value of a spin-1 parity even conserved operator in a traceless symmetric state $|(J,J), J_{34} = 2J, J_{12} = 0\rangle$ is [205]:

$$\begin{aligned}
\langle (J,J), 2J, 0 | j_0(\eta,\xi,\phi) | (J,J), 2J, 0\rangle &= R^{-3} \sum_{m=0}^{2J} a_m \sin^{2m}\eta\,,\\
\langle (J,J), 2J, 0 | j_\phi(\eta,\xi,\phi) | (J,J), 2J, 0\rangle &= R^{-3} \sum_{m=0}^{2J} b_m \sin^{2m}\eta\,,\\
\langle (J,J), 2J, 0 | j_\xi(\eta,\xi,\phi) | (J,J), 2J, 0\rangle &= 0\,,
\end{aligned} \tag{6.69}$$

where a_m and b_m are arbitrary theory dependent real coefficients, subject to the constraint $\sum_m b_m = 0$. Then the EFT gives

$$a_m = \begin{cases} \frac{Q}{2\pi^2}, & \text{if } m = 0\,, \\ 0, & \text{if } 1 \le m \ll Q^{1/3}\,; \end{cases} \qquad b_m = \begin{cases} \frac{3Q^{2/3}}{8\pi^2\alpha_1}, & \text{if } m = 0\,, \\ 0, & \text{if } 1 \le m \ll Q^{1/3}\,. \end{cases} \tag{6.70}$$

---

[3] To leading order, scalar insertions read as in the homogeneous phase [35].

Predictions are made only for $m \ll Q^{1/3}$ since the EFT breaks for distances of order of the inverse cutoff (6.20) from the vortex, which lies at $\eta = \pi/2$. [4]

A similar analysis can be done for the vortex crystal states in (6.53) and (6.55). Consider first the traceless symmetric case $Q \ll J_{34} \ll Q^{4/3}$ and $J_{12} = 0$. Using (6.52), eq. (6.66) reads

$$\langle j_0 \rangle = \frac{Q}{2\pi^2 R^3}\,, \qquad \langle j_\phi \rangle = \frac{e^2}{2\pi^2 R}\frac{J}{Q}\cos^2\eta\,, \qquad \langle j_\xi \rangle = 0\,. \tag{6.71}$$

This expression holds on scales larger than the vortex separation $\sim 1/\sqrt{\mathcal{J}} \sim \sqrt{Q/J}$, on which the continuous approximation (6.52) can be used. It is then convenient to rewrite eq. (6.69) in Fourier basis

$$\begin{aligned} \langle (J,J), 2J, 0 | j_0(\eta,\xi,\phi) | (J,J), 2J, 0 \rangle &= R^{-3} \sum_{m=0}^{2J} \tilde{a}_m \cos(2m\,\eta)\,, \\ \langle (J,J), 2J, 0 | j_\phi(\eta,\xi,\phi) | (J,J), 2J, 0 \rangle &= R^{-3} \sum_{m=0}^{2J} \tilde{b}_m \cos(2m\,\eta)\,. \end{aligned} \tag{6.72}$$

Cutting off the sums at $m \ll \sqrt{\mathcal{J}}$, we obtain the following predictions

$$\tilde{a}_m = \begin{cases} \frac{Q}{2\pi^2}, & \text{if } m = 0\,, \\ 0, & \text{if } 1 \le m \ll \sqrt{J/Q}\,; \end{cases} \qquad \tilde{b}_m = \begin{cases} \frac{3}{8\pi^2\alpha_1}\frac{J_{34}}{Q^{1/3}}, & \text{if } m = 0, 1\,, \\ 0, & \text{if } 2 \le m \ll \sqrt{J/Q}\,. \end{cases} \tag{6.73}$$

Analogously, for the state (6.55) with $Q \ll J_{12}, J_{34} \ll Q^{4/3}$, the EFT gives

$$\langle j_0 \rangle = \frac{Q}{2\pi^2 R^3}\,, \qquad \langle j_\phi \rangle = \frac{e^2}{2\pi^2 R}\frac{J_{34}}{Q}\cos^2\eta\,, \qquad \langle j_\xi \rangle = \frac{e^2}{2\pi^2 R}\frac{J_{12}}{Q}\sin^2\eta\,. \tag{6.74}$$

Without loss of generality, we assume $J_{12} \le J_{34}$. The three-point function of a spin-1 conserved operator in a mixed symmetric state $|(J,\bar{J}), J_{34}, J_{12}\rangle$, where J_{34} and J_{12} are related to $(J,\bar{J})$ as in (6.1), can be conveniently written as [212, 213]:

$$\begin{aligned} \langle (J,\bar{J}), J_{34}, J_{12} | j_0(\eta,\xi,\phi) | (J,\bar{J}), J_{34}, J_{12} \rangle &= R^{-3} \sum_{m=0}^{2|J-\bar{J}|} a_m \cos(2m\,\eta)\,, \\ \langle (J,\bar{J}), J_{34}, J_{12} | j_\phi(\eta,\xi,\phi) | (J,\bar{J}), J_{34}, J_{12} \rangle &= R^{-3} \sum_{m=0}^{2|J-\bar{J}|+1} b_m \cos(2m\,\eta)\,, \\ \langle (J,\bar{J}), J_{34}, J_{12} | j_\xi(\eta,\xi,\phi) | (J,\bar{J}), J_{34}, J_{12} \rangle &= R^{-3} \sum_{m=0}^{2|J-\bar{J}|+1} c_m \cos(2m\,\eta)\,. \end{aligned} \tag{6.75}$$

Here a_m, b_m and c_m are real coefficients, which satisfy the constraints $\sum_m (-1)^m b_m =$

---

[4] To appreciate this, it is useful to write $\sin^{2m}\eta \approx \exp\left(-m\,\delta\eta^2\right)$ for $m \gg 1$ and $\delta\eta = \pi/2 - \eta \ll 1$, which is exponentially suppressed away from the vortex core for $m \gtrsim Q^{1/3}$.

$\sum_m c_m = 0$ and $b_{2|J-\bar{J}|+1} = -c_{2|J-\bar{J}|+1}$. We then obtain the following results for the OPE coefficients:

$$\begin{aligned}
a_m &= \begin{cases} \frac{Q}{2\pi^2}, & \text{if } m = 0\,, \\ 0, & \text{if } 1 \leq m \ll \sqrt{J_{12}/Q}\,; \end{cases} \\
b_m &= \begin{cases} \frac{3}{8\pi^2\alpha_1}\frac{J_{34}}{Q^{1/3}}, & \text{if } m = 0, 1\,, \\ 0, & \text{if } 2 \leq m \ll \sqrt{J_{12}/Q}\,; \end{cases} \\
c_m &= \begin{cases} \frac{(-1)^m 3}{8\pi^2\alpha_1}\frac{J_{12}}{Q^{1/3}}, & \text{if } m = 0, 1\,, \\ 0, & \text{if } 2 \leq m \ll \sqrt{J_{12}/Q}\,. \end{cases}
\end{aligned} \tag{6.76}$$

6.5 Vortices in arbitrary dimensions

Based on the considerations of this and the previous chapter, it is not hard to understand the qualitative feature of the vortex EFT in higher spacetime dimensions. We give some brief comments here for completeness. We focus on the derivation of the scaling dimensions for traceless symmetric operators.

We first need to construct the dual of the d dimensional Lagrangian (3.8) in terms of a $d-2$ form gauge field A. Proceeding as in sec. 6.2.1, this reads

$$\mathcal{L} = -\kappa \left|H \cdot H\right|^{\frac{d}{2(d-1)}}\,, \qquad H = dA. \tag{6.77}$$

As in (6.18), the gauge and the scalar description are related by $*H \propto j$, where $*$ stands for the Hodge dual. The action (6.77) can be expanded to quadratic order in terms of a non-propagating *hydrophoton* $d-2$ gauge form and a longitudinal vector corresponding to the phonon. The cutoff of the action is given by $\Lambda \sim Q^{\frac{1}{d-1}}$. The energy of the homogeneous ground state reads

$$\Delta_Q = \alpha_1 Q^{\frac{d}{d-1}} + \alpha_2 Q^{\frac{d-2}{d-1}} + \dots\,. \tag{6.78}$$

Vortices are $d-2$ membranes which couple to the gauge field A through a Kalb Ramond like interaction. Calling $X_p^\mu(\bar{\sigma})$ their line elements, where $\bar{\sigma} = (\tau, \sigma_1, \dots)$ parametrizes the membrane coordinates, this coupling reads

$$S_{KR} = -\sum_p \lambda_p \int dX_p^{\mu_1} \wedge dX_p^{\mu_2} \wedge \dots \wedge dX_p^{\mu_{d-2}} A_{\mu_1\mu_2\dots\mu_{d-2}}\,. \tag{6.79}$$

One can similarly write the Nambu-Goto like action for the membrane [64]; we do not report here the expression since its detailed form will not be needed in the following.

One can now proceed as in sec. 6.3. From the energy momentum tensor, one finds that the leading contribution to the vortex energy comes from the hydrophoton gauge field. Generalizing eq.s (5.27) and (6.40), the angular momentum is proportional to the volume enclosed by the vortex in embedding coordinates.

For $J \ll Q^{\frac{1}{d-1}}$ the lowest dimension operator corresponds to a phonon propagating in the superfluid, with scaling dimension given by

$$\Delta = \Delta_Q + \sqrt{\frac{J(J+d-2)}{d-1}}\,, \qquad J \ll Q^{\frac{1}{d-1}}\,, \tag{6.80}$$

where Δ_Q is given by (6.78).

For $Q^{\frac{1}{d-1}} \ll J \leq Q$, the minimal energy state corresponds to a single spherical vortex in embedding space. The leading contribution to the vortex energy arises from the running of the tension, induced by the hydrophoton contribution to the self-energy as in (6.44). This can be computed using a flat space approximation for the gauge field Green function and a UV hard cutoff $\Lambda \sim Q^{\frac{1}{d-1}}/R$ to regulate the result:

$$\Delta = \Delta_Q + \frac{d-1}{2d\,\alpha_1} J^{\frac{d-3}{d-2}} Q^{\frac{1}{(d-1)(d-2)}} \log\left(J/Q^{\frac{1}{d-1}}\right), \qquad Q^{\frac{1}{d-1}} \ll J \leq Q, \tag{6.81}$$

where Δ_Q is given by (6.78). We expect d-dependent corrections to eq. (6.81), of order $J^{\frac{d-3}{d-2}} Q^{\frac{1}{(d-1)(d-2)}}$, similarly to eq. (6.45); these contributions however will not be logarithmically enhanced by the cutoff.

As in section 6.3.3, for $Q \ll J \ll Q^{\frac{d}{d-1}}$ we can identify the minimal energy state as a vortex crystal. Following the same steps which lead to (6.53), we find the energy of this state:

$$\Delta = \Delta_Q + \frac{d-1}{4\alpha_1}\frac{J^2}{Q^{\frac{d}{d-1}}}, \qquad Q \ll J \ll Q^{\frac{d}{d-1}}. \tag{6.82}$$

Eq.s (6.81) and (6.82) match the results obtained for $d = 3, 4$.

Conclusions to Part III

To summarize, in this part of the thesis we studied the properties of operators with large global charge and large spin in $U(1)$ invariant CFTs by combining the state-operator correspondence with the EFT of vortices in superfluids. We also calculated correlation functions with two such operators and the Noether current. Other correlators as well as higher order corrections can be systematically computed.

Our results apply to any CFT that satisfies three conditions: first, its large charge sector can be described as a superfluid; second, this superfluid admits vortices; third, the only low energy degrees of freedom are the Goldstone modes of the superfluid. These are the simplest and most natural conditions we can imagine. Because of this, we believe–but cannot prove–that our results apply to a wide range of CFTs with a $U(1)$ global symmetry. For example, we expect that they apply to the critical $O(2)$ model [103] in three dimensions and can be tested in principle. In light of the discussion in sec. 4.1, we expect our results to apply to theories with $SU(2)$ global symmetry as well.

The most direct extension of this work would be a detailed analysis of higher order corrections, both in three and four dimensions. In particular, a refinement of the continuum approximation used for $J \gg Q$ might allow for the study of collective excitations in the vortex crystal phase, corresponding to an unexplored class of universal CFT operators, possibly similar to the Tkachenko modes [214, 215], recently studied via effective field theory techniques in [93, 94].

It should be possible to study explicitly the operators discussed in chapters 5 and 6 in perturbative theories. The three-dimensional $U(1)$ gauge theories discussed in [104, 111, 136, 137, 142–147] at large N provide examples of weakly coupled *magnetic* theories, in the language of sec. 5.6.1, in which we expect our results to apply. Relatedly, vortices were also studied in the "holographic superconductors" states [148–150] using the AdS/CFT correspondence [216]. The Wilson-Fisher fixed points within the epsilon expansion [103] are examples of weakly coupled *electric* models in which our description should apply. We will discuss them in some detail in part IV of the thesis, but we will not address the question concerning operators with large charge and large spin. We also mention that, recently, large charge spinning operators were studied by very similar techniques in non-relativistic conformal field theories [217].

Perhaps AdS/CFT can also teach us how to study operators with $J \sim \Delta$ using EFT techniques, as this was the original motivation for the large spin bootstrap work [169–172, 184–190]. The idea was that these operators should be described as widely separated—and therefore weakly interacting—objects in AdS space [170, 184]. [5] This weak interaction suggests an EFT description, and such an EFT would then apply to all CFTs.

---

[5] A similar picture was proposed in [168], with no reference to the gravity dual.

Part IV

The ε-expansion meets semiclassics

So far we have investigated the properties of conformal field theories at large internal charge, mostly focusing on strongly coupled theories. However, it is natural to ask how the results we have discussed arise in a perturbative setting. Indeed, while the effective superfluid description should equally well apply to strongly and weakly coupled theories, in the latter case it is also possible to work directly in the full theory, bypassing the EFT construction, or, in fact, deriving it. The goal of this last part of the thesis is to illustrate this point. We shall do so computing the scaling dimensions of the lightest operator of charge n in two different models which can be studied within the ε-expansion: the $O(2)$ Wilson-Fisher (WF) fixed point in $4-\varepsilon$ dimensions [103], that we study in chapter 7, and the tricritical $U(1)$ CFT in $3-\varepsilon$ dimensions [218], that we discuss in chapter 8.

Besides providing a concrete "UV" realization of the conformal superfluid EFT discussed in the previous chapters, studying correlators of large charge operators in these perturbative theories presents an additional element of interest. Indeed, let us consider the scaling dimension Δ_{ϕ^n} of the lightest charge n operator, ϕ^n, at the WF fixed point. As we will show in detail in chapter 7, within diagrammatic perturbation theory the latter is given by a polynomial in ε and n:

$$\Delta_{\phi^n}=n\sum_k\varepsilon^k\left(c_kn^k+\ldots+c_1\right)=n+\mathcal{O}\left(\varepsilon n^2\right)\,. \tag{IV.1}$$

At fixed order in perturbation theory, eq. (IV.1) is clearly incompatible with the expected behaviour at large charge, $\Delta_n\propto n^{\frac{d}{d-1}}$. The key observation is that the perturbative parameter controlling the diagrammatic expansion for Δ_n is not ε, but εn. As the charge increases, $\varepsilon n\to 1$, and the perturbative result cannot be trusted anymore. This is a specific instance of a general issue: the breakdown of the perturbative expansion in the study of multi-legged amplitudes. [1] How shall we proceed in this case?

In chapter 7 we will show that, in the Wilson-Fisher fixed point, we can overcome this issue by working in a double-scaling limit, given by $\varepsilon\to 0$ with $\varepsilon n=$ fixed. In this limit, the scaling dimension of the operator ϕ^n can be computed through a systematic expansion around a non-trivial trajectory in the path-integral, yielding the result in the form

---

[1] As we review in the introduction of chapter 7, these were previously studied in relation to the production of a large number of massive particles [133].

$$\Delta_{\phi^n} = \frac{1}{\varepsilon}\Delta_{-1}(\varepsilon n) + \Delta_0(\varepsilon n) + \varepsilon\Delta_1(\varepsilon n) + \dots\,, \tag{IV.2}$$

with $\Delta_{\ell-1}$ representing the ℓ-th loop contribution. This expansion matches the result of Feynman diagram calculations for $\varepsilon n \ll 1$, in which case each function $\Delta_k(\varepsilon n)$ nontrivially resums the result of an infinite number of loop diagrams, while matching the predictions of the large charge expansion when $\varepsilon n \gg 1$.

Before discussing the details of the derivation of eq. (IV.2), it is useful to discuss a simple example, in the form of an ordinary integral, which illustrates the origin of this result. [2]

Invitation: perturbation theory for an ordinary integral

Consider the following ordinary integral defining the function $g(\lambda, n)$: [3]

$$\Gamma\left(n+\frac{1}{2}\right) g(\lambda,n) = \int_{-\infty}^{\infty} dx\, x^{2n} \exp\left[-S(x)\right]\,, \qquad S(x) = x^2 + \frac{\lambda}{4}x^4\,. \tag{IV.3}$$

We shall treat λ as a small parameter, analogous to a perturbative coupling in quantum field theory. The standard perturbative analysis amounts at expanding the quartic term in the exponential as $e^{-\lambda x^4} = 1 - \lambda x^4 + \frac{\lambda^2}{2}x^8 + \dots$. This is equivalent to performing a saddle point analysis for $\lambda \to 0$ with n fixed. The result is conveniently written in terms of the logarithm of g as

$$\log g(\lambda,n) = -\frac{\lambda}{16}\left(4n^2+8n+3\right) + \frac{\lambda^2}{32}\left(4n^3+16n^2+19n+6\right) + \mathcal{O}(\lambda^3 n^4). \tag{IV.4}$$

Clearly, the perturbative expansion breaks down for $\lambda n/4 \gtrsim 1$, analogously to the Feynman diagram expansion for Δ_{ϕ^n} in (IV.1), where the role of λ is played by ε.

To understand the origin of this issue, let us write $x^{2n} = e^{n\log x^2}$ so that eq. (IV.3) can be rewritten as

$$\Gamma\left(n+\frac{1}{2}\right) g(\lambda,n) = \int_{-\infty}^{\infty} dx\, \exp\left[-S_{mod}(x)\right]\,, \tag{IV.5}$$

where we defined a *modified action* as

$$S_{mod}(x) = x^2 + \frac{\lambda x^4}{4} - n\log x^2\,. \tag{IV.6}$$

To get to equation (IV.4) we expanded the integrand around the point $x = 0$, corresponding to a saddle-point approximation in which x^{2n} is treated as a perturbation. However, as n increases, the minimum of the *modified action* (IV.6), given by $x_0^2 = \frac{\sqrt{1+2\lambda n}-1}{\lambda} = n + \mathcal{O}\left(\lambda n^2\right)$, moves away from the origin and this approximation breaks down.

---

[2] The same example is also discussed in [219, 220].

[3] This integral defines the confluent hypergeometric function $g(\lambda,n) = \lambda^{-n/2-1/4}U\left(\frac{n}{2}+\frac{1}{4}, \frac{1}{2}, \frac{1}{\lambda}\right)$.

It is then clear how to overcome the issue with perturbation theory at large λn: we should expand around a saddle-point of the full exponential (IV.6). As it can be seen by rescaling $x \to x/\sqrt{\lambda}$, this will provide an asymptotic expansion for $\lambda \to 0$ with λn fixed. Using the Stirling formula for the Gamma function, the result is then recast in the form

$$g(\lambda, n) \simeq \exp\left[\frac{1}{\lambda}F_{-1}(\lambda n) + F_0(\lambda n) + \dots\right], \tag{IV.7}$$

where

$$\begin{aligned} F_{-1}(\lambda n) &= \frac{1+\lambda n - \sqrt{1+2\lambda n}}{2} + \lambda n \log\left(\frac{\sqrt{1+2\lambda n}-1}{\lambda n}\right), \\ F_0(\lambda n) &= -\frac{1}{4}\log\left(1+2\lambda n\right). \end{aligned} \tag{IV.8}$$

In particular, expanding the result for small λn, we see that it matches the previous calculation (IV.4):

$$\log g(\lambda, n) = -\lambda\left(\frac{n^2}{4}+\frac{n}{2}\right) + \frac{1}{8}\lambda^2\left(n^3+4n^2\right) + \mathcal{O}\left(\lambda^2 n\right) + \mathcal{O}\left(\lambda^3 n^4\right). \tag{IV.9}$$

Notice that the agreement is up to a term of order $\lambda^2 n = \lambda \times \lambda n$ which arises at the next order in the expansion of eq. (IV.7). At large λn we obtain a qualitatively different behaviour:

$$\log g(\lambda, n) = -\frac{1}{\lambda}\left\{\frac{\lambda n}{2}\left[\log\left(\lambda n\right) - 1 - \log 2\right] + \sqrt{2}\sqrt{\lambda n} + \mathcal{O}\left((\lambda n)^0\right)\right\} + \mathcal{O}\left(\lambda^0 \log \lambda n\right). \tag{IV.10}$$

The calculation of a generic amplitude in a perturbative quantum field theory presents several analogies with this simple example. The standard perturbative approach corresponds to performing a small field expansion in the path-integral, analogously to the one with which we obtained eq. (IV.4). However, in certain situations, such as the calculation of correlators of ϕ^n with $n \gtrsim 1/\varepsilon$ in the ε-expansion, the operator insertions in the path integral cannot be treated as small fluctuations on the vacuum; in this case, one should look for a new saddle in the path-integral, which accounts for their effect, as we did in eq. (IV.6) including the contribution of x^{2n} in the *action*. We shall discuss how this procedure concretely allows computing the scaling dimension Δ_{ϕ^n}. Analogously to eq. (IV.7), the result will be organized as a perturbative expansion in the double scaling limit, $\varepsilon \to 0$ with εn fixed.

7 Large charge operators and multilegged amplitudes at the Wilson-Fisher fixed point

The most common practice in particle physics concerns processes involving a few weakly interacting particles, for instance 1 → 2, 2 → 2, 2 → 3, etc. That corresponds to computing quantum fluctuations around the vacuum trajectory in a weakly coupled path integral. On the other hand it is well known that, even in weakly coupled QFT, when considering processes whose number of legs n grows, perturbation theory eventually fails [133]. This issue was investigated in some details in the 80's and 90's, where, focussing on massive $\lambda\phi^4$, some remarkable results were obtained. In particular, it was shown that the computation could be organized as a semiclassical expansion around a non-trivial trajectory [221–223]. Mostly technical difficulties, but also some conceptual ones, however slowed progress down. A recent revival [224] did not greatly progress, in our opinion, towards the tackling of the difficulties (see for instance [219,225] for a critical assessment). This remains an important problem, not only technically and conceptually, but also phenomenologically, when considering the fate of scattering amplitudes involving many W, Z and Higgs bosons in the Standard Model (SM) at energies that may be approachable at the next generation of colliders.

While keeping the fate of the SM in our mind, in the present chapter we shall focus on a simpler problem, plausibly the simplest one in the context of multilegged amplitudes. We shall study the correlator of the operator of charge n, ϕ^n, in $U(1)$ invariant scalar QFT with quartic interaction $(\bar{\phi}\phi)^2$. In particular we shall study its scaling dimension, mostly focussing on the Wilson-Fisher fixed point in $d = 4 - \varepsilon$, at small ε where the coupling is weak. The main conceptual result of this chapter is that the operator's scaling dimension Δ_{ϕ^n} can be computed through a systematic expansion around a non-trivial trajectory, yielding

$$\Delta_{\phi^n} = \frac{1}{\lambda_*}\Delta_{-1}(\lambda_* n) + \Delta_0(\lambda_* n) + \lambda_*\Delta_1(\lambda_* n) + \dots \qquad (7.1)$$

with $\lambda_*/16\pi^2 = \varepsilon/5 + \dots$ the fixed point coupling, and with $\Delta_{\ell-1}$ representing the ℓ-th loop contribution. This result will be made concrete through the explicit computation of the leading and subleading terms, Δ_{-1} and Δ_0. Eq. (7.1) shows the existence of a double scaling limit, where $\lambda_* \to 0$ and $n \to \infty$ with $\lambda_* n$ fixed, where λ_* remains the loop expansion parameter, while the effects of large n are controlled by the classical parameter $\lambda_* n$. Our system, when weakly coupled around the vacuum, thus remains weakly coupled also at large n. However our result applies equally well to large and to small $\lambda_* n$, where one can also compute using Feynman diagrams. On the one hand this illustrates that the poor behaviour of standard perturbation theory as $\lambda_* n$ is increased is simply tied to a poor choice of the path integral trajectory around which to expand. On the other hand it allows to compare our semiclassical computation to the results obtained using Feynman diagrams. In that doing we shall not only find perfect agreement, but also be able to combine our result with finite order calculations and predict expansion coefficients that are beyond the order reached by each method when taken individually.

The simplicity of the problem we consider, we believe, illuminates previous literature in related but different contexts. As concerns multilegged scattering amplitude, the structure of our computation is precisely the same, and precisely identical is the emergence of a double scaling limit, $\lambda \to 0$ with λn fixed. This indicates a sort of universality in the structure of multilegged observables, with λn acting like a sort of 't Hooft coupling, and motivates further investigations into the more difficult problem of particle production. At the same time, on the CFT side, this result directly connects to the general properties of large charge operators [34, 35], discussed at length in this thesis. In this context, it shows more concretely how the superfluid configuration of the leading trajectory emerges and it offers a concrete “UV" complete realization of the effective field theory describing the superfluid. In particular the parameter $\lambda_* n$ controls the occurrence of the pure superfluid regime: at small $\lambda_* n$ the leading trajectory corresponds to a superfluid interacting with a light radial excitation, while at large $\lambda_* n$ the latter decouples. In our amusingly simple scenario, the parameter $\lambda_* n$ thus seems to play a role similar to the 't Hooft coupling in AdS/CFT, where it controls the gap between stringy and supergravity modes. Finally, our systematic expansion in ε invites a comparison with the results of Monte Carlo simulations in $d = 3$ [118]. While we are aware that taking $\varepsilon = 1$ is a significant stunt, we nonetheless find the comparison encouraging already with the first two orders we computed. This warrants computation of the next order, Δ_1.

This chapter is organized as follows. In section 7.1 we setup our conventions and we review the standard perturbative calculation of the anomalous dimension of ϕ^n. In section 7.2 we derive the existence of the expansion (7.1) and we show how to compute the leading term Δ_{-1} for small $\lambda_* n$ within the proposed approach. Section 7.3 deals with the explicit calculation of the first two leading terms in (7.1) for arbitrary values of $\lambda_* n$; the result is analyzed at length in section 7.4.

7.1 Perturbation theory around the vacuum

7.1.1 Conventions

We will consider massless $U(1)$ symmetric $\lambda(\bar{\phi}\phi)^2$ theory in $d = 4 - \varepsilon$ dimensional euclidean space-time with lagrangian

$$\mathcal{L} = \partial\bar{\phi}\partial\phi + \frac{\lambda_0}{4}\left(\bar{\phi}\phi\right)^2. \tag{7.2}$$

We will first consider general coupling, but we shall later derive more specific results by focussing on the Wilson-Fisher fixed point. Renormalized field and coupling are defined according to

$$\phi = Z_\phi[\phi], \quad \lambda_0 = M^\varepsilon \lambda Z_\lambda, \tag{7.3}$$

where M is the sliding scale. We will adopt the minimal subtraction scheme, where Z_ϕ and Z_λ are expressed as an ascending series of pure poles. In particular we have

$$\log Z_\lambda = \sum_k \frac{z_k(\lambda)}{\varepsilon^k} = \frac{c_{11}\lambda + c_{12}\lambda^2 + \dots}{\varepsilon} + \frac{c_{22}\lambda^2 + \dots}{\varepsilon^2} + \dots, \tag{7.4}$$

where

$$z_1(\lambda) = 5\frac{\lambda}{(4\pi)^2} - \frac{15}{2}\frac{\lambda^2}{(4\pi)^4} + \mathcal{O}\left(\frac{\lambda^3}{(4\pi)^6}\right). \tag{7.5}$$

Notice moreover that $Z_\phi = 1$ up to two loop corrections. Using (7.3) one can easily show that the β-function equals

$$\frac{\partial\lambda}{\partial\log M} \equiv \beta(\lambda) = -\varepsilon\lambda + \beta_4(\lambda), \tag{7.6}$$

with

$$\beta_4(\lambda) = \lambda^2\frac{\partial z_1}{\partial\lambda} = 5\frac{\lambda^2}{(4\pi)^2} - 15\frac{\lambda^3}{(4\pi)^4} + \mathcal{O}\left(\frac{\lambda^4}{(4\pi)^6}\right). \tag{7.7}$$

At the Wilson-Fisher fixed point, defined by $\lambda = \lambda_*$ such that $\beta(\lambda_*) = 0$, the theory is invariant under conformal transformations. The fixed point coupling λ_* is non-trivially determined by the space-time dimensionality

$$\frac{\lambda_*}{(4\pi)^2} = \frac{\varepsilon}{5} + \frac{3}{25}\varepsilon^2 + \mathcal{O}(\varepsilon^3). \tag{7.8}$$

For $\varepsilon \ll 1$ the theory is weakly coupled [103]. As we will show in the next subsection, this does not prevent perturbation theory around the vacuum to break down for specific observables.

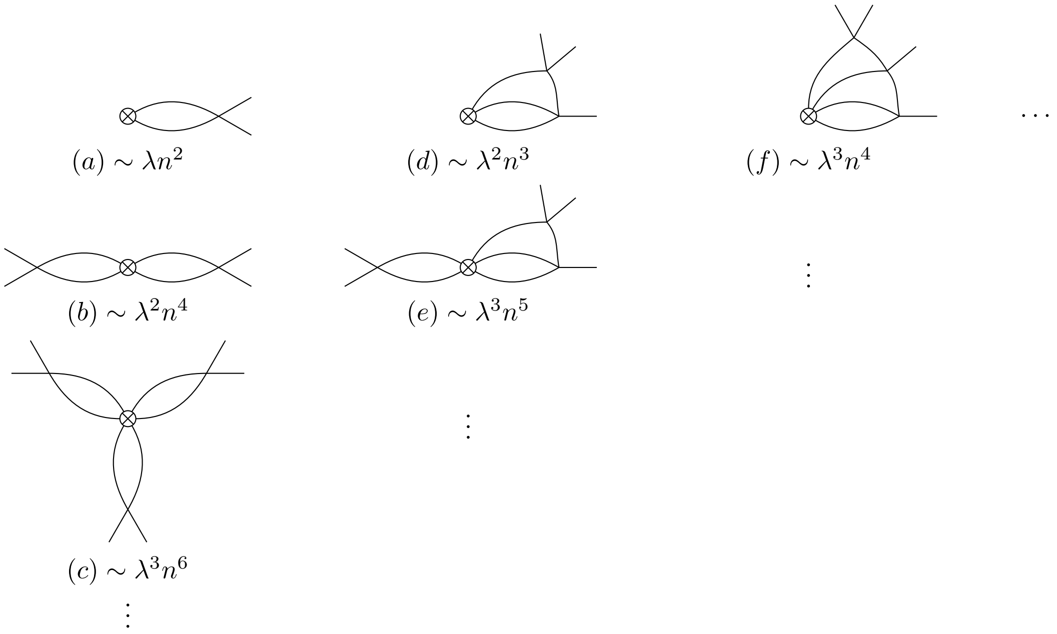

$(a) \sim \lambda n^2$ $(d) \sim \lambda^2 n^3$ $(f) \sim \lambda^3 n^4$

$(b) \sim \lambda^2 n^4$ $(e) \sim \lambda^3 n^5$

$(c) \sim \lambda^3 n^6$

Figure 7.1 – Some characteristic Feynman diagrams that appear with the ϕ^n operator.

7.1.2 Anomalous dimension of large charge operators

We will study the scaling dimension of the simplest operator with $U(1)$ charge[1] n ($-n$), denoted by $[\phi^n]$ ($[\bar{\phi}^n]$) and related to the bare field by

$$\phi^n = Z_{\phi^n}[\phi^n]\,. \tag{7.9}$$

where Z_{ϕ^n} is a multiplicative renormalization factor. The anomalous dimension is then given by

$$\gamma_{\phi^n} = \frac{\partial \log Z_{\phi^n}}{\partial \lambda}\,\left[-\varepsilon\lambda + \beta_4(\lambda)\right]\,. \tag{7.10}$$

For arbitrary λ, γ_{ϕ^n} is scheme dependent and thus unphysical beyond leading order. That can easily be seen by changing the scheme according to $[\phi^n] \to f(\lambda)[\phi^n]$ and $Z_{\phi^n} \to Z_{\phi^n}/f(\lambda)$, with $f(\lambda)$ a power series with finite coefficients. In the new scheme the anomalous dimension is modified according to $\gamma_{\phi^n} \to \gamma_{\phi^n} - \beta(\partial_\lambda \ln f)$. On the other hand $\beta(\lambda_*) = 0$, so that γ_{ϕ^n} is scheme independent and physical at the fixed point. Indeed, a straightforward solution of the Callan-Symanzik equation for $\langle[\bar{\phi}^n][\phi^n]\rangle$ shows that the operator's physical dimension at the fixed point is

$$\Delta_{\phi^n} = n(d/2-1) + \gamma_{\phi^n}(\lambda_*)\,. \tag{7.11}$$

We want to focus on $n \gg 1$, the regime of large charge or many legs. A first diagrammatic analysis shows multiplicity factors that grow with n, see figure 7.1. Considering any loop order $\ell \ll n$, one finds contributions to Z_{ϕ^n} that range from $\lambda^\ell n^{2\ell}$, for the daisy diagrams in the leftmost column of figure 7.1, down to $\lambda^\ell n$, for corrections on single legs. In particular the “connected diagrams", for which the number of legs picked from the ϕ^n equals $\ell+1$, like those in the top line of figure 7.1, scale like $\lambda^\ell n^{\ell+1}$. However, a more detailed analysis shows that the terms with the highest powers of n at any given loop order simply exponentiate terms from lower loops[2]. As a consequence, in the expansion of $\ln Z_{\phi^n}$, and thus of γ_{ϕ^n}, the leading contribution at order k scales like the connected diagram, $\lambda^\ell n^{\ell+1}$. That is

---

[1] In our conventions, $\phi, \bar{\phi}$ have charge, respectively, 1 and -1.

$$\gamma_{\phi^n} = n\sum_{\ell=1}\lambda^\ell P_\ell(n)\,, \tag{7.12}$$

with P_ℓ a polynomial of degree ℓ. In truth we have explicitly checked that only up to four loops, but in the next section we shall give a general argument bypassing the diagrammatic analysis. The above result shows that, no matter how weakly coupled the theory is, for sufficiently large λn, perturbation theory breaks down. The series in eq. (7.12) can also be organized in terms of leading and subleading n-powers, in close analogy with leading and subleading logs in the RG resummation

$$\gamma_{\phi^n} = n\sum_{\kappa=0}\lambda^\kappa F_\kappa(\lambda n)\,. \tag{7.13}$$

Very much like for the RG, this alternative rewriting of the series suggests an alternative loop expansion, performed after resumming (or straight out computing) all powers of λn. Again, the physics underlying this alternative interpretation will be made manifest in the next subsections. Notice in passing, and consistently with the results in the next section, that the leading-n contribution $F_0(\lambda n)$ is unaffected by changes in the subtraction scheme, like for instance $\lambda\to\lambda+a\lambda^2$ or $Z_{\phi^n}\to Z_{\phi^n}(1+bn^2\lambda)$, the latter corresponding to a simple reshuffling of the finite terms in the daisy diagram (a).

Before moving forward we would like to present the results of the explicit computation at 2-loops, whose details are given in the appendix D.1. We shall need these in order to compare to the results of the more powerful method we shall develop in the next sections. Working in the minimal subtraction scheme, we find

$$Z_{\phi^n} = 1-\frac{\lambda n(n-1)}{(16\pi^2)2\varepsilon}+\frac{\lambda^2}{(16\pi^2)^2}\left(\frac{n^4-2n^3-9n^2+10n}{8\varepsilon^2}+\frac{2n^3-2n^2-n}{8\varepsilon}\right), \tag{7.14}$$

which implies

$$\gamma_{\phi^n} = n\left[\frac{\lambda}{16\pi^2}\frac{(n-1)}{2}-\left(\frac{\lambda}{16\pi^2}\right)^2\frac{2n^2-2n-1}{4}\right]. \tag{7.15}$$

Considering the theory at the fixed point this implies

$$\Delta_{\phi^n} = n\left[\left(\frac{d}{2}-1\right)+\frac{\varepsilon}{10}(n-1)-\frac{\varepsilon^2}{100}(2n^2-8n+5)\right]. \tag{7.16}$$

---

[2] As an illustration, it is simple to check that the sum over daisy diagrams exponentiate the λn^2 contribution from the single petal diagram (a).

7.2 Semiclassical approach

The scaling dimension of $[\phi^n]$ can also be directly computed by considering the two-point function

$$\langle\bar{\phi}^n(x_f)\phi^n(x_i)\rangle \equiv \frac{\int \mathcal{D}\phi\mathcal{D}\bar{\phi}\,\bar{\phi}^n(x_f)\phi^n(x_i)\exp\left[-\int\mathcal{L}\right]}{\int \mathcal{D}\phi\mathcal{D}\bar{\phi}\,\exp\left[-\int\mathcal{L}\right]} \equiv Z^2_{\phi^n}\langle[\bar{\phi}^n](x_f)[\phi^n](x_i)\rangle\,. \tag{7.17}$$

The above integral can be cast in a form which exhibits its semiclassical nature in the small λ regime independently of the size of n. First it is convenient to rescale the field $\phi\to\phi/\sqrt{\lambda_0}$ to exhibit λ_0 as the loop counting parameter

$$\int\mathcal{L}\to\frac{1}{\lambda_0}\int\left[\partial\bar{\phi}\partial\phi+\frac{1}{4}\left(\bar{\phi}\phi\right)^2\right]\equiv\frac{S}{\lambda_0}\,. \tag{7.18}$$

Secondly $\bar{\phi}^n(x_f)\phi^n(x_i)$ can be brought up in the exponent, obtaining

$$Z^2_{\phi^n}\lambda_0^n\langle[\bar{\phi}^n](x_f)[\phi^n](x_i)\rangle = \frac{\int\mathcal{D}\phi\mathcal{D}\bar{\phi}\,e^{-\frac{1}{\lambda_0}\left[\int\partial\bar{\phi}\partial\phi+\frac{1}{4}\left(\bar{\phi}\phi\right)^2-\lambda_0 n\left(\ln\bar{\phi}(x_f)+\ln\phi(x_i)\right)\right]}}{\int\mathcal{D}\phi\mathcal{D}\bar{\phi}\,e^{-\frac{1}{\lambda_0}\left[\int\partial\bar{\phi}\partial\phi+\frac{1}{4}\left(\bar{\phi}\phi\right)^2\right]}}\,. \tag{7.19}$$

The dependence on λ_0 and n, shows that we can perform the path integral using a saddle point expansion in the limit of small λ_0, while keeping $\lambda_0 n$ fixed. This limit thus encompasses the case where $\lambda_0 n$ is (arbitrarily) large[3]. Independently of the detailed form of the field configuration furnishing the steepest descent, the right hand side of eq. (7.19) will then take the form

$$\lambda_0^{-1/2}\,e^{\frac{1}{\lambda_0}\Gamma_{-1}(\lambda_0 n,x_{fi})+\Gamma_0(\lambda_0 n,x_{fi})+\lambda_0\Gamma_1(\lambda_0 n,x_{fi})+\ldots}\,,\qquad x_{fi}=x_f-x_i. \tag{7.20}$$

The factor $\lambda_0^{-1/2}$ is understood as follows. The path integral in the denominator is computed through a saddle-point expansion around the trivial point $\phi=\bar{\phi}=0$, while the action of the path integral in the numerator is stationary on a continuous family of nontrivial configurations with $\phi,\bar{\phi}\neq 0$ and parametrized by the zero mode associated to the corresponding spontaneous breaking of the $U(1)$ symmetry. As the integral over the zero mode is clearly independent of the value of the action, this results in a mismatch of the powers of $\lambda_0^{1/2}$ in between the numerator and the denominator, leading to (7.20) [4].

---

[3] Of course we are making here a formal statement by using the bare coupling, which is a power series in the renormalized coupling. In terms of renormalized quantities the limit is thus $\lambda(M)$ small with $\lambda(M)n$ fixed.

[4] The situation is fully analogous to the following example involving two dimensional integrals:

$$I(\lambda,n)=\frac{\int_{\mathbb{C}}dzd\bar{z}(z\bar{z})^n\exp\left\{-\frac{1}{\lambda}\left[z\bar{z}+\frac{1}{4}(z\bar{z})^2\right]\right\}}{\int_{\mathbb{C}}dzd\bar{z}\exp\left\{-\frac{1}{\lambda}\left[z\bar{z}+\frac{1}{4}(z\bar{z})^2\right]\right\}}=\frac{\int_{\mathbb{C}}dzd\bar{z}\exp\left\{-\frac{1}{\lambda}\left[z\bar{z}+\frac{1}{4}(z\bar{z})^2-\lambda n\log(z\bar{z})\right]\right\}}{\int_{\mathbb{C}}dzd\bar{z}\exp\left\{-\frac{1}{\lambda}\left[z\bar{z}+\frac{1}{4}(z\bar{z})^2\right]\right\}}.$$

The integral in the denominator is performed in an expansion around $z=\bar{z}=0$ and is thus proportional to λ due to the gaussian integration on the two directions of the plane. The exponent in the numerator is instead stationary on the whole circle defined by $z\bar{z}=\sqrt{1+2\lambda n}-1$; in this case, while the integral over the radial direction produces a factor of $\sqrt{\lambda}$, angular integration gives an overall factor of 2π. The

Now, notice that by using Stirling's formula the expression $\lambda_0^{n+1/2} n!$ can be written in the same form as the exponential factor in eq. (7.20). It is then convenient to redefine the Γ_k's so as to factor out a $\lambda_0^{n+1/2} n!$ in the exponential factor in eq. (7.20) and rewrite that equation as

$$Z_{\phi^n}^2 \lambda_0^n \langle [\bar{\phi}^n](x_f)[\phi^n](x_i)\rangle = \lambda_0^n n!\, e^{\frac{1}{\lambda_0}\Gamma_{-1}(\lambda_0 n, x_{fi}) + \Gamma_0(\lambda_0 n, x_{fi}) + \lambda_0 \Gamma_1(\lambda_0 n, x_{fi}) + \dots} \tag{7.21}$$

Comparing to eq. (7.17), we deduce that the exponential factor in eq. (7.21) coincides at weak coupling and finite n with the loop expansion we discussed in the previous section. In particular, given

$$D(x) = \frac{1}{\Omega_{d-1}(d-2)(x^2)^{d/2-1}} = \langle \bar{\phi}(x)\phi(0)\rangle_{free}\,, \qquad \Omega_{d-1} = \frac{2\pi^{d/2}}{\Gamma(d/2)} \tag{7.22}$$

one has

$$\lim_{\lambda_0 \to 0} e^{\frac{1}{\lambda_0}\Gamma_{-1}(\lambda_0 n, x_{fi}) + \Gamma_0(\lambda_0 n, x_{fi}) + \lambda_0 \Gamma_1(\lambda_0 n, x_{fi}) + \dots} = D(x_{fi})^n\,. \tag{7.23}$$

Moreover, in order to match the diagrammatic expansion, the Γ_κ's must possess a power series expansion in λ_0 with fixed n, starting at order λ_0^κ. Renormalization is simply performed by separating out the UV divergent part in each term in the exponent

$$\lambda_0^\kappa \Gamma_\kappa(\lambda_0 n, x_{fi}) = \lambda^\kappa \Gamma_\kappa^{div}(\lambda n, \lambda) + \lambda^\kappa \Gamma_\kappa^{ren}(\lambda n, \lambda, x_{fi}, M) \tag{7.24}$$

where of course $\lambda \equiv \lambda(M)$ and where the resulting $\lambda^\kappa \bar{\Gamma}_\kappa$ behave like power series at $\lambda = 0$. From eqs. (7.19,7.21) we can then write

$$Z_{\phi^n}^2 = e^{\sum_{\kappa=-1} \lambda^\kappa \Gamma_\kappa^{div}(\lambda n, \lambda)} \equiv e^{\sum_{\kappa=-1} \lambda^\kappa \bar{\Gamma}_\kappa^{div}(\lambda n)} \tag{7.25}$$

and

$$\langle [\bar{\phi}^n](x_f)[\phi^n](x_i)\rangle = n!\, e^{\sum_{\kappa=-1} \lambda^\kappa \Gamma_\kappa^{ren}(\lambda n, \lambda, x_{fi}, M)} \equiv n!\, e^{\sum_{\kappa=-1} \lambda^\kappa \bar{\Gamma}_\kappa^{ren}(\lambda n, x_{fi}, M)}\,. \tag{7.26}$$

where, in the rightmost expressions, we rearranged the expansion in λ using the (asymptotic) power series expansion of the $\lambda^\kappa \Gamma_\kappa$. Eq. (7.25) provides a formal proof of eqs. (7.12,7.13). In the above expression the $\bar{\Gamma}_\kappa$ represents the $(\kappa+1)$-loop correction to the saddle point approximation. In particular $\bar{\Gamma}_{-1}^{div}(\lambda n)$ and $\bar{\Gamma}_{-1}^{ren}$, represent the leading semiclassical contribution, the exponent at the saddle point[5]. However, they fully determine the leading-n contribution $F_0(\lambda n)$ in eq. (7.13), thus resumming at once the largest powers of n up to arbitrarily high-loop orders in the standard diagrammatic approach! The remarkable result highlighted by our formal derivation and by eq. (7.13),

---

full result, for arbitrary λn, is thus proportional to $\lambda^{-1/2}$:

$$I(\lambda, n) = \sqrt{\frac{2\pi}{\lambda}}\, \frac{e^{-\frac{\lambda n + \sqrt{1+2\lambda n} - 1}{2\lambda}} \left(\sqrt{1+2\lambda n} - 1\right)^{n+\frac{1}{2}}}{(1+2\lambda n)^{1/4}} \left[1 + \mathcal{O}(\lambda)\right].$$

[5] As we shall illustrate in a moment and, as it must be according to our derivation, the divergent part appears from purely classical properties of the saddle point solution.

is that the result is organized as a 't Hooft expansion in which λn is the fixed 't Hooft coupling while $\lambda \ll 1$ and $n \gg 1$.

The rest of the chapter is devoted to explicitly deriving these expressions, at leading (LO) and next-to-leading (NLO) order in the λ expansion with λn fixed. In the next subsection we will perform a warm up computation by working at small but fixed λn. In the later sections we shall develop the case of arbitrary λn by focussing on the Wilson-Fisher fixed point, where conformal invariance permits to tackle some technical difficulties in the computation.

7.2.1 Semiclassics at small fixed λn

At small λn ordinary perturbation theory works. In this case the path integral eq. (7.17) can be computed by expanding around the trivial background $\phi = \bar{\phi} = 0$. In that case the insertions of ϕ^n and $\bar{\phi}^n$, are not included in the exponent (as the exponent of eq. (7.19) is singular at $\phi = \bar{\phi} = 0$) and are purely determined by the quantum fluctuation $\delta\phi$ around the trivial solution, i.e. $\phi \equiv 0 + \delta\phi$. The loop expansion is purely generated by the small quartic term $\lambda\phi^4$. For instance, working at order λ one finds

$$\langle \bar{\phi}^n(x_f)\phi^n(x_i)\rangle = \frac{n!\left[1 - \frac{\lambda n(n-1)}{2(4\pi)^2}\left(\frac{2}{\varepsilon} + \log x_{fi}^2 + 1 + \gamma + \log\pi\right) + \mathcal{O}\left(\frac{\lambda^2}{(4\pi)^4}\right)\right]}{\left[\Omega_{d-1}(d-2)\right]^n (x_{fi}^2)^{n\left(\frac{d}{2}-1\right)}}. \tag{7.27}$$

compatibly with the one-loop contribution to γ_{ϕ^n} derived in section 7.1.

As λn grows, the fluctuations of $\bar{\phi}^n(x_f)\phi^n(x_i)$ become significant, and for sufficiently large λn they cannot be captured by perturbation theory. However eq. (7.19) invites us to perform the computation around the stationary points of

$$S_{eff} \equiv \int d^dx \left[\partial\bar{\phi}\partial\phi + \frac{1}{4}\left(\bar{\phi}\phi\right)^2\right] - n\lambda_0\left(\log\bar{\phi}(x_f) + \log\phi(x_i)\right). \tag{7.28}$$

The equations of motion defining the stationary configuration include the operator insertions as a source

$$\begin{aligned} \partial^2\phi(x) - \frac{1}{2}\phi^2(x)\bar{\phi}(x) &= -\frac{\lambda_0 n}{\bar{\phi}(x_f)}\delta^{(d)}(x - x_f), \\ \partial^2\bar{\phi}(x) - \frac{1}{2}\phi(x)\bar{\phi}^2(x) &= -\frac{\lambda_0 n}{\phi(x_i)}\delta^{(d)}(x - x_i). \end{aligned} \tag{7.29}$$

Before discussing the details of the general computation, it is instructive to discuss the solution of (7.29) for small λn. Namely, we compute the function $\Gamma_{-1}(\lambda n)$ in (7.21) to order $\mathcal{O}\left(\lambda^2 n^2/(4\pi)^4\right)$ and we check that the result agrees with (7.27). As we work at first order in the coupling, in what follows we will take $\lambda_0 = \lambda$. Now, for small λn the equations (7.29) can be solved perturbatively; to this aim, it is convenient to expand the fields as

$$\phi = (\lambda n)^{1/2}\left[\phi^{(0)} + \phi^{(1)} + \dots\right], \qquad \bar{\phi} = (\lambda n)^{1/2}\left[\bar{\phi}^{(0)} + \bar{\phi}^{(1)} + \dots\right], \tag{7.30}$$

where $\phi^{(k)}, \bar{\phi}^{(k)} = \mathcal{O}\left(\lambda^k n^k\right)$. At the zeroth order, the equations of motion read

$$\begin{aligned} \partial^2\phi^{(0)}(x) &= -\frac{1}{\bar{\phi}^{(0)}(x_f)}\delta^{(d)}(x-x_f), \\ \partial^2\bar{\phi}^{(0)}(x) &= -\frac{1}{\phi^{(0)}(x_i)}\delta^{(d)}(x-x_i), \end{aligned} \tag{7.31}$$

whose solution is uniquely defined up to one free parameter and has the form

$$\begin{aligned} \phi^{(0)}(x) &= \frac{c_0}{\Omega_{d-1}(d-2)}\frac{1}{|x-x_f|^{d-2}}, \\ \bar{\phi}^{(0)}(x) &= \frac{\bar{c}_0}{\Omega_{d-1}(d-2)}\frac{1}{|x-x_i|^{d-2}}; \end{aligned} \tag{7.32}$$

with the parameters c_0 and $\bar{c}_0$ related by

$$c_0\bar{c}_0 = \Omega_{d-1}(d-2)|x_f - x_i|^{d-2}. \tag{7.33}$$

Notice that on the saddle-point, i.e. on the solution of (7.31), the fields ϕ and $\bar{\phi}$ are analytically continued away from the original integration contour, since they are not related by complex conjugation. As a consequence, the fields appearing in the source terms in the right hand side of (7.31) have a finite value and no regularization procedure is needed to find the solution (7.32). Finally, the arbitrariness in the solution is related to the symmetry $(\phi, \bar{\phi}) \to (\alpha\phi, \alpha^{-1}\bar{\phi})$ of the action (7.28) analytically continued to arbitrary values of the fields. The one free parameter in the solution precisely corresponds to the presence of the one zero mode we mentioned before.

The next to leading contribution is determined by

$$\begin{aligned} \partial^2\phi^{(1)}(x) &= \frac{\lambda n}{2}\left[\phi^{(0)}(x)\right]^2\bar{\phi}^{(0)}(x) + \frac{\bar{\phi}^{(1)}(x_f)}{\left[\bar{\phi}^{(0)}(x_f)\right]^2}\delta^{(d)}(x-x_f), \\ \partial^2\bar{\phi}^{(1)}(x) &= \frac{\lambda n}{2}\left[\bar{\phi}^{(0)}(x)\right]^2\phi^{(0)}(x) + \frac{\phi^{(1)}(x_i)}{\left[\phi^{(0)}(x_i)\right]^2}\delta^{(d)}(x-x_i). \end{aligned} \tag{7.34}$$

The solution reads

$$\begin{aligned} \phi^{(1)}(x) &= -\frac{\lambda n}{2}\int d^dy D(x-y)\left[\phi^{(0)}(y)\right]^2\bar{\phi}^{(0)}(y) - D(x-x_f)\frac{\bar{\phi}^{(1)}(x_f)}{\left[\bar{\phi}^{(0)}(x_f)\right]^2}, \\ \bar{\phi}^{(1)}(x) &= -\frac{\lambda n}{2}\int d^dy D(x-y)\left[\bar{\phi}^{(0)}(y)\right]^2\phi^{(0)}(y) - D(x-x_i)\frac{\phi^{(1)}(x_i)}{\left[\phi^{(0)}(x_i)\right]^2}, \end{aligned} \tag{7.35}$$

where $\phi^{(1)}(x_i)$ and $\bar{\phi}^{(1)}(x_f)$ satisfy

$$\frac{\phi^{(1)}(x_i)}{c_0}+\frac{\bar{\phi}^{(1)}(x_f)}{\bar{c}_0}=-\frac{\lambda n}{2}\int d^dy D^2(x_i-y)D^2(x_f-y). \tag{7.36}$$

There is a one parameter arbitrariness in the solution due to the aforementioned symmetry. The integrals are formally divergent in $d=4$ and thus are performed via standard dimensional regularization techniques. Plugging the solution in the action (7.28), we find

$$\begin{aligned} S_{eff} &= \lambda n-\lambda n\log\left[\frac{\lambda n}{\Omega_{d-1}(d-2)}\frac{1}{(x_{fi}^2)^{d/2-1}}\right] \\ &+ \lambda^2 n^2\left(\frac{1}{16\pi^2\varepsilon}+\frac{1+\gamma+\log\pi}{32\pi^2}\right)+\frac{\lambda^2n^2}{32\pi^2}\log x_{fi}^2\,. \end{aligned} \tag{7.37}$$

$e^{-S_{eff}/\lambda}$ must represent the leading term

$$\lambda^n n! e^{\frac{\Gamma_{-1}}{\lambda}} \tag{7.38}$$

in eq. (7.21) with Γ_{-1} expanded up to $\mathcal{O}(\lambda^2 n^2)$. It is easy to see it does. In particular, $\log n!\approx n\log n-n$ ensures that Γ_{-1} has a well defined power series in λn as expected. The correlator, according to eqs. (7.17,7.19), then reads

$$\langle\bar{\phi}^n(x_f)\phi^n(x_i)\rangle=\frac{n^ne^{-n}\exp\left[-\lambda n^2\left(\frac{1}{16\pi^2\varepsilon}+\frac{1+\gamma+\log\pi}{32\pi^2}\right)\right]}{\left[\Omega_{d-1}(d-2)\right]^n(x_{fi}^2)^{n\left(\frac{d}{2}-1\right)+\frac{\lambda n^2}{32\pi^2}}}. \tag{7.39}$$

This expression[6] reproduces the result of the standard perturbative computation (7.27) up to subleading terms at large n. Remarkably, the $\mathcal{O}(\lambda n^2)$ correction to the scaling dimension results in (7.27) from a genuine one-loop computation, while it results in (7.39) from the *classical* solution of the saddle point equations (7.29). According to our discussion, the subleading $\mathcal{O}(\lambda n)$ contribution to γ_{ϕ^n} in eq. (7.27), would instead arise from the first quantum correction around the saddle, i.e. from Γ_0 in eq. (7.21). Our alternative semiclassical computation shows that the $\mathcal{O}(\lambda n^2)$ contribution to γ_{ϕ^n} is a genuinely classical contribution, while the $\mathcal{O}(\lambda n)$ is intrinsically quantum. The emergence of classical physics in the presence of large quantum numbers, n in this case, is a crucial fact of physics. Our case here is closely analogous to the relation between the classical approximation to the squared angular momentum, ℓ^2, and the exact quantum result, $\ell(\ell+1)$ (see ref. [35] for an illustration).

---

[6] This expression was recently derived also in [226], where the authors considered the correlator in the $\lambda\to 0$ limit with λn^2 fixed, clearly corresponding to small λn. This is just a particular limit of the general formula (7.26), as our approach makes clear.

7.3 Finite λn on the cylinder

Finding the general solution of (7.29) is in general a technically challenging task, but symmetries can help tackle the difficulties. In the case at hand the relevant ones are $U(1)$ symmetry, rotational invariance and dilations. Starting with $U(1)$, the conservation of the associated Noether current

$$j_\mu = \bar{\phi}\partial_\mu\phi - \phi\partial_\mu\bar{\phi}. \tag{7.40}$$

provides powerful insight. The field insertions in (7.28) act as a source for the current (7.40). Indeed, from the equations of motion (7.29) we get

$$\partial_\mu j^\mu = n\delta^{(d)}(x-x_i) - n\delta^{(d)}(x-x_f). \tag{7.41}$$

We can then use Gauss law to determine the flux of the current through a sphere centered at x_i with radius r:

$$\oint_{x_i} d\Omega_{d-1}\, r^{d-1} j^\mu(x) n_\mu(x) = n\,\theta\left(|x_f - x_i| - r\right), \tag{7.42}$$

where $n_\mu(x)$ is the unit vector orthogonal to the sphere at point x. Sufficiently close to the point x_i, i.e. for $|x-x_i| \ll |x_f - x_i|$, we expect the solution of (7.29) to be approximately spherically symmetric. In this regime, we then conclude from eq. (7.42) that the current is given by

$$j_\mu(x) = \frac{n}{\Omega_{d-1}}\frac{(x-x_i)_\mu}{|x-x_i|^d}\left[1 + \mathcal{O}\left(\frac{|x-x_i|}{|x_f-x_i|}\right)\right]. \tag{7.43}$$

This equation provides a simple constraint involving both ϕ and $\bar{\phi}$. Unfortunately it is not enough to fix their coordinate dependence. In fact, even in the regime $|x-x_i| \ll |x_f - x_i|$, where spherical symmetry is expected, the radial dependence of the solution is non-trivial, as one can convince oneself by making eq. (7.35) explicit. The origin of such a complicated dependence is the lack of dilation invariance of generic $\lambda\phi^4$ in d-dimension. Notice, instead, that in the free case, where dilations are a symmetry, the solution displays a simple scaling behaviour. Working in strictly $d = 4$, where ϕ^4 is scale invariant is also not an option, because of the need for regulation[7]. We thus conclude that the only way forward in order to more easily derive the solution is to work directly at the Wilson-Fisher fixed point, where we can profit from the bonus of scale invariance. That also matches well, and not unrelatedly, the fact that only at the fixed point is the anomalous dimension a fully physical quantity.

The advantage of working at the fixed point is that we can exploit the power of conformal invariance. As reviewed in appendix B.1, that allows to map our theory from the plane to the cylinder

$$\mathbb{R}^d \to \mathbb{R}\times S^{d-1}, \tag{7.44}$$

---

[7] If we contented ourselves with the leading semiclassical approximation we could work in $d = 4$ and regulate ϕ^n by point splitting.

in such a way that the dilations on the plane are mapped to time translations on the cylinder. Correspondingly, the spectrum of operator dimensions on the plane, the eigenvalues of the dilation charge D, are mapped to the energy spectrum on the cylinder, the eigenvalues of H_{cyl}. Our goal of computing the dimension of $[\phi^n]$ is thus mapped into the computation of the energy of the corresponding state on the cylinder. The advantage offered by this viewpoint is that time translations on the cylinder, unlike dilations on the plane, are a symmetry also away from the fixed point. When mapping our semiclassical computation to the cylinder, we will thus have an additional symmetry controlling the classical solution, even away from criticality. In other words, while, in the approach of the previous section, a simple scaling ansatz for the radial dependence of the solution is inconsistent, given the lack of scale invariance in the regulated theory, on the cylinder it is possible to consistently look for a solution that is stationary in time. That enormously simplifies our task. Of course, we must stress that this very non trivial simplification only works at the fixed point.

Let us briefly recall our conventions. Parametrizing $\mathbb{R}^d$ by polar coordinates (r, Ω_{d-1}), where Ω_{d-1} collectively denotes the coordinates on S^{d-1}, and $\mathbb{R} \times S^{d-1}$ by (τ, Ω_{d-1}), the mapping to the cylinder is simply given by $r = Re^{\tau/R}$ with R the sphere radius. The cylinder metric is then related to the flat one by a Weyl rescaling (B.20). The action of the theory on the cylinder reads[8]

$$S_{cyl} = \int d^d x \sqrt{g} \left[g^{\mu\nu} \partial_\mu \bar{\phi} \partial_\nu \phi + m^2 \bar{\phi}\phi + \frac{\lambda_0}{4} \left(\bar{\phi}\phi\right)^2 \right], \tag{7.45}$$

where the mass term $m^2 = \left(\frac{d-2}{2R}\right)^2$ arises from the $\mathcal{R}(g)\bar{\phi}\phi$ coupling to the Ricci scalar which is enforced by conformal invariance[9] [227].

Weyl invariance at the fixed point ensures that the flat space theory (7.2) is equivalent to the one on the cylinder described by (7.45). In particular, eq. (B.23) implies that the two-point function $\langle \bar{\phi}^n(x_f) \phi^n(x_i) \rangle$, with $\tau_{f,i} = \pm T/2$, for $T \to \infty$ directly yields the scaling dimension Δ_{ϕ^n}

$$\langle \bar{\phi}^n(x_f) \phi^n(x_i) \rangle \overset{T\to\infty}{=} \mathcal{N} e^{-E_{\phi^n} T}, \qquad E_{\phi^n} = \Delta_{\phi^n}/R, \tag{7.46}$$

where the (divergent) coefficient $\mathcal{N}$ is independent of T.

To compute the two point function we can then proceed with the methodology discussed at the beginning of sec. 7.2. The result will have the structure of eq. (7.21). Upon separating out the divergent and finite part of the $\lambda_0^\kappa \Gamma_\kappa$'s, we will have a T independent divergent piece determining the normalization factor $\mathcal{N}$, while the T dependent part will be finite when written in terms of $\lambda(M)$ and linear in T for $T \gg R$. The linearity in T will follow provided the solution is stationary in time, which it will be, thanks to time translation invariance of the action regardless of the theory being at the fixed point.

---

[8] From this point forward we will be working with canonically normalized fields.

[9] Hence, at the fixed point, m^2 is not renormalized by loop effects.

Similarly to eq. (7.26) we shall thus have

$$\begin{aligned} RE_{\phi^n} &= \frac{1}{\lambda_0}e_{-1}(\lambda_0 n,d)+e_0(\lambda_0 n,d)+\lambda_0 e_1(\lambda_0 n,d)+\dots \\ &= \frac{1}{\lambda}\bar{e}_{-1}(\lambda n,RM,d)+\bar{e}_0(\lambda n,RM,d)+\lambda\bar{e}_1(\lambda n,RM,d)+\dots, \end{aligned} \tag{7.47}$$

where $\lambda \equiv \lambda(M)$ and $\bar{e}_k$ is defined from the e_k's analogously to $\bar{\Gamma}_k$ in eq. (7.25). By choosing $\lambda=\lambda_*$ the dependence on RM will have to drop by scale invariance giving a result of the form

$$\Delta_{\phi^n}=\frac{1}{\lambda_*}\Delta_{-1}(\lambda_* n)+\Delta_0(\lambda_* n)+\lambda_*\Delta_1(\lambda_* n)+\dots. \tag{7.48}$$

In the remaining sections of the chapter we shall explicitly compute the leading semiclassical contribution Δ_{-1} and the first quantum correction Δ_0.

7.3.1 Leading order: Δ_{-1}

In this section we compute the dimension Δ_{ϕ^n} at the leading order in λ using the operator state correspondence described above. More precisely, at this order, we shall compute the dimension of the lowest dimension operator with charge n as a function of λn. For sufficiently small λn, such operator of lowest dimension obviously coincides with ϕ^n as shown by a perturbative analysis. Indeed, any other operator with charge n, such as $\phi^{n-2}(x)(\partial\phi(x))^2$, clearly possesses a larger scaling dimension in the free limit, and for small enough λn the ordering is not affected. For generic λn, we *define* the operator ϕ^n to be the lowest dimension charge n operator. While this seems natural to us, the precise relation between such lowest dimension operator and its explicit functional expression in terms of field variables in the path integral, is not obvious in the regime $\lambda n \gg (4\pi)^2$. It should however become clear from our discussion that the precise form of the lowest dimension operator is a separate issue. It does not affect our computation of its scaling dimension but it matters for the computation of the normalization of the correlator, and thus for the computation of higher point functions. We plan to explore this in future work. [10]

Having said that, we further proceed as we did in chapter 3, the only difference being that here we can work in the full theory, without introducing an effective description. Namely, we compute the expectation of the evolution operator e^{-HT} in an arbitrary state $|\psi_n\rangle$ with fixed charge n. As long as there is an overlap between the state $|\psi_n\rangle$ and the lowest energy state (with charge n), in the limit $T\to\infty$ the expectation gets saturated by the latter

$$\langle\psi_n|e^{-HT}|\psi_n\rangle \underset{T\to\infty}{=} \tilde{\mathcal{N}}e^{-E_{\phi^n}T}. \tag{7.49}$$

---

[10] In [4] the analyticity of Δ_{ϕ^n} in λn as it directly emerges from the computation was taken as indication that there is no level crossing as λn is varied. However, unlike argued in [4], we now realize that it does not imply that the field expression for the lowest dimension charge n operator remains ϕ^n for all values of λn.

Now the choice of the state $|\psi_n\rangle$ is completely in our hands. In analogy with the discussion of the hydrogen atom at the beginning of part II, we take it to be

$$|\psi_n\rangle = \int \mathcal{D}\alpha(\vec{n}) \, \exp\left[i\frac{n}{\Omega_{d-1}}\int d\Omega_{d-1}\,\alpha(\vec{n})\right]|f,\alpha(\vec{n})\rangle, \tag{7.50}$$

where $\vec{n}$ denotes collectively the coordinates on the $d-1$ dimensional sphere and the state $|f,\alpha(\vec{n})\rangle$ is the one with fixed values of the fields[11] $\rho(\vec{n}) = f$ and $\chi(\vec{n}) = \alpha(\vec{n})$ defined as

$$\phi = \frac{\rho}{\sqrt{2}}e^{i\chi}, \quad \bar{\phi} = \frac{\rho}{\sqrt{2}}e^{-i\chi}. \tag{7.51}$$

The result for E_{ϕ^n} is independent of the constant value f, however, a specific choice, that will be derived later, makes computations much simpler. Plugging (7.51) into (7.49) and using the path integral representation for the evolution operator we obtain

$$\langle\psi_n|e^{-HT}|\psi_n\rangle = \mathcal{Z}^{-1}\int \mathcal{D}\chi_i\mathcal{D}\chi_f e^{-i\frac{n}{\Omega_{d-1}}\left[\int d\Omega_{d-1}(\chi_f-\chi_i)\right]}\int_{\rho=f,\ \chi=\chi_i}^{\rho=f,\ \chi=\chi_f}\mathcal{D}\rho\mathcal{D}\chi e^{-S}, \tag{7.52}$$

where we defined

$$\mathcal{Z} = \int \mathcal{D}\phi\mathcal{D}\bar{\phi}\, e^{-S}, \tag{7.53}$$

ensuring that the vacuum to vacuum amplitude is normalized to unity, $\langle 0|e^{-HT}|0\rangle = 1$. Using that the boundary conditions imply

$$\int d\Omega_{d-1}(\chi_f-\chi_i) = \int_{-T/2}^{T/2}d\tau\int d\Omega_{d-1}\dot{\chi} \tag{7.54}$$

where $\dot{\chi}\equiv\partial_\tau\chi$, eq. (7.52) can be rewritten as a finite time path integral with boundary conditions only for ρ :

$$\langle\psi_n|e^{-HT}|\psi_n\rangle = \mathcal{Z}^{-1}\int_{\rho=f}^{\rho=f}\mathcal{D}\rho\mathcal{D}\chi e^{-S_{eff}}, \tag{7.55}$$

where the action on the right hand side is given by

$$S_{eff} = \int_{-T/2}^{T/2}d\tau\int d\Omega_{d-1}R^{d-1}\left[\frac{1}{2}(\partial\rho)^2+\frac{1}{2}\rho^2(\partial\chi)^2+\frac{m^2}{2}\rho^2+\frac{\lambda_0}{16}\rho^4+i\frac{n}{R^{d-1}\Omega_{d-1}}\dot{\chi}\right]. \tag{7.56}$$

We can now perform the path integral in (7.55) via a saddle point approximation. The variation of the action (7.56) provides the equations of motion for the fields

$$-\partial^2\rho+\left[(\partial\chi)^2+m^2\right]\rho+\frac{\lambda_0}{4}\rho^3 = 0, \qquad i\partial_\mu\left(\rho^2 g^{\mu\nu}\partial_\nu\chi\right) = 0, \tag{7.57}$$

---

[11] The fields are independent of τ as the state is defined in Schrödinger picture.

supplemented by the following condition which fixes the value of the charge

$$i\rho^2\dot{\chi} = \frac{n}{R^{d-1}\Omega_{d-1}}. \tag{7.58}$$

By a proper choice of the initial and final value $\rho_i = \rho_f = f$ in the wave-function, the stationary configuration for the action (7.56) takes the familiar form of a superfluid solution [23], discussed at length in this thesis:

$$\rho = f\,, \qquad\qquad \chi = -i\mu\tau + \text{const.}\,, \tag{7.59}$$

with homogeneous charge density $j_0 = \mu f^2$ and chemical potential given by μ. The constants f and μ are fixed by the first equation in (7.57) and by (7.58)

$$(\mu^2 - m^2) = \frac{\lambda_0}{4} f^2, \qquad\qquad \mu f^2 R^{d-1}\Omega_{d-1} = n. \tag{7.60}$$

Given the constraint $f^2 \geq 0$, imposed by the boundary condition $\rho_i = \rho_f = f \in \mathbb{R}$, these equations admit a unique solution for f^2 and μ. On this profile χ is analytically continued to the complex plane (see the comments below (7.32)). Notice that the condition $f^2 \geq 0$ implies that the solution for μ is discontinuous at $\lambda_0 n = 0$. This can be seen easily substituting $f^2 \propto n/\mu$ in the first equation in (7.60):

$$\mu(\mu^2 - m^2) = \frac{\lambda_0 n}{4R^{d-1}\Omega_{d-1}} \quad \text{with} \quad n/\mu \geq 0, \tag{7.61}$$

where the last inequality follows from the reality condition on f. It is then obvious that the, otherwise analytical, solution of (7.61) satisfies $\mu(\lambda_0 n) = -\mu(-\lambda_0 n)$, implying the existence of a discontinuity for $\lambda_0 n \to 0$, where $\mu \simeq \text{sgn}(n)\left[m + \mathcal{O}\left(\lambda_0 n\right)\right]$. As a consequence of the latter, also the scaling dimension Δ_{ϕ^n} will be non-analytic at $\lambda n = 0$. This reflects the physical fact that the scaling dimension of ϕ^n and the operator with opposite charge, $\bar{\phi}^n$, are the same; as the expansion (7.12) contains odd powers of n, the physical scaling dimension cannot be continuous at $n = 0$. In the following, we implicitly consider only $n > 0$.

The action (7.56) evaluated on such configuration provides the leading order value for the energy (7.47):

$$\frac{1}{\lambda_0}\frac{e_{-1}(\lambda_0 n, d)}{R} = S_{eff}/T = \frac{n}{2}\left(\frac{3}{2}\mu + \frac{1}{2}\frac{m^2}{\mu}\right). \tag{7.62}$$

Had we chosen $\rho_i, \rho_f \neq f$, $\rho(\tau)$ would have approached exponentially fast the value $\rho = f$ away from the boundaries. As a result, in the $T \to \infty$ limit the contribution of the action growing linearly in time is independent of the precise value of the boundary conditions for ρ.

To obtain the leading order Δ_{-1} in (7.48), we consider the classical value for the chemical potential obtained from (7.60) setting $\lambda_0 = \lambda_*$ and $d = 4$ everywhere else:

$$R\mu_* = \frac{3^{1/3} + \left[9\frac{\lambda_* n}{(4\pi)^2} - \sqrt{81\frac{(\lambda_* n)^2}{(4\pi)^4} - 3}\right]^{2/3}}{3^{2/3}\left[9\frac{\lambda_* n}{(4\pi)^2} - \sqrt{81\frac{(\lambda_* n)^2}{(4\pi)^4} - 3}\right]^{1/3}}. \tag{7.63}$$

Taking the complex conjugate of this expression, one can check that $R\mu^*$ is real for $\lambda_* n \geq 0$. Plugging in (7.62) and taking $m = 1/R$ we conclude that the classical contribution to the scaling dimension is

$$\frac{1}{\lambda_*}\Delta_{-1} = nF_0\left(\lambda_* n\right), \tag{7.64}$$

where the function F_0 reads:

$$\begin{aligned} F_0(16\pi^2 x) \quad &= \quad \frac{3\left[9x - \sqrt{81x^2 - 3}\right]^{1/3} + 3^{2/3}\left[9x - \sqrt{81x^2 - 3}\right]}{\left[\left(9x - \sqrt{81x^2 - 3}\right)^{2/3} + 3^{1/3}\right]^2} \\ &+ \quad \frac{9 \times 3^{1/3} x\left[9x - \sqrt{81x^2 - 3}\right]^{2/3}}{2\left[\left(9x - \sqrt{81x^2 - 3}\right)^{2/3} + 3^{1/3}\right]^2}. \end{aligned} \tag{7.65}$$

Though not obvious, for $x > 0$ this is a real and positive function, which grows monotonically with x. Remarkably, eq. (7.64) explicitly resums the contribution of infinitely many Feynman diagrams.

The form of the result becomes particularly simple (and interesting) in the two extreme regimes, $\lambda_* n \ll (4\pi)^2$ and $\lambda_* n \gg (4\pi)^2$, where eq. (7.64) reads

$$\frac{\Delta_{-1}}{\lambda_*} = \begin{cases} n\left[1 + \frac{1}{2}\left(\frac{\lambda_* n}{16\pi^2}\right) - \frac{1}{2}\left(\frac{\lambda_* n}{16\pi^2}\right)^2 + \mathcal{O}\left(\frac{(\lambda_* n)^3}{(4\pi)^6}\right)\right], & \text{for} \quad \lambda_* n \ll (4\pi)^2, \\ \\ \frac{8\pi^2}{\lambda_*}\left[\frac{3}{4}\left(\frac{\lambda_* n}{8\pi^2}\right)^{4/3} + \frac{1}{2}\left(\frac{\lambda_* n}{8\pi^2}\right)^{2/3} + \mathcal{O}\left(1\right)\right], & \text{for} \quad \lambda_* n \gg (4\pi)^2. \end{cases} \tag{7.66}$$

The first line of (7.66) reproduces the result (7.15) up to higher orders and thus provides a non trivial check of our approach. Notice that the agreement is independent of the precise value of λ_*, since at tree-level the Lagrangian (7.2) is Weyl invariant for every value of the coupling and the theory can be safely mapped to the cylinder through a change of coordinates and a field redefinition. In the opposite regime, the result is organized as an expansion in powers of $(\lambda_* n)^{2/3}$, in agreement with the predictions of the large charge expansion in CFT [34, 35] (see eq. (3.14)).

The parameter which marks the difference between the two regimes is the chemical potential μ_*, since, as expected on general grounds and as we will see explicitly in the next section, the latter controls the gap of the radial mode. For small $\lambda_* n$ the chemical potential, is of order of R^{-1}, while in the opposite regime its value is proportional to $(\lambda j_0)^{1/3} \gg R^{-1}$. In this regime, the leading contribution in the second line of (7.66) follows simply by dimensional analysis [34]. More precisely, momentarily restoring units of $\hbar$ to count powers of λ [68], the quantity $(\lambda j_0)^{1/3}$ has mass units. The energy density of the homogeneous ground state, $E/(\Omega_3 R^3)$, is then expected to be proportional to $(\lambda j_0)^{4/3}/\lambda$, as in eq. (7.66).

7.3.2 One-loop correction: Δ_0

Let us now compute the first subleading correction Δ_0. To this aim we expand the fields around the saddle point configuration:

$$\rho(x) = f + r(x), \qquad \chi(x) = -i\mu\tau + \frac{1}{f\sqrt{2}}\pi(x). \tag{7.67}$$

The action (7.56) at quadratic order in the fluctuations reads

$$S^{(2)} = \int_{-T/2}^{T/2} d\tau \int d\Omega_{d-1} R^{d-1} \left[\frac{1}{2}(\partial r)^2 + \frac{1}{2}(\partial\pi)^2 - 2i\mu\, r\partial_\tau \pi + (\mu^2 - m^2) r^2\right]. \tag{7.68}$$

This action describes a gapped and a gapless mode, with dispersion relations given by

$$\omega_\pm^2(\ell) = J_\ell^2 + 3\mu^2 - m^2 \pm \sqrt{4J_\ell^2\mu^2 + (3\mu^2 - m^2)^2}, \tag{7.69}$$

where $J_\ell^2 = \ell(\ell + d - 2)/R^2$ is the eigenvalue of the Laplacian on the sphere. The gapless mode is the Goldstone boson for the spontaneously broken $U(1)$ symmetry. The gap of the first mode is:

$$\omega_+^2(0) = 6\mu^2 - 2m^2. \tag{7.70}$$

Notice also that the $\ell = 1$ excitation of the gapless mode has unit energy, $\omega_-(1) = 1/R$ and corresponds to a descendant state.

As anticipated, in the large λn limit the gap of the radial mode grows as $(\lambda n)^{1/3}/R$. Henceforth, in this regime we can integrate out this mode and the lightest states at charge n are described by an effective theory for the Goldstone mode only. We reviewed the form of the effective theory and studied the spectrum at large charge in a generic $U(1)$ invariant CFT in chapter 3, where we derived the form of the expansion in the second line of (7.66). We now see how those results emerge for a UV complete theory in a perturbative setting. As expected, in this regime, the squared sound speed of the Goldstone mode, given by

$$\left(\frac{d\omega_-^2}{dJ_\ell^2}\right)_{\ell=0} = \frac{\mu^2 - m^2}{3\mu^2 - m^2}, \tag{7.71}$$

approaches the value 1/3 dictated by scale invariance in a fluid.

To extract the first correction to the energy (7.47) we consider the one-loop expression for the path-integral (7.55):

$$\begin{aligned}\langle\psi_n|e^{-HT}|\psi_n\rangle &= e^{-\frac{e_{-1}(\lambda_0 n,d)T}{\lambda_0 R}}\frac{\int\mathcal{D}r\mathcal{D}\pi\,\exp\left[-S^{(2)}\right]}{\int\mathcal{D}\phi\mathcal{D}\bar{\phi}\,\exp\left[-\int_{-T/2}^{T/2}\left(\partial\phi\partial\bar{\phi}+m^2\phi\bar{\phi}\right)\right]}\\ &= \tilde{\mathcal{N}}\exp\left\{-\left[\frac{1}{\lambda_0}e_{-1}(\lambda_0 n,d)+e_0(\lambda_0 n,d)\right]\frac{T}{R}\right\},\end{aligned}\tag{7.72}$$

where the normalization factor $\tilde{\mathcal{N}}$ is T-independent. The latter contains a factor $\lambda_0^{-1/2}$ coming form the integration over the zero mode (see the comments below (7.20)). The denominator in the first line of (7.72) arises from the normalization factor (7.53). In the second line, the correction to the energy arises from the fluctuation determinant of the Gaussian integrals in the numerator and the denominator. It can be written explicitly in terms of the expressions (7.69) and the formula for the free dispersion relation $\omega_0^2(\ell)=J_\ell^2+m^2=\left(\ell+\frac{d-2}{2}\right)^2/R^2$:

$$\begin{aligned}T\frac{e_0}{R}=\log\frac{\sqrt{\det S^{(2)}}}{\det\left(-\partial_\tau^2-\Delta_{S^{d-1}}+m^2\right)} &= \frac{T}{2}\sum_{\ell=0}^{\infty}n_{\ell,d}\int\frac{d\omega}{2\pi}\log\frac{\left[\omega^2+\omega_-^2(\ell)\right]\left[\omega^2+\omega_-^2(\ell)\right]}{\left[\omega^2+\omega_0^2(\ell)\right]^2}\\ &= \frac{T}{2}\sum_{\ell=0}^{\infty}n_{\ell,d}\left[\omega_+(\ell)+\omega_-(\ell)-2\omega_0(\ell)\right],\end{aligned}\tag{7.73}$$

where $n_{\ell,d}$ is the multiplicity of the Laplacian on the $(d-1)$-dimensional sphere:

$$n_{\ell,d}=\frac{(2\ell+d-2)\Gamma(\ell+d-2)}{\Gamma(\ell+1)\Gamma(d-1)}.\tag{7.74}$$

In $d=4$ the multiplicity is $n_{\ell,d}=(1+\ell)^2$. In dimensional regularization, we can use the following identities which hold for sufficiently negative d

$$\sum_{\ell=0}^{\infty}n_{\ell,d}=\sum_{\ell=0}^{\infty}n_{\ell,d}\,\ell=0\qquad\Longrightarrow\qquad\sum_{\ell=0}^{\infty}n_{\ell,d}\,\omega_0(\ell)=0.\tag{7.75}$$

Finally we formally find the second term in the expansion (7.47) as a sum of zero point energies, as it could have been intuitively expected:

$$e_0(\lambda_0 n,d)=\frac{R}{2}\sum_{\ell=0}^{\infty}n_{\ell,d}\left[\omega_+(\ell)+\omega_-(\ell)\right].\tag{7.76}$$

We can now compute the leading correction to the scaling dimension (7.48). The details of the calculation are given in the appendix D.2.1. The result is formally written in terms of the classical value of the chemical potential (7.63) and a convergent infinite sum:

$$\Delta_0=-\frac{15\mu_*^4R^4+6\mu_*^2R^2-5}{16}+\frac{1}{2}\sum_{\ell=1}^{\infty}\sigma(\ell)+\frac{\sqrt{3\mu_*^2R^2-1}}{\sqrt{2}},\tag{7.77}$$

where $\sigma(\ell)$ is obtained by subtracting the divergent piece from the summand in (7.76)

$$\sigma(\ell) = (1+\ell)^2 R\left[\omega_+^*(\ell)+\omega_-^*(\ell)\right] - 2\ell^3 - 6\ell^2 - \left(2\mu_*^2 R^2 + 4\right)\ell - 2R^2\mu_*^2 + \frac{5\left(\mu_*^2 R^2 - 1\right)^2}{4\ell}. \tag{7.78}$$

As in equation (7.63), the star stresses that all quantities are evaluated setting $\lambda_0 = \lambda_*$ and $d = 4$ everywhere else.

In the small $\lambda_* n$ limit, we can compute the sum in (7.77) analytically and we find

$$\Delta_0 = -\frac{3\lambda_* n}{(4\pi)^2} + \frac{\lambda_*^2 n^2}{2(4\pi)^4} + \mathcal{O}\left(\frac{\lambda_*^3 n^3}{(4\pi)^6}\right). \tag{7.79}$$

Summing this to the leading order result (7.66) and recalling the relation between the coupling and the number of space dimensions (7.8), we determine Δ_{ϕ^n} as:

$$\Delta_{\phi^n} = n\left(\frac{d}{2}-1\right) + \frac{\varepsilon}{10}n(n-1) - \frac{\varepsilon^2}{50}n(n^2-4n) + \mathcal{O}\left(\varepsilon^2 n, \varepsilon^3 n^4\right). \tag{7.80}$$

This is in perfect agreement with the diagrammatic calculation in eq. (7.16).

In the large $\lambda_* n$ limit the result (7.77) develops a contribution proportional to $\log(\lambda_* n)$, which arises from the divergent tail of the sum in (7.76). As in (7.66), the result can be expanded in powers of $(\lambda_* n)^{2/3}$ and reads:

$$\Delta_0 = \left[a_1 + \frac{5}{24}\log\left(\frac{\lambda_* n}{8\pi^2}\right)\right]\left(\frac{\lambda_* n}{8\pi^2}\right)^{4/3} + \left[a_2 - \frac{5}{36}\log\left(\frac{\lambda_* n}{8\pi^2}\right)\right]\left(\frac{\lambda_* n}{8\pi^2}\right)^{2/3} + \mathcal{O}(1), \tag{7.81}$$

where the coefficients a_1 and a_2 are

$$a_1 = -0.5753315(3), \qquad a_2 = -0.93715(9). \tag{7.82}$$

The logarithmic terms are computed analytically, while the coefficients a_1 and a_2 follow from a numerical fit. Details of the calculation are given in the appendix D.2.2. The structure of the result (7.81) is in agreement with the expected form of the large charge expansion in d dimensions. This is evident summing (7.81) to the leading order in (7.66) and writing the result in the form

$$\begin{aligned}\Delta_{\phi^n} = {} & \frac{1}{\varepsilon}\left(\frac{2}{5}\varepsilon n\right)^{\frac{4-\varepsilon}{3-\varepsilon}}\left[\frac{15}{8} + \varepsilon\left(a_1 + \frac{3}{8}\right) + \mathcal{O}\left(\varepsilon^2\right)\right] \\ & + \frac{1}{\varepsilon}\left(\frac{2}{5}\varepsilon n\right)^{\frac{2-\varepsilon}{3-\varepsilon}}\left[\frac{5}{4} + \varepsilon\left(a_2 - \frac{1}{4}\right) + \mathcal{O}\left(\varepsilon^2\right)\right] + \mathcal{O}\left((\varepsilon n)^0\right).\end{aligned} \tag{7.83}$$

The change in the exponents of the (εn) terms with respect to the leading order (7.66) account for the logarithms in (7.81). Recalling that $d = 4 - \varepsilon$, eq. (7.83) is clearly in agreement with the structure of the large charge expansion (3.19) predicted in [34, 35]:

$$\Delta_n = n^{\frac{d}{d-1}} \left[\alpha_1(d) + \alpha_2(d) n^{-\frac{2}{d-1}} + \alpha_3(d) n^{-\frac{4}{d-1}} + \dots\right] \\ + n^0 \left[\beta_0(d) + \beta_1(d) n^{-\frac{2}{d-1}} + \dots\right]. \tag{7.84}$$

From the point of view of the large charge EFT, the first term is a purely classical contribution, while the second term is the one-loop Casimir energy of the Goldstone mode. We have checked that the coefficients of the logarithms multiplied by subleading powers of $(\lambda_* n)$ ensure the agreement between our result and the predicted structure (7.84) also in the subleading orders in n. The large $\lambda_* n$ expansion of the classical result determines the coefficients $\alpha_i(d)$ at leading order, while eq. (7.83) determines $\alpha_1(d)$ and $\alpha_2(d)$ to order $\mathcal{O}(\varepsilon)$. Even though we computed also the coefficient of the $(\lambda_* n)^0$ term in (7.81) (see eq. (D.28)), in the expansion of (7.84) for $d = 4 - \varepsilon$ to first order, we cannot disentangle the first correction in ε to $\alpha_3(d)$ and the leading order value of $\beta_0(d)$ (which is zero at tree-level).

7.4 Discussion

7.4.1 Large order behavior

Expanding all functions Δ_ℓ in a power series in $\lambda_* n$

$$\Delta_\ell = \sum_k f_{\ell,k} (\lambda_* n)^k, \tag{7.85}$$

it naively seems that the anomalous dimension (7.48) has, at fixed order in the semiclassical expansion, contributions from arbitrarily large powers of n. This, however, does not match the diagrammatic computation which is valid for small $\lambda_* n$ but virtually large n. Indeed, beyond order $\lfloor n/2 \rfloor$ in the ordinary loop expansion the operator ϕ^n does not have enough free legs to provide terms with higher and higher powers of n.

To understand what happens from the semiclassical perspective, we can compare contributions to the anomalous dimension that are of the same order in λ_* but which come from different orders in the semiclassical expansion. For instance we can consider Δ_ℓ and $\Delta_{\ell+1}$. The contributions of the same order in λ_* are controlled by $\lambda_*^{\ell+k} f_{\ell,k} n^k$ and $\lambda_*^{\ell+k} f_{\ell+1,k-1} n^{k-1}$ respectively. Therefore, if

$$\frac{f_{\ell+1,k-1}}{f_{\ell,k}} \sim k, \tag{7.86}$$

there can be a potential cancellation at order $k \sim n$, thus resulting in the correct behavior of the anomalous dimensions for k beyond roughly $\lfloor n/2 \rfloor$. We checked that this is precisely what happens for $f_{-1,k}$ and $f_{0,k-1}$.

7.4.2 Boosting diagrammatic loop calculations

At the Wilson-Fisher fixed point, the expansion in (7.12) for the anomalous dimension of ϕ^n, valid for small εn, is written as

$$\gamma_{\phi^n} = n \sum_{\ell=1} \varepsilon^\ell P_\ell(n), \tag{7.87}$$

Hence, at any fixed order ℓ in (7.87) there are ℓ independent coefficients to be determined. We can thus take advantage of existing results in the literature, as well as of the small $\lambda_* n$ expansion of our results (7.64) and (7.77), to fix some or all of them. The anomalous dimensions of ϕ, ϕ^2 and ϕ^4 are known to order ε^5 with analytical coefficients [113, 228], while the anomalous dimension of ϕ^3 is known to the same order with numerical coefficients [229]. These results then provide four constraints on each of the first five orders in (7.87) and are enough to fix all the coefficients in $P_1(n), P_2(n)$ and $P_3(n)$. Furthermore, expanding the results (7.64) and (7.77) derived in this chapter to order $\mathcal{O}(\varepsilon^5 n^5)$, we fix the first two coefficients of all the polynomials $P_\ell(n)$. Combining our result and the perturbative calculations, we have six constraints on each of the first five orders in (7.87). This fully fixes the form of the five polynomials $P_1(n), P_2(n), \ldots, P_5(n)$. The form of the first two was given in (7.15), while the others read

$$P_3(n) = \frac{n^3}{125} + \frac{n^2\,[16\zeta(3) - 29]}{500} + \frac{n\,[599 - 672\zeta(3)]}{5000} + \frac{[1024\zeta(3) - 603]}{10000}, \tag{7.88}$$

$$\begin{aligned} P_4(n) = &- \frac{21n^4}{5000} + \frac{n^3\,[214 - 77\zeta(3) - 80\zeta(5)]}{5000} + \frac{n^2\left[66336\zeta(3) + 160\pi^4 - 89491\right]}{600000} \\ &+ \frac{n\left[41073 - 45864\zeta(3) + 46720\zeta(5) - 224\pi^4\right]}{200000} \\ &+ \frac{75888\zeta(3) - 130560\zeta(5) + 512\pi^4 - 53717}{600000}, \end{aligned} \tag{7.89}$$

$$\begin{aligned} P_5(n) = &\frac{n^5 8}{3125} + \frac{n^4\,[476\zeta(3) + 480\zeta(5) + 448\zeta(7) - 1683]}{50000} \\ &+ 0.00093n^3 - 0.01067n^2 - 0.2460n + 0.2680. \end{aligned} \tag{7.90}$$

We checked that $P_3(n)$ agrees both with the previous literature and our results, providing another non trivial check of our approach. The polynomial $P_4(n)$ was determined using our results and those in the literature for ϕ, ϕ^2 and ϕ^4; we checked that it agrees numerically within 10% level with the coefficient reported in [229] for ϕ^3. We do not know if this discrepancy is due to the numerical uncertainty of this result, as the latter is not reported in [229]. For the same reason, we cannot quote the uncertainty on the last four coefficients of $P_5(n)$.

7.4.3 Comparison with Monte-Carlo results at large charge

We can compare our result in the large $(\lambda_* n)$ limit, given by (7.83) in the first two leading orders, with the recent results of Monte-Carlo lattice simulations of the three-dimensional

	α_1	α_2
Monte-Carlo [118]	0.337(3)	0.27(4)
ε-expansion: LO	0.47	0.79
ε-expansion: NLO	0.42	0.04

Table 7.1 – Comparison of the Monte-Carlo results in [118] with the ε-expansion for the coefficients in eq. (7.91); we display both the leading order (LO) result as well as the next to leading order (NLO).

$O(2)$ model [118]. There, the authors computed the scaling dimensions of the lightest charge n operator for various values of n and compared their result with the predicted form in $d = 3$, which we recall here for convenience:

$$\Delta_n \simeq \alpha_1 n^{3/2} + \alpha_2 n^{1/2} - 0.0937 + \alpha_3 n^{-1/2} + \mathcal{O}\left(n^{-1}\right). \tag{7.91}$$

The authors there determined the coefficients α_1 and α_2 fitting the result of the lattice computation.

We compared the coefficients they obtained with those which follow from (7.83) putting $\varepsilon = 1$. The results are displayed in the table 7.1. Using the next to leading order contribution as an estimate of the error, the result for α_1 is roughly within two standard deviations from the Monte-Carlo result, while for α_2 the error is as big as the leading order, making a quantitative analysis impossible. It is however interesting to notice that for both coefficients the next to leading order values are closer than the leading order ones to the results obtained by the Monte-Carlo. It would be interesting to compute the two-loop order result to explore the convergence properties of the expansion.

8 Feynman diagrams and the large charge expansion in $3-\varepsilon$ dimensions

The methodology discussed in the previous chapter can be straightforwardly applied to different theories, as well as to the calculations of different observables. Here we shall illustrate this concretely by computing the scaling dimension of ϕ^n in $(\bar{\phi}\phi)^3$ at its conformally invariant point in $3-\varepsilon$ dimensions. The result follows the same pattern observed in $(\bar{\phi}\phi)^2$ in $4-\varepsilon$ dimensions. Besides confirming the generality of the method, the main interest of $(\bar{\phi}\phi)^3$ in $d=3-\varepsilon$ lies in the possibility of non-trivially comparing to the universal predictions of the large charge EFT of 3d CFT [34]. Indeed the β function of $(\bar{\phi}\phi)^3$ arises only at 2-loops. At the 1-loop level the theory is therefore conformally invariant at $d=3$ for any value of λ. At this order, as λn is varied from small to large, our formulae non trivially interpolate between the prediction of standard Feynman diagram computations and those of the universal superfluid description of large charge states in 3d CFT. In particular for $t \equiv \lambda n/\sqrt{3}\pi \gg 1$ our result for the scaling dimension takes the form:

$$\Delta_{\phi^n} = t^{3/2}\left[\tilde{\alpha}_1 + \tilde{\alpha}_2 t^{-1} + \ldots\right] + t^0\left[\tilde{\beta}_0 + \tilde{\beta}_1 t^{-1} + \ldots\right] , \tag{8.1}$$

with $\tilde{\alpha}$'s and $\tilde{\beta}$'s having specific calculable values. We use the tilde to distinguish them, due to the definition of t, from the α's and β's used in part II and III of this thesis, defined in eq. (3.19). This result nicely matches the universal predictions of the large charge EFT, illustrated in chapter 3, where the $\tilde{\alpha}_k$'s are model-dependent Wilson coefficients, but the $\tilde{\beta}$'s are universally calculable effects associated to the 1-loop Casimir energy. Our result for the $\tilde{\beta}$'s should thus match the general theory, and they do. In particular, we find

$$\tilde{\beta}_0 = -0.0937255(3) \tag{8.2}$$

in agreement with eq. (3.20) [35]. The prediction of $\tilde{\beta}_1$ is similarly matched to eq. (3.20). Previously, eq.s (8.1) and (8.2) were verified at large N for monopole operators [136]; the results of Monte-Carlo simulations for the $O(2)$ model at criticality are consistent with the expansion (8.1) [118], though their present precision is not sufficient to check the universal prediction for $\tilde{\beta}_0$. Here we provide an alternative verification where the large charge regime is continuously connected, as λn is varied, to diagrammatic perturbation theory. The prediction for $\tilde{\beta}_1$ was not verified before.

8.1 Lagrangian and Feynman diagrams

We consider the following $U(1)$ symmetric theory in $d = 3 - \varepsilon$ dimensional euclidean space-time

$$\mathcal{L} = \partial\bar{\phi}\partial\phi + \frac{\lambda_0^2}{36}\left(\bar{\phi}\phi\right)^3 . \tag{8.3}$$

Within this convention for the Lagrangian, one can easily realize that λ_0 is the loop counting parameter by rescaling $\phi \to \phi/\sqrt{\lambda_0}$. The renormalized coupling and field are defined as

$$\phi = Z_\phi[\phi], \quad \lambda_0 = M^\varepsilon \lambda Z_\lambda \, , \tag{8.4}$$

where M denotes the sliding scale. The β-function is given by [218]

$$\frac{\partial\lambda}{\partial\log M} \equiv \beta(\lambda) = \lambda\left[-\varepsilon + \frac{7\lambda^2}{48\pi^2} + \mathcal{O}\left(\frac{\lambda^4}{(4\pi)^4}\right)\right] . \tag{8.5}$$

For $\varepsilon \ll 1$, this implies the existence of an IR-stable fixed point at

$$\frac{\lambda_*^2}{(4\pi)^2} = \frac{3}{7}\varepsilon + \mathcal{O}\left(\varepsilon^2\right) . \tag{8.6}$$

Notice that the β-function (8.5) starts at two-loop order at $\varepsilon = 0$. Hence the model is conformally invariant up to $\mathcal{O}(\lambda)$ in exactly $d = 3$. This observation will be important for what follows. The field wave-function renormalization starts at four loops and we shall always neglect it in the following.

We focus on the calculation of the scaling dimension of the $U(1)$ charge n operator ϕ^n, *defined* as the lowest dimension charge n operator (see the discussion at the beginning of 7.3.1) focusing on the regime $n \gg 1$. In complete analogy with the $(\phi\bar{\phi})^2$ case discussed before, the diagrammatic calculation for the anomalous dimension takes the form (7.12), where the loop order ℓ contribution grows as $\lambda^\ell n^{\ell+1}$ for $\ell \leq n$, implying that the diagrammatic expansion breaks down for sufficiently large λn. Re-organizing the series as in (7.13), the scaling dimension can also be expanded as

$$\Delta_{\phi^n} = n\left(\frac{d}{2} - 1\right) + \gamma_{\phi^n} = \sum_{\kappa=-1} \lambda^\kappa \Delta_\kappa(\lambda n). \tag{8.7}$$

The main result of chapter 7 is that it is possible to compute the functions $\Delta_\kappa(\lambda n)$ for arbitrary λn via a perturbative *semiclassical calculation* around a non-trivial saddle; the

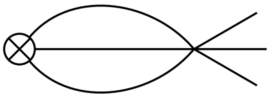

Figure 8.1 – Two-loop diagram contributing to the ϕ^n anomalous dimension. The crossed circle denotes the ϕ^n insertion.

result can be organized as an expansion in $\lambda \ll 4\pi$ while treating λn as a fixed parameter, closely analogous to the 't Hooft coupling of large N theories. The goal of this chapter is to compute the leading term and the first subleading correction in (8.7).

The scaling dimension (8.7) is a physical (scheme-independent) quantity only at the fixed-point (8.6). However, in light of the observation at the end of the previous section, working at order $\mathcal{O}(\lambda)$ we can take $\varepsilon \to 0$ without affecting the conformal invariance of the theory[1]. The leading order term $\Delta_{-1}(\lambda n)$ and the one-loop correction $\Delta_0(\lambda n)$ are hence scheme-independent for generic λ.

Working at fixed n, at leading order in λ, the anomalous dimension of $\phi^n(x)$ is determined by the diagram in Fig. 8.1 and it is given by

$$\gamma_{\phi^n}=\frac{\lambda^2 n(n-1)(n-2)}{36(4\pi)^2}+\mathcal{O}\left(\frac{\lambda^4 n^5}{(4\pi)^4}\right). \tag{8.8}$$

Comparing with (8.7), one can readily extract the lowest order terms in the expansion of Δ_{-1} and Δ_0 at small λn. We will use this expression as a check of the more general result that we will derive in the next section.

8.2 Semiclassical computation

To compute the scaling dimension Δ_{ϕ^n} for arbitrary λn we proceed as in chapter 7. We first use a Weyl transformation to map the theory to the cylinder $\mathbb{R}\times S^{d-1}$. The Lagrangian of the theory on the cylinder reads:

$$\mathcal{L}_{cyl}=\partial\bar{\phi}\partial\phi+m^2\bar{\phi}\phi+\frac{\lambda^2}{36}\left(\bar{\phi}\phi\right)^3, \tag{8.9}$$

where, as in eq. (7.45), $m^2=\left(\frac{d-2}{2R}\right)^2\overset{d=3}{=}\frac{1}{4R^2}$ arises from the $\mathcal{R}(g)\bar{\phi}\phi$ coupling to the Ricci scalar which is enforced by conformal invariance. Working at $\mathcal{O}(\lambda)$, we neglect the difference between bare and renormalized coupling, as that arises at $\mathcal{O}(\lambda^2)$. Then, as we discussed in sec. 7.3.1, Δ_{ϕ^n} is directly determined by studying the expectation value of the evolution operator e^{-HT} in an arbitrary state $|\psi_n\rangle$ with fixed charge n using eq. (7.49) with $E_{\phi^n}=\Delta_{\phi^n}/R$. Working in polar coordinates for the field $\phi=\frac{\rho}{\sqrt{2}}e^{i\chi}$, we then consider the following path integral:

---

[1] Dimensional regularization is still used in the intermediate steps.

$$\langle\psi_n|e^{-HT}|\psi_n\rangle = \mathcal{Z}^{-1}\int \mathcal{D}\chi_i\mathcal{D}\chi_f\psi_n(\chi_i)\psi_n^*(\chi_f)\times\int_{\rho=f,\ \chi=\chi_i}^{\rho=f,\ \chi=\chi_f}\mathcal{D}\rho\mathcal{D}\chi e^{-S}\,, \qquad (8.10)$$

where the insertions of the wave-functional

$$\psi_n(\chi) = \exp\left(\frac{i\,n}{\Omega_{d-1}}\int d\Omega_{d-1}\chi\right)\,. \qquad (8.11)$$

ensure that the initial and final states have charge n, while the boundary value f for ρ is arbitrary and will be fixed later by convenience. The factor $\mathcal{Z}$ ensures that the vacuum to vacuum amplitude is normalized to unity as in eq. (7.53). The structure of the expansion (8.7) follows from performing the path-integral in a saddle-point approximation. This is easily seen rewriting eq. (8.10) as

$$\langle\psi_n|e^{-HT}|\psi_n\rangle = \mathcal{Z}^{-1}\int_{\rho=f}^{\rho=f}\mathcal{D}\rho\mathcal{D}\chi e^{-S_{eff}}\,, \qquad (8.12)$$

where the action on the right hand side is given by

$$S_{eff} = \int_{-T/2}^{T/2}d\tau\int d^{d-1}x\sqrt{g}\left[\frac{1}{2}(\partial\rho)^2+\frac{1}{2}\rho^2(\partial\chi)^2+\frac{m^2}{2}\rho^2+\frac{\lambda^2}{2(12)^2}\rho^6+i\frac{n}{R^{d-1}\Omega_{d-1}}\dot{\chi}\right]\,. \qquad (8.13)$$

Rescaling then the field as $\rho\to\rho/\lambda^{1/2}$ and collecting up front the overall λ^{-1}, one immediately recognizes eq. (8.7) as the result of performing the path-integral (8.12) as a systematic loop expansion around a saddle-point .

Unsurprisingly, properly tuning the initial and final value $\rho_i=\rho_f=f$ in eq. (8.12), the stationary configuration for the action (8.13) is given again by a superfluid configuration as in (7.59), where now μ and f satisfy

$$\mu^2-m^2=\frac{\lambda^2}{48}f^4, \qquad \mu f^2R^{d-1}\Omega_{d-1}=n\,. \qquad (8.14)$$

Given the constraint $f^2\geq 0$, the eq.s (8.14) admit a unique solution. In particular, in $d=3$ and for $n>0$, μ reads:

$$R\mu = \frac{\sqrt{1+\sqrt{1+\frac{\lambda^2n^2}{12\pi^2}}}}{2\sqrt{2}}\,. \qquad (8.15)$$

For $\lambda n<0$ the chemical potential is given by minus the expression in (8.15) and is hence discontinuous at $\lambda n=0$ and the same comments below eq. (7.61) apply here. In the following we always assume $\lambda n>0$.

Plugging the solution into the classical action we extract the leading order contribution to the scaling dimension:

$$S_{eff}/T = \frac{n}{3}\left(2\mu + \frac{m^2}{\mu}\right) \overset{d=3}{=} \frac{1}{R}\frac{\Delta_{-1}(\lambda n)}{\lambda}\,. \tag{8.16}$$

Explicitly, the result reads

$$\Delta_{-1}(\lambda n) = \lambda n\, F_{-1}\left(\frac{\lambda^2 n^2}{12\pi^2}\right)\,, \tag{8.17}$$

where

$$F_{-1}(x) = \frac{1+\sqrt{1+x}+x/3}{\sqrt{2}\,(1+\sqrt{1+x})^{3/2}}\,. \tag{8.18}$$

To compute the one-loop correction we expand the fields around the saddle point configuration as in sec. 7.3.2. Putting $\rho(x) = f + r(x)$, and $\chi(x) = -i\mu\tau + \frac{1}{f\sqrt{2}}\pi(x)$, the action (8.13) at quadratic order in the fluctuations reads

$$S^{(2)} = \int_{-T/2}^{T/2} d\tau \int d\Omega_{d-1} R^{d-1}\left[\frac{1}{2}(\partial r)^2 + \frac{1}{2}(\partial\pi)^2 - 2i\mu\, r\partial_\tau\pi + 2(\mu^2-m^2)r^2\right]\,. \tag{8.19}$$

This action describes two modes, with dispersion relations given by

$$\omega_\pm^2(\ell) = J_\ell^2 + 2(2\mu^2-m^2) \pm 2\sqrt{J_\ell^2\mu^2 + (2\mu^2-m^2)^2}\,, \tag{8.20}$$

where $J_\ell^2 = \ell(\ell+d-2)/R^2$ is the eigenvalue of the Laplacian on the sphere. The first mode has a gap $\omega_+(0) = 2\sqrt{2\mu^2-m^2} \propto \sqrt{\lambda n}$ for $\lambda n \gg 1$. The dispersion relation $\omega_-(\ell)$ describes instead a gapless mode, the Goldstone boson for the spontaneously broken $U(1)$ symmetry. These modes, except for the zero mode of the Goldstone which relates different charge sectors, provide a basis for the Fock space describing charge n operators with higher scaling dimension. In particular, the descendants, obtained by acting q times with the P_i generators of the conformal algebra, correspond to states involving a number q of massless spin one quanta, each increasing the energy by $\omega_-(1) = 1/R$. Other modes describe different primaries; non-trivially, the expressions (8.20) include the leading λn corrections to the free theory values, effectively resumming the effect of infinitely many loop diagrams in standard diagrammatic calculations.

In the large λn regime, where we can integrate out the gapped mode and describe the lightest states at charge n through the superfluid effective theory for the gapless mode described in chapter 3, the dispersion relation of the Goldstone boson can be expanded in inverse powers of λn and reads

$$R\omega_-(\ell) = \left[\frac{1}{\sqrt{2}} - \frac{\sqrt{3}\pi}{\sqrt{2}\lambda n} + \mathcal{O}\left(\frac{1}{(\lambda n)^2}\right)\right] J_\ell + \left[\frac{\sqrt{3}\pi}{2\sqrt{2}} + \mathcal{O}\left(\frac{1}{\lambda n}\right)\right]\frac{J_\ell^3}{\lambda n} + \mathcal{O}\left(\frac{J_\ell^5}{(\lambda n)^2}\right)\,. \tag{8.21}$$

From this expression we see that the Goldstone sound speed approaches the value $c_s = 1/\sqrt{2}$ as $\lambda n \to \infty$, as dictated by conformal invariance in the superfluid phase.

The one-loop correction Δ_0 is determined by the fluctuation determinant around the leading trajectory. Explicitly, we find[2]

$$\Delta_0(\lambda n) = \frac{1}{2}\sum_{\ell=0}^{\infty} n_{\ell,d}\left[\omega_+(\ell) + \omega_-(\ell) - 2\omega_0(\ell)\right] , \tag{8.22}$$

where $\omega_0^2(\ell) = J_\ell^2 + m^2 = \left(\ell + \frac{d-2}{2}\right)^2/R^2$ is the free theory dispersion relation and $n_{\ell,d}$ is the multiplicity of the Laplacian on the $(d-1)$-dimensional sphere given by (7.74). The analytic continuation to negative d of the sum (8.22) is convergent; the final result is finite in the limit $d \to 3$, consistently with the coupling not being renormalized at one-loop. Proceeding as in the previous chapter, Δ_0 can be written in terms of an infinite convergent sum:

$$\Delta_0(\lambda n) = \frac{1}{4} - 3(R\mu)^2 + \frac{\sqrt{8R^2\mu^2 - 1}}{2} + \frac{1}{2}\sum_{\ell=1}^{\infty}\sigma(\ell) , \tag{8.23}$$

where $\sigma(\ell)$ is obtained from the summand in (7.73) by subtracting the divergent piece:

$$\sigma(\ell) = (1+2\ell)R\left[\omega_+(\ell) + \omega_-(\ell)\right] - 4\ell\left(\ell+1\right) - \left(6R^2\mu^2 - \frac{1}{2}\right) . \tag{8.24}$$

In (8.23) all quantities are evaluated in $d = 3$, hence μ is given by eq. (7.63) and $m = \frac{1}{2R}$.

8.3 Analysis of the result

Eq.s (8.17) and (8.23) provide the first two terms of the expansion (8.7) for the scaling dimension of the operator ϕ^n, Δ_{ϕ^n}. The result holds for arbitrary values of λn. Here we explicitly show that Δ_{ϕ^n} matches the diagrammatic result (8.8) and the large charge prediction (8.1) in the two extreme regimes of, respectively, small and large λn.

Let us consider first the small λn regime. From eq. (7.63) it follows that the chemical potential, and consequently all the functions Δ_κ, can be expanded in powers of $\lambda^2 n^2$. Explicitly neglecting terms of order $\mathcal{O}\left(\frac{\lambda^6 n^7}{(4\pi)^6}\right)$, we get:

$$\Delta_{\phi^n} = \frac{n}{2} + \frac{\lambda^2}{(4\pi)^2}\left[\frac{n^3 - 3n^2}{36} + \mathcal{O}(n)\right] - \frac{\lambda^4}{(4\pi)^4}\left[\frac{n^5}{144} - \frac{n^4(64 - 9\pi^2)}{1152} + \mathcal{O}\left(n^3\right)\right] + \dots . \tag{8.25}$$

In this regime we can compare eq. (8.25) with the diagrammatic result (8.8), finding perfect agreement.

---

[2] In (7.73) we neglect the integration over the zero mode associated to the $U(1)$ symmetry, whose result is independent of T and hence does not contribute to E_{ϕ^n} in eq. (7.49).

Let us now discuss the large λn regime. The classical result (8.17) is easily seen to admit an expansion in inverse powers of λn with the expected form. The one-loop contribution (8.23) can be evaluated numerically for large $\mu \sim (\lambda n)^{1/2}$ and then fitted[3] to the functional form (8.1), as we did for the Wilson-Fisher fixed point in the appendix D.2.2. In doing this we also verified that the coefficients of terms which might modify the form of the expansion, such as a term linear in λn, are compatible with zero within the numerical uncertainty. The final result reads

$$\Delta_{\phi^n} = t^{3/2}\left[\tilde{\alpha}_1 + \tilde{\alpha}_2 t^{-1} + \tilde{\alpha}_3 t^{-2} + \dots\right] + \left[\tilde{\beta}_0 + \tilde{\beta}_1 t^{-1} + \dots\right], \tag{8.26}$$

where we defined $t = \frac{\lambda n}{\sqrt{3}\pi}$ and the coefficients read

$$\begin{aligned}
\tilde{\alpha}_1 &= \frac{\sqrt{3}\pi}{6\lambda} - 0.0653 + \mathcal{O}\left(\frac{\lambda}{\sqrt{3}\pi}\right), \\
\tilde{\alpha}_2 &= \frac{\sqrt{3}\pi}{2\lambda} + 0.2088 + \mathcal{O}\left(\frac{\lambda}{\sqrt{3}\pi}\right), \\
\tilde{\alpha}_3 &= -\frac{\sqrt{3}\pi}{4\lambda} - 0.2627 + \mathcal{O}\left(\frac{\lambda}{\sqrt{3}\pi}\right), \\
\tilde{\beta}_0 &= -0.0937255(3), \\
\tilde{\beta}_1 &= 0.096(1) + \mathcal{O}\left(\frac{\lambda}{\sqrt{3}\pi}\right).
\end{aligned} \tag{8.27}$$

The parentheses show the numerical error on the last digit, when the latter is not negligible at the reported precision.

To discuss this result, let us rewrite the large charge EFT for the superfluid Goldstone field in $d=3$ setting $c_i = \tilde{c}_i/\lambda$ in (3.9): [4]

$$\begin{aligned}
\mathcal{L}/\sqrt{g} = -\frac{1}{\lambda}\Bigg\{&\tilde{c}_1|\partial\chi|^3 - \tilde{c}_2|\partial\chi|\left[\mathcal{R} + 2\frac{(\partial_\mu|\partial\chi|)^2}{|\partial\chi|^2}\right] + \tilde{c}_3\Bigg[\mathcal{R}_{\mu\nu}\frac{\partial^\mu\chi\partial^\nu\chi}{|\partial\chi|} \\
&+2\frac{(\partial^\mu\chi\partial_\mu|\partial\chi|)^2}{(\partial\chi)^3} + \nabla_\mu\left(\frac{\partial^\mu\chi\partial^\nu\chi}{|\partial\chi|^2}\right)\partial_\nu|\partial\chi|\Bigg] + \dots\Bigg\}.
\end{aligned} \tag{8.28}$$

The factor $1/\lambda$ in front ensures that the Wilson coefficients $\tilde{c}_i$ scale as λ^0, as we will see explicitly below in the matching. We recall that in the EFT the derivative expansion coincides with an expansion in inverse powers of $\mu^2 \sim \lambda n$. From eq. (8.28) we can also infer that the loop counting parameter is $\lambda/(\lambda n)^{3/2}$ instead. It follows that the scaling dimension of the lightest charged operator takes the form (8.26), where the first line corresponds to short distance (classical plus quantum) contribution from both the radial and Goldstone mode, while the second line corresponds the one-loop Casimir energy of the Goldstone mode. This second contribution is thus a genuinely long distance one. Matching the explicit calculation in the full theory with the result of the effective theory we can determine the Wilson coefficients $\tilde{c}_1$ and $\tilde{c}_3$ to next to leading order in λ through the relations:

---

[3] We computed Δ_0 numerically for $R\mu = 10, 11, \dots 210$ to perform the fit; the final results are obtained using six fitting parameters in the expansion (8.1).

[4] In [5] the last term of the Lagrangian, proportional to $\tilde{c}_3|_{here} = \alpha_2|_{there}$, was missing the last two contributions in eq.s (8.28). This led to two typos in eq.s (36) and (38) there, which we correct here in eq.s (8.30) and (8.31), but did not affect the main result of that work, as the matching of the full theory gives $\tilde{c}_3|_{here} = \alpha_2|_{there} = 0$ (see below).

$$\lambda\tilde{\alpha}_1 = \frac{\pi}{3^{3/4}\sqrt{\tilde{c}_1}}, \qquad \lambda\tilde{\alpha}_2 = \frac{4\pi\tilde{c}_2}{3^{1/4}\sqrt{\tilde{c}_1}}. \tag{8.29}$$

From these we extract $\tilde{c}_1 = 4/\sqrt{3} + 0.3326\,\lambda + \mathcal{O}(\lambda^2)$ and $\tilde{c}_2 = \sqrt{3}/4 + 0.0644\,\lambda + \mathcal{O}(\lambda^2)$. Recall also that the coefficient $\tilde{c}_3$ does not contribute to the scaling dimension at order $(\lambda n)^{1/2}$ since $\mathcal{R}_{00} = 0$.

To discuss the value of the coefficients $\tilde{\beta}$'s in eq. (8.27), recall that within the EFT one derives the dispersion relation of the Goldstone boson, in eq. (3.25). Using the normalization in eq. (8.28) for the Lagrangian, the latter reads

$$R\omega_-(\ell) = \left[\frac{1}{\sqrt{2}} - \frac{4\pi\,(\tilde{c}_2+\tilde{c}_3)}{\sqrt{2}\,\lambda n} + \mathcal{O}\left(\frac{1}{(\lambda n)^2}\right)\right] J_\ell + \left[\sqrt{2}\pi\,(\tilde{c}_2+\tilde{c}_3) + \mathcal{O}\left(\frac{1}{\lambda n}\right)\right]\frac{J_\ell^3}{\lambda n} + \dots\,. \tag{8.30}$$

Comparing this equation to eqs. (8.21), (8.27) and (8.29), at leading order we find $\tilde{c}_3 = 0$, and we can also check the consistency of the result for $\tilde{c}_2$: $\tilde{c}_2 = \sqrt{3}/4$. [5] Moreover we have seen that eq. (8.30) determines the one-loop Casimir energy of the Goldstone mode. Using (3.20), we can write the second line of (8.26) in terms of the EFT Wilson coefficients:

$$\tilde{\beta}_0 = -0.0937255\,, \tag{8.31}$$

$$\tilde{\beta}_1 = (\tilde{c}_2 + \tilde{c}_3) \times 0.2236\,. \tag{8.32}$$

The result of the explicit computation in the full model (8.27) agrees with the theory-independent prediction (8.31) almost to seven digits accuracy. Using the previously extracted values for the $\tilde{c}_i$, the EFT prediction in eq. (8.32) gives $\tilde{\beta}_1 = 0.0968$, again in agreement with the explicit result in eq. (8.27) within its numerical accuracy.

---

[5] That $\tilde{c}_3 = 0$ at the tree level in the effective lagrangian simply follows from the fact that, in the microscopic lagrangian, χ only appears through $(\partial\chi)^2$.

Conclusions to Part IV

In chapter 7 we illustrated a situation where amplitudes involving a large number n of legs can be reliably computed through a systematic semiclassical expansion. That the large number of legs be related to a large conserved charge was essential to achieve our goal, but also the specialization to a conformally invariant fixed point made the task technically easier. The main conceptual result, obtained in the context of the $U(1)$ Wilson-Fisher fixed point, is given by the existence of the expansion in eq. (7.1) for the scaling dimension Δ_{ϕ^n}. This result was concretely exemplified with the calculation of the tree-level and one-loop contribution in the double scaling limit, given, respectively, by (7.64) and (7.77). For small charge, the result matches, and in fact improve, the available diagrammatic expansions. In the large charge limit instead, the scaling dimension takes the form predicted by the large charge expansion, providing a concrete “UV" realization of the conformal superfluid phase discussed in part I of this thesis.

In chapter 8, we computed the scaling dimension of the operator ϕ^n in the tricritical $U(1)$ CFT in $3-\varepsilon$ dimensions at the next-to-leading order in the coupling λ, but for arbitrary values of λn. Our results nicely interpolate between the small λn regime, when it is given by (8.25), in agreement with diagrammatic calculations, and the large λn regime, where it reads as in (8.26) and it agrees with the expectation for the universal conformal superfluid phase of CFTs at large charge. The remarkable agreement between the form of the quantum corrections in eq.s (8.31) and (8.32) and the explicit result (8.26) provides a nontrivial check of the validity of our methodology.

The techniques discussed in this part of the thesis cleary allow for several applications and extensions. First, one can study other models [134, 138, 139, 141], such as the Wilson-Fisher fixed points in models with non-Abelian symmetry, like the $O(N)$ models, recently addressed in [135] within the epsilon expansion and in [140] at large N. These studies might illustrate the more general, but abstract, construction presented in chapter 4 of this thesis, as well as in several other works [78, 79, 120], in particular concerning the role of gapped Goldstones discussed in chapter 4. Similar ideas were also shown to be relevant in the study of extremal correlators in $\mathcal{N}=2$ superconformal theories [230, 231], with the double expansion remarkably associated to a dual matrix model description [161].

Perhaps, the most famous example of a double scaling limit at large quantum numbers supersymmetric theories is given by the BMN limit of $\mathcal{N}=4$ Yang-Mills (SYM) theory [162–165], corresponding to $N\to\infty$, $J\to\infty$ with J^2/N fixed, where J is the R-charge of the theory. While most of the original works focused on the integrability of the spectrum and its interpretation in the dual string theory, these ideas were recently revived in [166, 167] for the study of correlators of half-BPS operators. Perhaps, a semiclassical approach along the lines of our discussion might prove useful also in that setup.

Another straightforward application concerns the study of the n-point functions of light operators in between two arbitrary charge n states, [6] which would provide a concrete illustration of the transition from diagrammatic perturbation theory to the superfluid semiclassical description of correlators [35] discussed in section 3.3. A more technically involved problem concerns the computation of 3-point functions of the form $\langle\bar{\phi}^{n_1+n_2}\phi^{n_1}\phi^{n_2}\rangle$ with $n_{1,2}$ large, which would extend control to the full set of CFT data. The result requires a numerical analysis of the saddle-point solution. The same technology might allow for the calculation of correlators involving three large charge operators in the superfluid EFT discussed in chapter 3. We are currently investigating this issue.

It might be interesting to study the scaling dimension of charged operators with large spin. In particular, one could explore the transition in the description for the lowest energy state at fixed angular momentum. As discussed in section 5.6.1, the latter is expected to be described, as the spin is increased: first by a single phonon excitation, then by a multi-phonon state, and finally by a semiclassical configuration with non-zero vorticity. A quantitative description might be possible using ideas analogous to the one discussed in this part of the thesis for the scaling dimension of charged scalar operators.

Scattering processes involving a critical number of W, Z and Higgs bosons in the Standard Model (SM), which defy perturbation theory, may occur in the next generation of colliders [234]. Therefore, it might be of phenomenological relevance to revisit the issue of multi-particle production in massive quantum field theories. Perhaps, the development of some of the ideas which we discussed might prove useful in this direction as well.

---

[6] Some correlators of these kind have been computed in [232, 233], where however the authors focused only on the limt $\lambda\to 0$ with $\lambda n^2=$ fixed, corresponding to the small λn limit discussed in sec. 7.2.1.

Appendix Part V

A Appendices to Part I

A.1 Dimensionless coefficients in the model of two complex doublets

Here we provide the precise value of the dimensionless coefficients in eq.s (1.42), (1.43), (1.44), (1.45) and (1.46). We give them to leading order in the small chemical potential expansion, but for $\gamma^{(\pi_\mu)}$ which we give exactly. We write them in terms of the following dimensionless ratios

$$x = \frac{v_1}{v_2}\,, \qquad y = \frac{\mu_1}{\mu_2}\,, \qquad w = \frac{\lambda_{12}}{\lambda_2}\,, \qquad z = \frac{\lambda_1}{\lambda_2}\,. \tag{A.1}$$

The list follows:

$$\gamma^{(\pi)}_{1/2} = \frac{8xy\sqrt{z}\left(z - w^2\right)}{z\left(x^2 z + y^2\right) - w\left(x^2 y^2 z + z\right) \mp \sqrt{g_1(x,y,w,z)}}\,, \tag{A.2}$$

$$\gamma^{(r)}_{1} = \frac{z\left(1 - wx^2 - w + x^2 z\right) - \sqrt{g_2(x,w,z)}}{2x^2 z\left(z - w^2\right)}\,, \tag{A.3}$$

$$\gamma^{(r)}_{2} = \frac{z\left(1 - wx^2 - w + x^2 z\right) + \sqrt{g_2(x,w,z)}}{2\left(z - w^2\right)}\,, \tag{A.4}$$

$$\gamma^{(\pi_\mu)} = (1+y)\,\frac{\left\{\lambda_2 v_2^2\left[\left(x^2+1\right)z - w\left(x^2 z + 1\right)\right] + 2\mu_2^2\left[y^2 + z - w\left(y^2+1\right)\right]\right\}}{2\left\{\lambda_2 v_2^2\left[z + yw - x^2 z(w+y)\right] + 2\mu_2^2\left[z - y\left(yw - w + y^2\right)\right]\right\}}\,, \tag{A.5}$$

$$\gamma^{(\tilde{\pi}_\mu)} = \frac{z\left[1 - (1+w)x^2\right] + w}{z\left[1 + (1-w)x^2\right] - w}\,, \tag{A.6}$$

$$\gamma^{(\psi)}_{0} = \sqrt{\frac{z\left[1 + (1-w)x^2\right] - w}{2x\left(z - w^2\right)}}\,, \tag{A.7}$$

$$\gamma^{(\psi)}_{1} = \frac{z\left[1 - x^2(w+y)\right] + wy}{(1+y)\left\{z\left[1 + x^2(1-w)\right] - w\right\}}\,. \tag{A.8}$$

Here we defined the following functions:

$$\begin{aligned} g_1(x,y,w,z) =& \, 4w^3y^2z\left(wx^2-1\right)+2x^2z^3\left[w\left(x^2y^2-1\right)-y^2\right]+x^4z^4 \\ &+z^2\left[y^4-4w^3x^4y^2+\left(wx^2y^2+w\right)^2+w\left(2y^2-2x^2y^4\right)\right]\,, \qquad \text{(A.9)} \\ g_2(x,w,z) =& \, 4w^3z\left(wx^2-1\right)+z^2\left[1-4w^3x^4+w^2\left(1+x^2\right)^2+2w\left(1-x^2\right)\right] \\ &+2x^2z^3\left[w\left(x^2-1\right)-1\right]+x^4z^4\,. \qquad \text{(A.10)} \end{aligned}$$

A.2 Details on amplitudes in the triplet model

A.2.1 Coefficients of the gapped Goldstone annihilation

The coefficients in (2.4) are given by

$$\begin{aligned} \alpha &= \frac{2\left(5\mu^2-3m^2-\sqrt{4\mu^4+\left(\mu^2-m^2\right)^2}\right)}{2\mu^2+\sqrt{4\mu^4+\left(\mu^2-m^2\right)^2}}\,, \\ \beta &= \frac{-8\,\mu^2\left(\mu^2-m^2\right)^2}{29\mu^6-m^2\mu^4+3m^4\mu^2-m^6+\left(13\mu^4+2m^2\mu^2+m^4\right)\sqrt{4\mu^4+\left(\mu^2-m^2\right)^2}}\,. \end{aligned}$$

Those in (2.5) are

$$\begin{aligned} \gamma =& \frac{\lambda^2\mu^3\left[\frac{\sqrt{5\mu^4+m^4-2m^2\mu^2}+m^2}{5\mu^4+m^4-2m^2\mu^2}\right]^{1/2}}{15\pi\left(\mu^2-m^2\right)^6}\times \\ &\times\left[2085\mu^{10}-49m^{10}+441m^8\mu^2-1762m^6\mu^4+3842m^4\mu^6-4429m^2\mu^8+\right. \\ &\left.-\left(935\mu^8+55m^8-432m^6\mu^2+1314m^4\mu^4-1808\mu^6m^2\right)\sqrt{5\mu^4+m^4-2m^2\mu^2}\right]\,, \\ \delta =& \frac{-2\lambda^2\mu^2\left(\mu^2-m^2\right)^2\left(2\mu+\frac{4\mu^3}{\sqrt{5\mu^4+m^4-2m^2\mu^2}}\right)\left(\sqrt{5\mu^4+m^4-2m^2\mu^2}+m^2\right)^{5/2}}{15\pi\left[29\mu^6+m^6+3\mu^2m^4-m^2\mu^4+\left(13\mu^4+m^4+2m^2\mu^2\right)\sqrt{5\mu^4+m^4-2\mu^2m^2}\right]^2}\,. \end{aligned}$$

A.2.2 Gapped Goldstone decay

In the linear triplet model discussed in the main text, the accidental discrete $\mathbb{Z}_2$ symmetry forbids the decay of the gapped Goldstone. However, in more general theories the gapped Goldstone can decay into arbitrary lighter states. Here we provide a simple example of such a modification of the Lagrangian (1.24). The resulting decay rate vanishes with the velocity of the gapped Goldstone, in agreement with the general discussion of section 2.1.

To induce a decay channel for θ, we need to break explicitly the $\mathbb{Z}_2$ symmetry of the Lagrangian (1.24). In order to do that, we couple the $O(3)$ triplet $\boldsymbol{\Phi}$ to a complex $U(2)$ doublet Ψ. We hence add the following term to the linear triplet model Lagrangian:

$$\delta\mathcal{L} = |\partial\Psi|^2 - m_\Psi^2 |\Psi|^2 - \frac{\lambda_\Psi}{4} |\Psi|^4 - g \left(\Psi^\dagger \frac{\boldsymbol{\sigma}}{2}\Psi\right) \cdot \boldsymbol{\Phi} - \frac{\gamma}{4} |\Psi|^2 \boldsymbol{\Phi}^2 . \tag{A.11}$$

Here $\boldsymbol{\sigma} = (\sigma_1, \sigma_2, \sigma_3)$ are the Pauli matrices. Adding this term to (1.24), the resulting Lagrangian is the most general renormalizable theory of a doublet and a triplet preserving a global $SU(2) \times U(1)$ symmetry. Crucially, the coupling g breaks the discrete $\mathbb{Z}_2$ symmetry which prevented θ from decaying. All parameters are positive. When not specified otherwise, all parameters with the same coupling and mass dimensions are assumed to be of the same order [68].

We expand around the vev (1.25) for the triplet with $\Psi = 0$, which is a minimum for

$$\gamma \geq 2\frac{g}{\phi_0} + \frac{\mu^2 - 4m_\Psi^2}{\phi_0^2} . \tag{A.12}$$

This leaves the $U(1)$ acting as $\Psi \mapsto e^{i\alpha}\Psi$ unbroken. In this case the fluctuations for $\boldsymbol{\Phi}$ are parametrized as before (see eq. (1.26)) while Ψ can be written as

$$\Psi = e^{-i(\mu t + \psi(x)/\phi_0)\frac{\sigma_3}{2}} \begin{pmatrix} \Psi_1(x) \\ \Psi_2(x) \end{pmatrix} , \qquad \Psi_1,\ \Psi_2\ \in \mathbb{C}. \tag{A.13}$$

Notice that we explicitly factored out a time dependent rotation, which makes explicit that unbroken time translations correspond to $H + \mu Q_3$. To find the spectrum, consider the quadratic contribution from $\delta\mathcal{L}$:

$$\begin{aligned} \delta\mathcal{L}^{(2)} = {} & |\partial\Psi_1|^2 + |\partial\Psi_2|^2 + \frac{1}{2} i\mu \left(\Psi_1^*\dot{\Psi}_1 - \Psi_2^*\dot{\Psi}_2 - \text{c.c.}\right) - \frac{g}{2}\phi_0 \left(\Psi_1^*\Psi_2 + \text{c.c.}\right) \\ & - \left[m_\Psi^2 + \frac{\gamma}{4\lambda} m^2 + (\gamma/\lambda - 1)\,\mu^2/4\right] \left(|\Psi_1|^2 + |\Psi_2|^2\right) . \end{aligned} \tag{A.14}$$

The fields Ψ_1 and Ψ_2 interpolate four quasi-particles: $\{|\Psi_+(\boldsymbol{k})\rangle , |\Psi_-(\boldsymbol{k})\rangle , |\bar{\Psi}_+(\boldsymbol{k})\rangle, |\bar{\Psi}_-(\boldsymbol{k})\rangle\}$. Under the unbroken $U(1)$, $|\Psi_\pm(\boldsymbol{k})\rangle$ have positive charge while $|\bar{\Psi}_\pm(\boldsymbol{k})\rangle$ have negative charge. As a consequence of the symmetry $\Psi_1 \leftrightarrow \Psi_2^*$ of the quadratic Lagrangian, oppositely charged modes have dispersion relations equal in pair, given by:

$$\omega_\pm^2(k) = \bar{\omega}_\pm^2(k) = \frac{\mu^2}{4} + m_\Psi^2 + \frac{\gamma}{4}\phi_0^2 + k^2 \pm \sqrt{\frac{\gamma\mu^2}{4}\phi_0^2 + \frac{g^2}{4}\phi_0^2 + \mu^2 m_\Psi^2 + k^2\mu^2} . \tag{A.15}$$

Here $\omega_+(k) = \bar{\omega}_+(k)$ is the dispersion relation of $|\Psi_+(\boldsymbol{k})\rangle$ and $|\bar{\Psi}_+(\boldsymbol{k})\rangle$, while $\omega_-(k) = \bar{\omega}_-(k)$ is the dispersion relation of $|\Psi_-(\boldsymbol{k})\rangle$ and $|\bar{\Psi}_-(\boldsymbol{k})\rangle$. Notice furhter that, because of the aforementioned symmetry of the quadratic Lagrangian, the wavefunctions of the fields on the states $\{|\Psi_-(\boldsymbol{k})\rangle\,,|\bar\Psi_-(\boldsymbol{k})\rangle\}$ satisfy

$$\langle 0|\Psi_{1/2}(0)|\Psi_-(\boldsymbol{k})\rangle = e^{i\alpha}\,\langle 0|\Psi^*_{2/1}(0)|\bar\Psi_-(\boldsymbol{k})\rangle\;, \qquad \alpha\in\mathbb{R} \tag{A.16}$$

where $e^{i\alpha}$ is an unphysical phase factor which depends upon the precise definition of the states $|\Psi_-(\boldsymbol{k})\rangle$ and $|\bar\Psi_-(\boldsymbol{k})\rangle$. We will use this relation in the following.

The gapped Goldstone couples linearly to the complex $U(2)$ doublet through the $\mathbb{Z}_2$ breaking coupling g:

$$-g\left(\Psi^\dagger\frac{\boldsymbol{\sigma}}{2}\Psi\right)\cdot\boldsymbol{\Phi}\supset\frac{g}{2}\theta\left(|\Psi_2|^2-|\Psi_1|^2\right)\;, \tag{A.17}$$

To induce a decay for θ, we need the gap of the modes $\{|\Psi_-(\boldsymbol{k})\rangle\,,|\bar\Psi_-(\boldsymbol{k})\rangle\}$ to be less than half of the gapped Goldstone mass: $\omega_-(0)=\bar\omega_-(0)\leq\mu/2$. This happens for[1]

$$m_\Psi^2+\frac{\gamma}{4}\phi_0^2-\sqrt{\frac{\gamma\mu^2}{4}\phi_0^2+\frac{g^2}{4}\phi_0^2+\mu^2m_\Psi^2}\leq 0\,. \tag{A.18}$$

Under this condition, the following decay channel exists for θ

$$\theta(\boldsymbol{p})\to\Psi_-(\boldsymbol{k}_1)+\bar\Psi_-(\boldsymbol{k}_2)\,. \tag{A.19}$$

It is easy to compute the associated matrix element induced by the vertex (A.17); we do not report the details of the calculation. Notice however that the relation (A.16) implies that the decay amplitude vanishes when the final states have the same momenta. Consequently, a gapped Goldstone at rest cannot decay, as expected. Noticing that $|\boldsymbol{k}_1|$ is generically of order $\mathcal{O}(\mu)$, to linear order in the velocity the matrix element reads

$$i\mathcal{M}=iC\frac{\boldsymbol{p}\cdot\boldsymbol{k}_1}{|\boldsymbol{k}_1|}+\mathcal{O}\left(\boldsymbol{p}^2/\mu,(\boldsymbol{p}\cdot\boldsymbol{k}_1)^2/\mu^3\right), \tag{A.20}$$

where C is

$$\begin{aligned}C=&\frac{g^2\mu\phi_0/2}{2\mu^2\left(\sqrt{g^2\phi_0^2+\mu^4}+\mu^2\right)+g^2\phi_0^2}\\&\times\sqrt{\frac{\left(2\sqrt{g^2\phi_0^2+\mu^4}+2\mu^2-\gamma\phi_0^2-4m_\Psi^2\right)}{3\mu^2+2\sqrt{g^2\phi_0^2+\mu^4}-2\sqrt{2\mu^2\left(\sqrt{g^2\phi_0^2+\mu^4}+\mu^2\right)+g^2\phi_0^2}}}\,.\end{aligned} \tag{A.21}$$

In the limit where μ is much bigger than all other mass parameters this expression simplifies to

---

[1] The conditions (A.12) and (A.18) are compatible, as it can be seen in the limit where μ is much bigger than all other mass parameters where they reduce to $\lambda\leq\gamma\leq4\lambda$.

$$C = \frac{g^2\sqrt{4\lambda-\gamma}}{8\lambda\mu^2} + \mathcal{O}\left(\mu^{-4}\right) . \tag{A.22}$$

The total decay rate finally takes the following simple form

$$\Gamma = c\frac{\boldsymbol{p}^2}{\mu} = \left[\frac{g^4(4\lambda-\gamma)^{3/2}}{1536\pi\lambda^{5/2}\mu^4} + \mathcal{O}\left(\mu^{-6}\right)\right]\frac{\boldsymbol{p}^2}{\mu} , \tag{A.23}$$

where c is a dimensionless constant which we wrote in the $\mu \to \infty$ limit for illustration in the right hand side.

A.3 Spacetime coset construction for the $SU(2)$ superfluid

In this section we review the standard coset construction in presence of broken spacetime symmetries. Our goal is to show how to recover the Lagrangian in eq. (2.13) from this approach. Furthermore, this construction provides a useful bookkeeping tool to build higher derivative terms in our action, which we do in appendix A.4.1.

Consider a relativistic system with an internal $SU(2)$ symmetry, whose charge Q_3 is at finite density. The ground state $|\mu\rangle$ of such a system minimizes the modified Hamiltonian $\bar{H} = H + \mu Q_3$ [33], and it can be chosen to satisfy[2]

$$\bar{H}\,|\mu\rangle = (H + \mu Q_3)\,|\mu\rangle = 0\,. \tag{A.24}$$

If Q_3 is spontaneously broken so is H, the generator of time translations. The generators of boosts, J_{0i}, and the other internal generators, Q_1 and Q_2, are broken too. The symmetry breaking pattern is then

$$\begin{aligned}
&\text{unbroken} = \begin{cases} \bar{H} = H + \mu Q_3 & \text{time translations}\,, \\ \bar{P}_i = P_i & \text{space translations}\,, \\ J_{ij} & \text{rotations}\,, \end{cases} \\
&\text{broken} = \begin{cases} J_{0i} & \text{boosts}\,, \\ Q_3, Q_1, Q_2 & \text{internal symmetries}\,. \end{cases}
\end{aligned} \tag{A.25}$$

Therefore we have a theory with a symmetry group, G, given by the product of Poincaré and the internal $SU(2)$, which is spontaneously broken down to the semidirect product of the modified translations, generated by $\bar{P}_\mu = \{\bar{H}, \bar{\boldsymbol{P}}\}$, and rotations. We denote the unbroken group with G'. Following the standard CCWZ procedure, the coset G/G' can be parametrized as

---

[2] In general, the ground state will satisfy $\bar{H}|\mu\rangle = \lambda|\mu\rangle$, with minimum λ. In the absence of gravity, one can always add a cosmological constant term to the Hamiltonian to set $\lambda = 0$, with no physical consequences [33].

$$\Omega = e^{i\bar{P}_\mu x^\mu} e^{i\eta^i J_{0i}} e^{i\pi_3 Q_3} e^{i\alpha \frac{Q_+}{2} + i\alpha^* \frac{Q_-}{2}} \,. \tag{A.26}$$

The way to construct an action which is invariant under the full symmetry group is to consider the Maurer-Cartan form, $\Omega^{-1}d\Omega$, and expand it in the basis of broken and unbroken generators. Its general expression reads

$$\Omega^{-1}\partial_\mu\Omega = i{e_\mu}^a \left(\bar{P}_a + \nabla_a\eta^i J_{0i} + \nabla_a\pi_3 Q_3 + \nabla_a\alpha \frac{Q_+}{2} + \nabla_a\alpha^* \frac{Q_-}{2} + \frac{1}{2}\omega_a^{ij} J_{ij} \right) . \tag{A.27}$$

Here ${e_\mu}^a$ transforms as a spacetime vielbein [64, 235], and we introduced latin indices $a, b = 0, 1, 2, 3$ and $i, j = 1, 2, 3$ to distinguish within the vielbein indices, as in the familiar geometrical case. The coefficients of the broken generators, $\nabla_a\eta^i$, $\nabla_a\pi_3$ and $\nabla_a\alpha$, are the covariant derivatives of the Goldstones. They have the property that, under the action of any element of the full group, they transform as a linear representation of the *unbroken* subgroup. Finally, ω_a^{ij} transforms as a spin connection [77], which can be used to build higher covariant derivatives of the Goldstone fields:

$$\nabla_a^H = {e_a}^\mu \partial_\mu + \frac{i}{2}\omega_a^{ij} J_{ij} \,. \tag{A.28}$$

The previous derivative can also act on additional matter fields that transform in some linear representation of the unbroken group G'. The most general Lagrangian for the Goldstones, which is invariant under nonlinearly realized symmetry G is then given by

$$\mathcal{L}_{\text{eff}} = F(\nabla_a\Psi, \nabla_a^H \nabla_b \Psi, \dots) \,, \tag{A.29}$$

where we have collectively represented the Goldstone fields as Ψ. Here F is any function that depends on combinations of its arguments that are manifestly invariant under the unbroken group.[3]

For the case at hand, let us define ${(e^{-i\eta^i J_{0i}})^a}_\mu = {(\Lambda^{-1})^a}_\mu = {\Lambda_\mu}^a$ and $\chi = \mu t + \pi_3$ [35]. The quantities defined in (A.27) then read

$$\begin{gathered} {e_\mu}^a = {\Lambda_\mu}^a \,, \qquad \nabla_a\eta^i = -{\Lambda^\mu}_a (\Lambda^{-1}\partial_\mu\Lambda)^{0i} \,, \qquad \omega_a^{ij} = -{\Lambda^\mu}_a (\Lambda^{-1}\partial_\mu\Lambda)^{ij} \,, \\ \nabla_a\pi_3 = {\Lambda^\mu}_a D_\mu\chi - \mu\delta_a^0 \,, \qquad \nabla_a\alpha = {\Lambda^\mu}_a D_\mu\alpha \,, \end{gathered} \tag{A.30}$$

where $D_\mu\alpha$ and $D_\mu\chi$ are the covariant derivatives for a Lorentz invariant EFT of completely broken $SU(2)$ symmetry in (2.10).

It often happens that, in presence of broken spacetime symmetries, some of the Goldstones can be algebraically eliminated in favor of the others. This is done imposing the so-called inverse Higgs constraints [80]. In this case, we can eliminate the Goldstones associated to the boost generators by imposing[4]

---

[3] In this case, this just means that space indices $i, j, \dots$ should be contracted in a rotationally invariant way.

$$\nabla_i \pi_3 = 0 \qquad \Longrightarrow \qquad \frac{\eta^i}{\eta}\tanh\eta = -\frac{D_i\chi}{D_0\chi} = -\frac{\partial_i \pi_3}{\mu} + \dots\,. \tag{A.31}$$

Crucially, thanks to the transformation properties of the covariant derivative, this constraint is compatible with all the symmetries. Consequently it is always *possible* to impose it. The physical reason is that, when the system breaks spacetime symmetries, the same physical fluctuation can be described as the action of different generators. In this case, a small fluctuation generated by a boost could be obtained from the action of Q_3 as well [39, 63], making the field η_i redundant.

Once the condition (A.31) has been imposed, all the remaining invariants are expressed in terms of $D_\mu\chi$ and $D_\mu\alpha$ only—i.e. the covariant derivatives of the simpler completely broken $SU(2)$ theory. Without making further calculations, we know that the most general $SU(2)$ and Lorentz invariant Lagrangian written in terms of these objects is given by eq. (2.13).

We can also see this explicitly by writing the invariants obtained combining (A.30) and (A.28). To this aim, it is convenient to notice that eq. (A.31) implies

$$\Lambda_\mu^{\ 0} = \frac{D_\mu\chi}{\sqrt{D_\mu\chi D^\mu\chi}} \equiv n_\mu\,, \qquad \Lambda_\mu^{\ i}\Lambda_\nu^{\ i} = -\eta_{\mu\nu} + n_\mu n_\nu \equiv P_{\mu\nu}\,. \tag{A.32}$$

Here we have conveniently defined a unit four-vector $n_\mu \simeq \delta_\mu^0 + \dots$ in the direction of the superfluid velocity and a projector $P_{\mu\nu}$ orthogonal to it. Using these quantities, the leading order invariants take the form:

$$\begin{aligned} \nabla_0\pi_3 &= n^\mu D_\mu\chi - \mu\,, & \nabla_0\alpha &= n^\mu D_\mu\alpha\,,\\ \nabla_i\alpha\nabla_i\alpha^* &= D_\mu\alpha P^{\mu\nu} D_\nu\alpha^*\,, & \nabla_i\alpha\nabla_i\alpha &= D_\mu\alpha P^{\mu\nu} D_\nu\alpha\,. \end{aligned} \tag{A.33}$$

The first three expressions here agree with eq. (2.31) when written in terms of the fields

---

[4] We use that, in our convention, the boost matrix can be written as [64]

$$\Lambda^0{}_0 = \gamma \quad \Lambda^0{}_i = \gamma\beta_i \quad \Lambda^i{}_0 = \gamma\beta^i \quad \Lambda^i{}_j = \delta^i{}_j + (\gamma-1)\frac{\beta^i\beta_j}{\beta^2}\,,$$

with the velocity related to the Goldstone by $\beta_i = \frac{\eta_i}{\eta}\tanh\eta$ and $\gamma^2 = \frac{1}{1-\beta^2}$.

in (2.9) using (2.26). Higher order invariants are similarly obtained, for instance:

$$\begin{aligned}
&\nabla_i \eta^i = \partial_\mu n^\mu \ , \\
&\nabla_0^H \nabla_0 \pi_3 = n^\mu \partial_\mu (n^\rho D_\rho \chi) \ , \\
&\nabla_i \alpha^* \nabla_0^H \nabla_i \alpha = -D_\mu \alpha^* P^{\mu\sigma} n^\rho \partial_\rho (P_{\sigma\nu} D^\nu \alpha) \ , \\
&\nabla_j \eta^i \nabla_j \eta^i = -P^{\mu\nu} \partial_\mu n^\rho \partial_\nu n_\rho \ , \\
&\nabla_0 \eta^i \nabla_0 \eta^i = -(n^\mu \partial_\mu n^\rho) \eta_{\rho\sigma} (n^\nu \partial_\nu n^\sigma) \ , \\
&(\nabla_j \nabla_i \alpha^*)(\nabla_j \nabla_i \alpha) = -P^{\rho\sigma} \partial_\sigma \left(P^{\mu\nu} D_\nu \alpha^* \right) \partial_\rho \left(P_{\mu\lambda} D^\lambda \alpha \right) \ .
\end{aligned} \tag{A.34}$$

We checked up to fourth order in derivatives that all invariants obtained combining (A.30) and (A.28) can be written contracting in a Lorentz invariant way ∂_μ, $D_\mu \chi$ and $D_\mu \alpha$, as in eq. (2.13).

A.3.1 The inverse Higgs constraint in the NREFT

Within the spacetime coset construction presented in the previous section, there exists also the possibility of imposing an extra Inverse-Higgs constraint of the form[5] $\nabla_0 \alpha_1 = \mathrm{Re}[\nabla_0 \alpha] \simeq \dot{\alpha}_1 + \mu \alpha_2 = 0$, which eliminates one of the two real components of $\alpha = \alpha_1 + i\alpha_2$. Here we discuss the interpretation of this constraint within the NREFT.

In section 2.2.3 we showed that the NREFT describes two modes, corresponding to the gapless and the gapped Goldstones. In particular, the complex field $\pi = e^{i\chi}\alpha$ interpolates a single degree of freedom, as typical of a nonrelativistic field. However, there exists an analogous description in terms of a real field. To see this, let us rewrite the quadratic action (2.33) to leading order in derivatives in terms of the real fields α_1 and α_2, with all time derivatives acting on the first and discarding total derivatives. One gets

$$\mathcal{L} \supset -c^{(1)} \mu^3 \left[\alpha_2 \dot{\alpha}_1 + \mu \frac{\alpha_1^2 + \alpha_2^2}{2} \right] - c_3^{(2)} \mu^2 \left[(\boldsymbol{\nabla} \alpha_1)^2 + (\boldsymbol{\nabla} \alpha_2)^2 \right] . \tag{A.35}$$

Since there is no time derivative acting on it, α_2 is an auxiliary field, which can be integrated out on its equation of motion. This gives

$$0 = \dot{\alpha}_1 + \mu \alpha_2 + \mathcal{O}\left(\boldsymbol{\nabla}^2 / \mu \right) \simeq \nabla_0 \alpha_1 + \mathcal{O}\left(\boldsymbol{\nabla}^2 / \mu \right) \ . \tag{A.36}$$

We hence recovered the inverse Higgs constraint[6] $\nabla_0 \alpha_1 = 0$. Since we integrated out an auxiliary field, the number of degrees of freedom and all the other properties of the action are unaffected. Indeed, plugging back the solution of (A.36) in the Lagrangian we find that α_1 becomes a real field with gap μ. In practice, in a nonrelativistic setting it is easier to work with a complex field, which makes particle number conservation manifest. We did not explore the possibility of building the action using only two real fields from start, e.g. working with an $SU(2)/U(1)$ coset $\Omega = e^{i\chi Q_3} e^{i\alpha_1 Q_1}$ around the background $\chi = \mu t$, $\alpha_1 = 0$.

---

[5] Of course, one could alternatively consider $\nabla_0 \alpha_2 = \mathrm{Im}[\nabla_0 \alpha] \simeq \dot{\alpha}_2 - \mu \alpha_1 = 0$.

[6] With the current parametrization the inverse Higgs constraint corresponds to the equations of motion of α_2 only to linear order in the fields. However, the equality is true at all nonlinear orders in the Euler parametrization of the Goldstones: $\Omega = e^{i\chi Q_3} e^{i\alpha_1 Q_1} e^{i\alpha_2 Q_2}$. In other words, there is a field redefinition for which to impose the inverse Higgs constraint corresponds to integrate out α_2 to leading orders in derivatives but to all orders in the field expansion.

This inverse Higgs constraint was also discussed in [39]. However, the authors there focused on a different setup, where the derivative expansion is controlled by a scale $\Lambda \gg \mu$. In that case, imposing or not the inverse Higgs constraint leads to physically distinct theories, providing a different interpretation for it. Let us briefly review these previous findings, in order to compare them with our construction.

When the inverse Higgs constraint is imposed, the construction of [39] leads to an EFT describing the gapless and the gapped Goldstone, with cutoff $\Lambda \gg \mu$. In this setup, the symmetry is partially restored in the limit $\mu \to 0$, if this limit exists.[7] As discussed in the introduction of section 2.2, this EFT applies for instance in the linear sigma model for $m^2 < 0$ when the radial mode is much heavier than the gapped Goldstone, i.e. when $|m^2| \gg \mu^2$.

The situation is different when the inverse Higgs constraint is not imposed. Indeed, when $\Lambda \gg \mu$, the leading order quadratic Lagrangian for the complex field α is second order in time derivatives, implying that α interpolates two modes rather than one as in our nonrelativistic construction. One mode is the gapped Goldstone, while the mass of the other depends on the coefficients of the Lagrangian and it is formally proportional to μ. This mode is usually referred to as a gapped Goldstone with unfixed gap [39]. In this case, if the limit $\mu \to 0$ is smooth, the theory breaks the internal $SU(2)$ symmetry completely also at zero chemical potential; the extra mode then provides the third Goldstone required by the relativistic Goldstone theorem.

In general, the presence of the unfixed gap mode and its properties are not fixed by the symmetry breaking pattern only and depend on the structure of the theory at scales $\Lambda \gg \mu$. Thus, for the purposes of our construction in which the chemical potential itself provides the cutoff, this mode, if present in the UV theory, behaves rather like any other matter field and is thus integrated out in our setup. The nonrelativistic EFT, similarly to the standard relativistic CCWZ construction, provides the minimal structure required to realize nonlinearly all the symmetries; in practice, this means that the NREFT describes only the gapless and the gapped Goldstones. Of course, while we expect this simple setup to correspond to the most generic situation, specific theories may contain additional light degrees of freedom, e.g. gauge fields, which can be added to the EFT in the standard way.

---

[7] This is not obvious even for $\Lambda \gg \mu$, since the cutoff itself might depend on the chemical potential, e.g. as $\Lambda^2 \sim f\mu$ with $f \gg \mu$; see [39] for details.

A.4 NREFT details

A.4.1 NREFT action to $\mathcal{O}(\partial^4)$

In this section, we write the Lagrangian for the non-relativistic effective theory to fourth order in derivatives. To this aim, we find a convenient bookkeeping tool to use the invariants written using the spacetime coset construction presented in appendix A.3. We assume parity invariance for simplicity.

The effective nonrelativistic Lagrangian is written using the prescription presented in section 2.2.1, namely imposing the $U(1)$ invariance $\pi \to e^{i\xi}\pi$ and using the nonrelativistic derivative (2.28). In the notation of the previous section, the latter amounts at building higher derivative terms using, rather than the one given in eq. (A.28), the following covariant derivative:

$$e_a{}^{\mu}\hat{\partial}_\mu + \frac{i}{2}\omega_a^{ij}J_{ij} = \nabla_a^H + i\left(\mu + \nabla_0\pi_3\right)\delta_a^0[Q_3,\cdot\,]\,. \tag{A.37}$$

In practice, we performed calculations using the following

$$\hat{\nabla}_a^H \equiv \nabla_a^H + i\,\mu\delta_a^0[Q_3,\cdot\,]\,. \tag{A.38}$$

This definition corresponds to a slightly different form of the nonrelativistic derivative, obtained multiplying $D_\mu\chi$ in eq. (2.28) by $\mu/\sqrt{D_\mu\chi D^\mu\chi}$. As commented below that equation, this redefinition does not affect the key property (2.29), which is needed in order to have a well-structured derivative expansion.

We can now proceed to formally write the Lagrangian in a ∇/μ expansion as

$$\mathcal{L} = \mathcal{L}_\nabla^{(1)} + \mathcal{L}_\nabla^{(2)} + \mathcal{L}_\nabla^{(3)} + \mathcal{L}_\nabla^{(4)} + \dots\,, \tag{A.39}$$

where $\mathcal{L}_\nabla^{(i)}$ contains all terms which are of order i in terms of ∇'s covariant derivatives. We have:

$$\mathcal{L}_\nabla^{(1)}/\mu^3 = c^{(1)}\nabla_0\pi_3\,, \tag{A.40}$$

$$\mathcal{L}_\nabla^{(2)}/\mu^2 = c_1^{(2)}(\nabla_0\pi_3)^2 + c_2^{(2)}|\nabla_0\alpha|^2 - c_3^{(2)}|\nabla_i\alpha|^2\,, \tag{A.41}$$

$$\begin{aligned}\mathcal{L}_\nabla^{(3)}/\mu &= c_1^{(3)}(\nabla_0\pi_3)^3 + c_2^{(3)}\nabla_0\pi_3|\nabla_0\alpha|^2 + c_3^{(3)}\nabla_0\pi_3|\nabla_i\alpha|^2 \\ &+ c_4^{(3)}\left[i\nabla_0\alpha^*\hat{\nabla}_0^H\left(\nabla_0\alpha\right) + c.c.\right] + c_5^{(3)}\left[i\nabla_i\alpha^*\hat{\nabla}_0^H\left(\nabla_i\alpha\right) + c.c.\right] \\ &+ c_6^{(3)}\left[\nabla_i\alpha^*\hat{\nabla}_i^H\left(\nabla_0\alpha\right) + c.c.\right] + c_7^{(3)}\left[i\nabla_i\alpha^*\hat{\nabla}_i^H\left(\nabla_0\alpha\right) + c.c.\right] \\ &+ c_8^{(3)}\nabla_0\pi_3(\mu\nabla_i\eta^i)\,.\end{aligned} \tag{A.42}$$

We can expand these in terms of the $SU(2)$ covariant derivatives in eq. (2.10) and their derivatives. Doing so and defining $D_\mu\pi_3 \equiv D_\mu\chi - \mu\delta_\mu^0$, we can rewrite the Lagrangian in a standard derivative expansion:

$$\mathcal{L}^{(1)}/\mu^3 = c^{(1)} D_0\pi_3\,, \tag{A.43}$$

$$\mathcal{L}^{(2)}/\mu^2 = c_1^{(2)}(D_0\pi_3)^2 - \frac{c^{(1)}}{2}(D_i\pi_3)^2 + c_2^{(2)}|D_0\alpha|^2 - c_3^{(2)}|D_i\alpha|^2\,, \tag{A.44}$$

$$\begin{aligned}
\mathcal{L}^{(3)}/\mu = {} & \left[\frac{c^{(1)}}{2} - c_1^{(2)}\right] D_0\pi_3(D_i\pi_3)^2 + \left[c_2^{(2)} - c_3^{(2)} - c_7^{(3)}\right](D_0\alpha^* D_i\alpha D_i\pi_3 + \text{c.c.}) \\
& + c_6^{(3)}\left(iD_i\alpha^* D_i\pi_3 D_0\alpha + \text{c.c.}\right) + c_1^{(3)}(D_0\pi_3)^3 + c_2^{(3)} D_0\pi_3|D_0\alpha|^2 + c_3^{(3)} D_0\pi_3|D_i\alpha|^2 \\
& + c_4^{(3)}\left[iD_0\alpha^*(\partial_0 + i\mu)\left(D_0\alpha\right) + \text{c.c.}\right] + c_5^{(3)}\left[iD_i\alpha^*(\partial_0 + i\mu)\left(D_i\alpha\right) + \text{c.c.}\right] \\
& + c_6^{(3)}\left[D_i\alpha^*\partial_i\left(D_0\alpha\right) + \text{c.c.}\right] + c_7^{(3)}\left[iD_i\alpha^*\partial_i\left(D_0\alpha\right) + \text{c.c.}\right] - c_8^{(3)} D_0\pi_3(\partial_i D_i\pi_3)\,.
\end{aligned} \tag{A.45}$$

Notice that terms with $D_i\pi_3$ always appear from the expansion of the ∇ covariant derivatives in connection with lower derivative ones.
The fourth order in derivatives can be constructed similarly. Here we just report the fourth order term in (A.39)

$$\begin{aligned}
\mathcal{L}_{\nabla}^{(4)} = {} & c_1^{(4)}(\nabla_0\pi_3)^4 + c_2^{(4)}(\nabla_0\pi_3)^2|\nabla_0\alpha|^2 + c_3^{(4)}(\nabla_0\pi_3)^2|\nabla_i\alpha|^2 \\
& + c_4^{(4)}|\nabla_0\alpha|^4 + c_5^{(4)}|\nabla_0\alpha|^2|\nabla_i\alpha|^2 + c_6^{(4)}\left[(\nabla_i\alpha)^2(\nabla_0\alpha^*)^2 + \text{c.c.}\right] \\
& + c_7^{(4)}\left[i(\nabla_i\alpha)^2(\nabla_0\alpha^*)^2 + \text{c.c.}\right] + c_8^{(4)}|\nabla_i\alpha|^2|\nabla_j\alpha|^2 \\
& + c_9^{(4)}(\nabla_i\alpha)^2(\nabla_j\alpha^*)^2 + c_{10}^{(4)}(\hat{\nabla}_0^H\nabla_0\pi_3)|\nabla_0\alpha|^2 + c_{11}^{(4)}(\nabla_0\pi_3)\left[i\nabla_0\alpha^*\hat{\nabla}_0^H\nabla_0\alpha + \text{c.c.}\right] \\
& + c_{12}^{(4)}(\hat{\nabla}_0^H\nabla_0\pi_3)|\nabla_i\alpha|^2 + c_{13}^{(4)}(\nabla_0\pi_3)\left[i\nabla_i\alpha^*\hat{\nabla}_0^H\nabla_i\alpha + \text{c.c.}\right] \\
& + c_{14}^{(4)}(\hat{\nabla}_i^H\nabla_0\pi_3)\left[\nabla_i\alpha^*\nabla_0\alpha + \text{c.c.}\right] + c_{15}^{(4)}(\hat{\nabla}_i^H\nabla_0\pi_3)\left[i\nabla_i\alpha^*\nabla_0\alpha + \text{c.c.}\right] \\
& + c_{16}^{(4)}\nabla_0\pi_3\left[\hat{\nabla}_i^H(\nabla_0\alpha)\nabla_i\alpha^* + \text{c.c.}\right] + c_{17}^{(4)}\nabla_0\pi_3\left[i\hat{\nabla}_i^H(\nabla_0\alpha)\nabla_i\alpha^* + \text{c.c.}\right] \\
& + c_{18}^{(4)}(\hat{\nabla}_0^H\nabla_0\pi_3)^2 + c_{19}^{(4)}(\hat{\nabla}_i^H\nabla_0\pi_3)^2 + c_{20}^{(4)}|\hat{\nabla}_0^H\nabla_0\alpha|^2 \\
& + c_{21}^{(4)}|\hat{\nabla}_i^H\nabla_0\alpha|^2 + c_{22}^{(4)}\left[\hat{\nabla}_i^H\nabla_i\alpha^*\hat{\nabla}_0^H\nabla_0\alpha + \text{c.c.}\right] + c_{23}^{(4)}\left[i\hat{\nabla}_i^H\nabla_i\alpha^*\hat{\nabla}_0^H\nabla_0\alpha + \text{c.c.}\right] \\
& + c_{24}^{(4)}|\hat{\nabla}_0^H\nabla_i\alpha|^2 + c_{25}^{(4)}|\hat{\nabla}_i^H\nabla_i\alpha|^2 + c_{26}^{(4)}|\hat{\nabla}_j^H\nabla_i\alpha|^2 + c_{27}^{(4)}\mu^2\nabla_0\eta^i\nabla_0\eta^i + c_{28}^{(4)}\mu^2(\nabla_i\eta^i)^2 \\
& + c_{29}^{(4)}\mu^2\nabla_i\eta^j\nabla_i\eta^j + c_{30}^{(4)}\mu\nabla_i\eta^i\hat{\nabla}_0^H\nabla_0\pi_3 + c_{31}^{(4)}\mu(\nabla_0\pi_3)^2\nabla_i\eta^i + c_{32}^{(4)}\mu|\nabla_0\alpha|^2\nabla_i\eta^i \\
& + c_{33}^{(4)}\mu|\nabla_i\alpha|^2\nabla_j\eta^j + c_{34}^{(4)}\mu\nabla_i\eta^j\left[\nabla_i\alpha\nabla_j\alpha^* + \text{c.c.}\right] + c_{35}^{(4)}\mu\nabla_i\eta^j\left[i\nabla_i\alpha\nabla_j\alpha^* + \text{c.c.}\right] \\
& + c_{36}^{(4)}\mu\nabla_0\eta^i\left[\nabla_i\alpha\nabla_0\alpha^* + \text{c.c.}\right] + c_{37}^{(4)}\mu\nabla_0\eta^i\left[i\nabla_i\alpha\nabla_0\alpha^* + \text{c.c.}\right]\,.
\end{aligned} \tag{A.46}$$

We did not write terms which effectively contribute at fifth order in derivatives after expanding the ∇'s as before.

A.4.2 Feynman rules to leading order in ∂/μ

Before introducing a process dependent velocity power counting, it might be useful to consider a power counting in ∂/μ. Here we list the Feynman rules to leading order within this counting. We use the field parametrization (2.9). Black solid lines correspond to gapped Goldstones with four-momentum $p = (\mu + \epsilon, \boldsymbol{p})$, while dashes stand for gapless Goldstones, whose four-momentum is denoted as $k = (\omega, \boldsymbol{k})$.

- $|\pi|^2\pi_3$ **vertex:**

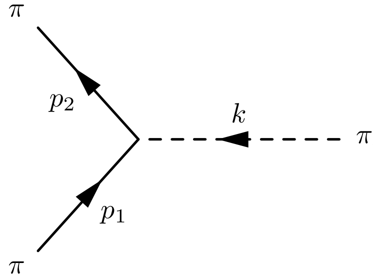

$$= \frac{1}{2\mu^2 c_s \sqrt{c^{(1)}}} \left[(\epsilon_1 + \epsilon_2)\omega_k - c_s^2(\boldsymbol{p}_1 + \boldsymbol{p}_1) \cdot \boldsymbol{k}\right]. \tag{A.47}$$

- π_3^3 **vertex:**

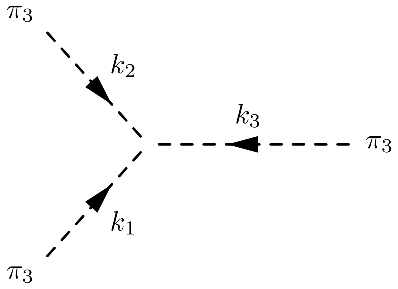

$$\begin{aligned} &= \frac{-c_s(c_s^2 - 1)}{\mu^2\sqrt{c^{(1)}}} \left(\omega_1 \boldsymbol{k}_2 \cdot \boldsymbol{k}_3 + \omega_2 \boldsymbol{k}_3 \cdot \boldsymbol{k}_1 + \omega_3 \boldsymbol{k}_1 \cdot \boldsymbol{k}_2\right) \\ &\quad - \frac{6c_1^{(3)} c_s^3}{\mu^2 \left[c^{(1)}\right]^{3/2}} \omega_1\omega_2\omega_3. \end{aligned} \tag{A.48}$$

- $|\pi|^4$ **vertex:**

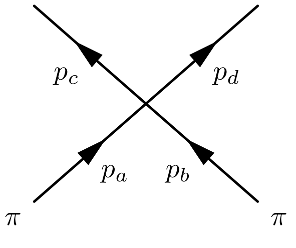

$$\begin{aligned} &= -\frac{i}{6c^{(1)}\mu^3}(\epsilon_a + \epsilon_b + \epsilon_c + \epsilon_d) \\ &\quad + i\frac{2c_m - 3}{12c^{(1)}\mu^4}\left[2\boldsymbol{p}_a \cdot \boldsymbol{p}_b + 2\boldsymbol{p}_c \cdot \boldsymbol{p}_d + (\boldsymbol{p}_a + \boldsymbol{p}_b) \cdot (\boldsymbol{p}_c + \boldsymbol{p}_d)\right] \\ &\quad + \frac{i\left(3c^{(1)} - 8c_2^{(2)}c_s^2\right)}{12\left[c^{(1)}\right]^2 c_s^2\mu^4}\left[2\epsilon_a\epsilon_b + 2\epsilon_c\epsilon_d + (\epsilon_a + \epsilon_b)(\epsilon_c + \epsilon_d)\right]. \end{aligned} \tag{A.49}$$

- **$|\pi|^2\pi_3^2$ vertex:**

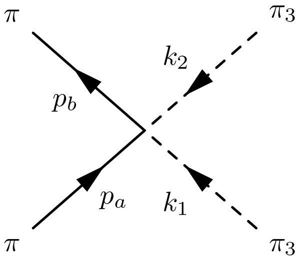

$$\begin{aligned}&= i\frac{c_s^2-1}{2c^{(1)}\mu^4}\left[(\boldsymbol{k}_1\cdot\boldsymbol{k}_2)(\epsilon_a+\epsilon_b)+(\omega_1\boldsymbol{k}_2+\omega_2\boldsymbol{k}_1)\cdot(\boldsymbol{p}_a+\boldsymbol{p}_b)\right]\\ &\quad + i\frac{3c_1^{(3)}c_s^2}{\left[c^{(1)}\right]^2\mu^4}(\epsilon_a+\epsilon_b)\omega_1\omega_2.\end{aligned} \tag{A.50}$$

- **π_3^4 vertex:**

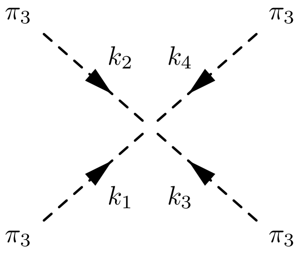

$$\begin{aligned}&= i\frac{2c_s^2\left(c^{(1)}-c^{(1)}c_s^2-3c_1^{(3)}c_s^2\right)}{\left[c^{(1)}\right]^2\mu^4}\left[\omega_1\omega_2\boldsymbol{k}_3\cdot\boldsymbol{k}_4+\text{permutations}\right]\\ &\quad + i\frac{c_s^2(1-c_s^2)}{c^{(1)}\mu^4}\left[(\boldsymbol{k}_1\cdot\boldsymbol{k}_2)(\boldsymbol{k}_3\cdot\boldsymbol{k}_4)+\text{permutations}\right]\\ &\quad + i\frac{24c_1^{(4)}c_s^4}{\left[c^{(1)}\right]^2\mu^4}\omega_1\omega_2\omega_3\omega_4.\end{aligned} \tag{A.51}$$

A.4.3 Coefficients of $\pi\pi$ scattering to order $\mathcal{O}(v^4)$

The coefficients of the π dispersion relation (2.44) to subleading order is given by

$$c_m^{(2)} = 16\frac{c^{(1)}\left[c^{(1)}\left(c_{25}^{(4)}+c_{26}^{(4)}\right)+4c_3^{(2)}\left(c_5^{(3)}+c_7^{(3)}\right)\right]+4c_2^{(2)}\left(c_3^{(2)}\right)^2}{(c^{(1)})^3}\,. \tag{A.52}$$

The b_i's in (2.43) are

$$b_1 = -\frac{c^{(1)}c_m^2(c_s-1)-4c_s\left[c_m(c_2^{(2)}+c_3^{(3)})+2c_5^{(3)}(c_m-1)-2c_7^{(3)}\right]}{8c_s}\,, \tag{A.53}$$

$$\begin{aligned}b_2 &= \frac{1}{4}\left(c_m\left[4c_3^{(3)}-3c^{(1)}c_m+4c_2^{(2)}(2c_m+3)\right]-2c^{(1)}c_m^{(2)}\right)\\ &\quad + 6c_5^{(3)}(c_m-1)+c_7^{(3)}(4c_m-6)\,,\end{aligned} \tag{A.54}$$

$$b_3 = -4\left(2c_5^{(3)}-4c_9^{(4)}+2c_{26}^{(4)}+c_{29}^{(4)}+2c_{35}^{(4)}\right)\,, \tag{A.55}$$

$$b_4 = 2\left(2c_5^{(3)}+4c_8^{(4)}+2c_{26}^{(4)}+c_{29}^{(4)}+2c_{35}^{(4)}\right)\,. \tag{A.56}$$

A.4.4 Loops in dimensional regularization

We can regulate the NREFT at quantum level with a hard space cutoff $\Lambda \lesssim \mu$. However powers of the cutoff spoil power counting [92] and complicate computations. It is hence preferable to use a mass independent regulator, such as dimensional regularization. In a nonrelativistic EFT, if this is done naïvely retaining the standard form of propagators, loops involving both massive and massless particle become dominated by hard momenta $|\boldsymbol{k}| \sim \mu$, which should not enter in the NREFT computations (c.f [83] within the context of NRQCD). This is due to the fact that the gapped dispersion relation $k_0 \sim \boldsymbol{k}^2/\mu$ and the gapless one $k_0 \sim |\boldsymbol{k}|$ can be simultaneously satisfied only for $|\boldsymbol{k}| \sim \mu$. A consistent formulation of NREFTs with both heavy and light fields was devised by Griesshammer [86, 87], as a development of the method of regions [236], and then further refined with the formulation of vNRQCD [88, 237]. In this appendix we review the key points and their application to our EFT, focusing on the power counting of diagrams. We refer to the original works for details.

The first step is to identify a consistent set of modes, according to their scaling with velocity v. According to standard NRQCD results [83,84], these are given by soft, potential and ultrasoft modes listed in (2.40). Fields are split accordingly as explained in section 2.2.5. To enforce power counting, one should retain in the denominators of propagators only momenta with the same scaling in v, expanding the subleading ones in an infinite series. In particular, they will be given by [8]

$$
\begin{aligned}
&G^{\mathrm{s}}_{\pi_3}(\omega, \boldsymbol{k}) = G^{\mathrm{us}}_{\pi_3}(\omega, \boldsymbol{k}) = \frac{i}{\omega^2 - c_s^2 \boldsymbol{k}^2}\,, \qquad G^{\mathrm{p}}_{\pi_3}(\omega, \boldsymbol{k}) = \frac{-i}{c_s^2 \boldsymbol{k}^2} \sum_{n=0}^{\infty} \left(\frac{\omega^2}{c_s^2 \boldsymbol{k}^2} \right)^n\,, \\
&G^{\mathrm{s}}_{\pi}(\epsilon, \boldsymbol{p}) = G^{\mathrm{us}}_{\pi}(\epsilon, \boldsymbol{p}) = \frac{i}{\epsilon} \sum_{n=0}^{\infty} \left(\frac{c_m \boldsymbol{p}^2}{2\mu\epsilon} \right)^n\,, \qquad G^{\mathrm{p}}_{\pi}(\epsilon, \boldsymbol{p}) = \frac{i}{\epsilon - \frac{c_m \boldsymbol{p}^2}{2\mu}}\,,
\end{aligned}
\tag{A.57}
$$

where we omitted the $+i0$ prescription. For instance, the soft $G^s_\pi(\epsilon, \boldsymbol{p})$ propagator and the potential $G^p_\pi(\epsilon, \boldsymbol{p})$ propagators are not equivalent beyond tree-level, since infinite sums and integration do not commute in dimensional regularization [236]. After the splitting into different modes is performed, and hence all propagators are properly expanded, all loops in dimensional regularization are made only of light scales. This also makes it straightforward to power count diagrams in v.

---

[8] Naively performing these expansions inside loops sometimes leads to unphysical *pinch* singularities, e.g. in box integrals. However, a careful analysis shows that these arise from an over-counting of the contribution of a certain region and that loops are indeed regular after the proper *zero-bin* subtractions have been performed [237]. These subtleties do not affect the simple power counting rules that we discuss here, hence we will neglect them in what follows.

As a simple illustration, consider the one-loop correction to the $G^p_\pi(\epsilon,\boldsymbol{p})$ propagator [9]

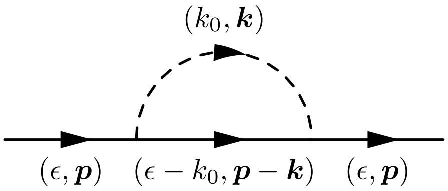
$(k_0,\boldsymbol{k})$
$(\epsilon,\boldsymbol{p})$
$(\epsilon-k_0,\boldsymbol{p}-\boldsymbol{k})$
$(\epsilon,\boldsymbol{p})$

$$= \frac{i}{4\mu^4 c^{(1)} c_s^2} I_{\pi\pi}, \tag{A.58}$$

where in a hard cutoff approach we would write the loop integral as

$$I_{\pi\pi} = -i\int \frac{d^4k}{(2\pi)^4}\frac{\left[(2\epsilon-k_0)k_0 - c_s^2(2\boldsymbol{p}-\boldsymbol{k})\cdot\boldsymbol{k}\right]^2}{\left[(\epsilon-k_0)-c_m\frac{(\boldsymbol{p}-\boldsymbol{k})^2}{2\mu}+i0\right]\left(k_0^2-c_s^2\boldsymbol{k}^2+i0\right)}. \tag{A.59}$$

To perform this computation in $d=4-\varepsilon$ dimensions, we need to take into account four different integrals, depending on the specific modes running in the loop:

1. $\pi_3^s : (k_0,\boldsymbol{k}) \sim (\mu v, \mu v)$ and $\pi^s : (\epsilon-k_0,\boldsymbol{p}-\boldsymbol{k}) \sim (\mu v,\mu v)$;
2. $\pi_3^p : (k_0,\boldsymbol{k}) \sim (\mu v^2, \mu v)$ and $\pi^p : (\epsilon-k_0,\boldsymbol{p}-\boldsymbol{k}) \sim (\mu v^2,\mu v)$;
3. $\pi_3^p : (k_0,\boldsymbol{k}) \sim (\mu v^2, \mu v)$ and $\pi^{us} : (\epsilon-k_0,\boldsymbol{p}-\boldsymbol{k}) \sim (\mu v^2,\mu v^2)$;
4. $\pi_3^{us} : (k_0,\boldsymbol{k}) \sim (\mu v^2, \mu v^2)$ and $\pi^p : (\epsilon-k_0,\boldsymbol{p}-\boldsymbol{k}) \sim (\mu v^2,\mu v)$.

Consider for illustration the $\pi^s - \pi_3^s$ loop. We have $k_0 \gg \epsilon, (\boldsymbol{p}-\boldsymbol{k})^2/\mu$, hence we should enforce this expanding the gapped NGB propagator in an infinite series

$$\frac{i}{(\epsilon-k_0)-c_m\frac{(\boldsymbol{p}-\boldsymbol{k})^2}{2\mu}+i0} \quad\longrightarrow\quad \frac{i}{-k_0+i0}\left[1+\frac{\epsilon-c_m\frac{(\boldsymbol{p}-\boldsymbol{k})^2}{2\mu}}{k_0-i0}+\dots\right] \tag{A.60}$$

The integral here is:

$$I^{(1)}_{\pi\pi} = -iM^\varepsilon\int \frac{d^dk}{(2\pi)^d}\frac{[\dots]^2}{(-k_0+i0)\left(k_0^2-c_s^2\boldsymbol{k}^2+i0\right)}\left[1+\frac{\epsilon-c_m\frac{(\boldsymbol{p}-\boldsymbol{k})^2}{2\mu}}{k_0-i0}+\dots\right]=0, \tag{A.61}$$

where M is the sliding scale. The loop vanishes since, after performing the k^0 integration with the residue's theorem, the integral can be divided in a sum of contributions proportional to $\int d^{d-1}\boldsymbol{k}/|\mathbf{k}|^n = 0$. Similarly one can check that the $\pi_3^p - \pi^p$ and $\pi_3^p - \pi^s$ loops vanish[10] to all orders in v.

The only nontrivial contribution comes from the ultrasoft $\pi_3^{us} - \pi^p$ loop. We have $\boldsymbol{k}^2 \ll \boldsymbol{p}^2$, implying that the π^p propagator should be expanded as

---

[9] We neglected a scaleless tadpole vanishing in dimensional regularization.

[10] Within this approach this is a common fact, for instance one can prove that π^{us} never contributes inside loops [86].

$$\frac{i}{(\epsilon-k_0)-c_m\frac{(\boldsymbol{p}-\boldsymbol{k})^2}{2\mu}+i0}\quad\longrightarrow\quad\frac{i}{(\epsilon-k_0)-c_m\frac{\boldsymbol{p}^2}{2\mu}+i0}\left(1-\frac{c_m\frac{\boldsymbol{p}\cdot\boldsymbol{k}}{\mu}}{\epsilon-k_0-c_m\frac{\boldsymbol{p}^2}{2\mu}}+\dots\right). \tag{A.62}$$

We can power count the measure according to the momentum of the softest propagator, which sets the size of the *integration box.* In this case thus $d^4k\sim\mu^4v^8$. The leading contribution is

$$I^{(4)}_{\pi\pi}=M^{\varepsilon}\int\frac{d^dk}{(2\pi)^d}\frac{-ic_s^4(\boldsymbol{p}\cdot\boldsymbol{k})^2}{\left[(\epsilon-k_0)-c_m\frac{\boldsymbol{p}^2}{2\mu}+i0\right]\left(k_0^2-c_s^2\boldsymbol{k}^2+i0\right)}\sim\mathcal{O}\left(v^8\right). \tag{A.63}$$

The integral is simple to perform, giving an $\mathcal{O}(v^8)$ contribution:

$$I^{(4)}_{\pi\pi}=\frac{\boldsymbol{p}^2\left(\epsilon-c_m\frac{\boldsymbol{p}^2}{2\mu}\right)^3}{3\pi^2c_s}\left\{\frac{1}{\varepsilon}-\log\left(\frac{\epsilon-c_m\frac{\boldsymbol{p}^2}{2\mu}+i0}{-c_sM}\right)-\frac{\gamma}{2}+\frac{4}{3}+\frac{\log\pi}{2}\right\}. \tag{A.64}$$

The divergence renormalizes the Lagrangian term $\frac{1}{\mu^5}\nabla_i\pi^*\left(i\hat{\nabla}^H_0-\frac{c_m}{2\mu}\hat{\nabla}^H_i\hat{\nabla}^H_i\right)^3\nabla_i\pi=\frac{1}{\mu^5}D^\lambda\pi^*P_{\lambda\mu}\left\{\left[in^\rho\hat{\partial}_\rho-\frac{c_m}{2\mu}\hat{\partial}_\rho\left(P^{\rho\sigma}\hat{\partial}_\sigma\right)\right]^3P^{\mu\nu}D_\nu\pi\right\}$, in the notation of app. A.3. In practice many tree-level higher derivative terms have to be taken into account at the lower orders.

In (A.64) we found a $\sim\log\left(\mu v^2/M\right)$ contribution. Indeed in general ultrasoft loops give rise to logarithms of the *ultrasoft* scale μv^2. Instead soft and potential loops lead to logarithms of the *soft* scale μv [88]. For instance, the leading loop contribution to $\pi^p_3\pi^p_3$ potential propagator comes from a soft loop and takes the form

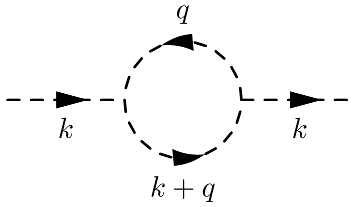

$$=\frac{i}{\mu^4c^{(1)}}\boldsymbol{k}^4k_0^2\left[-\frac{\alpha}{\varepsilon/2}+\alpha\log\left(\frac{\boldsymbol{k}^2-i0}{M^2}\right)+\beta\right]+\mathcal{O}\left(v^{10}\right). \tag{A.65}$$

Finally, one can now consistently power count loop contributions to the $\pi\pi$ elastic scattering, computed to $\mathcal{O}(v^4)$ at tree-level in sec. 2.2.5. Using the Feynman rules in A.4.2, one easily concludes that the first corrections arise only at $\mathcal{O}(v^5)$. Specifically, three kinds of loop corrections exist. First, corrections to the $G^p_{\pi_3}$ propagator in exchange diagrams of fig. 2.2, which however start at $\mathcal{O}(v^8)$ as eq. (A.65) shows. Then corrections to the $\pi^p_3|\pi^p|^2$ vertex appearing in the same kind of diagrams. For instance, the leading

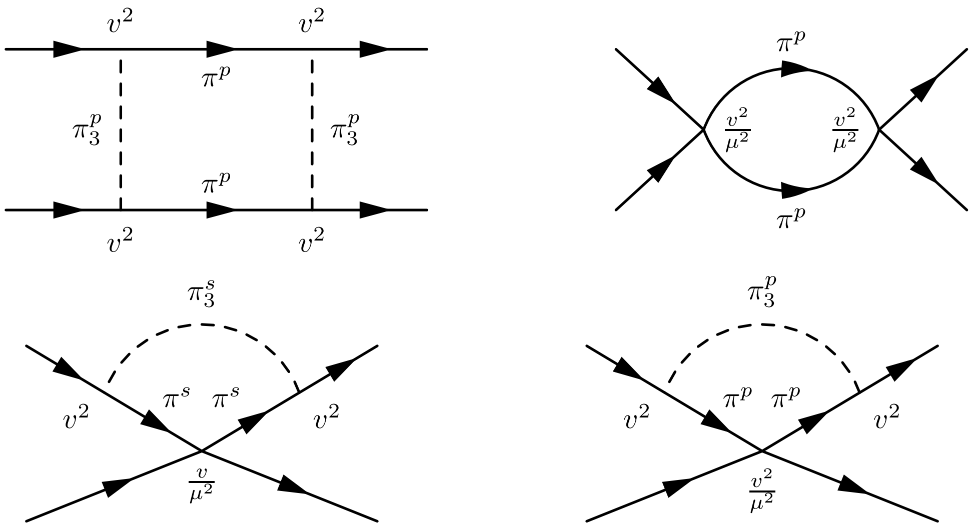

Figure A.1 – Leading loop topologies which correct the contact interaction in $\pi\pi$ scattering. The scaling of vertices and the modes in the loop are displayed.

correction in this class is given by a loop of π^p and π_3^p:

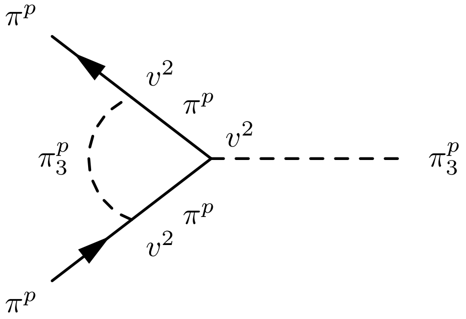

$$\sim \mu^4 v^5 \times \frac{1}{\mu^4 v^6} \times v^6 \sim v^5. \tag{A.66}$$

Here we showed explicitly the scaling of the vertices with v and we power counted the result as *measure*×*propagators*×*vertices*. Finally we have those that we can interpret as corrections to the contact vertex in fig. 2.1. The leading corrections in this class are also $\mathcal{O}(v^5)$ and are displayed in figure A.1.

We remark that this formulation of the NREFT differs in some points from the modern vNRQCD [88]. First, we did not separate explicitly the fields momenta in soft, potential and ultra-soft components in the Lagrangian, as it is customarily done in NRQCD [84]. Of course, this is possible and it might be useful in performing more refined computations, especially to account for the proper *zero-bin* subtractions [237]. Furthermore, here off-shell modes are not integrated out explicitly and the *pull-up* mechanism is not explicitly implemented [88], i.e. we do not renormalize soft and ultrasoft fields separately. These differences stem from the fact that we want to preserve the nonlinearly realized $SU(2)$ invariance in the Lagrangian, which relates the different modes of π_3 and π. In particular, this implies that all modes of a given operator have the same anomalous dimensions [87], differently than in vNRQCD. There, renormalizing them separately allows to efficiently resum logarithms of both the *soft* and *ultrasoft* scale, via the velocity Renormalization Group.[11] This is not possible within our approach, but it is only a minor drawback. Indeed, as typical for Goldstone bosons, all interactions are irrelevant, so that logarithms are always multiplied by powers of the velocity.

---

[11] For instance, in vNRQCD ultrasoft and soft fields are allowed to interact via gauge couplings evaluated at different sliding scales.

B Appendices to Part II

B.1 Basics of Conformal Field Theories

Conformal field theories (CFTs) are local[1] quantum field theories (QFTs), invariant under conformal transformations. Here we review their basic properties and introduce our conventions, referring the reader to [238–240] for further details. We will focus our discussion on $d > 2$ Euclidean space dimensions (see [241] for $d = 2$).

B.1.1 The conformal algebra and primary operators

In Euclidean signature, the conformal group in d dimensions is isomorphic to $SO(d+1,1)$. Its generators, P_μ, $J_{\mu\nu}$, K_μ and D, satisfy the following algebra

$$\begin{gathered} [J_{\mu\nu}, J_{\rho\sigma}] = -i\left(\delta_{\mu\sigma} J_{\nu\rho} + \delta_{\nu\rho} J_{\mu\sigma} - \delta_{\mu\rho} J_{\nu\sigma} - \delta_{\nu\sigma} J_{\mu\rho}\right) , \\ [P_\rho, J_{\mu\nu}] = i\delta_{\rho\nu} P_\mu - i\delta_{\rho\mu} P_\nu \,, \qquad [K_\rho, J_{\mu\nu}] = i\delta_{\rho\nu} K_\mu - i\delta_{\rho\mu} K_\nu \,, \\ [D, P_\mu] = -iP_\mu \,, \qquad [D, K_\mu] = +iK_\mu \,, \qquad [P_\mu, K_\nu] = -2i(D\delta_{\mu\nu} + J_{\mu\nu}) \,. \end{gathered} \tag{B.1}$$

P_μ and $J_{\mu\nu}$ correspond to the generators of the Poincaré group. D generates rigid scale transformations $x^\mu \to \lambda x^\mu$ with $\lambda > 0$. Finally K_μ corresponds to special conformal transformations, whose finite action is given by

$$x^\mu \longrightarrow \frac{x^\mu - b^\mu x^2}{1 - 2b\cdot x + b^2 x^2} \,. \tag{B.2}$$

P^μ and K^μ are conjugated under the the action of the inversion $IP^\mu I = K^\mu$, where I acts as $x^\mu \to x^\mu / x^2$. As a consequence, special conformal transformations map the origin to itself, as translations do with the point at infinity.

---

[1] By this we mean that the spectrum of operators of the theory includes a conserved spin-2 operator, the energy-momentum tensor.

Operators are classified in irreducible representations of the conformal group. We call *primaries* the operators which are annihilated by the action of special conformal transformations at the origin $[K^\mu, \mathcal{O}^{(\Delta)}_{\mu_1\ldots\mu_\ell}(0)] = 0$. These are labelled by their scaling dimension Δ, determining their properties under rigid rescaling $\mathcal{O}^{(\Delta)}_{\mu_1\ldots}(x) \to \lambda^\Delta \mathcal{O}^{(\Delta)}_{\mu_1\ldots}(\lambda x)$, and by the representation of the rotation group under which they transform. The action of the conformal generators on a primary operator at an arbitrary point reads:

$$\begin{aligned}
&[J_{\mu\nu}, \mathcal{O}^{(\Delta)}_{\mu_1\ldots\mu_\ell}(x)] = i(x_\mu\partial_\nu - x_\nu\partial_\mu)\mathcal{O}^{(\Delta)}_{\mu_1\ldots\mu_\ell}(x) - \rho^{(\ell)}\,[J_{\mu\nu}]^{\nu_1\ldots\nu_\ell}_{\mu_1\ldots\mu_\ell}\,\mathcal{O}^{(\Delta)}_{\nu_1\ldots\nu_\ell}(x)\,,\\
&[P_\mu, \phi(x)] = -i\partial_\mu\phi(x)\,,\\
&[D, \mathcal{O}^{(\Delta)}_{\mu_1\ldots\mu_\ell}(x)] = -i(x^\mu\partial_\mu + \Delta)\mathcal{O}^{(\Delta)}_{\mu_1\ldots\mu_\ell}(x)\,,\\
&[K_\mu, \mathcal{O}^{(\Delta)}_{\mu_1\ldots\mu_\ell}(x)] = i(2x_\mu x^\nu\partial_\nu - x^2\partial_\mu + 2\Delta x_\mu)\mathcal{O}^{(\Delta)}_{\mu_1\ldots\mu_\ell}(x)\\
&\qquad\qquad + 2x^\nu\rho^{(\ell)}\,[J_{\nu\mu}]^{\nu_1\ldots\nu_\ell}_{\mu_1\ldots\mu_\ell}\,\mathcal{O}^{(\Delta)}_{\nu_1\ldots\nu_\ell}(x)\,,
\end{aligned} \tag{B.3}$$

where $\rho^{(\ell)}\,[J_{\nu\mu}]$ stands for the appropriate representation of the $SO(d)$ generators. Operators which are not annihilated by K^μ at the origin are called *descendants* and are obtained taking an arbitrary number k of derivatives of primary operators, e.g. $\partial_{\nu_1}\ldots\partial_{\nu_k}\mathcal{O}^{(\Delta)}_{\mu_1\ldots\mu_\ell}$, and transform with scaling dimension $\Delta + k$ under rigid rescaling. Therefore, correlation functions of descendant operators are fully determined from the ones of the primaries. In the following we will restrict our attention to primary operators. For the sake of simplicity, we will only consider traceless symmetric operators.

B.1.2 Correlation functions and CFT data

Basic observables in CFTs are correlation functions of local operators. These in turn are highly constrained from conformal symmetry. Let us briefly review the basic results.

The two-point function of two primary operators vanishes unless they have the same spin and scaling dimension; its general form is determined by the conformal symmetry up to a constant c_{ab}:

$$\langle \mathcal{O}^{(\Delta_a)}_{\mu_1\ldots\mu_{\ell_a}}(x)\mathcal{O}^{(\Delta_b)}_{\nu_1\ldots\nu_{\ell_b}}(0)\rangle = \delta_{\Delta_a\,\Delta_b}\delta_{\ell_a\,\ell_b}\frac{c_{ab}}{c_{d,\ell_a}}\,\frac{\Pi^{\rho_1\ldots\rho_{\ell_a}}_{\mu_1\ldots\mu_{\ell_a}}\,I_{\rho_1\nu_1}(x)\ldots I_{\rho_{\ell_a}\nu_{\ell_a}}(x)}{x^{2\Delta_a}}\,, \tag{B.4}$$

where

$$I_{\mu\nu}(x) = \delta_{\mu\nu} - \frac{2x_\mu x_\nu}{x^2}\,, \tag{B.5}$$

$\Pi^{\rho_1\ldots\rho_\ell}_{\mu_1\ldots\mu_\ell}$ is the projector onto the space of traceless symmetric tensors[2] and we conventionally introduced the following normalization factor

$$c_{d,\ell} = \frac{\ell!}{2^\ell\left(\frac{d-2}{2}\right)_\ell}\,, \tag{B.6}$$

---

[2] For instance, taking $\ell = 2$ it reads $\Pi^{\nu_1\nu_2}_{\mu_1\mu_2} = \frac{1}{2}\left(\delta^{\nu_1}_{\mu_1}\delta^{\nu_2}_{\mu_2} + \delta^{\nu_2}_{\mu_1}\delta^{\nu_1}_{\mu_2}\right) - \frac{1}{d}\delta_{\mu_1\mu_2}\delta^{\nu_1\nu_2}$ [205].

where $(x)_y = \Gamma(x+y)/\Gamma(x)$ is the Pochhammer symbol. This factor will be convenient when mapping the theory to the cylinder. We can always work in a basis of operators such that $c_{ab} = \delta_{ab}$, with the exception of conserved operators; these cannot be rescaled without changing the conventions of the group algebra which they generate. Therefore, the normalization coefficients of two-point functions of conserved operators are physical constants, usually referred as *central charges* [242], whose value depends on the specific theory under consideration.

The structure of three-point functions is similarly constrained by conformal symmetry, that fixes their form up to a finite number of constants, called *OPE coefficients* for reasons which will become clear later. For instance, the three-point function of two scalars and a spin ℓ primary reads

$$\langle \mathcal{O}^{(\Delta_c)}_{\mu_1\ldots\mu_\ell}(x_3)\mathcal{O}^{(\Delta_b)}(x_2)\mathcal{O}^{(\Delta_a)}(x_1)\rangle = \frac{\lambda_{abc}}{c_{d,\ell}}\frac{\Pi^{\nu_1\ldots\nu_\ell}_{\mu_1\ldots\mu_\ell} Z_{\nu_1}(x_1,x_2;x_3)\ldots Z_{\nu_\ell}(x_1,x_2;x_3)}{x_{12}^{\Delta_a+\Delta_b-\Delta_c}x_{23}^{\Delta_b+\Delta_c-\Delta_a}x_{31}^{\Delta_c+\Delta_a-\Delta_b}}\,, \tag{B.7}$$

where λ_{abc} is a theory-dependent OPE coefficient, $x_{ij} = x_i - x_j$ and

$$Z^\mu(x_1,x_2;x_3) = \sqrt{\frac{x_{13}^2 x_{23}^2}{x_{12}^2}}\left(\frac{x_{23}^\mu}{x_{23}^2} - \frac{x_{13}^\mu}{x_{13}^2}\right)\,. \tag{B.8}$$

More general three-point functions may depend upon a larger number of theory-dependent coefficients. This is for instance the case for the correlator of a scalar, a vector J^μ and a spin $\ell \geq 1$ operator, which depends upon two OPE coefficients [205]:

$$\langle \mathcal{O}^{(\Delta_\ell)}_{\mu_1\ldots\mu_\ell}(x_3)J_\mu(x_2)\mathcal{O}^{(\Delta_s)}(x_1)\rangle = c_{d,\ell}^{-1}\frac{\lambda^{(1)}_{sJ\ell}T_{\mu\mu_1\ldots\mu_\ell} + \lambda^{(2)}_{sJ\ell}\left[T_{\mu\mu_1\ldots\mu_\ell} + \tilde{T}_{\mu\mu_1\ldots\mu_\ell}\right]}{x_{12}^{\Delta_s+\Delta_J-\Delta_\ell}x_{23}^{\Delta_J+\Delta_\ell-\Delta_s}x_{31}^{\Delta_s+\Delta_\ell-\Delta_J}}\,, \tag{B.9}$$

where we defined the following tensor structures

$$T_{\mu\mu_1\ldots\mu_\ell} = Z_\mu(x_3,x_1;x_2)\,\Pi^{\nu_1\ldots\nu_\ell}_{\mu_1\ldots\mu_\ell}Z_{\nu_1}(x_1,x_2;x_3)\ldots Z_{\nu_\ell}(x_1,x_2;x_3)\,, \tag{B.10}$$

$$\tilde{T}_{\mu\mu_1\ldots\mu_\ell} = I_{\mu\nu_1}(x_{23})\Pi^{\nu_1\ldots\nu_\ell}_{\mu_1\ldots\mu_\ell}Z_{\nu_2}(x_1,x_2;x_3)\ldots Z_{\nu_\ell}(x_1,x_2;x_3)\,. \tag{B.11}$$

We conventionally associated specific tensor structures to the three-point function coefficients in eq. (B.9) for future convenience. When the vector J_μ is conserved, corresponding to $\Delta_J = d-1$, the constraint $\partial^\mu J_\mu = 0$ implies a linear relation between the OPE coefficients, which allows to express one in terms of the other:

$$\lambda^{(2)}_{sJ\ell} = \frac{(\Delta_s - \Delta_\ell)}{\ell + d - 2}\lambda^{(1)}_{sJ\ell}\,. \tag{B.12}$$

Similarly, the three-point function of a conserved current and two scalars vanishes unless these two have the same scaling dimension and opposite charge under the corresponding generator. Calling Q such charge and assuming the scalar operator to be normalized as explained above, the Ward identity fix it to be

$$\langle \mathcal{O}_{-Q}(x_3) J_\mu(x_2) \mathcal{O}_Q(x_1)\rangle = \frac{Q}{\Omega_{d-1}} \frac{Z_\mu(x_1, x_3; x_2)}{x_{12}^{d-1} x_{23}^{d-1} x_{31}^{2\Delta_{\mathcal{O}}-d+1}} \,, \tag{B.13}$$

where $\Omega_{d-1} = \frac{2\pi^{d/2}}{\Gamma(d/2)}$ is the volume of the $d-1$-dimensional sphere.

The structure of higher-point functions is less constrained. This is because there exist scalar combinations of four or more points, called cross ratios, that are conformal invariant and can be used to construct invariant functions. For instance, the correlator of four identical scalars $\mathcal{O}$ depends on a function of two variables:

$$\langle \mathcal{O}(x_4)\mathcal{O}(x_3)\mathcal{O}(x_2)\mathcal{O}(x_1)\rangle = \frac{f(u,v)}{x_{12}^{2\Delta_{\mathcal{O}}} x_{34}^{2\Delta_{\mathcal{O}}}} \,, \tag{B.14}$$

where the cross-ratios read

$$u = \frac{x_{12}^2 x_{34}^2}{x_{13}^2 x_{24}^2} \,, \qquad v = \frac{x_{14}^2 x_{23}^2}{x_{13}^2 x_{24}^2} \,. \tag{B.15}$$

Nonetheless, it turns out that correlators of $n \geq 4$ operators do not contain additional information with respect to two- and three-point functions. This is thanks to the, arguably, most important property of conformal theories: the Operator Product Expansion (OPE). This is a standard tool in QFT, which allows to replace the product of two operators $\mathcal{O}_a(x_1)\mathcal{O}_b(x_2)$ for $|x_1 - x_2|$ sufficiently small by an infinite sum of local operators $\sum_c C_{ab}^c(x_1 - x_2)\mathcal{O}_c(x_2)$. However, while in generic QFTs this series is believed to be asymptotic [28], in CFTs the OPE has a finite radius of convergence [127], as it could have been expected by scale invariance [243]. Therefore, it can be used to systematically reduce n-point functions to a sum of two-point functions, whose general form is fixed by symmetry. Furthermore, the structure of the OPE is fully determined by conformal invariance and by the coefficients appearing in the three-point functions. For instance, the OPE of two identical scalar primaries takes the form

$$\mathcal{O}(x)\mathcal{O}(0) = \sum_{primaries} \lambda_{\mathcal{O}\mathcal{O}\phi} C_{\Delta_{\mathcal{O}},\Delta}^{\mu_1\ldots\mu_\ell}(x^\mu, \partial_\mu)\phi^{(\Delta)}_{\mu_1\ldots\mu_\ell}(0) \,, \tag{B.16}$$

where $\lambda_{\mathcal{O}\mathcal{O}\phi}$ is the coefficient appearing in eq. (B.7) and the functional $C_{\Delta_{\mathcal{O}},\Delta}^{\mu_1\ldots\mu_\ell}(x^\mu, \partial_\mu)$ depends only on the scaling dimension and spin of the operator $\phi^{(\Delta)}_{\mu_1\ldots\mu_\ell}(0)$. Using this formula in eq. (B.7) and expanding for $x_1 \to x_2$, its form can be found as a series in $|x|$; the leading term is given by:

$$C_{\Delta_{\mathcal{O}},\Delta}^{\mu_1\ldots\mu_\ell}(x^\mu, \partial_\mu) = \frac{x^{\mu_1}\ldots x^{\mu_\ell}}{x^{2\Delta_{\mathcal{O}}-\Delta+\ell}} + \ldots \,. \tag{B.17}$$

Therefore, the full *dynamical* information specifying the CFT is encoded in the spectrum of primaries and in the OPE coefficients specifying their three-point correlators. This set of number goes under the name of *CFT data* and determines all local correlation functions of the theory. [3] For instance, using the OPE in eq. (B.14) between the operators at x_1 and x_2 and those at x_3 and x_4, we can express the function $f(u,v)$ as

$$f(u,v) = \sum_{primaries} \lambda^2_{\mathcal{O}\mathcal{O}\phi} g_{\Delta,\ell}(u,v)\,, \tag{B.18}$$

where $g_{\Delta,\ell}(u,v)$ is called a *conformal block* and it is fully specified by conformal invariance in terms of the scaling dimension Δ and spin ℓ of the *exchanged* primary operator ϕ. Explcit expressions for $g_{\Delta,\ell}(u,v)$ in even dimensions, as well as a series representation holding for every d, were derived in [244, 245]. Similar conformal block decompositions exist for arbitrary conformal four-point functions. We shall discuss in detail a case of interest for this thesis in sec. B.4.2.

It should be stressed that most possible set of scaling dimensions, spins and OPE coefficients do not specify a consistent theory, as the CFT data should satisfy a number of non-trivial constraints. The most stringent ones arise from imposing the associativity of the OPE in four-point functions. The study of these constraints is called the *conformal bootstrap* [25, 97]. Recently, unitarity and OPE associativity were used to obtain detailed predictions on the spectrum of specific theories [98, 116, 117], as well as to unveil some universal properties of general CFTs [169, 170, 173, 246].

B.1.3 The map to the cylinder and the state-operator correspondence

In all local unitary CFTs, the energy momentum tensor is traceless [105, 241]:

$$T^\mu_\mu = 0\,. \tag{B.19}$$

This further implies that the theory is invariant under Weyl rescaling of the metric. In particular, this allows to map our theory from the plane to the cylinder $\mathbb{R}^d \to \mathbb{R}\times S^{d-1}$. To see this, let us parametrize $\mathbb{R}^d$ by polar coordinates (r,Ω_{d-1}), where Ω_{d-1} collectively denotes the coordinates on S^{d-1}, and $\mathbb{R}\times S^{d-1}$ by (τ,Ω_{d-1}); the mapping is then simply given by $r = Re^{\tau/R}$ with R the sphere radius. The cylinder metric is then related to the flat one by a Weyl rescaling

$$ds^2_{cyl} = d\tau^2 + R^2 d\Omega^2_{d-1} = \frac{R^2}{r^2} ds^2_{flat}\,. \tag{B.20}$$

---

[3] Besides the correlation functions of local operators one can consider extended operators, such as conformal defects, as well as the correlation functions on various non-trivial manifolds. In order to be able to compute these quantities, in general, one has to extend the notion of CFT data.

Weyl invariance[4] ensures that the flat space theory is equivalent to the one on the cylinder. In particular, a correlation function of n primary operators with scaling dimensions $\Delta_1, \ldots, \Delta_n$ and spin $\ell_1, \ldots \ell_n$, with all spacetime indices lowered, is related to the flat space one by [239]

$$\langle \mathcal{O}_n(x_n) \ldots \mathcal{O}_1(x_1) \rangle_{\text{cyl}} = |x_n|^{\Delta_n - \ell_n} \ldots |x_1|^{\Delta_1 - \ell_1} \langle \mathcal{O}_n(x_n) \ldots \mathcal{O}_1(x_1) \rangle_{\text{flat}} \,. \tag{B.21}$$

When considering the mapping in eq. (B.21), dilations on the plane are mapped to time translations on the cylinder. Correspondingly, the spectrum of operator dimensions on the plane, the eigenvalues of the dilation charge D, is mapped to the energy spectrum on the cylinder, the eigenvalues of H_{cyl}. To illustrate this point, consider a two-point function of a (real) scalar primary $\mathcal{O}$:

$$\langle \mathcal{O}(x_f) \mathcal{O}(x_i) \rangle_{cyl} = \frac{|x_f|^{\Delta} |x_i|^{\Delta}}{x_{if}^{2\Delta}} \,. \tag{B.22}$$

Now, the limit $x_i \to 0$ on the plane translates to $\tau_i \to -\infty$ on the cylinder and the above equation becomes

$$\langle \mathcal{O}(x_f) \mathcal{O}(x_i) \rangle_{\text{cyl}} \overset{\tau_i \to -\infty}{=} e^{-E_{\mathcal{O}}(\tau_f - \tau_i)} \,, \qquad E_{\mathcal{O}} = \Delta_{\mathcal{O}}/R \,. \tag{B.23}$$

More precisely one can check that the rate of approach to the above limiting result is controlled by $e^{\tau_i/R}$, so that the above equation holds with exponential precision for $|\tau_i/R| \gg 1$. By eq. (B.23) the action of $\mathcal{O}(x_i)$ at $\tau_i \to -\infty$ simply creates a state with energy $\Delta_{\mathcal{O}}/R$ and carrying all the global quantum numbers of $\mathcal{O}$. This is the operator state correspondence, which greatly illuminates many aspects of conformal field theory when viewed on the cylinder. Calling this state $|\mathcal{O}\rangle = \mathcal{O}(0)\,|0\rangle$, we can also recover states associated to descendants acting with the translation generators: $P^{\mu_1} \ldots P^{\mu_\ell}\,|\mathcal{O}\rangle$. The set composed of $|\mathcal{O}\rangle$ and all its descendants is called *conformal multiplet.*

Given a real operator $\mathcal{O}_{\mu_1 \ldots \mu_\ell}(\tau, \Omega)$ on the cylinder, the natural definition of conjugation in Euclidean signature is [239]

$$\mathcal{O}^{\dagger}_{\mu_1 \ldots \mu_\ell}(\tau, \Omega) = \hat{I}^{\nu_1}_{\mu_1} \ldots \hat{I}^{\nu_\ell}_{\mu_\ell} \mathcal{O}_{\nu_1 \ldots \nu_\ell}(-\tau, \Omega) \,, \tag{B.24}$$

where $\hat{I}^{\nu}_{\mu} = \delta^{\nu}_{\mu} - 2\delta^{0}_{\mu}\delta^{\nu}_{0}$ is the reflection in the cylinder time direction. When mapping back to the plane, this definition is equivalent to the action of the inversion operator I:

$$\mathcal{O}^{\dagger}_{\mu_1 \ldots \mu_\ell}(x^\mu) = I \mathcal{O}_{\mu_1 \ldots \mu_\ell}(x^\mu) I = x^{-\Delta_{\mathcal{O}}} I_{\mu_1 \nu_1} \ldots I_{\mu_\ell \nu_\ell} \mathcal{O}^{\nu_1 \ldots \nu_\ell}(x^\mu / x^2) \,, \tag{B.25}$$

where $I_{\mu\nu}$ is given in eq. (B.5). As a consequence $P^{\dagger}_{\mu} = I P_\mu I = K_\mu$ and $D^\dagger = IDI = -D$.

Combining unitarity and the state-operator correspondence we may derive constraints on the spectrum of operators of the theory. For instance, imposing positivity of the norm of the first descendant state $P_\mu |\mathcal{O}\rangle$ of the conformal multiplet of a scalar operator we get

---

[4] The Weyl anomaly does not affect correlation functions of local operators [239].

$$||P_\mu |\mathcal{O}\rangle||^2 = \langle \mathcal{O}|K_\mu P_\mu|\mathcal{O}\rangle = 2\Delta \langle \mathcal{O}|\mathcal{O}\rangle \geq 0 \qquad \Longrightarrow \qquad \Delta \geq 0\,. \tag{B.26}$$

Here we used the algebra (B.1) and $K_\mu |\mathcal{O}\rangle = 0$. Imposing positivity of the norm of descendant states for general conformal multiplets, one finds that the scaling dimension of a spin ℓ traceless symmetric primary operator satisfies the following *unitarity bound*:

$$\Delta \geq \begin{cases} \frac{d-2}{2} & \ell = 0 \\ d-2+\ell & \ell \geq 1\,. \end{cases} \tag{B.27}$$

The bound for scalars is saturated only by the free field, while that for $\ell \geq 1$ is saturated by conserved operators $\partial^{\mu_1}\mathcal{O}_{\mu_1\ldots\mu_\ell}(x) = 0$. Conversely, any conserved operator saturates the unitarity bound. In particular, conserved operators with $\ell = 1$ are Noether currents for internal symmetries, while the only conserved operator with $\ell = 2$ is the energy-momentum tensor. Higher spin conserved operators exist only in free theories [247, 248].

Finally, we comment on the normalization of states. First, notice that from eq. (B.4), different conformal multiplets are orthogonal. Furthermore, from the definition (B.24) we obtain the normalization of spin ℓ primary states as [240]:

$$\langle \mathcal{O}_{\nu_1\ldots\nu_\ell}|\mathcal{O}^{\mu_1\ldots\mu_\ell}\rangle = \lim_{\substack{x_i\to 0\\ x_f\to\infty}} \langle \mathcal{O}^\dagger_{\nu_1\ldots\nu_\ell}(x_f)\, \mathcal{O}^{\mu_1\ldots\mu_\ell}(x_i)\rangle = c_{d,\ell}^{-1}\Pi^{\mu_1\ldots\mu_\ell}_{\nu_1\ldots\nu_\ell}\,, \tag{B.28}$$

where we work in a basis such that $c_{ab} = \delta_{ab}$ in eq. (B.5). Despite the odd looking factor $c_{d,\ell}^{-1}$, the normalization (B.28) is a convenient one when considering the theory quantized on the cylinder. Indeed, it is often useful to decompose a spin ℓ operator as

$$\mathcal{O}_{\mu_1\ldots\mu_\ell}(x) = \sum_m T^{(\ell,m)}_{\mu_1\ldots\mu_\ell}\mathcal{O}_{(\ell,m)}(x)\,, \tag{B.29}$$

where m collectively labels the eigenvalues of the Cartan generators of $SO(d)$ and the tensors $T^{(\ell,m)}_{\mu_1\ldots\mu_\ell}$ provide the basis of traceless symmetric tensors defining the normalized hyperspherical harmonics as

$$\hat{n}^{\mu_1}\ldots\hat{n}^{\mu_\ell}T^{(\ell,m)}_{\mu_1\ldots\mu_\ell} = \sqrt{\frac{(d-2)\Omega_{d-1}}{(2\ell+d-2)}}\,Y^\ell_m(\hat{n}^\mu)\,, \qquad \hat{n}^\mu = x^\mu/|x|\,, \tag{B.30}$$

The conventional prefactor on the right-hand will be useful when considering the conformal block decomposition of four-point functions. The square root of the volume of S^{d-1}, Ω_{d-1}, ensures that for $\ell = 0$ we have $T^{(0,0)} = 1$, making the decomposition (B.29) trivial for scalars. In this basis, the normalization in eq. (B.28) simply reads:

$$\langle \mathcal{O}_{(\ell,m')}|\mathcal{O}_{(\ell,m)}\rangle = \delta_{m'\,m}\,. \tag{B.31}$$

B.2 Conformal superfluid from the coset construction

Here we provide a derivation of the conformal Abelain superfluid Lagrangian (3.9) on the cylinder, using the CCWZ technique. In order to apply the coset construction in a curved manifold, it is convenient (but not necessary) to gauge spacetime symmetries, specifying the preferred value for the metric only at the end of calculations [64]. [5] To proceed in this way, we consider the generators acting in a locally flat chart of the manifold, denoted $\{\widehat{D}, \widehat{P}^\mu, \widehat{K}^\mu, \widehat{J}_{\mu\nu}\}$. These are naturally associated with those acting on the plane considering the formal $R \to \infty$ limit on $\mathbb{R} \times S^{d-1}$:

$$D = -R\widehat{P}_0, \qquad J_{ij} = \widehat{J}_{ij}, \qquad J_{0i} = -R\widehat{P}_i, \qquad P_0 = \widehat{P}_0 + \frac{\widehat{D}}{R} + \frac{\widehat{K}_0}{2R^2},$$
$$K_0 = \frac{1}{2}\widehat{K}_0 - R\widehat{D} + R^2\widehat{P}_0, \qquad P_i = \widehat{P}_0 + \frac{\widehat{J}_{0i}}{R} - \frac{\widehat{K}_i}{2R^2}, \qquad K_i = \frac{1}{2}\widehat{K}_i + R\widehat{J}_{0i} - R^2\widehat{P}_i. \tag{B.32}$$

These expressions are derived considering the differential representations for the conformal generators in the coordinate system (τ, y_i) on the cylinder, specified by $Re^{\tau/R} = \sqrt{x_0^2 + x_i^2}$ and $y_i = x_i$ in terms of the flat space coordinates (x_0, x_i) in Euclidean signature, and then taking the limit $R \to \infty$ [35]. Notice that in this limit, quite intuitively, the translations $\widehat{P}_i$ are proportional to the rotations around x_0, while the Hamiltonian $\widehat{P}_0$ is proportional to the dilatation generator.

The symmetry breaking pattern (3.7) discussed in sec. 3.1 can now be rewritten in terms of the hatted generators in eq. (B.32). Doing so and specializing to an internal symmetry group $G = U(1)$, we get:

$$\begin{cases} \widehat{\overline{P}}_0 = \widehat{P}_0 + \mu\, Q,\ \widehat{P}_i,\ \widehat{J}_{ij} & \text{unbroken,} \\ \widehat{J}_{0i},\ \widehat{K}_\mu,\ \widehat{Q} & \text{broken.} \end{cases} \tag{B.33}$$

Following [35], we gauge all spacetime symmetries, including dilatation. This amounts at constructing the Maurer-Cartan one-form using the following covariant derivative:

$$D_\mu = \partial_\mu + i\tilde{e}^a_\mu P_a + \frac{i}{2}\omega^{ab}_\mu J_{ab} + iA_\mu D \tag{B.34}$$

where $\tilde{e}^a_\mu$, ω^{ab}_μ and A_μ are gauge connections. Indices $a, b = 0, 1, \dots$ label the gauged Poincaré generators and should not be confused with spacetime indices $\mu, \nu, \dots$ [235, 249]. Notice that, in this approach, special conformal transformations are obtained as local scale transformations. Thus we did not include them in the covariant derivative (B.34), which already cointains a gauge field associated to dilatations. Similarly, we do not need to introduce separate Goldstone fields for them in the coset representative. Thus, working from now on in Lorentzian time and dropping the hat from generators, we parametrize the coset representative as

---

[5] This approach, when the metric is treated as a dynamical field rather than a background one, produces dynamical gravitational theories [235, 249].

$$\Omega = e^{iy^a \bar{P}_a} e^{i\sigma D} e^{i\eta^i J_{0i}} e^{i\pi Q} = e^{iy^a P_a} e^{i\sigma D} e^{i\eta^i J_{0i}} e^{i\chi Q}, \qquad \chi = \mu t + \pi. \tag{B.35}$$

The first step of the construction is to consider the Maurer-Cartan (MC) one form:

$$\Omega^{-1} D_\mu \Omega = i E^a_\mu \left(\bar{P}_a + \nabla_a \sigma D + \nabla_a \pi Q + \nabla_a \eta^i J_{0i} + \frac{1}{2} \Omega^{ij}_a J_{ij} \right); \tag{B.36}$$

where

$$\begin{aligned} E^a_\mu = e^{-\sigma} e^b_\mu \Lambda_b^{\ a}\,, \qquad \nabla_a \pi = e^\sigma e^\mu_b \Lambda^b_{\ a} \partial_\mu \chi - \mu \delta^0_a\,, \qquad \nabla_a \sigma = e^\sigma e^\mu_b \Lambda^b_{\ a} \left(\partial_\mu \sigma + A_\mu\right)\,, \\ \nabla_a \eta^i = e^\sigma e^\mu_b \Lambda^b_{\ a} \left[-(\Lambda^{-1} \partial_\mu \Lambda)^{0i} + \omega^{cd}_\mu \Lambda_c^{\ 0} \Lambda_d^{\ i} \right]\,, \\ \Omega^{ij}_a = e^\sigma e^\mu_b \Lambda^b_{\ a} \left[-(\Lambda^{-1} \partial_\mu \Lambda)^{ij} + \omega^{cd}_\mu \Lambda_c^{\ i} \Lambda_d^{\ j} \right]\,. \end{aligned} \tag{B.37}$$

Here we introduced the Lorentz matrix $(e^{-i\eta^i J_{0i}})^a_{\ b} = \Lambda_b^{\ a}$. The field $e^a_\mu = \tilde{e}^a_\mu + \partial_\mu y^a - \omega^{a}_{\mu\ b} y^b + A_\mu y_a$ has the right transformation properties to be interpreted as a spacetime vielbein and similarly ω^{ab}_μ is a spin connection. The associated field strengths follow from

$$\Omega^{-1}[D_\mu, D_\nu]\Omega = i E^a_\mu E^b_\mu \left(T^c_{ab} P_c + \frac{1}{2} R^{cd}_{ab} J_{cd} + A_{ab} D \right), \tag{B.38}$$

where, calling E^μ_a the inverse of E^a_μ in eq. (B.37),

$$\begin{aligned} T^c_{ab} &= E^\mu_a E^\nu_b \left(\partial_\mu e^d_\nu - \partial_\nu e^d_\mu - \omega^{d}_{\mu\ e} e^e_\nu + \omega^{d}_{\nu\ e} e^e_\mu + A_\mu e^d_\nu - A_\nu e^d_\mu \right) \Lambda_d^{\ c} e^{-\sigma}, \\ R^{cd}_{ab} &= E^\mu_a E^\nu_b \left(\partial_\mu \omega^{gh}_\nu - \partial_\nu \omega^{gh}_\mu - \omega^{g}_{\mu\ e} \omega^{eh}_\nu + \omega^{g}_{\nu\ e} \omega^{eh}_\mu \right) \Lambda_g^{\ c} \Lambda_h^{\ d}, \\ A_{ab} &= E^\mu_a E^\nu_b (\partial_\mu A_\nu - \partial_\nu A_\mu). \end{aligned} \tag{B.39}$$

The E^a_μ in eq. (B.37) are used to construct an invariant measure as $\det E = e^{-d\sigma}$. The Lagrangian is then built considering $SO(d-1)$ invariant contractions of the covariant derivatives of the Goldstones, $\nabla_a \pi$, $\nabla_a \sigma$ and $\nabla_a \eta^i$ in eq. (B.37), and the curvature invariants in eq. (B.39). Higher derivatives of these invariants are obtained using

$$\nabla^H_a = E^\mu_a \partial_\mu + \frac{1}{2} \Omega^{ij}_a J_{ij}. \tag{B.40}$$

As we have seen concerning broken boosts in part I of this thesis, for spontaneously broken space-time the number of Goldstone modes is usually smaller than the number of broken generators [63, 77, 80, 250]. This might be interpreted either as if the missing Goldstones do not parametrize flucutations which are independent of the physical ones [39], either as if some of the Goldstone fields become massive, with a theory-dependent gap, and therefore are not visible from the low energy perspective [64]. This feaure is implemented in the coset construction via imposing covariant *inverse Higgs constraints*, that allow to express the would-be massive Goldstone fields in terms of the rest. We have already seen an example of this kind in appendix A.3, where the boost Goldstones of the superfluids were eliminated in this way.

Here we focus on the simplest possible description of the system, in which the only light modes are those whose existence is required by the symmetry. To this aim, we impose the maximal number of inverse Higgs constraints, given by

$$\nabla_a\sigma = 0\,, \qquad T^a_{bc} = 0\,, \qquad \nabla_0\pi = 0\,, \qquad \nabla_i\pi = 0\,. \tag{B.41}$$

The first two constraints are geometric in nature, and are used to eliminate the gauge field associated to dilatations and select the spin connection compatible with the modified metric $\hat{g}_{\mu\nu} = e^{-2\sigma}g_{\mu\nu}$:

$$\begin{aligned} A_\mu &= -\,\partial_\mu\sigma\,, && \text{(B.42)}\\ \omega_\mu^{ab} &= -\frac{1}{2}\Big[e^{\nu a}(\partial_\mu e^b_\nu - \partial_\nu e^b_\mu) - e^{\nu b}(\partial_\mu e^a_\nu - \partial_\nu e^a_\mu) - e_{\mu c}e^{\nu a}e^{\lambda b}(\partial_\nu e^c_\lambda - \partial_\lambda e^c_\nu)\Big] && \text{(B.43)}\\ &\quad + (e^a_\mu e^b_\nu - e^a_\nu e^b_\mu)\partial^\nu\sigma\,. \end{aligned}$$

Notice that eq. (B.42) implies $A_{ab} = 0$. The others are used to express σ and η^i in terms of the other fields:

$$\mu e^{-\sigma} = (e^{\mu a}e^\nu_a\partial_\mu\chi\partial_\nu\chi)^{1/2}\,, \qquad \frac{\eta^i}{\eta}\tanh\eta = -\frac{e^\mu_i\partial_\mu\chi}{e^\mu_0\partial_\mu\chi}\,, \tag{B.44}$$

where $\eta \equiv \sqrt{\eta^i\eta^i}$ and $(\partial\chi) = (e^{a\mu}e^\nu_a\partial_\mu\chi\partial_\nu\chi)^{1/2}$. Eventually, we are left with a single independent Goldstone field $\chi(x) = \mu t + \pi(x)$.

We are finally in position to build invariants. To this aim we take the metric $g_{\mu\nu} = e^a_\mu e^b_\nu\eta_{ab}$ to be the cylinder one. After having set to zero the covariant derivatives of the Goldstone π, to leading order in derivatives we only have the invariant measure at hand. This reads:

$$\mu^d \det E = \sqrt{g}(\partial\chi)^d = \sqrt{\hat{g}}\,, \tag{B.45}$$

where we introduced the Weyl invariant modified metric $\hat{g}_{\mu\nu} = (\partial\chi)^2 g_{\mu\nu}$ as in sec. 3.2.1. This clearly agrees with eq. (3.8). We may also build higher derivative terms. In the same notation of sec. 3.2.1, the ones in eq. (3.9) are obtained as

$$\mu^{-2}R^{ab}_{ab} = \hat{\mathcal{R}}\,, \qquad \mu^{-2}R^{0a}_{0a} = \hat{\mathcal{R}}^{\mu\nu}g_{\mu\nu}\,. \tag{B.46}$$

Finally, at the same order in the derivative expansion we also have the following terms[6]

$$\begin{aligned}\mu^{-1}\nabla_i\eta^i &= \hat{\nabla}^\mu\partial_\mu\chi\,,\\ \mu^{-2}\nabla_a\eta^i\nabla_a\eta^i &= -\mu^{-2}\nabla_i\eta^j\nabla_j\eta^i = \left(\hat{\nabla}_\mu\partial_\nu\chi\right)\hat{g}^{\mu\rho}\hat{g}^{\nu\sigma}\left(\hat{\nabla}_\rho\partial_\sigma\chi\right)\,,\end{aligned}\tag{B.47}$$

Discarding total derivatives and using the equations of motion deriving from the leading order Lagrangian (3.8), which reads $\hat{\nabla}^\mu\partial_\mu\chi=0$, these reduce to zero or to the ones above.

Finally, let us comment that we can use the coset construction to build operators transforming in linear representations of the full group [35]. Specifically, consider any operator ϕ built out of the Goldstone fields or, possibly, additional matter fields transforming in a linear representation ρ of the unbroken rotation group $SO(d)$. We may build an operator transforming in a rep. $\kappa\supset\rho$ of the full group as

$$\Phi=\kappa\left(e^{i\sigma D}e^{i\eta^i J_{0i}}e^{i\chi Q}\right)\tilde{\phi}\,,\tag{B.48}$$

where $\tilde{\phi}=(\phi,0)$ is the simplest embedding of the operator ϕ in the representation κ of the full symmetry group. For instance, eq. (3.32) for a primary scalary field in the main text is obtained with this procedure taking

$$\tilde{\phi}=C^{(1)}_{\delta,q}-C^{(2)}_{\delta,q}\mu^{-2}R^{ab}_{ab}+\dots\,.\tag{B.49}$$

Similarly, the spinning operator in eq. (3.43) is obtained taking

$$\tilde{\phi}_{a_1\dots a_\ell}=C^{(1)}_{\delta,\ell,q}\delta^0_{a_1}\dots\delta^0_{a_\ell}+\dots\,.\tag{B.50}$$

B.3 Casimir energy of the $U(1)$-conformal superfluid

Here we compute thq quantum correction to the superfluid energy (3.17) in $d=3$ and $d=4$ spacetime dimensions. To regulate the calculation compatibly with all the symmetries, at intermediate steps we shall work in generic d spacetime dimensions. The value of β_0 in $d=3$ was previously derived using zeta function regularization in [251].

Let us start evaluating the leading order contribution, given by

$$\delta\Delta^{(1)}_Q\frac{T}{R}=\frac{1}{2}\log\det\left[-\partial_\tau^2-\frac{1}{d-1}\Delta^{(S^{(d-1)})}\right]=\frac{T}{2}\int\frac{d\omega}{2\pi}\sum_{\ell=0}^{\infty}n_{\ell,d}\log\left(\omega^2+\frac{1}{d-1}J_\ell^2\right)\,,\tag{B.51}$$

where $J_\ell^2=\ell(\ell+d-2)/R^2$ are the eigenvalues of the Laplacian on the S^{d-1} and $n_{\ell,d}$ is their multiplicity, given by

---

[6] Notice also that $\nabla_0\eta^i\nabla_0\eta^i=\left[\partial_\mu\chi\hat{\nabla}^\mu\left(\partial_\nu\chi\right)\right]\left[\partial_\sigma\chi\hat{\nabla}^\sigma\left(\hat{g}^{\nu\rho}\partial_\rho\chi\right)\right]=\left[\hat{\nabla}_\rho\left(\hat{g}^{\mu\nu}\partial_\nu\chi\partial_\mu\chi\right)\right]^2=0$.

$$n_{\ell,d} = \frac{(2\ell+d-2)\Gamma(\ell+d-2)}{\Gamma(\ell+1)\Gamma(d-1)}\,. \tag{B.52}$$

For sufficiently negative d the sum in eq. (B.51) is convergent. Nonetheless, exchanging the sum and the integral leads to an apparently divergent result. To remedy this we use the following identity which holds in dimensional regularization:

$$\sum_{\ell=0}^{\infty} n_{\ell,d} = 0\,. \tag{B.53}$$

It is then convenient to subtract from eq. (B.51) a vanishing contribution of the form $\int \frac{d\omega}{2\pi}\sum_{\ell=0}^{\infty} n_{\ell,d}\log(\omega^2+m^2)$, where m is an arbitrary mass scale which will eventually drop from the final result. Doing so we get

$$\frac{1}{2}\log\det\left[-\partial_\tau^2-\frac{1}{d-1}\Delta^{(S^{(d-1)})}\right]=\frac{T}{2}\int\frac{d\omega}{2\pi}\sum_{\ell=0}^{\infty} n_{\ell,d}\log\left(\frac{\omega^2+\frac{1}{d-1}J_\ell^2}{\omega^2+m^2}\right)\,. \tag{B.54}$$

We may now exchange the sum and the integral, finding

$$\begin{aligned}\delta\Delta_Q^{(1)} &= \frac{1}{2}\sum_{\ell=0}^{\infty} n_{\ell,d}\left(\frac{RJ_\ell}{\sqrt{d-1}}+Rm\right)+\mathcal{O}\left(\frac{1}{R^2\mu^2}\right)\\ &= \frac{1}{2\sqrt{d-1}}\sum_{\ell=1}^{\infty} n_{\ell,d}RJ_\ell+\mathcal{O}\left(\frac{1}{R^2\mu^2}\right)\,,\end{aligned} \tag{B.55}$$

where we used again the property (B.53); as expected, m does not contribute to the final result. Eq. (B.55) is correct in any dimensions and it is interpreted as the Casimir energy of the superfluid on the cylinder.

Let us evaluate (B.55) in $d=3$ first. It is convenient to isolate the divergent contribution by expanding the summand for $\ell\to\infty$:

$$n_{\ell,d}RJ_\ell = \sum_{k=1}^{4}\gamma_k\ell^{d-k}+\sigma(\ell)\,, \tag{B.56}$$

where

$$\sigma(\ell)=\sqrt{\ell(\ell+1)}(1+2\ell)-2\ell^2-2\ell-\frac{1}{4}+\mathcal{O}\left(d-3\right)\xrightarrow{\ell\to\infty}-\frac{1}{64\ell^2} \tag{B.57}$$

so that its infinite sum converges directly in $d = 3$, and the coefficients γ_k's are:

$$\begin{aligned} \gamma_1 &= 2 + \mathcal{O}\left(d-3\right) , & \gamma_2 &= 2 + \mathcal{O}\left(d-3\right) , \\ \gamma_3 &= \frac{1}{4} + \mathcal{O}\left(d-3\right) , & \gamma_4 &= \frac{3-d}{24} + \mathcal{O}\left((d-3)^2\right) . \end{aligned} \tag{B.58}$$

Using then $\sum_{\ell=1}^{\infty} \ell^k = \zeta(-k)$ and recalling that the zeta function is analytic on the real axis except for a simple pole at $k = 1$, we realize that the only divergent contribution for $d \to 3$ arises from the sum $\sum_{\ell=1}^{\infty} \ell^{d-4} = \zeta(4-d) \sim \frac{1}{3-d}$; however, this contribution is multiplied by the coefficient γ_4 in eq. (B.58), which has a simple zero for $d = 3$. The result is then finite in the limit $d \to 3$, as expected. Eventually, expanding appropriately the zeta functions and evaluating numerically the infinite convergent sum, we find

$$\sum_{\ell=1}^{\infty} n_{\ell,d} R J_\ell = \left[\sum_{k=1}^{4} c_k \zeta(k-d) + \sum_{\ell=1}^{\infty} \sigma(\ell) \right] = -0.265096 + \mathcal{O}\left(3-d\right) . \tag{B.59}$$

Using this result in eq. (B.55), we recover β_0 in eq. (3.20).

The same procedure can be used to evaluate the sum in $d = 4$. One finds

$$\delta\Delta_Q^{(1)} = \frac{1}{2\sqrt{d-1}} \sum_{\ell=1}^{\infty} n_{\ell,d} R J_\ell = -\frac{1}{16\sqrt{3}(4-d)} - 0.113876 + \mathcal{O}\left(4-d\right) . \tag{B.60}$$

In this case, the result displays a simple pole for $d \to 4$. Thus this contribution renormalizes one of the Wilson coefficients of the effective Lagrangian. It is instructive to identify which one. To this aim, we should construct the effective Lagrangian to fourth order in derivatives. In practice, since we need to renormalize the Casimir energy, we can focus only on the terms which are non-vanishing on the background solution. These are built contracting the modified Riemann tensor $\hat{\mathcal{R}}_{\mu\nu\rho\sigma}$ with itself and the modified metric, in the notation of section 3.2.1. We therefore consider the following three invariants:

$$\sqrt{\hat{g}}\hat{\mathcal{R}}^2 , \qquad \sqrt{\hat{g}}\hat{W}_{\mu\nu\rho\sigma}\hat{W}^{\mu\nu\rho\sigma} , \qquad \sqrt{\hat{g}}\hat{E} , \tag{B.61}$$

where $\hat{W}_{\mu\nu\rho\sigma}$ and $\hat{E}$ are, respectively, the Weyl tensor and the Gauss-Bonnet term [252]:

$$\begin{aligned} \hat{W}_{\mu\nu\rho\sigma} &= \hat{\mathcal{R}}_{\mu\nu\rho\sigma} + \frac{1}{d-2}\left(\hat{g}_{\mu\sigma}\hat{\mathcal{R}}_{\nu\rho} - \hat{g}_{\mu\rho}\hat{\mathcal{R}}_{\nu\sigma} + \hat{g}_{\nu\rho}\hat{\mathcal{R}}_{\mu\sigma} - \hat{g}_{\nu\sigma}\hat{\mathcal{R}}_{\mu\rho}\right) \\ &\quad + \frac{1}{(d-1)(d-2)}\hat{\mathcal{R}}\left(\hat{g}_{\mu\rho}\hat{g}_{\nu\sigma} - \hat{g}_{\mu\sigma}\hat{g}_{\nu\rho}\right) \end{aligned} \tag{B.62}$$

$$\hat{E} = \hat{\mathcal{R}}^2 - 4\hat{\mathcal{R}}_{\mu\nu}\hat{\mathcal{R}}^{\mu\nu} + \hat{\mathcal{R}}_{\mu\nu\rho\sigma}\hat{\mathcal{R}}^{\mu\nu\rho\sigma} . \tag{B.63}$$

The contribution from the last two terms vanishes exactly for every value of χ. Indeed the first is Weyl invariant and the metric $\hat{g}_{\mu\nu}$ is conformally equivalent to flat space, while the second one in four dimensions coincides with the Euler density, whose integral is a topological invariant and vanishes on the cylinder. Finally, due to the Weyl anomaly in four dimensions, the effective action must include the following Wess-Zumino term [34, 253]:

$$S_{WZ} = \int d^4x\sqrt{g}\log(\partial\chi)\left[-aE + cW_{\mu\nu\rho\sigma}W^{\mu\nu\rho\sigma}\right] + \mathcal{O}\left(\mathcal{R}\left[\nabla(\partial\chi)\right]^2\right) , \tag{B.64}$$

where a and c are the trace anomalies. This term however vanishes on the superfluid background by considerations similar to the ones above. Therefore, in the action (3.9), the divergence in eq. (B.60) is renormalized by the contribution of the following term

$$\delta S = c_{div}\int d^dx\sqrt{g}(\partial\chi)^{d-4}\hat{\mathcal{R}}^2 \propto c_{div}T(R\mu)^{d-4} . \tag{B.65}$$

Choosing c_{div} so to cancel the pole in (B.60) and expanding the result for $d \to 4$ we then find the following result

$$\delta\Delta_Q^{(1)}|_{renormalized} = -\frac{1}{16\sqrt{3}}\log R\mu + \alpha_3 , \tag{B.66}$$

where we absorbed in α_3 both the classical and the quantum contributions of order μ^0. Using the relation (3.13) we obtain eq. (3.21).

We may easily extend this calculation to include the first subleading contribution to the one-loop Casimir energy. With steps similar to those with which we obtained eq. (B.55), we find

$$\begin{aligned}\delta\Delta_Q^{(1)} = {} & \frac{1}{2}\left[\frac{1}{\sqrt{d-1}} - (R\mu)^{-2}\frac{(d-2)\left[c_2(d-2)+c_3\right]}{c_1 d\sqrt{d-1}}\right]\sum_{\ell=1}^{\infty} n_{\ell,d}RJ_\ell \\ & + (R\mu)^{-2}\frac{(d-2)\left[c_2(d-2)+c_3\right]}{2c_1 d(d-1)^{3/2}}\sum_{\ell=1}^{\infty} n_{\ell,d}R^3J_\ell^3 + \mathcal{O}\left(\frac{1}{R^4\mu^4}\right) ,\end{aligned} \tag{B.67}$$

as it could have been guessed form the dispersion relation of the superfluid phonon (3.25). To evaluate this contribution in $d = 3$, we use eq. (B.59) and the analogously derived result

$$\sum_{\ell=1}^{\infty} n_{\ell,d}R^3J_\ell^3 = 0.017496 + \mathcal{O}\left(d-3\right) . \tag{B.68}$$

Using the expression of the chemical potential (3.13) we find the value for β_1 in eq. (3.20). In $d = 4$ instead we use

$$\sum_{\ell=1}^{\infty} n_{\ell,d}R^3J_\ell^3 = \frac{1}{16(4-d)} + \text{finite} . \tag{B.69}$$

Analogously to eq. (B.65), this subleading contribution is renormalized by the classical contributions to Δ_Q, such as $(\partial\chi)^{d-6}\hat{\mathcal{R}}^3$. Irrespectively of the precise structure of the involved terms, choosing the divergent part of the μ^{d-6} classical contribution to the energy so to have a finite result for $d \to 4$, as we did in eq. (B.66), we find the result (3.21).

B.4 Details on correlation functions in the large charge EFT

B.4.1 Three-point function with a $U(1)$-charged scalar insertion to the first subleading order

Here we evaluate the first correction to the OPE coefficient (3.40) by solving the equation (3.36) to linear order in the fluctuation $\pi(x)=\chi+i\mu\tau-\pi_0$. This reads:

$$ic_1 d(d-1)\mu^{d-2}\left(\partial_\tau^2+\Delta^{S^{d-1}}\right)\pi(\tau,\hat{n})=q\delta(\tau-\tau_c)\delta^{d-1}(\hat{n}-\hat{n}_c)/\sqrt{g}\,. \tag{B.70}$$

This equation can be straightforwardly solved expanding the field into Gegenbauer polynomials[7]

$$\begin{aligned}\pi(x)=&\, i\frac{q/(R^{d-1}\Omega_{d-1})}{c_1 d(d-1)\mu^{d-2}}\left[(\tau-\tau_c)\theta(\tau-\tau_c)-\sum_{\ell=1}^{\infty}\frac{2\ell+d-2}{d-2}\frac{e^{-\omega_\ell|\tau-\tau_c|}}{2\omega_\ell}C_\ell^{\left(\frac{d}{2}-1\right)}(\hat{n}\cdot\hat{n}_c)\right]\\&+\mathcal{O}\left(\frac{q^2/c_1^2}{(R\mu)^{2d-3}},\frac{q/c_i}{(R\mu)^d}\right),\end{aligned} \tag{B.71}$$

where $\omega_\ell=J_\ell/\sqrt{d-1}$ is the phonon energy (3.25) and we estimated the size of corrections induced both from the nonlinear terms and the higher derivative contributions which we neglected in eq. (B.70). In particular, we see that the linear approximation holds as long as $q/(R\mu)^{(d-1)}\sim q/Q\ll 1$. Since the variation of the action vanishes on the solution of the equations of motion, we can use eq. (B.71) to evaluate the modified action to second order in the field expansion:

$$\begin{aligned}S_{mod}[\chi]&=\Delta_Q(\tau_f-\tau_{in})/R+\mu q(\tau_f-\tau_c)+i\frac{q}{2}\left[\pi_f-\pi(\tau_c,\hat{n}_c)\right]\\&=\Delta_Q(\tau_f-\tau_{in})/R+\left[q\frac{\partial\Delta_Q}{\partial Q}+\frac{q^2}{2}\frac{\partial^2\Delta_Q}{\partial Q^2}\right](\tau_f-\tau_c)/R-\frac{q^2}{c_1(R\mu)^{d-2}}N(d)\,,\end{aligned} \tag{B.72}$$

where $N(d)$ is a formally divergent contribution, given by the following sum

$$N(d)=iq^{-2}c_1(R\mu)^{d-2}\pi(\tau_c,\hat{n}_c)=\sum_{\ell=1}^{\infty}\frac{2\ell+d-2}{d(d-1)(d-2)\Omega_{d-1}}\frac{C_\ell^{\left(\frac{d}{2}-1\right)}(1)}{2R\omega_\ell} \tag{B.73}$$

The contribution which grows linear in time in the action agrees with eq. (3.33) to the order we are working. Expanding the exponential, the last term in eq. (B.72) instead provides a correction to the OPE coefficient:

$$\lambda^{(\delta)}_{(Q+q),q,Q}=C^{(1)}_{(\delta,q)}(R\mu)^{\delta}\left[1-\frac{q^2}{c_1(R\mu)^{d-2}}N(d)+\dots\right]+C^{(2)}_{(\delta,q)}(R\mu)^{\delta-2}+\dots \tag{B.74}$$

---

[7] These are the generalization to arbitrary dimensions of the Legendre polynomials, to which they reduce in $d=3$.

Similarly to the discussion below eq. (3.19) on the quantum corrections to the ground state energy, the situation is slightly different between even and odd spacetime dimensions. Let us consider for concreteness the physically interesting cases $d=3$ and $d=4$. In $d=3$, the term proportional to $N(d)$ in eq. (B.74) is suppressed only by one power of $\mu\sim\sqrt{Q}$ with respect to the leading term and provides the dominant correction. Therefore, its value cannot be renormalized by $C^{(2)}_{(\delta,q)}$ or any other Wilson coefficient contributing to the matching in eq. (3.32). Correspondingly, it must be finite and calculable. Proceeding as we did in appendix B.3 for the Casimir energy, we can evaluate the sum (B.73) in dimensional regularization and take the limit $d\to 3$ to find

$$N(3)=-0.0164523\,. \tag{B.75}$$

Absorbing all the anyway unknown constants in a new Wilson parameter $\eta^{(1)}_{(\delta,q)}$, we finally recast eq. (B.74) as [8]

$$\lambda^{(\delta)}_{(Q+q),q,Q}\Big|_{d=3}=Q^{\delta/2}\left[\eta^{(1)}_{(\delta,q)}\left(1-\frac{q^2\sqrt{12\pi}}{\sqrt{c_1 Q}}N(3)\right)+\mathcal{O}\left(\max\left\{q^4Q^{-1},\delta^2Q^{-3/2}\right\}\right)\right]. \tag{B.76}$$

Corrections arise from the subleading term in the expansion of the exponential and from the expansion of $(\partial\chi)^\delta$ to second order in *quantum* fluctuations, which provides a term of the form $\delta^2\langle[\partial\pi(\tau_c,\hat{n}_c)]^2\rangle\mu^{\delta-2}\sim\delta^2\mu^{\delta-3}$, [9] implying that the result (B.76) holds only for $\delta^2\ll Q^{3/2}$.

In $d=4$ instead the contribution proportional to $N(4)$ in eq. (B.74) is divergent:

$$N(4)=\frac{1}{32\sqrt{3}\pi^2(4-d)}+\text{finite}\,, \tag{B.77}$$

where we work in dimensional regularization. This divergence is renormalized writing the Wilson coefficient $C^{(2)}_{(\delta,q)}$ as:

$$C^{(2)}_{(\delta,q)}=-\frac{q^2C^{(1)}_{(\delta,q)}}{c_1 32\sqrt{3}\pi^2(d-4)}+\text{finite}\,. \tag{B.78}$$

Using these equations and eq. (3.13) in (B.74), the final result reads

$$\begin{aligned}\lambda^{(\delta)}_{(Q+q),q,Q}\Big|_{d=4}=Q^{\delta/3}\Bigg[&\eta^{(1)}_{(\delta,q)}\left(1-\frac{q^2/Q^{2/3}}{24\sqrt{3}\pi^{2/3}c_1^{1/3}}\log Q\right)+\eta^{(2)}_{(\delta,q)}Q^{-2/3}\\&+\mathcal{O}\left(\max(q^4,\delta^2)\times Q^{-4/3}\right)\Bigg]\,.\end{aligned} \tag{B.79}$$

---

[8] Notice that the term arising from the expansion of $(\partial\chi)^\delta\simeq\mu^\delta+i\mu^{\delta-1}\dot{\pi}$ just renormalizes $C^{(2)}_{(\delta,q)}$ using eq. (B.71).

[9] Here we used that the canonically normalized field scales as $\pi\sim\mu^{-1/2}$ from eq. (3.23).

As in eq. (3.21), there is a universal logarithmic calculable subleading contribution to the result. Corrections are estimated as before.

B.4.2 Conformal block decomposition at large charge

Let us consider the following four-point function for the theory on the Euclidean cylinder

$$F^{\delta,\delta}_{-q,q} = \langle Q,\tau_{out}|\mathcal{O}^{(\delta)}_{-q}(\tau_2,\hat{n}_2)\mathcal{O}^{(\delta)}_{q}(\tau_1,\hat{n}_1)|Q,\tau_{in}\rangle \, , \qquad \tau_2>\tau_1\, , \tag{B.80}$$

where $\mathcal{O}^{(\delta)}_q$ is a scalar primary operator, whose scaling dimension δ and charge q we assume of order one for simplicity. As we commented in section B.1, we may systematically use the OPE to compute the correlator (B.80), reducing it to a sum of *conformal blocks* multiplied by the corresponding OPE coefficients as in eq. (B.18). Here we show this concretely considering the operators exchanged in the s-channel OPE $\mathcal{O}^{(\delta)}_q\times\mathcal{O}_Q$ in eq. (B.80). We shall comment at the end on the case where we replace one or both of these operators with the time component of the current.

To this aim, we insert the decomposition of the identity in terms of conformal families in between the two operators:

$$F^{\delta,\delta}_{-q,q} = \sum_{\Delta,\ell}\langle Q,\tau_{out}|\mathcal{O}^{(\delta)}_{-q}(\tau_2,\hat{n}_2)\,|\mathcal{O}^{(\Delta,\ell)}_{Q+q}|\,\mathcal{O}^{(\delta)}_{q}(\tau_1,\hat{n}_1)|Q,\tau_{in}\rangle \tag{B.81}$$

where the contribution of a single family is given by:

$$|\mathcal{O}^{(\Delta,\ell)}_{Q+q}| = \sum_{\alpha,\beta=\mathcal{O},P_\mu\mathcal{O},\dots}|\alpha\rangle\,\mathcal{N}^{-1}_{\alpha\beta}\,\langle\beta|\, , \qquad \mathcal{N}_{\alpha\beta}\equiv\langle\alpha|\beta\rangle\, . \tag{B.82}$$

Considering separatly the contribution of each single family to eq. (B.81), we define the *conformal block* decomposition as

$$R^{2\delta}F^{\delta,\delta}_{-q,q} = e^{-\Delta_Q(\tau_{out}-\tau_{in})/R}\sum_{\Delta,\ell}\left|\lambda_{\langle\mathcal{O}^{(\Delta,\ell)}_{-Q-q}\mathcal{O}^{(\delta)}_q\mathcal{O}_Q\rangle}\right|^2 g^{\mathcal{O}_Q,\mathcal{O}^{(\delta)}_q}_{\Delta,\ell}(\tau_2-\tau_1,\hat{n}_2\cdot\hat{n}_1)\, . \tag{B.83}$$

Here $\lambda_{\langle\mathcal{O}^{(\Delta,\ell)}_{-Q-q}\mathcal{O}^{(\delta)}_q\mathcal{O}_Q\rangle}$ is the OPE coefficient in the normalization introduced in eq. (B.7), [10] and the conformal block $g^{\mathcal{O}_Q,\mathcal{O}^{(\delta)}_q}_{\Delta,\ell}(\tau,x)$ is fully fixed by conformal invariance in terms of the quantum numbers of the exchanged operator and of those of the operators whose OPE we are considering, $\mathcal{O}^{(\delta)}_q$ and $\mathcal{O}_Q$.

Generically, the expression for the conformal blocks is quite involved, as all the states in the multiplet (B.82) contribute. However, within the kinematic regime of validity of the EFT, we consider exchanges of operators with scaling dimension $\Delta\sim\Delta_{Q+q}\simeq\Delta_Q+\mathcal{O}\left(Q^{\frac{d-2}{d-1}}\right)$

---

[10] Our normalization agrees with that of [109].

and spin $\ell \ll Q^{\frac{1}{d-1}} \ll \Delta$. In this case the contribution of the k-th level descendants in eq. (B.82) is suppressed with respect to the $k-1$-th level by at least a power of [109]

$$\frac{(\Delta-\Delta_Q)^2}{\Delta} \lesssim \frac{1}{\Delta_Q}\left(\frac{\partial\Delta_Q}{\partial Q}\right)^2 \sim Q^{-\frac{d-2}{d-1}}\,. \tag{B.84}$$

This implies that we can consider the contributions from descendants perturbatively when matching the EFT predictions with a conformal block decomposition. We prove this property below. Along the way, we will also illustrate a simple way to compute the conformal blocks in this limit.

Let us consider first the contribution from the primary and the first descendant states. Working in the notation explained below eq. (B.28) and using $\Delta \gg \ell$, we can compute the norm matrix from

$$\begin{aligned}
&\langle\mathcal{O}^{(\Delta,\ell)}_{Q+q,m}|\mathcal{O}^{(\Delta,\ell)}_{Q+q,m'}\rangle = \delta_{m\,m'}\,,\\
&\langle\mathcal{O}^{(\Delta,\ell)}_{Q+q,m}|K_\nu P_\mu|\mathcal{O}^{(\Delta,\ell)}_{Q+q,m'}\rangle = \delta_{m\,m'}2\Delta\delta_{\mu\nu} + 2i\,\langle\mathcal{O}^{(\Delta,\ell)}_{Q+q,m}|J_{\mu\nu}|\mathcal{O}^{(\Delta,\ell)}_{Q+q,m'}\rangle \approx 2\Delta\delta_{m\,m'}\,,
\end{aligned} \tag{B.85}$$

where we used the commutator in eq. (B.1) and that the primary state $|\mathcal{O}^{(\Delta,\ell)}_{Q+q,m'}\rangle$ is annihilated by K_ν. Here m labels collectively the eigenvalues of the Cartan generators of the rotation group. We then write the contribution of a conformal family as

$$|\mathcal{O}^{(\Delta,\ell)}_{Q+q}| = \sum_m |\mathcal{O}^{(\Delta,\ell)}_{Q+q,m}\rangle\,\langle\mathcal{O}^{(\Delta,\ell)}_{Q+q,m}| + \sum_m P_\mu\,|\mathcal{O}^{(\Delta,\ell)}_{Q+q,m}\rangle\,\frac{\delta^{\mu\nu}}{2\Delta}\,\langle\mathcal{O}^{(\Delta,\ell)}_{Q+q,m}|\,K_\nu + \ldots\,. \tag{B.86}$$

To proceed, we notice that time translational and rotational symmetry imply the following structure for the matrix element of $\mathcal{O}^{(\delta)}_q$ in between $|Q\rangle$ and $|\mathcal{O}^{(\Delta,\ell)}_{Q+q,m}\rangle$:

$$\langle\mathcal{O}^{(\Delta,\ell)}_{Q+q,m}|\mathcal{O}^{(\delta)}_q(\tau,\hat{n})|Q\rangle = \sqrt{\frac{(d-2)\Omega_{d-1}}{(2\ell+d-2)}} \times \lambda_{\langle\mathcal{O}^{(\Delta,\ell)}_{-Q-q}\mathcal{O}^{(\delta)}_q\mathcal{O}_Q\rangle}\left[Y^\ell_m(\hat{n})\right]^* e^{(\Delta-\Delta_Q)\tau/R}/R^\delta\,, \tag{B.87}$$

where the OPE coefficient precisely coincides with λ_{abc} in eq. (B.7) (and with $\lambda^{(1)}_{sJ\ell}$ in eq. (B.9) for $\mathcal{O}^{(\delta)}_{-q} = J_0$), when mapping this equation to the plane. Using eq. (B.87) and the action of the conformal generators (B.3), we may further estimate the matrix element with the first descendant state. Indeed, recalling the map (B.21) between $\mathbb{R}^d$ and $\mathbb{R}\times S^{d-1}$, we find

$$\begin{aligned}
\langle Q|\mathcal{O}^{(\delta)}_{-q}(\tau,\hat{n})P_\mu|\mathcal{O}^{(\Delta,\ell)}_{Q+q,m}\rangle &= \langle Q|[\mathcal{O}^{(\delta)}_{-q}(\tau,\hat{n}),P_\mu]|\mathcal{O}^{(\Delta,\ell)}_{Q+q,m}\rangle\\
&= i\left(\frac{\partial}{\partial x^\mu} - \delta\frac{x_\mu}{x^2}\right)\langle Q|\mathcal{O}^{(\delta)}_{-q}(\tau,\hat{n})|\mathcal{O}^{(\Delta,\ell)}_{Q+q,m}\rangle\\
&\sim (\Delta-\Delta_Q)\,\langle Q|\mathcal{O}^{(\delta)}_{-q}(\tau,\hat{n})|\mathcal{O}^{(\Delta,\ell)}_{Q+q,m}\rangle\,,
\end{aligned} \tag{B.88}$$

where x^μ is the coordinate on $\mathbb{R}^d$, and, to estimate the size of the matrix element, we noticed that the most important contribution is given by the derivative of the exponential in eq. (B.87). Similarly, setting $\tilde{x}^\mu = x^\mu/x^2$, we find

$$\begin{aligned}\langle \mathcal{O}^{(\Delta,\ell)}_{Q+q,m}|K_\nu \mathcal{O}^{(\delta)}_q(\tau,\hat{n})|Q\rangle &= -i\left(\frac{\partial}{\partial \tilde{x}^\mu} - \delta\frac{\tilde{x}_\mu}{\tilde{x}^2}\right)\langle \mathcal{O}^{(\Delta,\ell)}_{Q+q,m}|\mathcal{O}^{(\delta)}_q(\tau,\hat{n})|Q\rangle \\ &\sim (\Delta-\Delta_Q)\,\langle \mathcal{O}^{(\Delta,\ell)}_{Q+q,m}|\mathcal{O}^{(\delta)}_q(\tau,\hat{n})|Q\rangle \ .\end{aligned} \tag{B.89}$$

Combining these results and eq. (B.86), we find that the contribution of the first descendant is suppressed by a power of $(\Delta-\Delta_Q)^2/\Delta$ with respect to that of the primary state. We may further use eq.s (B.87), (B.88) and (B.89) to compute explicitly the conformal blocks. Indeed, from the following relation between hyperspherical harmonics and Gegenbauer polynomials [108]

$$\sum_m Y^\ell_m(\hat{n}_1)\left[Y^\ell_m(\hat{n}_1)\right]^* = \frac{2\ell+d-2}{(d-2)\Omega_{d-1}}C_\ell^{\left(\frac{d}{2}-1\right)}(\hat{n}_2\cdot\hat{n}_1)\ , \tag{B.90}$$

we find (notice that the prefactor of eq. (B.90) precisely cancels that of eq. (B.87))

$$\begin{aligned} g_{\Delta,\ell}^{\mathcal{O}_Q,\mathcal{O}^{(\delta)}_q}(\tau,\hat{n}_2\cdot\hat{n}_1) &= e^{-(\Delta-\Delta_Q)\tau/R}C_\ell^{\left(\frac{d}{2}-1\right)}(\hat{n}_2\cdot\hat{n}_1) \\ &+\frac{e^{-(\Delta-\Delta_Q+1)\tau/R}}{2\Delta}\left[\tilde{a}_{1,\ell+1}C_{\ell+1}^{\left(\frac{d}{2}-1\right)}(\hat{n}_2\cdot\hat{n}_1)+\tilde{a}_{1,\ell-1}C_{\ell-1}^{\left(\frac{d}{2}-1\right)}(\hat{n}_2\cdot\hat{n}_1)\right] \\ &+\mathcal{O}\left(\frac{(\Delta-\Delta_Q)^4}{\Delta^2}\right)\ ,\end{aligned} \tag{B.91}$$

$$\tilde{a}_{1,\ell+1} = \frac{(\ell+1)(\Delta-\Delta_Q+\delta+\ell)^2}{2\ell+d-2}\ ,\quad \tilde{a}_{1,\ell-1} = \frac{(\ell+d-3)(\Delta-\Delta_Q+\delta-\ell-d+2)^2}{2\ell+d-2}\ . \tag{B.92}$$

We can straightforwardly generalize the previous argument to show that the contribution to the conformal block of a generic k-th level descendant is suppressed by $(\Delta-\Delta_Q)^{2k}/\Delta^k$ with respect to the primary state. Indeed, eq. (B.86) schematically takes the form

$$|\mathcal{O}| = \sum_n P^n\,|\mathcal{O}\rangle\,\mathcal{N}_n^{-1}\,\langle\mathcal{O}|\,K^n\,. \tag{B.93}$$

From the conformal algebra, we may estimate the norm as

$$\mathcal{N}_k \sim \langle\mathcal{O}|K^kP^k|\mathcal{O}\rangle \sim \Delta^k\,, \tag{B.94}$$

while, by repeatedly commuting the conformal generators with the operator, eq.s (B.88) and (B.89) generalize to

$$\langle Q|\mathcal{O}^{(\delta)}_{-q}P^k|\mathcal{O}\rangle \sim \langle\mathcal{O}|K^k\mathcal{O}^{(\delta)}_q|Q\rangle \sim (\Delta-\Delta_Q)^k\,\langle Q|\mathcal{O}^{(\delta)}_{-q}|\mathcal{O}\rangle\ , \tag{B.95}$$

which implies that the contribution from the k-th level descendants scales as

$$\begin{aligned}\langle Q|\mathcal{O}_{-q}^{(\delta)}P^k|\mathcal{O}\rangle\,\mathcal{N}_k^{-1}\,\langle\mathcal{O}|K^k\mathcal{O}_q^{(\delta)}|Q\rangle &\sim \frac{(\Delta-\Delta_Q)^{2k}}{\Delta^k}\,\langle Q|\mathcal{O}_{-q}^{(\delta)}|\mathcal{O}\rangle\,\langle\mathcal{O}|\mathcal{O}_q^{(\delta)}|Q\rangle \\ &\lesssim Q^{-k\frac{d-2}{d-1}}\times\langle Q|\mathcal{O}_{-q}^{(\delta)}|\mathcal{O}\rangle\,\langle\mathcal{O}|\mathcal{O}_q^{(\delta)}|Q\rangle\,.\end{aligned} \tag{B.96}$$

By precisely evaluating the matrix elements with descendant states we may further compute the conformal block explicitly as a series expansion. In practice, the expression for the conformal block as a sum over descendants was found in [244, 245] and reads

$$g_{\Delta,\ell}^{\mathcal{O}_Q,\mathcal{O}_q^{(\delta)}}(\tau,\hat{n}_2\cdot\hat{n}_1)=e^{-(\Delta-\Delta_Q)\tau}\sum_{n=0}^{\infty}\sum_{k=0}^{n}a_{n,\ell-n+2k}\,e^{-n\tau/R}C_{\ell-n+2k}^{\left(\frac{d}{2}-1\right)}(\hat{n}_2\cdot\hat{n}_1)\,, \tag{B.97}$$

with the convention that Gegenbauer polynomials with negative subscript vanish. The first few coefficients are [109]

$$a_{0,\ell}=1\,, \tag{B.98}$$

$$a_{1,\ell+1}=\frac{(\ell+1)(\Delta-\Delta_Q+\delta+\ell)^2}{2(2\ell+d-2)(\Delta+\ell)}\,, \tag{B.99}$$

$$a_{1,\ell-1}=\frac{(\ell+d-3)(\Delta-\Delta_Q+\delta-\ell-d+2)^2}{2(2\ell+d-2)(\Delta-\ell-d+2)}\,, \tag{B.100}$$

in agreement with eq. (B.91) derived before for $\Delta\gg\ell$. We shall also need the $n=2$ coefficients for $\ell=0$, which read

$$a_{2,2}=\frac{(\Delta-\Delta_Q+\delta)^2(\Delta-\Delta_Q+\delta+2)^2}{4d(d-2)\Delta(\Delta+1)}\,, \tag{B.101}$$

$$a_{2,0}=\frac{(\Delta-\Delta_Q+\delta)^2(\Delta-\Delta_Q+\delta-d+2)^2}{4d\,\Delta(2\Delta-d+2)}\,. \tag{B.102}$$

A final comment concerns the case in which we replace the $\mathcal{O}_Q^{(\delta)}$ insertions with the time component of the Noether current, J_0. On the one hand, for what concerns the power counting of the descendant contributions, nothing changes. On the other hand, due to the term proportional to the $SO(d)$ generator $\rho^{(\ell)}[J_{\nu\mu}]$ in the action of K_μ (B.3), the detailed form of the conformal block will not coincide with eq. (B.97) in general. Nonetheless eq. (B.91) still correctly reproduces the conformal block for J_0 to leading order, where no descendants are considered, since J_0 behaves as a scalar under rotations. Furthermore, by carefully repeating the steps above for the current, and using that the matrix element of a spatial component (on the cylinder) of the current in between two scalar states vanishes by rotationally invariance $\langle\mathcal{O}|J_i(\tau,\hat{n})|Q\rangle=0$, one finds that eq. (B.91) correctly reproduces the first descendant contribution in the case of an exchanged scalar operator. These considerations justify eq.s (3.51) and (3.52) in the main text.

B.4.3 Two scalar insertions: subleading orders

Here we consider the correlator in eq. (3.54) to subleading orders; for an analogous discussion limited to $d = 3$ of the same correlator see [109]. Expanding the expression (3.32), we find

$$F^{\delta,\delta}_{q,-q} = e^{-\Delta_Q(\tau_{out}-\tau_{in})/R} e^{-\mu q(\tau_2-\tau_1)} R^{2\delta} \left|\lambda^{(\delta)}_{(Q+q),q,Q}\right|^2 f^{\delta,\delta}_{q,-q}\,, \tag{B.103}$$

where

$$\begin{aligned} f^{\delta,\delta}_{q,-q} &= 1 + q\frac{\delta}{R\mu}\frac{\partial^2\Delta_Q}{\partial Q^2} \\ &+ \left[\left(q - \frac{\delta}{\mu}\partial_{\tau_2}\right)\left(q + \frac{\delta}{\mu}\partial_{\tau_1}\right) + \mathcal{O}\left(\frac{1}{(R\mu)^2}\right)\right]\langle\pi_2\pi_1\rangle \\ &+ \left[\frac{q^4}{2} + \mathcal{O}\left(\frac{1}{R\mu}\right)\right]\langle\pi_2\pi_1\rangle^2 + \dots\,, \end{aligned} \tag{B.104}$$

where the second terms arises from factoring out the OPE coefficient $\left|\lambda^{(\delta)}_{(Q+q),q,Q}\right|^2$ to subleading order. Power counting the field as $\pi \sim \mu^{-\frac{d-2}{2}}$ from eq. (3.16), we can see that eq. (B.104) includes all contributions up to order $\mu^{-(d-1)} \sim 1/Q$. In $d = 4$ the corrections to the propagator which we neglected in the first square parenthesis are of the same order of the last parenthesis in eq. (B.104); however, when matching to the s-channel OPE decomposition, the last parenthesis contributes to different terms than those corrections, namely the conformal blocks associated to the exchange of primary states with two phonons, which therefore may be reliably computed.

To proceed, we use eq. (3.56) and exponentiate in an obvious way the terms linear in $\tau_2 - \tau_1$, to write eq. (B.103) as

$$F^{\delta,\delta}_{q,-q} = e^{-\Delta_Q(\tau_{out}-\tau_{in})/R} e^{-(\Delta_{Q+q}-\Delta_Q)(\tau_2-\tau_1)} R^{2\delta} \left|\lambda^{(\delta)}_{(Q+q),q,Q}\right|^2 \tilde{f}^{\delta,\delta}_{q,-q} \tag{B.105}$$

where, calling $r = e^{-|\tau_2-\tau_1|/R}$ and $x = \hat{n}_2 \cdot \hat{n}_1$, $\tilde{f}^{\delta,\delta}_{q,-q}$ is given by

$$
\begin{aligned}
&\left.1+\frac{1}{2\Delta_Q}\left(q\frac{\partial\Delta_Q}{\partial Q}+\delta\right)^2 r\,x+\frac{q^4}{8\Delta_Q^2}\left(\frac{\partial\Delta_Q}{\partial Q}\right)^4 r^2\,x^2\right\}\Delta_{Q+q}\\
&\left.\begin{aligned}
&+\sum_{\ell=2}^{\infty}\frac{(2\ell+d-2)\left(q+\delta\frac{\omega_\ell}{\mu}\right)^2/(R\omega_\ell)}{2c_1d(d-1)(d-2)(R\mu)^{d-2}\Omega_{d-1}}r^{R\omega_\ell}C_\ell^{\left(\frac{d}{2}-1\right)}(x)\\
&+\frac{q^4}{2\Delta_Q}\left(\frac{\partial\Delta_Q}{\partial Q}\right)^2\sum_{\ell=2}^{\infty}\frac{(2\ell+d-2)q^2/(R\omega_\ell)}{2c_1d(d-1)(d-2)(R\mu)^{d-2}\Omega_{d-1}}r^{R\omega_\ell+1}x\,C_\ell^{\left(\frac{d}{2}-1\right)}(x)
\end{aligned}\right\}\Delta_{Q+q,\ell}\\
&\left.+\frac{q^4}{2}\sum_{\ell,j=2}^{\infty}\frac{(2\ell+d-2)(2j+d-2)\,r^{R(\omega_\ell+\omega_j)}C_\ell^{\left(\frac{d}{2}-1\right)}(x)\,C_j^{\left(\frac{d}{2}-1\right)}(x)}{\left[2c_1d(d-1)(d-2)(R\mu)^{d-2}\Omega_{d-1}\right]^2R^2\omega_j\omega_\ell}\,.\right\}\Delta_{Q+q,\ell,j}
\end{aligned}
\tag{B.106}
$$

We have grouped together the contributions referring to the same exchanged operator, specifying its conformal dimension on the right, Δ_{Q+q} for the ground state, $\Delta_{Q+q,\ell} = \Delta_{Q+q} + R\omega_\ell$ for a single phonon, and $\Delta_{Q+q,\ell,j} = \Delta_{Q+q} + R\omega_\ell + R\omega_j$ for two phonons. Indeed, using the following property of Gegenabuer polynomials:

$$
x\,C_\ell^{\left(\frac{d}{2}-1\right)}(x)=\frac{\ell+1}{2\ell+d-2}C_{\ell+1}^{\left(\frac{d}{2}-1\right)}(x)+\frac{\ell+d-3}{2\ell+d-2}C_{\ell-1}^{\left(\frac{d}{2}-1\right)}(x)\,,
\tag{B.107}
$$

we may check that the contributions associated to the ground state and the single phonon excitation match the corresponding expansion of the conformal blocks (B.97). We may also rewrite the last line in eq. (B.106) using the linearization formula for the Gegenbauer polynomials [254]

$$
C_\ell^{\left(\frac{d}{2}-1\right)}(x)C_j^{\left(\frac{d}{2}-1\right)}(x)=\sum_{\substack{k=|\ell-j|\\ k-|\ell-j|\ \text{even}}}^{\ell+j}\frac{(2k+d-2)\,\Gamma(k+1)}{(d-2)(d-2)_k}R^{(d)}_{\ell,j,k}\,C_k^{\left(\frac{d}{2}-1\right)}(x)\,,
\tag{B.108}
$$

where $R^{(d)}_{\ell,j,k}$ is fully symmetric in ℓ, j and k

$$
R^{(d)}_{\ell,j,k}=\frac{\left(\frac{d-2}{2}\right)_{\frac{1}{2}(\ell+j-k)}\left(\frac{d-2}{2}\right)_{\frac{1}{2}(j+k-\ell)}\left(\frac{d-2}{2}\right)_{\frac{1}{2}(k+\ell-j)}(d-2)_{\frac{1}{2}(\ell+j+k)}}{\Gamma\left(\frac{\ell+j-k}{2}+1\right)\Gamma\left(\frac{j+k-\ell}{2}+1\right)\Gamma\left(\frac{k+\ell-j}{2}+1\right)\left(\frac{d}{2}\right)_{\frac{1}{2}(\ell+j+k)}}\,.
\tag{B.109}
$$

Eventually, the correlator (B.103) matches the following conformal block expansion

$$\begin{aligned} F^{\delta,\delta}_{q,-q} = {} & \left|\lambda^{(\delta)}_{(Q+q),q,Q}\right|^2 g^{\mathcal{O}_Q,\mathcal{O}_q^{(\delta)}}_{\Delta_{Q+q},0}(\tau,\hat{n}_2\cdot\hat{n}_1) + \sum_{\ell=2}^{\infty}\left|\lambda^{[\ell],(\delta)}_{(Q+q),q,Q}\right|^2 g^{\mathcal{O}_Q,\mathcal{O}_q^{(\delta)}}_{\Delta_{Q+q,\ell},\ell}(\tau,\hat{n}_2\cdot\hat{n}_1) \\ & + \sum_{\ell=2}^{\infty}\sum_{j=2}^{\infty}\sum_{\substack{k=|\ell-j| \\ k-|\ell-j|\text{ even}}}^{\ell+j}\left|\lambda^{[\ell,j;k],(\delta)}_{(Q+q),q,Q}\right|^2 g^{\mathcal{O}_Q,\mathcal{O}_q^{(\delta)}}_{\Delta_{Q+q,\ell,j},k}(\tau,\hat{n}_2\cdot\hat{n}_1) + \ldots\,, \end{aligned} \tag{B.110}$$

where the OPE coefficients for $\mathcal{O}_Q^{(\delta)}$ in between the ground state and, respectively, one- and two-phonon primaries are given by:

$$\begin{aligned} \left|\lambda^{[\ell],(\delta)}_{(Q+q),q,Q}\right|^2 &= \left|\lambda^{(\delta)}_{(Q+q),q,Q}\right|^2 \times Q^{-\frac{d-2}{d-1}} \times \frac{\left[\frac{q}{\sqrt{R\omega_\ell}} + \delta\sqrt{R\omega_\ell}\left(\frac{c_1 d\Omega_{d-1}}{Q}\right)^{\frac{1}{d-1}} + \mathcal{O}\left(Q^{-\frac{2}{d-1}}\right)\right]^2}{2(2\ell+d-2)^{-1}(d-1)(d-2)(c_1 d\Omega_{d-1})^{\frac{1}{d-1}}} \\ \left|\lambda^{[\ell,j;k](\delta)}_{(Q+q),q,Q}\right|^2 &= \left|\lambda^{(\delta)}_{(Q+q),q,Q}\right|^2 \times Q^{-2\frac{d-2}{d-1}} \times q^4\left(1-\frac{\delta_{\ell j}}{2}\right) R^{(d)}_{\ell,j,k} \\ & \quad \times \frac{(2j+d-2)(2\ell+d-2)(2k+d-2)\Gamma(k+1)}{4(d-2)^3(d-1)^2(d-2)_k\,(c_1 d\Omega)^{\frac{2}{d-1}}}\left[1+\mathcal{O}\left(Q^{-\frac{1}{d-1}}\right)\right]. \end{aligned} \tag{B.111}$$

Notice that a two-phonon primary state is labeled by three indices: ℓ, j specify the energy $\Delta_{Q,\ell,j} = \Delta_Q + R\omega_\ell + R\omega_j$, and k is the angular momentum, whose value is contained in the decomposition $\ell \otimes j \supset |\ell-j| \oplus |\ell-j|+2 \oplus \ldots \oplus (\ell+j)$.

B.5 Continuum approximation and thermalization in the CFT spectrum

In every CFT, the density of states with energy $\Delta \gg \Delta_Q$ is expected to grow exponentially. This fact underlies the analysis of the strongly coupled case in sec. 4.3, where we study correlation functions of the non-Abelian components of the Noether current in a $SU(2)$-invariant CFT. In sec. B.5.1 we justify this statement. Motivated by the exponential density of states, in sec. B.5.2 we propose that the OPE coefficients $\lambda^{(\ell)}_{A,J_-,Q}$ in eq. (4.48) are described by an ansatz analogous to the eigenstate thermalization hypothesis (ETH) [125, 255, 256] for a strongly coupled theory. We then study the consequences of this ansatz for the correlator (4.50). As in sec. 4.3, we consider for concreteness a three-dimensional $SU(2)$-invariant CFT throughout this appendix.

B.5.1 The density of states

Here we estimate the density of states with energy $\sim \Delta_Q + \delta/\sqrt{2}$ with $1 \ll \delta \lesssim R\mu$ via a simple counting argument. To this aim, we suppose for simplicity that the CFT spectrum in this range consists only of the phonons discussed in sec. 3.2.2. Under this assumption, most possible states with fixed energy δ in the range of interest consist of n phonons with $1 \ll n \ll \delta$, each phonon having spin ℓ in the range $1 \ll \ell \ll \delta$. In this regime, we can reliably approximate the dispersion relation (3.25) with the simple expression $R\omega_\ell \simeq \ell/\sqrt{2}$. With these approximations at hand, we can easily proceed with a rough estimate of the density of states.

Consider first the n-phonon states whose gap above the ground state lies in the range

$$\Lambda_\delta = \left(\frac{\delta}{\sqrt{2}} - \frac{1}{2\sqrt{2}}, \frac{\delta}{\sqrt{2}} + \frac{1}{2\sqrt{2}}\right) . \tag{B.112}$$

Since $R\omega_\ell \simeq \ell/\sqrt{2}$, these are obtained considering all combinations of n integers ℓ_i, representing the angular momentum of each individual phonon, such that

$$\ell_1 + \ell_2 + \ldots + \ell_n = [\delta], \tag{B.113}$$

where $[x]$ denotes the integer part of x. To count the number of such states, we can solve eq. (B.113) for ℓ_n and sum over the remaining variables ℓ_i, $i = 1, \ldots, n-1$. Recalling that the multiplicity of an $SU(2)$ irrep. ℓ is given by $2\ell + 1$ and multiplying by $1/n!$ to avoid double counting, we find that the number of n-particle states with energy in the range (B.112) is given by

$$\begin{aligned} \#_\delta^{(n)} &\approx \frac{1}{n!} \sum_{\ell_1=1}^{\delta-n} \sum_{\ell_2=1}^{\delta-(n-1)} \cdots \sum_{\ell_{n-1}=1}^{\delta-1} \left[\prod_{i=1}^{n-1} (2\ell_i + 1)\right] \times \left[2\left(\delta - \sum_{i=1}^{n-1} \ell_i\right) + 1\right] \\ &\approx \frac{2^n}{n!(2n-1)!} \delta^{2n-1} . \end{aligned} \tag{B.114}$$

The overall number of states with energy included in the set (B.112) is obtained summing over n:

$$n_\Delta \approx \sum_{n=1}^{\sim\delta} \frac{2^n}{n!(2n-1)!} \delta^{2n-1} \approx \exp\left[\frac{3\,\delta^{2/3}}{2^{1/3}}\right] = \exp\left[\frac{3\,(\Delta - \Delta_Q)^{2/3}}{2^{2/3}}\right] , \tag{B.115}$$

where we dropped any sub-exponential dependence on $\delta \gg 1$.

Eq. (B.115) provides the exponential dependence of δ of the density of *all* states with energy δ. However, recalling that descendants are obtained considering the $\ell = 1$ mode of the phonon, it is easy to see that the density of primary states obeys a similar exponential behaviour. We expect a similar formula to hold for the density of states with energy δ in a given irreducible representation $\ell \ll \delta$ of the rotation group, but we did not prove it.

While the numerical coefficient in eq. (B.115) depends on our assumptions and, perhaps, our approximations, the behaviour $S \equiv \log n_\Delta \propto (\Delta - \Delta_Q)^{2/3}$ for the entropy of the system is general. Indeed, by the equivalence of the canonical and microcanonical ensembles in statistical mechanics, we expect the average properties of the CFT states with large energy to be given by thermodynamic averages at fixed temperature β^{-1} and chemical potential μ. Using that the entropy density scales as β^{-2} and that in a CFT the temperature is related to energy density above the ground state $\epsilon = (\Delta - \Delta_Q)/R^3$ as $\beta^{-1} \sim \epsilon^{1/3}$, we recover a behaviour similar to eq. (B.115) for the density of states $n_\Delta = e^S$. We refer to [176] for a detailed analysis of the thermodynamics of the superfluid phase of CFTs at large charge.

B.5.2 Continuum limit and thermalization of OPE coefficients

In a generic QFT, the matrix element of a light operator in between two states with large energy is expected to be effectively described by thermodynamics. Normally, this is quantitatively phrased in terms of the eigenstate thermalization hypothesis (ETH) [255,256]. In a CFT, this schematically states that the OPE coefficient for a light operator in between two states with large energy takes the following form [125]: [11]

$$\langle \Delta_A | \mathcal{O} | \Delta_B \rangle = \delta_{AB} \, \langle \mathcal{O} \rangle_\beta + R_{AB}^{\mathcal{O}} \sqrt{\frac{f_{\mathcal{O}}(E_A - E_B)}{n_{\bar{\Delta}}}} . \tag{B.116}$$

The first term of this formula states that the diagonal matrix elements of the light operator $\mathcal{O}$ in between two identical states with energy $E_{A/B} \gg 1$ is given by its thermal expectation value on average. Indeed, this property simply follows from the equivalence between the microcanonical and canonical ensemble in statistical mechanics. The second term in eq. (B.116) is less trivial. It is suppressed by the square root of the density of states n_Δ evaluated at $\bar{\Delta} \equiv \frac{\Delta_A + \Delta_B}{2}$. The $R_{AB}^{\mathcal{O}}$ are uncorrelated random variables with zero mean, unit variance and all other momenta of order unity. Finally, $f_{\mathcal{O}}(E_\alpha - E_\beta)$ is a smooth function, which may be related to the hydrodynamic two-point function of the operator $\mathcal{O}$ under certain hypotheses [176, 257].

Eq. (B.116) allows studying the OPE coefficients when the CFT spectrum is very dense at the energy of the two states $|\Delta_A\rangle$ and $|\Delta_B\rangle$ [125]. This idea has been recently explored in [176], where both neutral and charged heavy states were considered. There it was argued that the OPE coefficient of light operators in between states with energy $\Delta_{A/B} - \Delta_Q \gtrsim R\mu$ are governed by hydrodynamic fluctuations.

Here we consider instead the matrix-element for the current J_-^0 in between the superfluid ground state $|Q\rangle$ and a generic primary state $|\Delta_A, (\ell, m)\rangle$ with spin ℓ and energy $\Delta_A = \Delta_Q + \delta$, with $|\delta| \ll R\mu$:

$$\langle \Delta_A, (\ell, m) | J_-^0 | Q \rangle = \sqrt{\frac{4\pi}{2\ell + 1}} \times \lambda_{A, J_-, Q}^{(\ell)} \left[Y_m^\ell(\hat{n}) \right]^* e^{(\Delta_A - \Delta_Q)\tau/R} / R^2 . \tag{B.117}$$

---

[11] In (B.116) we neglect for simplicity the dependence on the angular momentum of $\mathcal{O}$ and the states.

These are the OPE coefficients which appear in eq. (4.48) and we expect the non-Abelian superfluid NREFT to provide informations on their average properties. To quantify this intuition, motivated by eq. (B.116) we assume that in a strongly coupled theory the OPE coefficients obey the following ansatz: [12]

$$\lambda^{(\ell)}_{A,J_-,Q} = R^{(\ell)}_A \sqrt{\frac{f_{J_-,Q}(\Delta_A - \Delta_Q)}{n^{(\ell)}_{\Delta_A}}}\,, \tag{B.118}$$

where $n^{(\ell)}_{\Delta}$ is the density of states with spin ℓ, energy Δ and charge $Q_3 = Q - 1$, $f_{J_-,Q}(\Delta_A - \Delta_Q)$ is a smooth function not growing exponentially and $R^{(\ell)}_A$ are uncorrelated random variables with zero mean, unit variance and all other momenta of order unity. The main difference with eq. (B.116) is that only one of the two states involved, namely $|\Delta_A, (\ell, m)\rangle$, belongs to the exponentially dense region of the spectrum. Correspondingly, the random variable depends on a single index.

At this stage, we are unable to justify eq. (B.118) if not by analogy with ETH. It would be interesting to investigate its validity in general theories. We leave this task for future work. Here we shall study instead the implications of eq. (B.118) for the continuum approximation discussed in sec. 4.3. Indeed eq. (B.118) provides a non-trivial setup in which to check the consistency of our ideas and estimate the accuracy of the approximations. We remark however that the analysis in the main text might hold even if eq. (B.118) will turn out to be wrong in the future.

Let us insert the ansatz (B.118) in eq. (4.50) replacing the infinitesimal ε with a finite $\bar{\varepsilon} > 0$. We find

$$\tilde{G}^{R\,(\ell)}_{J_+J_-}(\omega + i\bar{\varepsilon}) = \frac{i}{2\ell+1}\sum_{\phi^{(\ell)}_A} \frac{\left|R^{(\ell)}_A\right|^2}{n^{(\ell)}_{\Delta_A}} \frac{f_{J_-,Q}(\Delta_A - \Delta_Q)}{\omega - (\Delta_A - \Delta_Q)/R + i\bar{\varepsilon}} \equiv i\frac{\left|R^{(\ell)}_A\right|^2}{n^{(\ell)}_{\Delta_A}} F_A(\omega + i\bar{\varepsilon})\,, \tag{B.119}$$

where the sum runs over operators with charge $Q - 1$ and scaling dimensions in the range $[\Delta_Q - \delta, \Delta_Q + \delta]$ with $\delta \ll R\mu$ and we defined

$$F_A(\omega) \equiv \frac{f_{J_-,Q}(\Delta_A - \Delta_Q)}{(2\ell+1)\left[\omega - (\Delta_A - \Delta_Q)/R\right]}\,. \tag{B.120}$$

Due to the presence of the random variable, we should now formally treat (B.119) as a stochastic function; we distinguish it from the true CFT correlator via the supscript R. The physical observable is obtained upon taking its expectation value. Doing so and using $\left\langle \left| R^{(\ell)}_A \right|^2 \right\rangle = 1$, we easily see that we can turn the sum into an integral:

---

[12] A similar ansatz was recently proposed in [258] for $2d$ CFTs.

$$\begin{aligned}\tilde{G}^{(\ell)}_{J_+J_-}(\omega+i\bar{\varepsilon}) &= \left\langle \tilde{G}^{R\,(\ell)}_{J_+J_-}(\omega+i\bar{\varepsilon}) \right\rangle = \sum_A \frac{F_A\,(\omega+i\bar{\varepsilon})}{n^{(\ell)}_{\Delta_A}} \\ &= \frac{i}{2\ell+1}\int_{\Delta_Q-\delta}^{\Delta_Q+\delta} d\Delta \frac{f_{J_-,Q}(\Delta_A-\Delta_Q)}{\omega-(\Delta-\Delta_Q)/R+i\bar{\varepsilon}} + \mathcal{O}\left(\frac{1}{\bar{\varepsilon} n^{(\ell)}_{\Delta_Q}}\right) .\end{aligned} \tag{B.121}$$

From eq. (B.121) we identify $\rho^{reg\,(\ell)}_{J_-,Q}(\Delta) = f_{J_-,Q}(\Delta_A - \Delta_Q)$ in eq. (4.51). The estimate of the remainder in eq. (B.121) is obtained using standard calculus. However eq. (B.121) does not account for the corrections arising from the stochastic nature of the OPE coefficient (B.118). To estimate these contributions, we consider the variance of eq. (B.119):

$$\begin{aligned}\sigma^2 &= \left\langle \left| \tilde{G}^{R\,(\ell))}_{J_+J_-}(\omega+i\bar{\varepsilon}) - \left\langle \tilde{G}^{R\,(\ell))}_{J_+J_-}(\omega+i\bar{\varepsilon}) \right\rangle \right|^2 \right\rangle \\ &= \sum_{A,B} \left[\frac{F_A\,(\omega+i\bar{\varepsilon})\,F_B\,(\omega+i\bar{\varepsilon})}{n^{(\ell)}_{\Delta_A} n^{(\ell)}_{\Delta_B}} \left\langle \left|R^{(\ell)}_A\right|^2 \left|R^{(\ell)}_B\right|^2 \right\rangle \right] - \left[\sum_A \frac{F_A\,(\omega+i\bar{\varepsilon})}{n^{(\ell)}_{\Delta_A}} \right]^2 .\end{aligned} \tag{B.122}$$

From the assumption that the random variables $R^{(\ell)}_A$ are uncorrelated, we find

$$\left\langle \left|R^{(\ell)}_A\right|^2 \left|R^{(\ell)}_B\right|^2 \right\rangle = 1 + \delta_{AB} \times c_A \,, \tag{B.123}$$

where $c_A \geq 0$ is an order one quantity. Then, we obtain

$$\sigma^2 = \sum_A c_A \left[\frac{F_A\,(\omega+i\bar{\varepsilon})}{n^{(\ell)}_{\Delta_A}} \right]^2 \leq \max_{\Delta_A\in[\Delta_Q-\delta,\Delta_Q+\delta]} \left[c_A \frac{F_A\,(\omega+i\bar{\varepsilon})}{n^{(\ell)}_{\Delta_A}} \right] \times \tilde{G}^{(\ell)}_{J_+J_-}(\omega) \sim \frac{1}{\bar{\varepsilon}\, n^{(\ell)}_{\Delta_Q}} \,, \tag{B.124}$$

where the last estimate is obtained using that $f_{J_-,Q}(\Delta_A - \Delta_Q)$ and $\tilde{G}^{(\ell)}_{J_+J_-}(\omega)$ in eq. (B.121) do not depend exponentially on Δ_Q and recalling that $\delta \ll R\mu$. We conclude that, assuming eq. (B.118), the continuum approximation in eq. (4.51) holds up to corrections of order $\sigma \sim 1/\sqrt{\bar{\varepsilon}\, n^{(\ell)}_{\Delta_Q}}$.

C Appendices to Part III

C.1 Nambu-Goto action for superfluid vortices from the coset construction

In chapter 3, following [35], we argued that two charged scalar operators insertions in d dimensions at $x = 0$ and $x = \infty$ induce a specific symmetry breaking pattern for the leading trajectory in the path integral. A similar logic can be applied when the operators have also large spin J. As in the scalar case, translations P_μ, special conformal transformations K_μ and dilatation D are broken, with the combination $D + \mu Q$ left unbroken. Assuming the operator insertion to be polarized in the (x_1, x_2) plane, the Lorentz generators J_{1p}, J_{2p} with $p, q = 0, 3, \ldots$ must necessarily be broken. A vortex corresponds to the regime where it is energetically favorable for the system to still be in an almost homogeneous state, rotations being broken by a localized region of size $1/j_0 \sim R/Q^{\frac{1}{d-1}}$ in which the superfluid description breaks. This region naturally extends from 0 to ∞ along the directions orthogonal to the spin polarization, corresponding hence to a $d-2$ dimensional membrane. In this regime, J_{12} parametrizes rotation around the vortex and it is thus unbroken. We then identify the symmetry breaking pattern corresponding to a vortex as:

$$\begin{cases} \bar{D} = D + \mu\, Q, J_{12}, J_{pq} & \text{unbroken,} \\ D, P_\mu, K_\mu, J_{mp} & \text{broken.} \end{cases} \tag{C.1}$$

where we introduced the set of indices $m, n = 1, 2$ and $p, q = 0, 3, \ldots$.

As in appendix B.2, it is useful to rewrite the symmetry breaking pattern (C.1) in terms of the hatted generators (B.32), associated to a local chart of the cylinder. Focussing on

2 + 1 and 3 + 1 dimensions, we get

$$2+1:\begin{cases}\widehat{\bar{P}}_0=\widehat{P}_0+\mu\,Q,\widehat{J}_{12} & \text{unbroken,}\\ \widehat{P}_i,\widehat{J}_{0i},\widehat{K}_\mu,\widehat{Q} & \text{broken;}\end{cases}\qquad 3+1:\begin{cases}\widehat{\bar{P}}_p=\widehat{P}_p+\mu\delta^0_p\,Q,\widehat{J}_{12} & \text{unbroken,}\\ \widehat{P}_m,\widehat{J}_{0i},\widehat{J}_{n3},\widehat{K}_\mu,\widehat{Q} & \text{broken.}\end{cases}\tag{C.2}$$

From (C.2) we can construct the Nambu-Goto action for the vortex via the coset construction [26, 27], applied to the case of a membrane [64, 259].

C.1.1 2+1 dimensions

As in appendix B.2, we gauge all spacetime symmetries and specify the manifold only at the end of computations. We henceforth do not consider special conformal transformations anymore and work with the covariant derivative (B.34). From (C.1), the coset of a vortex line in 2 + 1 dimensions is formally identical to the conformal superfluid one

$$\Omega=e^{iy^a\bar{P}_a}e^{i\sigma D}e^{i\eta^iJ_{0i}}e^{i\pi Q}=e^{iy^aP_a}e^{i\sigma D}e^{i\eta^iJ_{0i}}e^{i\chi Q},\qquad \chi=\mu t+\pi,\tag{C.3}$$

where the notation is as in appendix B.2. The Maurer-Cartan (MC) one form reads thus as in eq. (B.36). One further need to consider the projection of the MC one form onto the vortex world-line $x^\mu(\lambda)$ [64]:

$$\dot{x}^\mu\Omega^{-1}D_\mu\Omega=iE\left(P_0+\nabla y^iP_i+\nabla\sigma D+\nabla\chi Q+\nabla\eta^iJ_{0i}+\frac{1}{2}\Omega^{ij}J_{ij}\right),\tag{C.4}$$

where

$$\begin{aligned}E&=\dot{x}^\mu e^{-\sigma}e^b_\mu\Lambda^0_b, &\qquad \nabla y^i&=E^{-1}\dot{x}^\mu e^{-\sigma}e^b_\mu\Lambda^i_b,\\ \nabla\chi&=E^{-1}\dot{x}^\mu\partial_\mu\chi, &\qquad \nabla\sigma&=E^{-1}\dot{x}^\mu\left(\partial_\mu\sigma+A_\mu\right).\end{aligned}\tag{C.5}$$

We can reduce the number of independent Goldstones setting to zero one or more of the invariants in (B.36), (B.38) or (C.4). When an algebraic solution exists, these conditions are called Inverse Higgs Constraints (IHCs) [63, 80]. In this case, the same IHCs (B.41) which lead to the superfluid action are imposed.

We now consider the leading order invariants in the world-line. Noticing that $\nabla\chi=\mu$ and $\nabla\sigma=0$, these are constructed out of the *einbein* E and the covariant derivative ∇y^i as:

$$\mu E=\dot{x}^\mu\partial_\mu\chi,\qquad \nabla y^i\nabla y^i=1-\frac{(\partial\chi)^2\dot{x}^\mu\dot{x}_\mu}{(\dot{x}^\mu\partial_\mu\chi)^2}.\tag{C.6}$$

The most general NG action is then written in terms of an arbitrary function:

$$S=\mu\int d\lambda\,E\,f\left(\nabla y^i\nabla y^i\right)=\int dt\sqrt{\dot{x}^\mu\dot{x}_\mu}(\partial\chi)F\left[\frac{(\dot{x}^\mu\partial_\mu\chi)^2}{(\partial\chi)^2\dot{x}^\mu\dot{x}_\mu}\right].\tag{C.7}$$

This is precisely the action in the last term of eq. (5.17).

C.1.2 3+1 dimensions

From (C.2), the coset is written as

$$\Omega = e^{iy^a P_a} e^{i\sigma D} e^{i\eta^i J_{0i}} e^{i\xi^n J_{n3}} e^{i\chi Q}. \tag{C.8}$$

We use indices $m, n = 1, 2$ and $p, q = 0, 3$. One can compute the MC one form as before

$$\Omega^{-1} D_\mu \Omega = i E^a_\mu \left(P_a + \nabla_a \sigma D + \nabla_a \chi Q + \nabla_a \eta^i J_{0i} + \nabla_a \xi^n J_{n3} + \Omega^{12}_a J_{12} \right); \tag{C.9}$$

with

$$E^a_\mu = e^{-\sigma} e^c_\mu \Lambda_c{}^b R_b{}^a, \qquad \nabla_a \chi = e^{\sigma} e^\mu_c \Lambda^c{}_b R^b{}_a \partial_\mu \chi, \qquad \nabla_a \sigma = e^{\sigma} e^\mu_c \Lambda^c{}_b R^b{}_a \left(\partial_\mu \sigma + A_\mu \right). \tag{C.10}$$

Here we introduced another Lorentz matrix $(e^{-i\xi^n J_{n3}})^a{}_b = R_b{}^a$. Curvature invariants are written as before. The MC form projected on the vortex world-sheet $X^\mu(\tau, \sigma)$ reads:

$$\partial_\alpha X^\mu \Omega^{-1} D_\mu \Omega = i E^p_\alpha \left(P_p + \nabla_p y^n P_n + \nabla_p \sigma D + \nabla_p \chi Q + \nabla_p \eta^i J_{0i} + \nabla_p \xi^n J_{n3} + \Omega^{12}_p J_{12} \right), \tag{C.11}$$

where $\alpha = \tau, \sigma$ and

$$\begin{gathered} E^p_\alpha = \partial_\alpha X^\mu e^{-\sigma} e^c_\mu \Lambda_c{}^b R_b{}^p, \qquad \nabla_p y^n = E^\alpha_p \partial_\alpha X^\mu e^{-\sigma} e^c_\mu \Lambda_c{}^b R_b{}^n, \\ \nabla_p \chi = E^\alpha_p \partial_\alpha X^\mu \partial_\mu \chi, \qquad \nabla_p \sigma = E^\alpha_p \partial_\alpha X^\mu \left(\partial_\mu \sigma + A_\mu \right). \end{gathered} \tag{C.12}$$

Here E^α_p is the inverse of the world-sheet vielbein: $E^p_\alpha E^\alpha_q = \delta^p_q$, $E^p_\alpha E^\beta_p = \delta^\alpha_\beta$. As before, the IHCs (B.41) are imposed. Since $[P_3, J_{n3}] \sim P_n$, we can also eliminate ξ^n imposing the following IHC

$$\nabla_3 y^n = 0 \qquad \Longrightarrow \qquad \frac{\xi^n}{\xi} \tan \xi = \frac{v^n}{v^3}, \tag{C.13}$$

where the vector v^i is given by

$$v^i = \frac{\left(\partial_3 X^\mu \partial_\mu \chi \right) \left(\partial_0 X^\mu e^c_\mu \Lambda_c{}^i \right) - \left(\partial_0 X^\mu \partial_\mu \chi \right) \left(\partial_3 X^\mu e^c_\mu \Lambda_c{}^i \right)}{(\partial \chi) \sqrt{-\det(G_{\alpha\beta})\, h_{\alpha\beta} G^{\alpha\beta}}}. \tag{C.14}$$

Here $G_{\alpha\beta}$ and $h_{\alpha\beta}$ are:

$$G_{\alpha\beta} = g_{\mu\nu} \partial_\alpha X^\mu \partial_\beta X^\nu, \qquad h_{\alpha\beta} = \frac{\partial_\mu \chi \partial_\nu \chi}{(\partial \chi)^2} \partial_\alpha X^\mu \partial_\beta X^\nu. \tag{C.15}$$

These expression agree with the previous definitions (6.27) and (6.28). Since $\nabla_p \chi = \mu \delta^0_p$ and $\nabla_p \sigma = 0$, leading order invariants are built out of the following objects

$$\mu^2 \det(E^p_\alpha) = (\partial \chi)^2 \sqrt{|\det(G_{\alpha\beta})|} \sqrt{G^{\alpha\beta} h_{\alpha\beta}}, \qquad \nabla_0 y^n \nabla_0 y^n = 1 - \frac{1}{h_{\alpha\beta} G^{\alpha\beta}}. \tag{C.16}$$

One finally writes the leading order action as

$$S=\mu^2\int d\tau d\sigma\,\det E^p_\alpha\, f\left(\nabla_0 y^n\nabla_0 y^n\right)=\int d\tau d\sigma(\partial\chi)^2\sqrt{|\det(G_{\alpha\beta})|}F[G^{\alpha\beta}h_{\alpha\beta}]. \tag{C.17}$$

Using (6.18), this agrees with the last line in (6.26).

C.2 Photon propagator on the sphere

Here we obtain the photon propagator on a D dimensional sphere following the simple method of [260, 261]. [1] In this section we set $R=1$.

Consider the action of a massless vector field coupled to a conserved current J^μ (in Euclidean signature):

$$S=\int d^Dx\sqrt{g}\left(\frac{1}{4}f_{\mu\nu}f^{\mu\nu}-a_\mu J^\mu\right),\qquad f_{\mu\nu}=\partial_\mu a_\nu-\partial_\nu a_\mu. \tag{C.18}$$

The gauge field on the equations of motion is given by

$$a_\mu(x)=\int d^Dx'\sqrt{g'}G_{\mu\nu'}(x,x')J^{\nu'}(x'), \tag{C.19}$$

where $G_{\mu\nu'}(x,x')$ satisfies the equation

$$\nabla^\mu\left(\partial_\mu G_{\nu\nu'}(x,x')-\partial_\nu G_{\mu\nu'}(x,x')\right)=-g_{\nu\nu'}(x)\frac{\delta(x-x')}{\sqrt{g'}}+\partial_{\nu'}\Lambda_\nu(x,x'). \tag{C.20}$$

Here Λ_ν is a pure gauge term which drops from physical observables; primed and unmprimed indices refer, respectively, to the points x and x'.

Let us define the following biscalar

$$u=\frac{1}{2}(X-X')^2, \tag{C.21}$$

where $(X-X')^2$ is the chordal distance in embedding coordinates. Given the isometries of the sphere, it is possible to parametrize the propagator as

$$G_{\nu\nu'}(x,x')=-\left(\partial_\nu\partial_{\nu'}u\right)F(u)+\partial_\nu\partial_{\nu'}S(u). \tag{C.22}$$

The last term is gauge dependent and drops from eq. (C.19).

The following properties hold:

1. $\nabla^\mu\partial_\mu u=d(1-u)$,

---

[1] A similar derivation in $4d$ de Sitter can be found in [262].

2. $g^{\mu\nu}\partial_\mu u \partial_\nu u = u(2-u)$,
3. $\nabla_\mu \partial_\nu u = g_{\mu\nu}(1-u)$,
4. $(\nabla^\mu u)(\nabla_\mu \partial_{\nu'} u) = (1-u)\partial_{\nu'} u$,
5. $(\nabla^\mu u)(\nabla_\mu \partial_\nu \partial_{\nu'} u) = -\partial_\nu u \partial_{\nu'} u$.

These can be explicitly verified in stereographic coordinates, for instance. It follows

$$\begin{aligned}\nabla^\mu\left(\partial_\mu G_{\nu\nu'}(x,x') - \partial_\nu G_{\mu\nu'}(x,x')\right) = &-\left(\partial_\nu \partial_{\nu'} u\right)\left[u(2-u)F'' + (d-1)(1-u)F'\right] \\ &+ \left(\partial_\nu u \partial_{\nu'} u\right)\left[(1-u)F'' + (1-d)F'\right]. \end{aligned} \tag{C.23}$$

By symmetry, we can write $\Lambda_\nu(x,x') = (\partial_\nu u)\Lambda(u)$. Then for $x \neq x'$ (C.20) gives two equations:

$$u(2-u)F'' + (d-1)(1-u)F' = -\Lambda, \tag{C.24}$$

$$(1-u)F'' - (d-1)F' = \Lambda'. \tag{C.25}$$

We can integrate the second and plug the result in the first to obtain

$$(2-u)uF''(u) + d(1-u)F'(u) - (d-2)F(u) = 0. \tag{C.26}$$

This is just Klein Gordon equation for a scalar field of mass $m^2 = D-2$ on S^D. The solution is fixed requiring a power low singularity for $u \to 0$ and regularity at the antipodal point $u \to 2$ [263]:

$$F(u) = \frac{\Gamma(D-2)}{(4\pi)^{\frac{D}{2}}\Gamma\left(\frac{D}{2}\right)}\, {}_2F_1\left(1, D-2; \frac{D}{2}; 1-\frac{u}{2}\right), \qquad D > 2. \tag{C.27}$$

The normalization is determined matching the short distance limit with the flat space propagator. Plugging in (C.22) and setting $D = d-1$, we get eq. (6.36) in the main text.

C.3 Vortex energy in 4d via dimensional regularization

To regulate the computation of the magnetostatic energy, it is convenient to work in d spacetime dimensions. It is natural to modify the Lagrangian (6.17) in a way which preserves Weyl invariance:

$$\mathcal{L} = -\kappa H^{d/3}. \tag{C.28}$$

The definition of H in terms of the two-form field $A_{\mu\nu}$ here is unchanged. Notice that working in arbitrary d with a 2-form field we loose the duality with a shift invariant scalar; instead, within this regularization the $U(1)$ symmetry is promoted to a $d-3$–form symmetry at intermediate steps in the calculation. [2] An alternative approach might be to promote $A_{\mu\nu}$ to a $d-2$ form field, preserving the Weyl invariance of the action. A more detailed investigation of this issue might be helpful in expanding our results to subleading orders.

Expanding the action (C.28) to quadratic order gives

$$\mathcal{L}_{fluct} = \frac{1}{4e^2(d)} f_{ij} f^{ij} + \frac{1}{2e^2(d)} \left[\dot{b}^i \dot{b}_i - \frac{(d-3)}{3} (\nabla_i b^i)^2 \right], \tag{C.29}$$

where we defined the electric coupling in d spacetime dimensions as

$$e^2(d) = \frac{\left(\sqrt{6}B\right)^{2-\frac{d}{3}}}{2d\kappa} = e^2 \left[1 - (d-4) \left(\log B^{\frac{1}{3}} + \frac{1}{4} + \frac{1}{6} \log 6 \right) + \mathcal{O}\left((d-4)^2\right) \right]. \tag{C.30}$$

The NG action discussed in section 6.2.2 is unchanged in d dimensions.

C.3.1 Vortex ring self-energy

Consider a single vortex moving on a trajectory given by (6.41). We want to compute the self-energy contribution due to the hydrophoton, i.e. the second term in eq. (6.43). In Hopf coordinates (6.13) and in dimensional regularization, it reads:

$$E_{mag} = \frac{e^2(d)}{2} R^2 \iint d\xi d\xi' G_{\xi\xi} \left((\eta, \xi, \phi); (\eta, \xi', \phi) \right) = \pi R e^2(d) R^{4-d} I(r,d), \tag{C.31}$$

where we isolated the integral

$$I(r,d) = r^2 \frac{\Gamma(d-3)}{(4\pi)^{\frac{d-1}{2}} \Gamma\left(\frac{d-1}{2}\right)} \int_0^{2\pi} d\xi \cos(\xi) \, {}_2F_1\left(1, d-3; \frac{d-1}{2}; 1 - \frac{1}{2} r^2 (1-\cos\xi)\right). \tag{C.32}$$

In $d=4$, the integral is logarithmically divergent for $\xi \to 0$, corresponding to the interaction of an infinitesimal line element with itself.

Setting $\frac{1}{2}(1-\cos\xi) = y$ in (C.32), we get

$$I(r,d) = 2r^2 \frac{\Gamma(d-3)}{(4\pi)^{\frac{d-1}{2}} \Gamma\left(\frac{d-1}{2}\right)} \int_0^1 dy \frac{(1-2y)}{\sqrt{(1-y)y}} \, {}_2F_1\left(1, d-3; \frac{d-1}{2}; 1 - r^2 y\right). \tag{C.33}$$

The divergent part comes from the first term in the expansion of the hypergeometric function when the argument goes to one:

$${}_2F_1(a,b;c;1-z) \xrightarrow{z\to 0} \frac{1}{z^{a+b-c}} \frac{\Gamma(c)\Gamma(a+b-c)}{\Gamma(a)\Gamma(b)}, \qquad a+b>c. \tag{C.34}$$

---

[2] Conversely, a cutoff approach as in chapter 5 breaks Weyl invariance.

We separate explicitly this contribution and recast the integral as:

$$I(r,d) = I_{div}(r,d) + I_{reg}(r,d), \tag{C.35}$$

where the divergent piece is

$$\begin{aligned} I_{div}(r,d) &= 2r^2 \frac{\Gamma\left(\frac{d-3}{2}\right)}{(4\pi)^{\frac{d-1}{2}}} \int_0^1 dy \frac{(1-2y)}{\sqrt{(1-y)y}} \left(\frac{1}{r^2 y}\right)^{\frac{d-3}{2}} \\ &= \frac{r}{2\pi(4-d)} + \frac{r\left[\log\left(4\pi r^2\right) - \gamma_E - 2\psi\left(3/2\right)\right]}{4\pi} + \mathcal{O}\left(4-d\right), \end{aligned} \tag{C.36}$$

and the regular part can be evaluated directly in $d=4$, where it reads

$$I_{reg}(r) \equiv I_{reg}(r,4) = \frac{r}{2\pi^2} \int_0^1 dy \frac{(1-2y)}{y\sqrt{1-y}} \left[\frac{\arcsin\left(\sqrt{1-r^2 y}\right)}{\sqrt{1-r^2 y}} - \frac{\pi}{2}\right]. \tag{C.37}$$

To compute the latter, it is convenient to use the following expansion

$$\frac{\arcsin\left(\sqrt{1-x^2}\right)}{\sqrt{1-x^2}} = \sum_{m=0}^{\infty} \frac{-(-2)^{m+1}\Gamma\left(\frac{m+3}{2}\right)^2}{(m+1)^2} \frac{x^m}{m!}, \qquad 0 \leq x < 1. \tag{C.38}$$

Interchanging sum and integral, the regular part gives

$$I_{reg}(r) = \frac{r^2}{4\pi^2} \sum_{m=1}^{\infty} \frac{(-1)^{m+1} 2\pi (m-1) r^{m-1}}{m(m+1)} = \frac{r}{\pi} - \frac{r}{2\pi}\log(r+1) - \frac{1}{\pi}\log(r+1). \tag{C.39}$$

Collecting everything and adding the tension contribution, we arrive at (6.44).

C.3.2 Kelvin waves frequency

The EOMs which derive from (6.59) give the oscillation frequency of Kelvin waves as

$$\frac{1}{2} B\omega_n = \gamma \frac{\pi B^{2/3}}{R^2}\left(n^2-1\right) + \frac{2\pi e^2(d) R^{4-d}}{R^2} \delta\omega_n^I, \tag{C.40}$$

where the second term comes from the nonlocal piece of the action and is written in terms of the following integral:

$$\begin{aligned} \delta\omega_n^I = \frac{1}{2}\int d\sigma \Big\{ &\left[n^2\cos(n\sigma) - \cos\sigma\right] F(1-\cos\sigma) \\ &+ \left[\cos^2\sigma - \cos(n\sigma)\cos\sigma\right] F'(1-\cos\sigma) \Big\}. \end{aligned} \tag{C.41}$$

Let us sketch the evaluation of (C.41). Changing variables as before, we write $\delta\omega_n^I$ as the sum of the following two contributions:

$$\begin{aligned} I_1(n) = {} & \frac{\Gamma(d-3)}{(4\pi)^{\frac{d-1}{2}}\Gamma\left(\frac{d-1}{2}\right)} \\ & \times \int_0^1 \frac{dy}{\sqrt{y(1-y)}} \left[n^2 T_n(1-2y) - (1-2y)\right] {}_2F_1(1, d-3; \frac{d-1}{2}; 1-y)\,, \end{aligned} \tag{C.42}$$

$$\begin{aligned} I_2(n) = {} & \frac{\Gamma(d-2)/2}{(4\pi)^{\frac{d-1}{2}}\Gamma\left(\frac{d+1}{2}\right)} \\ & \times \int_0^1 \frac{dy(1-2y)}{\sqrt{y(1-y)}} \left[T_n(1-2y) - (1-2y)\right] {}_2F_1(2, d-2; \frac{d+1}{2}; 1-y)\,. \end{aligned} \tag{C.43}$$

Here $T_n(x) = \cos\left(n \arccos(x)\right)$ is a Chebyshev polynomial. The divergent contributions are identified from the leading term of the Hypergeometric expansion (C.34) and can be evaluated using

$$\int_0^1 dy \frac{T_n(1-2y)}{\sqrt{y(1-y)}} y^{m-\frac{1}{2}} = \frac{\sqrt{\pi}\Gamma(m)\left(\frac{1}{2}-m\right)_n}{\Gamma\left(m+n+\frac{1}{2}\right)}\,. \tag{C.44}$$

To evaluate the regular parts, we use the following results:

$$\begin{aligned} \lambda_n \equiv {} & \int_0^1 dy \frac{T_n(1-2y)}{\sqrt{y(1-y)}} \left[\frac{\arcsin\left(\sqrt{1-y}\right)}{\sqrt{y}\sqrt{1-y}} - \frac{\pi}{2\sqrt{y}}\right] \\ = {} & \frac{\pi}{2}\left[\psi\left(\frac{n}{2}+1\right) + 2\psi\left(n+\frac{1}{2}\right) - \psi\left(\frac{n+1}{2}\right) - 2\psi\left(n+1\right)\right]\,, \end{aligned} \tag{C.45}$$

$$\begin{aligned} \rho_n \equiv {} & \int_0^1 dy \frac{1-2y}{\sqrt{y(1-y)}} T_n(1-2y) \left[{}_2F_1\left(2, 2; \frac{5}{2}; 1-y\right) - \frac{3\pi}{8y^{3/2}} + \frac{3\pi}{16y^{1/2}}\right] \\ = {} & \frac{3}{2}\pi\left\{\left(n^2+1\right)\left[\psi\left(\frac{n-1}{2}\right) - \psi\left(n-\frac{1}{2}\right) + \log 2\right] + \frac{4n^4+6n^2+3n-1}{4n^3-4n^2-n+1} + \frac{3}{8}\right\}\,. \end{aligned} \tag{C.46}$$

Using `Mathematica` we computed these integrals explicitly for fixed integer values of n and identified their functional form; the result was then verified numerically and using the $n \to \infty$ asymptotic expansion of the results (C.45) and (C.46). This indeed can be obtained explicitly truncating the series expansion of the Hypergeometric functions in the integrals and using (C.44). The regular contributions finally read

$$I_1^{reg}(n) = \frac{1}{4\pi^2}\left(n^2\lambda_n - \lambda_1\right)\,, \tag{C.47}$$

$$\begin{aligned} I_2^{reg}(n) &= \frac{1}{12\pi^2}(\rho_n - \rho_1) - \frac{1}{64\pi}\int_0^1 dy \frac{(1-2y)\left[T_n(1-2y)-(1-2y)\right]}{y\sqrt{(1-y)}} \\ &= \frac{1}{12\pi^2}(\rho_n - \rho_1) + \frac{3\psi\left(n+\frac{1}{2}\right) + 3\gamma_E - 4 + \log(64) - \frac{6}{4n^2-1}}{96\pi} . \end{aligned} \tag{C.48}$$

The second contribution in (C.48) arises since we subtracted the $\mathcal{O}\left(1/\sqrt{y}\right)$ term in the expansion of the Hypergeometric function from the first piece, in order to apply (C.46). Collecting everything and expanding for $d \to 4$, we find the following remarkably simple result:

$$\delta\omega_n^I = \frac{n^2-1}{8\pi(4-d)} + \frac{\left(n^2-1\right)\left[\log\pi - 2\psi\left(\frac{n+1}{2}\right) - \gamma_E - 1\right]}{16\pi} + \mathcal{O}\left(4-d\right) . \tag{C.49}$$

Eq. (6.61) then follows.

D Appendices to Part IV

D.1 Diagrammatic two loop computation in $\lambda|\phi|^4$

In this section we compute the anomalous dimension of the $[\phi^n]$ operator to two loop via diagrammatic techniques. For simplicity, we work in momentum space and we consider an insertion of the operator ϕ^n within n equal incoming momenta p. We want to compute, according to the definitions (7.3),(7.9):

$$\langle \phi^n \bar{\phi}(p)\bar{\phi}(p)\dots\bar{\phi}(p)\rangle = Z_{\phi^n} Z_\phi^n \langle [\phi^n]\,[\bar{\phi}](p)\,[\bar{\phi}](p)\dots[\bar{\phi}](p)\rangle \tag{D.1}$$

and find the right renormalization constant Z_{ϕ^n} such that $\langle [\phi^n]\,[\bar{\phi}](p)\,[\bar{\phi}](p)\dots[\bar{\phi}](p)\rangle$ is finite in the minimal subtraction (MS) scheme. At two loop Z_ϕ is [113]

$$Z_\phi = 1 - \frac{\lambda^2}{(16\pi^2)^2 8\varepsilon} + \mathcal{O}(\lambda^3). \tag{D.2}$$

We work within renormalized perturbation theory, the Feynman rules are:

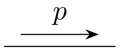

$= \dfrac{1}{p^2}\,,$

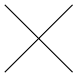

$= \,-\lambda\,,$

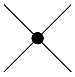

$= \,-\delta_\lambda\,,$ (D.3)

where $\delta_\lambda = \frac{5\lambda^2}{16\pi^2\varepsilon}$ is the coupling counterterm at one loop in MS [113]. The ϕ^n operator will be represented by a crossed vertex and normalized to

$$\otimes = 1. \tag{D.4}$$

All diagrams to two loop are displayed in figure D.1. We don't represent the incoming lines if they are directly connected to the ϕ^n operator, only those connected to other vertices are shown.

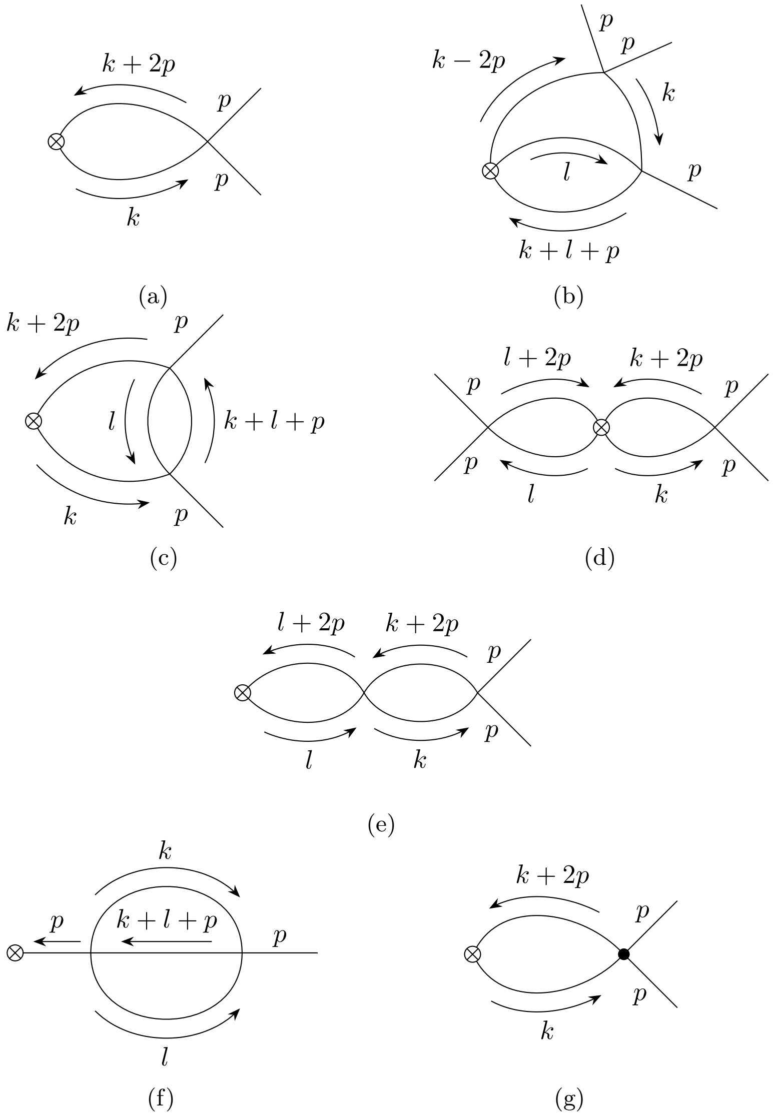
k + 2p
p
p
k
(a)
k − 2p
p
p
k
l
p
k + l + p
(b)
k + 2p
p
l
k + l + p
k
p
(c)
l + 2p
k + 2p
p
p
p
p
l
k
(d)
l + 2p
k + 2p
p
p
l
k
(e)
k
p
k + l + p
p
l
(f)
k + 2p
p
p
k
(g)

Figure D.1 – Feynman diagrams that contribute at two-loops.

The one loop diagram is:

$$
\begin{aligned}
(\mathrm{a}) = \; & \frac{n(n-1)}{2}\frac{1}{2}(-\lambda)\int\frac{\mathrm{d}^d k}{(2\pi)^d}\frac{1}{k^2}\frac{1}{(k+2p)^2} \\
= \; & -\frac{\lambda}{16\pi^2}\frac{n(n-1)}{4}\left(\frac{2}{\varepsilon}+2-\gamma+\log\left(\frac{\pi M^2}{p^2}\right)\right)+\mathcal{O}(\varepsilon)
\end{aligned}
\tag{D.5}
$$

where in the first line, the first factor $\frac{n(n-1)}{2}$ indicates the number of ways the external momenta can be connected to form this diagram: one has to chose 2 momenta among n. The next factor $\frac{1}{2}$ is the usual symmetry factor, then comes the vertex, and finally the loop integral. In the result, M is the scale introduced in (7.3).

Six diagrams have to be computed at two loop level. We need only the divergent piece of these diagrams. The procedure to compute the first two diagrams is described in [107]. The last diagram includes the one loop counterterm δ_λ.

$$\begin{aligned}(b) &= \frac{n(n-1)(n-2)}{2}\frac{1}{2}(-\lambda)^2\int\frac{\mathrm{d}^dk}{(2\pi)^d}\int\frac{\mathrm{d}^dl}{(2\pi)^d}\frac{1}{k^2}\frac{1}{(k-2p)^2}\frac{1}{l^2}\frac{1}{(k+l+p)^2} \\ &= \frac{\lambda^2}{(16\pi^2)^2}\frac{n(n-1)(n-2)}{4}\left(\frac{2}{\varepsilon^2}+\frac{5-2\gamma+2\log\left(\frac{\pi M^2}{p^2}\right)}{\varepsilon}\right)+\mathcal{O}(\varepsilon^0)\end{aligned} \tag{D.6}$$

$$\begin{aligned}(c) &= \frac{n(n-1)}{2}(-\lambda)^2\int\frac{\mathrm{d}^dk}{(2\pi)^d}\int\frac{\mathrm{d}^dl}{(2\pi)^d}\frac{1}{k^2}\frac{1}{(k+2p)^2}\frac{1}{l^2}\frac{1}{(k+l+p)^2} \\ &= \frac{\lambda^2}{(16\pi^2)^2}\frac{n(n-1)}{2}\left(\frac{2}{\varepsilon^2}+\frac{5-2\gamma+2\log\left(\frac{\pi M^2}{p^2}\right)}{\varepsilon}\right)+\mathcal{O}(\varepsilon^0)\end{aligned} \tag{D.7}$$

$$\begin{aligned}(d) &= \frac{n(n-1)(n-2)(n-3)}{8}\frac{1}{4}(-\lambda)^2\left(\int\frac{\mathrm{d}^dk}{(2\pi)^d}\frac{1}{k^2}\frac{1}{(k+2p)^2}\right)^2 \\ &= \frac{\lambda^2}{(16\pi^2)^2}\frac{n(n-1)(n-2)(n-3)}{8}\left(\frac{1}{\varepsilon^2}+\frac{2-\gamma+\log\left(\frac{\pi M^2}{p^2}\right)}{\varepsilon}\right)+\mathcal{O}(\varepsilon^0)\end{aligned} \tag{D.8}$$

$$\begin{aligned}(e) &= \frac{n(n-1)}{2}\frac{1}{4}(-\lambda)^2\left(\int\frac{\mathrm{d}^dk}{(2\pi)^d}\frac{1}{k^2}\frac{1}{(k+2p)^2}\right)^2 \\ &= \frac{\lambda^2}{(16\pi^2)^2}\frac{n(n-1)}{2}\left(\frac{1}{\varepsilon^2}+\frac{2-\gamma+\log\left(\frac{\pi M^2}{p^2}\right)}{\varepsilon}\right)+\mathcal{O}(\varepsilon^0)\end{aligned} \tag{D.9}$$

$$\begin{aligned}(f) &= n\frac{1}{2}(-\lambda)^2\frac{1}{p^2}\int\frac{\mathrm{d}^dk}{(2\pi)^d}\int\frac{\mathrm{d}^dl}{(2\pi)^d}\frac{1}{k^2}\frac{1}{l^2}\frac{1}{(k+l+p)^2} \\ &= -\frac{\lambda^2}{(16\pi^2)^2}\frac{n}{4\varepsilon}+\mathcal{O}(\varepsilon^0)\end{aligned} \tag{D.10}$$

$$\begin{aligned}(g) &= \frac{n(n-1)}{2}\frac{1}{2}(-\delta_\lambda)\int\frac{\mathrm{d}^dk}{(2\pi)^d}\frac{1}{k^2}\frac{1}{(k+2p)^2} \\ &= -\frac{\lambda^2}{(16\pi^2)^2}\frac{5n(n-1)}{4}\left(\frac{2}{\varepsilon^2}+\frac{2-\gamma+\log\left(\frac{\pi M^2}{p^2}\right)}{\varepsilon}\right)+\mathcal{O}(\varepsilon^0)\end{aligned} \tag{D.11}$$

Summing all contributions we get:

$$\begin{aligned}
&(D.4)+(D.5)+(D.6)+(D.7)+(D.8)+(D.9)+(D.10)+(D.11)\\
=&\left(1-\frac{\lambda n(n-1)}{(16\pi^2)2\varepsilon}+\frac{\lambda^2}{(16\pi^2)^2}\left(\frac{n^4-2n^3-9n^2+10n}{8\varepsilon^2}+\frac{n^3-n^2-n}{4\varepsilon}\right)\right)\\
&\times\left(1-\frac{\lambda n(n-1)\left(2-\gamma+\log\left(\frac{\pi M^2}{p^2}\right)\right)}{4(16\pi^2)}\right)+\mathcal{O}(\varepsilon,\lambda^2\varepsilon^0)
\end{aligned} \tag{D.12}$$

where the result, following (D.1), has been factored as $Z_{\phi^n}Z_{\phi}^{n}$, which contains only poles according to MS prescription, times the finite value of $\langle[\phi^n]\,[\bar\phi](p)\,[\bar\phi](p)\ldots[\bar\phi](p)\rangle$. This lets us compute the renormalization factor Z_{ϕ^n} using (D.2):

$$Z_{\phi^n}=1-\frac{\lambda n(n-1)}{(16\pi^2)2\varepsilon}+\frac{\lambda^2}{(16\pi^2)^2}\left(\frac{n^4-2n^3-9n^2+10n}{8\varepsilon^2}+\frac{2n^3-2n^2-n}{8\varepsilon}\right).$$

The anomalous dimension γ_{ϕ^n} is computed using (7.10) and yields (7.15).

D.2 One loop computation on the cylinder in $\lambda|\phi|^4$

D.2.1 Next to leading order corrections for generic λn

Here we discuss the derivation of (7.77) from (7.62). To this aim, we first compute $\bar e_0$ expanding the first line in (7.47) from the expression of the bare coupling (7.5):

$$\begin{aligned}
\bar e_0(\lambda n,RM,d)=e_0(\lambda n,d)+\Bigg\{&\frac{5}{8}(\mu^2R^2-1)^2\left[\frac{1}{\varepsilon}-\log(M\tilde R)\right]\\
&+\frac{1}{16}(\mu^2R^2+3)(\mu^2R^2-1)+\mathcal{O}(\varepsilon)\Bigg\}_{\lambda_0=\lambda},
\end{aligned} \tag{D.13}$$

where we defined $\tilde R\equiv\sqrt{\pi}e^{\gamma/2}R$ and we used the equations of motion (7.60) to expand the leading order in the coupling:

$$\frac{\partial}{\partial\lambda_0}\left[\frac{e_{-1}(\lambda_0 n,d)}{\lambda_0 R}\right]=\frac{R^{d-1}\Omega_{d-1}f^4}{16}. \tag{D.14}$$

To compute Δ_0 in (7.48), we need to evaluate (D.13) in $d=4$ and add the expansion of the leading order $\bar e_{-1}/\lambda$ to first order in ε (at fixed coupling)

$$\begin{aligned}
\Delta_0 &= \left\{\bar e_0(\lambda n,RM,4)+\frac{\partial}{\partial\varepsilon}\left[\frac{1}{\lambda}\bar e_{-1}(\lambda n,RM,4-\varepsilon)\right]_{\varepsilon=0}\right\}_{\lambda=\lambda_*}\\
&= \left\{\lim_{\varepsilon\to0}\left[\frac{R}{2}\sum_{\ell=0}^{\infty}n_{\ell,d}\left[\omega_+(\ell)+\omega_-(\ell)\right]+\frac{5}{8\varepsilon}(\mu^2R^2-1)^2\right]\right\}_{\lambda_0=\lambda_*}
\end{aligned} \tag{D.15}$$

where the limit $\varepsilon \to 0$ is taken at λ_0 fixed, we used eq. (7.8) and

$$\frac{1}{\lambda}\bar{e}_{-1}(\lambda n, RM, 4-\varepsilon) = \frac{1}{\lambda M^{\varepsilon}} e_{-1}(\lambda n M^{\varepsilon}, 4-\varepsilon). \tag{D.16}$$

As anticipated, at the fixed point the dependence on the sliding scale drops.

To proceed, we need to isolate the divergent contribution in the sum in eq. (D.15). We use the $\ell \to \infty$ expansion of the summand

$$n_{\ell,d}\left[\omega_+(\ell) + \omega_-(\ell)\right] \sim \sum_{n=1}^{\infty} c_n \ell^{d-n}. \tag{D.17}$$

The first five terms provide a divergent contribution in $d = 4$. The expansion in $4-\varepsilon$ dimensions of the coefficients is

$$\begin{gathered} c_1 = \frac{2}{R} + \mathcal{O}(\varepsilon), \quad c_2 = \frac{6}{R} + \mathcal{O}(\varepsilon), \quad c_3 = 2\mu^2 R + \frac{4}{R} + \mathcal{O}(\varepsilon), \quad c_4 = 2\mu^2 R + \mathcal{O}(\varepsilon), \\ c_5 = -\frac{5\left(\mu^2R^2-1\right)^2}{4R} + \varepsilon \frac{\left[113 + 50\mu^2R^2 - 225\mu^4R^4 + 150\gamma\left(\mu^2R^2-1\right)^2 +\right]}{120R} + \mathcal{O}\left(\varepsilon^2\right). \end{gathered} \tag{D.18}$$

We can now rewrite the sum isolating explicitly the divergent contribution as

$$\frac{1}{2}\sum_{\ell=0}^{\infty} n_{\ell,d}\left[\omega_+(\ell) + \omega_-(\ell)\right] = \frac{1}{2}\sum_{n=1}^{5} c_n \sum_{\ell=1}^{\infty} \ell^{d-n} + \frac{1}{2}\sum_{\ell=1}^{\infty}\bar{\sigma}(\ell) + \frac{1}{2}\omega_+(0), \tag{D.19}$$

where $\bar{\sigma}(\ell)$ is defined subtracting the first five terms in (D.17) from the original summand,

$$\bar{\sigma}(\ell) = n_{\ell,d}\left[\omega_+(\ell) + \omega_-(\ell)\right] - \sum_{n=1}^{5} c_n \ell^{d-n}, \tag{D.20}$$

and we used that $\omega_-(0) = 0$. From (D.17) we see that the sum over $\bar{\sigma}(\ell)$ is convergent and can be evaluated directly in $d = 4$. The first terms provide a divergent contribution which can be computed using $\sum_{\ell=1}^{\infty} \ell^x = \zeta(-x)$ and recalling $\zeta(1-\varepsilon) \sim -1/\varepsilon$:

$$\frac{1}{2}\sum_{n=1}^{5} c_n \sum_{\ell=1}^{\infty} \ell^{d-n} = -\frac{5\left(\mu^2R^2-1\right)^2}{8R\varepsilon} - \frac{15\mu^4R^4 - 6\mu^2R^2 + 7}{16R}. \tag{D.21}$$

Using eq.s (D.19) and (D.21) in (D.15), we obtain the result in the main text (7.77).

D.2.2 Next to leading order corrections for large λn

Here we discuss the derivation of the result (7.81). To this aim, it is convenient to start from eq. (D.15), derived in the previous appendix. We denote the summand in (7.76) with the bare coupling replaced by the renormalized one as

$$s(\ell,d)\equiv n_{\ell,d}R\left[\omega_+(\ell)+\omega_-(\ell)\right]_{\lambda_0=\lambda}. \tag{D.22}$$

We then separate the sum over $s(\ell,d)$ into two terms introducing a cutoff $AR\mu$, where $A\gtrsim 1$ is an arbitrary number such that $AR\mu_*$ is an integer:

$$\frac{1}{2}\sum_{\ell=0}^{\infty}s(\ell,d)=\frac{1}{2}\sum_{\ell=0}^{AR\mu}s(\ell,d)+\frac{1}{2}\sum_{AR\mu+1}^{\infty}s(\ell,d). \tag{D.23}$$

We can approximate the second sum using the Euler-Maclaurin formula:

$$\sum_{AR\mu+1}^{\infty}s(\ell,d)\simeq\int_{AR\mu}^{\infty}d\ell s(\ell,d)-\frac{s(AR\mu,4)}{2}-\sum_{k=1}^{N_1}\frac{B_{2k}}{(2k)!}s^{(2k+1)}(AR\mu,4)+\mathcal{O}(\varepsilon), \tag{D.24}$$

where B_{2k} are the Bernoulli numbers and N_1 is an integer. As $s^{(k)}(AR\mu)\sim(AR\mu)^{1-k}$ and $\frac{B_{2k}}{(2k)!}$ approaches zero exponentially fast as k grows, the error we make in (D.24) can be made arbitrarily small increasing N_1. The integral in (D.24) is approximately evaluated using the expansion (D.17) truncated after N_2 terms, giving

$$\begin{aligned}\frac{1}{2}\int_{AR\mu}^{\infty}d\ell s(\ell,d)&\simeq\frac{1}{2}(AR\mu)^d\sum_{n=1}^{N_2}\frac{c_n}{(AR\mu)^{n-1}(n-1-d)}\\&\equiv-\frac{5\left(\mu^2R^2-1\right)^2}{8\,\varepsilon}+\frac{5}{8}\left(R^2\mu^2-1\right)^2\log(R\mu)+f_{N_2,A}(R\mu)+\mathcal{O}(\varepsilon),\end{aligned} \tag{D.25}$$

where f is a regular function of $R\mu$. As before, increasing N_2 we can improve at will the precision of our calculation for $A\gtrsim 1$. Using (D.15) we then conclude

$$\Delta_0=\frac{5}{8}\left(R^2\mu_*^2-1\right)^2\log(R\mu_*)+F(R\mu_*), \tag{D.26}$$

where the function $F(R\mu_*)$ can be computed from

$$F(R\mu_*)\simeq f_{N_2,A}(R\mu_*)-\frac{s(AR\mu_*)}{2}+\left[\frac{1}{2}\sum_{\ell=0}^{AR\mu_*}s(\ell,4)-\sum_{k=1}^{N_1}\frac{B_{2k}}{(2k)!}s^{(2k+1)}(AR\mu_*)\right]_{\mu=\mu_*}. \tag{D.27}$$

The function $F(R\mu_*)$ can now be evaluated numerically and then fitted to the expected functional form, estimating the error from the first subleading terms neglected in the sums in (D.24) and (D.25). Using $N_1=4$, $N_2=10$ and $A=10$, we evaluated (D.27) for $R\mu_*=11,12,\dots 210$. The result was fitted with an expansion in $(R\mu_*)^{-2}$, starting from

$(R\mu_*)^4$, with four parameters[1]. The first three terms read:

$$F(R\mu_*) = -2.01444683(3)(R\mu_*)^4 + 2.49986(9)(R\mu_*)^2 - 0.55(4) + \mathcal{O}\left((R\mu_*)^{-2}\right) . \tag{D.28}$$

We have also verified that the coefficients of $(R\mu_*)$, $(R\mu_*)^3$, $(R\mu_*)^4 \log(R\mu_*)$ and $(R\mu_*)^2 \log(R\mu_*)$ are compatible with zero if included, individually or in combination, in the fit of the function in (D.27). Notice that the functional form (D.28) agrees with (7.84) for $d = 4$ after expanding $R\mu_*$ in terms of $(\lambda_* n)^{2/3}$.

The expansion of the first term in (D.26) produces logarithms of $\lambda_* n$:

$$\begin{aligned} \frac{5}{8}\left(R^2\mu_*^2 - 1\right)^2 \log(R\mu_*) =& 5\left(\frac{(\lambda_* n)^{4/3}}{384\pi^{8/3}} - \frac{(\lambda_* n)^{2/3}}{144\pi^{4/3}} + \frac{1}{72}\right)\log\left(\frac{\lambda_* n}{8\pi^2}\right) \\ &+ \frac{5}{288}\left(\frac{3(\lambda_* n)^{2/3}}{\pi^{4/3}} - 10\right) + \mathcal{O}\left(\left(\frac{\lambda_* n}{16\pi^2}\right)^{-2/3}\right) . \end{aligned} \tag{D.29}$$

As explained in the main text, the coefficients of the logarithms ensure that the one-loop result takes the form predicted by the large charge CFT predictions. Assuming that $F(R\mu_*)$ contains only powers of $R\mu_*$ (as we checked in (D.28)), one can verify that this is true for all the subleading orders in $(\lambda_* n)$ as well. Summing (D.28) and (D.29) and expanding $(R\mu_*)^2$ in powers of $(\lambda_* n)^{2/3}$, we obtain the result stated in the main text.

---

[1] A fit with three parameter produces the same results with smaller standard errors.

Bibliography

[1] G. Cuomo, A. Esposito, E. Gendy, A. Khmelnitsky, A. Monin and R. Rattazzi, *Gapped Goldstones at the cut-off scale: a non-relativistic EFT*, `2005.12924`.

[2] G. Cuomo, A. de la Fuente, A. Monin, D. Pirtskhalava and R. Rattazzi, *Rotating superfluids and spinning charged operators in conformal field theory*, *Phys. Rev.* **D97** (2018) 045012 [`1711.02108`].

[3] G. Cuomo, *Superfluids, vortices and spinning charged operators in 4d CFT*, *JHEP* **02** (2020) 119 [`1906.07283`].

[4] G. Badel, G. Cuomo, A. Monin and R. Rattazzi, *The Epsilon Expansion Meets Semiclassics*, *JHEP* **11** (2019) 110 [`1909.01269`].

[5] G. Badel, G. Cuomo, A. Monin and R. Rattazzi, *Feynman diagrams and the large charge expansion in* $3-\varepsilon$ *dimensions*, *Phys. Lett.* **B802** (2020) 135202 [`1911.08505`].

[6] L. Landau and E. Lifshitz, *Quantum Mechanics*, Course of Theoretical Physics. Butterworth-Heinemann, 3 ed., 1977.

[7] Y. Nambu, *Quasi-particles and gauge invariance in the theory of superconductivity*, *Phys. Rev.* **117** (1960) 648.

[8] J. Goldstone, A. Salam and S. Weinberg, *Broken Symmetries*, *Phys. Rev.* **127** (1962) 965.

[9] B. B. Brandt and M. Meineri, *Effective string description of confining flux tubes*, *Int. J. Mod. Phys. A* **31** (2016) 1643001 [`1603.06969`].

[10] T. Goto, *Relativistic quantum mechanics of one-dimensional mechanical continuum and subsidiary condition of dual resonance model*, *Prog. Theor. Phys.* **46** (1971) 1560.

[11] V. Barone, *Relatività. Principi e applicazioni*, Programma di mat. fisica elettronica. Bollati Boringhieri, 2004.

[12] G. F. Chew, *S-Matrix Theory of Strong Interactions without Elementary Particles*, *Rev. Mod. Phys.* **34** (1962) 394.

[13] S. Hellerman and I. Swanson, *String Theory of the Regge Intercept*, *Phys. Rev. Lett.* **114** (2015) 111601 [`1312.0999`].

[14] S. Dubovsky, R. Flauger and V. Gorbenko, *Evidence from Lattice Data for a New Particle on the Worldsheet of the QCD Flux Tube*, *Phys. Rev. Lett.* **111** (2013) 062006 [`1301.2325`].

[15] S. Dubovsky and V. Gorbenko, *Towards a Theory of the QCD String*, *JHEP* **02** (2016) 022 [`1511.01908`].

[16] S. Dubovsky, R. Flauger and V. Gorbenko, *Effective String Theory Revisited*, *JHEP* **09** (2012) 044 [`1203.1054`].

[17] O. Aharony and Z. Komargodski, *The Effective Theory of Long Strings*, *JHEP* **05** (2013) 118 [`1302.6257`].

[18] J. Polchinski and A. Strominger, *Effective string theory*, *Phys. Rev. Lett.* **67** (1991) 1681.

[19] S. Hellerman, S. Maeda, J. Maltz and I. Swanson, *Effective String Theory Simplified*, *JHEP* **09** (2014) 183 [`1405.6197`].

[20] J. Polchinski, *String Theory: Volume 1, An Introduction to the Bosonic String*, Cambridge Monographs on Mathematical Physics. Cambridge University Press, 1998.

[21] S. Hellerman and I. Swanson, *Boundary Operators in Effective String Theory*, *JHEP* **04** (2017) 085 [`1609.01736`].

[22] A. Nicolis, R. Penco, F. Piazza and R. Rattazzi, *Zoology of condensed matter: Framids, ordinary stuff, extra-ordinary stuff*, *JHEP* **06** (2015) 155 [`1501.03845`].

[23] D. T. Son, *Low-energy quantum effective action for relativistic superfluids*, `hep-ph/0204199`.

[24] I. Heemskerk, J. Penedones, J. Polchinski and J. Sully, *Holography from Conformal Field Theory*, *JHEP* **10** (2009) 079 [`0907.0151`].

[25] R. Rattazzi, V. S. Rychkov, E. Tonni and A. Vichi, *Bounding scalar operator dimensions in 4D CFT*, *JHEP* **12** (2008) 031 [`0807.0004`].

[26] S. R. Coleman, J. Wess and B. Zumino, *Structure of phenomenological Lagrangians. 1.*, *Phys. Rev.* **177** (1969) 2239.

[27] C. G. Callan, Jr., S. R. Coleman, J. Wess and B. Zumino, *Structure of phenomenological Lagrangians. 2.*, *Phys. Rev.* **177** (1969) 2247.

[28] S. Weinberg, *The quantum theory of fields. Vol. 2: Modern applications*. Cambridge University Press, 2013.

[29] R. V. Lange, *Goldstone Theorem in Nonrelativistic Theories*, *Phys. Rev. Lett.* **14** (1965) 3.

[30] H. B. Nielsen and S. Chadha, *On How to Count Goldstone Bosons*, *Nucl. Phys.* **B105** (1976) 445.

[31] H. Watanabe and H. Murayama, *Redundancies in Nambu-Goldstone Bosons*, *Phys. Rev. Lett.* **110** (2013) 181601 [`1302.4800`].

[32] T. Brauner, *Spontaneous Symmetry Breaking and Nambu-Goldstone Bosons in Quantum Many-Body Systems*, *Symmetry* **2** (2010) 609 [`1001.5212`].

[33] A. Nicolis and F. Piazza, *Spontaneous Symmetry Probing*, *JHEP* **06** (2012) 025 [`1112.5174`].

[34] S. Hellerman, D. Orlando, S. Reffert and M. Watanabe, *On the CFT Operator Spectrum at Large Global Charge*, *JHEP* **12** (2015) 071 [`1505.01537`].

[35] A. Monin, D. Pirtskhalava, R. Rattazzi and F. K. Seibold, *Semiclassics, Goldstone Bosons and CFT data*, *JHEP* **06** (2017) 011 [`1611.02912`].

[36] G. Morchio and F. Strocchi, *Effective Non-Symmetric Hamiltonians and Goldstone Boson Spectrum*, *Annals Phys.* **185** (1988) 241.

[37] F. Strocchi, *Symmetry Breaking*, vol. 732. 2008, 10.1007/978-3-540-73593-9.

[38] A. Nicolis and F. Piazza, *Implications of Relativity on Nonrelativistic Goldstone Theorems: Gapped Excitations at Finite Charge Density*, *Phys. Rev. Lett.* **110** (2013) 011602 [`1204.1570`].

[39] A. Nicolis, R. Penco, F. Piazza and R. A. Rosen, *More on gapped Goldstones at finite density: More gapped Goldstones*, *JHEP* **11** (2013) 055 [`1306.1240`].

[40] H. Watanabe, T. Brauner and H. Murayama, *Massive Nambu-Goldstone Bosons*, *Phys. Rev. Lett.* **111** (2013) 021601 [`1303.1527`].

[41] D. B. Kaplan and A. E. Nelson, *Strange Goings on in Dense Nucleonic Matter*, *Phys. Lett.* **B175** (1986) 57.

[42] G. E. Brown, V. Thorsson, K. Kubodera and M. Rho, *A Novel mechanism for kaon condensation in neutron star matter*, *Phys. Lett.* **B291** (1992) 355.

[43] D. T. Son and M. A. Stephanov, *QCD at finite isospin density*, *Phys. Rev. Lett.* **86** (2001) 592 [`hep-ph/0005225`].

[44] T. Schäfer, D. T. Son, M. A. Stephanov, D. Toublan and J. J. M. Verbaarschot, *Kaon condensation and Goldstone's theorem*, *Phys. Lett.* **B522** (2001) 67 [`hep-ph/0108210`].

[45] K. Rajagopal and F. Wilczek, *The Condensed matter physics of QCD*, pp. 2061–2151. 11, 2000. `hep-ph/0011333`. 10.1142/9789812810458_0043.

[46] L. Landau, E. Lifšic, E. Lifshitz, L. Pitaevskii, J. Sykes and M. Kearsley, *Statistical Physics: Theory of the Condensed State*, Course of theoretical physics. Elsevier Science, 1980.

[47] J. Polchinski, *Effective field theory and the Fermi surface*, in *Proceedings, Theoretical Advanced Study Institute (TASI 92): From Black Holes and Strings to Particles: Boulder, USA, June 1-26, 1992*, pp. 0235–276, 1992, `hep-th/9210046`.

[48] I. Z. Rothstein and P. Shrivastava, *Symmetry Realization via a Dynamical Inverse Higgs Mechanism*, *JHEP* **05** (2018) 014 [`1712.07795`].

[49] I. Z. Rothstein and P. Shrivastava, *Symmetry Obstruction to Fermi Liquid Behavior in the Unitary Limit*, *Phys. Rev.* **B99** (2019) 035101 [`1712.07797`].

[50] L. Alberte and A. Nicolis, *Spontaneously broken boosts and the Goldstone continuum*, *JHEP* **07** (2020) 076 [`2001.06024`].

[51] C. A. Orzalesi, *Charges and generators of symmetry transformations in quantum field theory*, *Rev. Mod. Phys.* **42** (1970) 381.

[52] T. Kugo and I. Ojima, *Local Covariant Operator Formalism of Nonabelian Gauge Theories and Quark Confinement Problem*, *Prog. Theor. Phys. Suppl.* **66** (1979) 1.

[53] H. Watanabe and T. Brauner, *On the number of Nambu-Goldstone bosons and its relation to charge densities*, *Phys. Rev. D* **84** (2011) 125013 [`1109.6327`].

[54] Y. Hidaka, *Counting rule for nambu-goldstone modes in nonrelativistic systems*, *Phys. Rev. Lett.* **110** (2013) 091601.

[55] H. Watanabe and H. Murayama, *Unified description of nambu-goldstone bosons without lorentz invariance*, *Phys. Rev. Lett.* **108** (2012) 251602.

[56] H. Watanabe, *Counting Rules of Nambu-Goldstone Modes*, *Ann. Rev. Condensed Matter Phys.* **11** (2020) 169 [`1904.00569`].

[57] H. J. Maris, *Phonon-phonon interactions in liquid helium*, *Rev. Mod. Phys.* **49** (1977) 341.

[58] D. Gaiotto, A. Kapustin, N. Seiberg and B. Willett, *Generalized Global Symmetries*, *JHEP* **02** (2015) 172 [`1412.5148`].

[59] S. Weinberg, *The Quantum theory of fields. Vol. 1: Foundations*. Cambridge University Press, 6, 2005.

[60] H. Georgi, *Lie algebras in particle physics*, vol. 54. Perseus Books, Reading, MA, 2nd ed. ed., 1999.

[61] H. Leutwyler, *Nonrelativistic effective Lagrangians*, *Phys. Rev.* **D49** (1994) 3033 [`hep-ph/9311264`].

[62] C. Burgess, *Goldstone and pseudoGoldstone bosons in nuclear, particle and condensed matter physics*, *Phys. Rept.* **330** (2000) 193 [`hep-th/9808176`].

[63] I. Low and A. V. Manohar, *Spontaneously broken space-time symmetries and Goldstone's theorem*, *Phys. Rev. Lett.* **88** (2002) 101602 [`hep-th/0110285`].

[64] L. V. Delacrétaz, S. Endlich, A. Monin, R. Penco and F. Riva, *(Re-)Inventing the Relativistic Wheel: Gravity, Cosets, and Spinning Objects*, *JHEP* **11** (2014) 008 [`1405.7384`].

[65] S. Dubovsky, T. Gregoire, A. Nicolis and R. Rattazzi, *Null energy condition and superluminal propagation*, *JHEP* **03** (2006) 025 [`hep-th/0512260`].

[66] L. Landau, E. Lifshitz and L. E. Reichl, *Statistical physics, part 1*, *Physics Today* **34** (1981) 74.

[67] T. Brauner and M. F. Jakobsen, *Scattering amplitudes of massive Nambu-Goldstone bosons*, *Phys. Rev.* **D97** (2018) 025021 [`1709.01251`].

[68] G. F. Giudice, C. Grojean, A. Pomarol and R. Rattazzi, *The Strongly-Interacting Light Higgs*, *JHEP* **06** (2007) 045 [`hep-ph/0703164`].

[69] A. Manohar and H. Georgi, *Chiral Quarks and the Nonrelativistic Quark Model*, *Nucl. Phys. B* **234** (1984) 189.

[70] H. Georgi, *Generalized dimensional analysis*, *Phys. Lett. B* **298** (1993) 187 [`hep-ph/9207278`].

[71] W. E. Caswell and G. P. Lepage, *Effective Lagrangians for Bound State Problems in QED, QCD, and Other Field Theories*, *Phys. Lett.* **167B** (1986) 437.

[72] P. Labelle, G. P. Lepage and U. Magnea, *Order m-alpha**8 contributions to the decay rate of orthopositronium*, *Phys. Rev. Lett.* **72** (1994) 2006 [`hep-ph/9310208`].

[73] E. Braaten, H. W. Hammer and G. P. Lepage, *Open Effective Field Theories from Deeply Inelastic Reactions*, *Phys. Rev.* **D94** (2016) 056006 [`1607.02939`].

[74] W. Kohn, *Cyclotron Resonance and de Haas-van Alphen Oscillations of an Interacting Electron Gas*, *Phys. Rev.* **123** (1961) 1242.

[75] M. Oshikawa and I. Affleck, *Electron spin resonance in $s = \frac{1}{2}$ antiferromagnetic chains*, *Phys. Rev. B* **65** (2002) 134410.

[76] M. E. Luke and M. J. Savage, *Power counting in dimensionally regularized NRQCD*, *Phys. Rev.* **D57** (1998) 413 [`hep-ph/9707313`].

[77] V. I. Ogievetsky, *Nonlinear realizations of internal and space-time symmetries*, *Proceedings of the Xth Winter School of Theoretical Physics in Karpacz* **1** (1974) 117.

[78] L. Alvarez-Gaume, O. Loukas, D. Orlando and S. Reffert, *Compensating strong coupling with large charge*, *JHEP* **04** (2017) 059 [`1610.04495`].

[79] S. Hellerman, N. Kobayashi, S. Maeda and M. Watanabe, *A Note on Inhomogeneous Ground States at Large Global Charge*, *JHEP* **10** (2019) 038 [`1705.05825`].

[80] E. A. Ivanov and V. I. Ogievetsky, *The Inverse Higgs Phenomenon in Nonlinear Realizations*, *Teor. Mat. Fiz.* **25** (1975) 164.

[81] M. H. Namjoo, A. H. Guth and D. I. Kaiser, *Relativistic Corrections to Nonrelativistic Effective Field Theories*, *Phys. Rev.* **D98** (2018) 016011 [`1712.00445`].

[82] G. T. Bodwin, E. Braaten and G. P. Lepage, *Rigorous QCD analysis of inclusive annihilation and production of heavy quarkonium*, *Phys. Rev.* **D51** (1995) 1125 [`hep-ph/9407339`].

[83] A. H. Hoang, *Heavy quarkonium dynamics*, `hep-ph/0204299`.

[84] I. Z. Rothstein, *TASI lectures on effective field theories*, 2003, `hep-ph/0308266`.

[85] A. Caputo, A. Esposito and A. D. Polosa, *Sub-MeV Dark Matter and the Goldstone Modes of Superfluid Helium*, *Phys. Rev. D* **100** (2019) 116007 [`1907.10635`].

[86] H. W. Griesshammer, *Threshold expansion and dimensionally regularized NRQCD*, *Phys. Rev.* **D58** (1998) 094027 [`hep-ph/9712467`].

[87] H. W. Griesshammer, *Power counting and Beta function in NRQCD*, *Nucl. Phys.* **B579** (2000) 313 [`hep-ph/9810235`].

[88] M. E. Luke, A. V. Manohar and I. Z. Rothstein, *Renormalization group scaling in nonrelativistic QCD*, *Phys. Rev.* **D61** (2000) 074025 [`hep-ph/9910209`].

[89] O. Loukas, D. Orlando and S. Reffert, *Matrix models at large charge*, *JHEP* **10** (2017) 085 [`1707.00710`].

[90] O. Loukas, *A matrix CFT at multiple large charges*, *JHEP* **06** (2018) 164 [`1711.07990`].

[91] S. Weinberg, *Nuclear forces from chiral Lagrangians*, *Phys. Lett. B* **251** (1990) 288.

[92] D. B. Kaplan, *Five lectures on effective field theory*, 2005, `nucl-th/0510023`.

[93] S. Moroz, C. Hoyos, C. Benzoni and D. T. Son, *Effective field theory of a vortex lattice in a bosonic superfluid*, *SciPost Phys.* **5** (2018) 039 [`1803.10934`].

[94] S. Moroz and D. T. Son, *Bosonic Superfluid on the Lowest Landau Level*, *Phys. Rev. Lett.* **122** (2019) 235301 [`1901.06088`].

[95] J. M. Maldacena, *The Large N limit of superconformal field theories and supergravity*, *Int. J. Theor. Phys.* **38** (1999) 1113 [`hep-th/9711200`].

[96] E. Witten, *Anti-de Sitter space and holography*, *Adv. Theor. Math. Phys.* **2** (1998) 253 [`hep-th/9802150`].

[97] A. M. Polyakov, *Nonhamiltonian approach to conformal quantum field theory*, *Zh. Eksp. Teor. Fiz.* **66** (1974) 23.

[98] D. Poland, S. Rychkov and A. Vichi, *The Conformal Bootstrap: Theory, Numerical Techniques, and Applications*, *Rev. Mod. Phys.* **91** (2019) 15002 [`1805.04405`].

[99] R. Rattazzi, "CFT data at large charge from Effective Field Theory." Princeton seminar, 2018.

[100] V. Papadopoulos, *Stage EPFL*, Master's thesis, École normale supérieure, 2018.

[101] D. Gaiotto, A. Kapustin, Z. Komargodski and N. Seiberg, *Theta, Time Reversal, and Temperature*, *JHEP* **05** (2017) 091 [`1703.00501`].

[102] S. Hellerman, S. Maeda and M. Watanabe, *Operator Dimensions from Moduli*, *JHEP* **10** (2017) 089 [`1706.05743`].

[103] K. G. Wilson and M. E. Fisher, *Critical exponents in 3.99 dimensions*, *Phys. Rev. Lett.* **28** (1972) 240.

[104] S. S. Pufu and S. Sachdev, *Monopoles in 2 + 1-dimensional conformal field theories with global U(1) symmetry*, *JHEP* **09** (2013) 127 [`1303.3006`].

[105] K. Farnsworth, M. A. Luty and V. Prilepina, *Weyl versus Conformal Invariance in Quantum Field Theory*, *JHEP* **10** (2017) 170 [`1702.07079`].

[106] G. K. Karananas and A. Monin, *Weyl vs. Conformal*, *Phys. Lett. B* **757** (2016) 257 [`1510.08042`].

[107] M. E. Peskin and D. V. Schroeder, *An Introduction to Quantum Field Theory*. Westview Press, 1995.

[108] J. S. Avery, *Harmonic polynomials, hyperspherical harmonics, and atomic spectra*, *Journal of Computational and Applied Mathematics* **233** (2010) 1366 .

[109] D. Jafferis, B. Mukhametzhanov and A. Zhiboedov, *Conformal Bootstrap At Large Charge*, *JHEP* **05** (2018) 043 [1710.11161].

[110] E. Vicari, *Critical phenomena and renormalization-group flow of multi-parameter Phi**4 field theories*, *PoS* **LATTICE2007** (2007) 023 [0709.1014].

[111] G. Murthy and S. Sachdev, *Action of Hedgehog Instantons in the Disordered Phase of the (2+1)-dimensional CP^{N-1} Model*, *Nucl. Phys.* **B344** (1990) 557.

[112] T. Banks and A. Zaks, *On the Phase Structure of Vector-Like Gauge Theories with Massless Fermions*, *Nucl. Phys. B* **196** (1982) 189.

[113] H. Kleinert and V. Schulte-Frohlinde, *Critical properties of phi**4-theories*. 2001.

[114] M. Campostrini, M. Hasenbusch, A. Pelissetto, P. Rossi and E. Vicari, *Critical behavior of the three-dimensional xy universality class*, *Phys. Rev. B* **63** (2001) 214503 [cond-mat/0010360].

[115] M. Campostrini, M. Hasenbusch, A. Pelissetto, P. Rossi and E. Vicari, *Critical exponents and equation of state of the three-dimensional Heisenberg universality class*, *Phys. Rev. B* **65** (2002) 144520 [cond-mat/0110336].

[116] F. Kos, D. Poland, D. Simmons-Duffin and A. Vichi, *Precision Islands in the Ising and $O(N)$ Models*, *JHEP* **08** (2016) 036 [1603.04436].

[117] S. M. Chester, W. Landry, J. Liu, D. Poland, D. Simmons-Duffin, N. Su et al., *Carving out OPE space and precise $O(2)$ model critical exponents*, *JHEP* **06** (2020) 142 [1912.03324].

[118] D. Banerjee, S. Chandrasekharan and D. Orlando, *Conformal dimensions via large charge expansion*, *Phys. Rev. Lett.* **120** (2018) 061603 [1707.00711].

[119] D. Banerjee, S. Chandrasekharan, D. Orlando and S. Reffert, *Conformal dimensions in the large charge sectors at the O(4) Wilson-Fisher fixed point*, *Phys. Rev. Lett.* **123** (2019) 051603 [1902.09542].

[120] S. Hellerman, N. Kobayashi, S. Maeda and M. Watanabe, *Observables in Inhomogeneous Ground States at Large Global Charge*, 1804.06495.

[121] D. Banerjee, S. Chandrasekharan and H. Singh. *work in progress*.

[122] A. Di Giacomo, *Lezioni di fisica teorica*. ETS, 1992.

[123] G. F. Giudice, R. Rattazzi and J. D. Wells, *Graviscalars from higher dimensional metrics and curvature Higgs mixing*, *Nucl. Phys. B* **595** (2001) 250 [hep-ph/0002178].

[124] G. F. Giudice, R. Rattazzi and J. D. Wells, *Quantum gravity and extra dimensions at high-energy colliders*, *Nucl. Phys. B* **544** (1999) 3 [hep-ph/9811291].

[125] N. Lashkari, A. Dymarsky and H. Liu, *Eigenstate Thermalization Hypothesis in Conformal Field Theory*, *J. Stat. Mech.* **1803** (2018) 033101 [`1610.00302`].

[126] M. Serone, "Notes on quantum field theory." https://www.sissa.it/tpp/phdsection/descriptioncourse.php?ID=1, 2020.

[127] D. Pappadopulo, S. Rychkov, J. Espin and R. Rattazzi, *OPE Convergence in Conformal Field Theory*, *Phys. Rev. D* **86** (2012) 105043 [`1208.6449`].

[128] S. Rychkov and P. Yvernay, *Remarks on the Convergence Properties of the Conformal Block Expansion*, *Phys. Lett. B* **753** (2016) 682 [`1510.08486`].

[129] B. Mukhametzhanov and A. Zhiboedov, *Analytic Euclidean Bootstrap*, *JHEP* **10** (2019) 270 [`1808.03212`].

[130] B. Mukhametzhanov and A. Zhiboedov, *Modular invariance, tauberian theorems and microcanonical entropy*, *JHEP* **10** (2019) 261 [`1904.06359`].

[131] J. Korevaar, *Tauberian Theory: A Century of Developments*, Die Grundlehren der mathematischen Wissenschaften in Einzeldarstellungen. Springer, 2004.

[132] A. de la Fuente and J. Zosso, *The large charge expansion and AdS/CFT*, *JHEP* **06** (2020) 178 [`2005.06169`].

[133] V. A. Rubakov, *Nonperturbative aspects of multiparticle production*, in *2nd Rencontres du Vietnam: Consisting of 2 parallel conferences: Astrophysics Meeting: From the Sun and Beyond / Particle Physics Meeting: Physics at the Frontiers of the Standard Model, Ho Chi Minh City, Vietnam, October 21-28, 1995*, 1995, `hep-ph/9511236`.

[134] M. Watanabe, *Accessing Large Global Charge via the ϵ-Expansion*, `1909.01337`.

[135] O. Antipin, J. Bersini, F. Sannino, Z.-W. Wang and C. Zhang, *Charging the $O(N)$ model*, *Phys. Rev. D* **102** (2020) 045011 [`2003.13121`].

[136] A. De La Fuente, *The large charge expansion at large N*, *JHEP* **08** (2018) 041 [`1805.00501`].

[137] É. Dupuis, M. Paranjape and W. Witczak-Krempa, *Transition from a Dirac spin liquid to an antiferromagnet: Monopoles in a QED3-Gross-Neveu theory*, *Phys. Rev. B* **100** (2019) 094443 [`1905.02750`].

[138] M. Watanabe, *Chern-Simons-Matter Theories at Large Global Charge*, `1904.09815`.

[139] D. Orlando, S. Reffert and F. Sannino, *A safe CFT at large charge*, *JHEP* **08** (2019) 164 [`1905.00026`].

[140] L. Alvarez-Gaume, D. Orlando and S. Reffert, *Large charge at large N*, *JHEP* **12** (2019) 142 [`1909.02571`].

[141] D. Orlando, S. Reffert and F. Sannino, *Charging the Conformal Window*, 2003.08396.

[142] V. Borokhov, A. Kapustin and X.-k. Wu, *Topological disorder operators in three-dimensional conformal field theory*, *JHEP* **11** (2002) 049 [hep-th/0206054].

[143] M. A. Metlitski, M. Hermele, T. Senthil and M. P. A. Fisher, *Monopoles in CP**(N-1) model via the state-operator correspondence*, *Phys. Rev.* **B78** (2008) 214418 [0809.2816].

[144] S. S. Pufu, *Anomalous dimensions of monopole operators in three-dimensional quantum electrodynamics*, *Phys. Rev.* **D89** (2014) 065016 [1303.6125].

[145] E. Dyer, M. Mezei and S. S. Pufu, *Monopole Taxonomy in Three-Dimensional Conformal Field Theories*, 1309.1160.

[146] E. Dyer, M. Mezei, S. S. Pufu and S. Sachdev, *Scaling dimensions of monopole operators in the* $\mathbb{CP}^{N_b-1}$ *theory in* $2+1$ *dimensions*, *JHEP* **06** (2015) 037 [1504.00368].

[147] S. M. Chester, L. V. Iliesiu, M. Mezei and S. S. Pufu, *Monopole Operators in* $U(1)$ *Chern-Simons-Matter Theories*, *JHEP* **05** (2018) 157 [1710.00654].

[148] S. A. Hartnoll, C. P. Herzog and G. T. Horowitz, *Building a Holographic Superconductor*, *Phys. Rev. Lett.* **101** (2008) 031601 [0803.3295].

[149] S. A. Hartnoll, C. P. Herzog and G. T. Horowitz, *Holographic Superconductors*, *JHEP* **12** (2008) 015 [0810.1563].

[150] S. A. Hartnoll, *Lectures on holographic methods for condensed matter physics*, *Classical and Quantum Gravity* **26** (2009) 224002 [0903.3246].

[151] A. Esposito, S. Garcia-Saenz and R. Penco, *First sound in holographic superfluids at zero temperature*, *JHEP* **12** (2016) 136 [1606.03104].

[152] M. Edalati, J. I. Jottar and R. G. Leigh, *Shear Modes, Criticality and Extremal Black Holes*, *JHEP* **04** (2010) 075 [1001.0779].

[153] M. Edalati, J. I. Jottar and R. G. Leigh, *Holography and the sound of criticality*, *JHEP* **10** (2010) 058 [1005.4075].

[154] O. Loukas, D. Orlando, S. Reffert and D. Sarkar, *An AdS/EFT correspondence at large charge*, *Nucl. Phys.* **B934** (2018) 437 [1804.04151].

[155] D. Son and M. Wingate, *General coordinate invariance and conformal invariance in nonrelativistic physics: Unitary Fermi gas*, *Annals Phys.* **321** (2006) 197 [cond-mat/0509786].

[156] S. M. Kravec and S. Pal, *Nonrelativistic Conformal Field Theories in the Large Charge Sector*, *JHEP* **02** (2019) 008 [`1809.08188`].

[157] S. Favrod, D. Orlando and S. Reffert, *The large-charge expansion for Schrödinger systems*, *JHEP* **12** (2018) 052 [`1809.06371`].

[158] S. Hellerman and S. Maeda, *On the Large R-charge Expansion in $\mathcal{N} = 2$ Superconformal Field Theories*, *JHEP* **12** (2017) 135 [`1710.07336`].

[159] S. Hellerman, S. Maeda, D. Orlando, S. Reffert and M. Watanabe, *Universal correlation functions in rank 1 SCFTs*, *JHEP* **12** (2019) 047 [`1804.01535`].

[160] S. Hellerman, S. Maeda, D. Orlando, S. Reffert and M. Watanabe, *S-duality and correlation functions at large R-charge*, `2005.03021`.

[161] A. Grassi, Z. Komargodski and L. Tizzano, *Extremal Correlators and Random Matrix Theory*, `1908.10306`.

[162] D. E. Berenstein, J. M. Maldacena and H. S. Nastase, *Strings in flat space and pp waves from N=4 superYang-Mills*, *JHEP* **04** (2002) 013 [`hep-th/0202021`].

[163] J. C. Plefka, *Lectures on the plane wave string / gauge theory duality*, *Fortsch. Phys.* **52** (2004) 264 [`hep-th/0307101`].

[164] J. M. Maldacena, *TASI 2003 lectures on AdS / CFT*, in *Theoretical Advanced Study Institute in Elementary Particle Physics (TASI 2003): Recent Trends in String Theory*, pp. 155–203, 9, 2003, `hep-th/0309246`.

[165] H. Nastase, *Introduction to the ADS/CFT Correspondence*. Cambridge University Press, 9, 2015.

[166] T. Bargheer, F. Coronado and P. Vieira, *Octagons I: Combinatorics and Non-Planar Resummations*, *JHEP* **19** (2020) 162 [`1904.00965`].

[167] T. Bargheer, F. Coronado and P. Vieira, *Octagons II: Strong Coupling*, `1909.04077`.

[168] L. F. Alday and J. M. Maldacena, *Comments on operators with large spin*, *JHEP* **11** (2007) 019 [`0708.0672`].

[169] Z. Komargodski and A. Zhiboedov, *Convexity and Liberation at Large Spin*, *JHEP* **11** (2013) 140 [`1212.4103`].

[170] A. L. Fitzpatrick, J. Kaplan, D. Poland and D. Simmons-Duffin, *The Analytic Bootstrap and AdS Superhorizon Locality*, *JHEP* **12** (2013) 004 [`1212.3616`].

[171] L. F. Alday and A. Zhiboedov, *Conformal Bootstrap With Slightly Broken Higher Spin Symmetry*, *JHEP* **06** (2016) 091 [`1506.04659`].

[172] D. Simmons-Duffin, *The Lightcone Bootstrap and the Spectrum of the 3d Ising CFT*, *JHEP* **03** (2017) 086 [`1612.08471`].

[173] S. Caron-Huot, *Analyticity in Spin in Conformal Theories*, *JHEP* **09** (2017) 078 [`1703.00278`].

[174] D. Simmons-Duffin, D. Stanford and E. Witten, *A spacetime derivation of the Lorentzian OPE inversion formula*, *JHEP* **07** (2018) 085 [`1711.03816`].

[175] P. Kravchuk and D. Simmons-Duffin, *Light-ray operators in conformal field theory*, *JHEP* **11** (2018) 102 [`1805.00098`].

[176] L. V. Delacretaz, *Heavy Operators and Hydrodynamic Tails*, `2006.01139`.

[177] P. Kovtun, *Lectures on hydrodynamic fluctuations in relativistic theories*, *J. Phys. A* **45** (2012) 473001 [`1205.5040`].

[178] R. Donnelly, *Quantized Vortices in Helium II*, no. 3 in Cambridge Studies in Low Temperature Physics. Cambridge University Press, 1991.

[179] B. Horn, A. Nicolis and R. Penco, *Effective string theory for vortex lines in fluids and superfluids*, *JHEP* **10** (2015) 153 [`1507.05635`].

[180] F. Lund and T. Regge, *Unified Approach to Strings and Vortices with Soliton Solutions*, *Phys. Rev.* **D14** (1976) 1524.

[181] R. L. Davis and E. P. S. Shellard, *Global strings and superfluid vortices*, *Phys. Rev. Lett.* **63** (1989) 2021.

[182] S. Endlich and A. Nicolis, *The incompressible fluid revisited: vortex-sound interactions*, `1303.3289`.

[183] R. Feynman, *Statistical Mechanics: A Set Of Lectures*, Advanced Books Classics. Avalon Publishing, 1998.

[184] A. L. Fitzpatrick, J. Kaplan and M. T. Walters, *Universality of Long-Distance AdS Physics from the CFT Bootstrap*, *JHEP* **08** (2014) 145 [`1403.6829`].

[185] L. F. Alday, A. Bissi and T. Lukowski, *Large spin systematics in CFT*, *JHEP* **11** (2015) 101 [`1502.07707`].

[186] L. F. Alday and A. Zhiboedov, *An Algebraic Approach to the Analytic Bootstrap*, *JHEP* **04** (2017) 157 [`1510.08091`].

[187] L. F. Alday, *Large Spin Perturbation Theory for Conformal Field Theories*, *Phys. Rev. Lett.* **119** (2017) 111601 [`1611.01500`].

[188] L. F. Alday, *Solving CFTs with Weakly Broken Higher Spin Symmetry*, *JHEP* **10** (2017) 161 [`1612.00696`].

[189] A. Kaviraj, K. Sen and A. Sinha, *Analytic bootstrap at large spin*, *JHEP* **11** (2015) 083 [`1502.01437`].

[190] A. Kaviraj, K. Sen and A. Sinha, *Universal anomalous dimensions at large spin and large twist*, *JHEP* **07** (2015) 026 [`1504.00772`].

[191] L. Landau and E. Lifshitz, *The Classical Theory of Fields*, Course of Theoretical Physics. Butterworth-Heinemann, 4 ed., 1975.

[192] N. Sivan and S. Levit, *Semiclassical quantization of interacting electrons in a strong magnetic field*, *Phys. Rev. B* **46** (1992) 2319.

[193] A. Entelis and S. Levit, *Quantum adiabatic expansion for dynamics in strong magnetic fields*, *Phys. Rev. Lett.* **69** (1992) 3001.

[194] T. Tochishita, M. Mizui and H. Kuratsuji, *Semiclassical quantization for the motion of the guiding center using the coherent state path integral*, *Physics Letters A* **212** (1996) 304 .

[195] G. V. Dunne, R. Jackiw and C. A. Trugenberger, *"topological" (chern-simons) quantum mechanics*, *Phys. Rev. D* **41** (1990) 661.

[196] G. Dunne and R. Jackiw, *"peierls substitution" and chern-simons quantum mechanics*, *Nuclear Physics B - Proceedings Supplements* **33** (1993) 114 .

[197] E. J. Yarmchuk, M. J. V. Gordon and R. E. Packard, *Observation of stationary vortex arrays in rotating superfluid helium*, *Phys. Rev. Lett.* **43** (1979) 214.

[198] E. B. Sonin, *Vortex oscillations and hydrodynamics of rotating superfluids*, *Rev. Mod. Phys.* **59** (1987) 87.

[199] T. T. Wu and C. N. Yang, *Dirac monopole without strings: Monopole harmonics*, *Nuclear Physics B* **107** (1976) 365 .

[200] S. Coleman, *The Magnetic Monopole Fifty Years Later*, pp. 21–117. Springer US, Boston, MA, 1983. 10.1007/978-1-4613-3655-6_2.

[201] M. Hatsuda, S. Iso and H. Umetsu, *Noncommutative superspace, supermatrix and lowest landau level*, *Nuclear Physics B* **671** (2003) 217 [`hep-th/0306251`].

[202] K. Hasebe, *Hopf Maps, Lowest Landau Level, and Fuzzy Spheres*, *SIGMA* **6** (2010) 071 [`1009.1192`].

[203] F. D. M. Haldane, *Fractional quantization of the hall effect: A hierarchy of incompressible quantum fluid states*, *Phys. Rev. Lett.* **51** (1983) 605.

[204] M. Greiter, *Landau level quantization on the sphere*, *Phys. Rev. B* **83** (2011) 115129 [`1101.3943`].

[205] M. S. Costa, J. Penedones, D. Poland and S. Rychkov, *Spinning Conformal Correlators*, *JHEP* **11** (2011) 071 [1107.3554].

[206] S. M. Chester, M. Mezei, S. S. Pufu and I. Yaakov, *Monopole operators from the* $4-\epsilon$ *expansion*, *JHEP* **12** (2016) 015 [1511.07108].

[207] Z. Komargodski, *Baryons as Quantum Hall Droplets*, 1812.09253.

[208] F. A. Berezin and M. S. Marinov, *Particle Spin Dynamics as the Grassmann Variant of Classical Mechanics*, *Annals Phys.* **104** (1977) 336.

[209] A. Barducci, R. Casalbuoni and L. Lusanna, *Supersymmetries and the Pseudoclassical Relativistic electron*, *Nuovo Cim.* **A35** (1976) 377.

[210] L. Brink, P. Di Vecchia and P. S. Howe, *A Lagrangian Formulation of the Classical and Quantum Dynamics of Spinning Particles*, *Nucl. Phys.* **B118** (1977) 76.

[211] B. S. Skagerstam and A. Stern, *Lagrangian descriptions of classical charged particles with spin*, *Physica Scripta* **24** (1981) 493.

[212] E. Elkhidir, D. Karateev and M. Serone, *General Three-Point Functions in 4D CFT*, *JHEP* **01** (2015) 133 [1412.1796].

[213] G. F. Cuomo, D. Karateev and P. Kravchuk, *General Bootstrap Equations in 4D CFTs*, *JHEP* **01** (2018) 130 [1705.05401].

[214] V. Tkachenko, *Stability of vortex lattices*, *Sov. Phys. JETP* **23** (1966) 1049.

[215] V. Tkachenko, *Elasticity of vortex lattices*, *Soviet J. Exp. Theor. Phys* **29** (1969) 945.

[216] Ó. J. C. Dias, G. T. Horowitz, N. Iqbal and J. E. Santos, *Vortices in holographic superfluids and superconductors as conformal defects*, *Journal of High Energy Physics* **2014** (2014) 96 [1311.3673].

[217] S. Kravec and S. Pal, *The Spinful Large Charge Sector of Non-Relativistic CFTs: From Phonons to Vortex Crystals*, *JHEP* **05** (2019) 194 [1904.05462].

[218] R. D. Pisarski, *Fixed point structure of* ϕ^6 *in three-dimensions at large* N, *Phys. Rev. Lett.* **48** (1982) 574.

[219] A. Monin, *Inconsistencies of higgsplosion*, 1808.05810.

[220] M. Dine, H. H. Patel and J. F. Ulbricht, *Behavior of Cross Sections for Large Numbers of Particles*, 2002.12449.

[221] L. S. Brown, *Summing tree graphs at threshold*, *Phys. Rev.* **D46** (1992) R4125 [hep-ph/9209203].

[222] M. B. Voloshin, *Multiparticle amplitudes at zero energy and momentum in scalar theory*, *Nucl. Phys.* **B383** (1992) 233.

[223] D. T. Son, *Semiclassical approach for multiparticle production in scalar theories*, *Nucl. Phys.* **B477** (1996) 378 [`hep-ph/9505338`].

[224] V. V. Khoze and M. Spannowsky, *Higgsplosion: Solving the Hierarchy Problem via rapid decays of heavy states into multiple Higgs bosons*, *Nucl. Phys. B* **926** (2018) 95 [`1704.03447`].

[225] A. Belyaev, F. Bezrukov, C. Shepherd and D. Ross, *Problems with Higgsplosion*, *Phys. Rev.* **D98** (2018) 113001 [`1808.05641`].

[226] G. Arias-Tamargo, D. Rodriguez-Gomez and J. Russo, *The large charge limit of scalar field theories and the Wilson-Fisher fixed point at* $\epsilon = 0$, *JHEP* **10** (2019) 201 [`1908.11347`].

[227] L. S. Brown and J. C. Collins, *Dimensional Renormalization of Scalar Field Theory in Curved Space-time*, *Annals Phys.* **130** (1980) 215.

[228] P. Calabrese, A. Pelissetto and E. Vicari, *Multicritical phenomena in* $O(n(1)) + O(n(2))$ *symmetric theories*, *Phys. Rev.* **B67** (2003) 054505 [`cond-mat/0209580`].

[229] M. De Prato, A. Pelissetto and E. Vicari, *Third harmonic exponent in three-dimensional* N *vector models*, *Phys. Rev.* **B68** (2003) 092403 [`cond-mat/0302145`].

[230] A. Bourget, D. Rodriguez-Gomez and J. G. Russo, *A limit for large R-charge correlators in* $\mathcal{N} = 2$ *theories*, *JHEP* **05** (2018) 074 [`1803.00580`].

[231] M. Beccaria, *On the large R-charge* $\mathcal{N} = 2$ *chiral correlators and the Toda equation*, *JHEP* **02** (2019) 009 [`1809.06280`].

[232] G. Arias-Tamargo, D. Rodriguez-Gomez and J. G. Russo, *Correlation functions in scalar field theory at large charge*, *JHEP* **01** (2020) 171 [`1912.01623`].

[233] G. Arias-Tamargo, D. Rodriguez-Gomez and J. G. Russo, *On the UV completion of the* $O(N)$ *model in* $6 - \epsilon$ *dimensions: a stable large-charge sector*, `2003.13772`.

[234] V. V. Khoze and J. Reiness, *Review of the semiclassical formalism for multiparticle production at high energies*, *Phys. Rept. C* **822** (2019) 1 [`1810.01722`].

[235] E. A. Ivanov and J. Niederle, *Gauge Formulation of Gravitation Theories. 1. The Poincare, De Sitter and Conformal Cases*, *Phys. Rev.* **D25** (1982) 976.

[236] M. Beneke and V. A. Smirnov, *Asymptotic expansion of Feynman integrals near threshold*, *Nucl. Phys.* **B522** (1998) 321 [`hep-ph/9711391`].

[237] A. V. Manohar and I. W. Stewart, *The Zero-Bin and Mode Factorization in Quantum Field Theory*, *Phys. Rev.* **D76** (2007) 074002 [`hep-ph/0605001`].

[238] S. Rychkov, *EPFL Lectures on Conformal Field Theory in $D \geq 3$ Dimensions*, SpringerBriefs in Physics. 2016, 10.1007/978-3-319-43626-5, [`1601.05000`].

[239] D. Simmons-Duffin, *The Conformal Bootstrap*, in *Proceedings, Theoretical Advanced Study Institute in Elementary Particle Physics: New Frontiers in Fields and Strings (TASI 2015): Boulder, CO, USA, June 1-26, 2015*, pp. 1–74, 2017, `1602.07982`, DOI.

[240] H. Osborn, "Lectures on conformal field theories." https://www.damtp.cam.ac.uk/user/ho/CFTNotes.pdf, 2019.

[241] P. Francesco, P. Mathieu and D. Sénéchal, *Conformal field theory*. Springer Science & Business Media, 2012.

[242] F. Kos, D. Poland, D. Simmons-Duffin and A. Vichi, *Bootstrapping the O(N) Archipelago*, *JHEP* **11** (2015) 106 [`1504.07997`].

[243] J. Cardy, *Scaling and Renormalization in Statistical Physics*, Cambridge Lecture Notes in Physics. Cambridge University Press, 1996, 10.1017/CBO9781316036440.

[244] F. Dolan and H. Osborn, *Conformal four point functions and the operator product expansion*, *Nucl. Phys. B* **599** (2001) 459 [`hep-th/0011040`].

[245] F. Dolan and H. Osborn, *Conformal partial waves and the operator product expansion*, *Nucl. Phys. B* **678** (2004) 491 [`hep-th/0309180`].

[246] T. Hartman, S. Kundu and A. Tajdini, *Averaged Null Energy Condition from Causality*, *JHEP* **07** (2017) 066 [`1610.05308`].

[247] J. Maldacena and A. Zhiboedov, *Constraining Conformal Field Theories with A Higher Spin Symmetry*, *J. Phys. A* **46** (2013) 214011 [`1112.1016`].

[248] V. Alba and K. Diab, *Constraining conformal field theories with a higher spin symmetry in $d > 3$ dimensions*, *JHEP* **03** (2016) 044 [`1510.02535`].

[249] E. A. Ivanov and J. Niederle, *Gauge Formulation of Gravitation Theories. 2. The Special Conformal Case*, *Phys. Rev.* **D25** (1982) 988.

[250] D. V. Volkov, *Phenomenological Lagrangians*, *Fiz. Elem. Chast. Atom. Yadra* **4** (1973) 3.

[251] A. Monin, *Partition function on spheres: How to use zeta function regularization*, *Phys. Rev. D* **94** (2016) 085013 [`1607.06493`].

[252] R. M. Wald, *General relativity*. Chicago Univ. Press, Chicago, IL, 1984.

[253] Z. Komargodski and A. Schwimmer, *On Renormalization Group Flows in Four Dimensions*, *JHEP* **12** (2011) 099 [`1107.3987`].

[254] T. H. Koornwinder et al., *Dual addition formulas associated with dual product formulas*, *arXiv preprint arXiv:1607.06053* (2018) .

[255] M. Srednicki, *Chaos and quantum thermalization*, *Phys. Rev. E* **50** (1994) 888.

[256] M. Srednicki, *Thermal fluctuations in quantized chaotic systems*, *J. Phys. A* **29** (1996) L75 [`chao-dyn/9511001`].

[257] L. V. Delacrétaz, T. Hartman, S. A. Hartnoll and A. Lewkowycz, *Thermalization, Viscosity and the Averaged Null Energy Condition*, *JHEP* **10** (2018) 028 [`1805.04194`].

[258] A. Belin and J. de Boer, *Random Statistics of OPE Coefficients and Euclidean Wormholes*, `2006.05499`.

[259] J. Gomis, K. Kamimura and J. M. Pons, *Non-linear Realizations, Goldstone bosons of broken Lorentz rotations and effective actions for p-branes*, *Nucl. Phys. B* **871** (2013) 420 [`1205.1385`].

[260] E. D'Hoker and D. Z. Freedman, *Gauge boson exchange in AdS(d+1)*, *Nucl. Phys.* **B544** (1999) 612 [`hep-th/9809179`].

[261] E. D'Hoker, D. Z. Freedman, S. D. Mathur, A. Matusis and L. Rastelli, *Graviton and gauge boson propagators in AdS(d+1)*, *Nucl. Phys.* **B562** (1999) 330 [`hep-th/9902042`].

[262] S. Domazet and T. Prokopec, *A photon propagator on de Sitter in covariant gauges*, `1401.4329`.

[263] B. Allen and T. Jacobson, *Vector Two Point Functions in Maximally Symmetric Spaces*, *Commun. Math. Phys.* **103** (1986) 669.

Gabriel Francisco Cuomo

Curriculum Vitae

Swiss address: Rue du Lac 43, 1020, Renens CH
Italian (permanent) address: Via Romano 6, Acireale (CT), 95024 IT
☎ *+41 77 9172296*
✉ *gabriel.cuomo@epfl.ch*
9th March 1993, Catania (CT), Italy

Research interests

My research interests encompass several aspects of quantum field theory and theoretical particle physics, including analytical methods in conformal field theories, finite density systems, and high energy electroweak physics.

Education and training

November 2016–present	**PhD in Theoretical Particle Physics**, *École Polytechnique Fédérale de Lausanne (EPFL), Laboratory of Theoretical Particle Physics (LPTP)*, Supervisor: Prof. Riccardo Rattazzi.
September 2014–October 2016	**International Master Programme in Theoretical Physics**, *University of Trento - SISSA (International School for Advanced Studies, Trieste)*, LM-17 - Fisica, Graduation Thesis: Kinematic aspects of n-point functions in 4d conformal field theories. Advisor: Prof. Marco Serone (SISSA). Average grade of the exams: 29.6/30. *110/110 with honor*
October 2011–October 2014	**Complementary bachelor honor program: Scuola Superiore di Catania**, *University of Catania*, Graduation thesis: Derivation of a Linblad equation for heavy quark diffusion in an Abelian plasma. Advisor: Prof. Pietro Faccioli (University of Trento). Excellence program of the University of Catania (acceptance rate $\lesssim 10\%$). *70/70 with honor*
October 2011–October 2014	**Bachelor degree in Physics**, *University of Catania*, L-30 - Scienze e tecnologie fisiche, Graduation thesis: Geometric Phases in Molecular Physics. Advisor: Prof. G.G.N. Angilella (University of Catania). Average grade of the exams: 29.9/30. *110/110 with honor*
2006–2011	**High School**, *Liceo Classico Gulli e Pennisi*, Acireale (CT). *100/100 with honor*

Publications

The following list is updated to July 1, 2020. An updated list is available at this *link*.

Published papers

2019 G. Cuomo, L. Vecchi and A. Wulzer,
"Goldstone Equivalence and High Energy Electroweak Physics",
SciPost Phys. 8 (2020) 5, 078
e-Print: arXiv:1911.12366 [hep-ph]

2019 G. Badel, G. Cuomo, A. Monin, and R. Rattazzi,
"Feynman diagrams and the large charge expansion in $3-\varepsilon$ dimensions",
Phys.Lett. B802 (2020) 135202,
e-Print: arXiv:1911.08505 [hep-th]

2019 G. Badel, G. Cuomo, A. Monin, and R. Rattazzi,
"The epsilon expansion meets semiclassics",
JHEP 1911 (2019) 110,
e-Print: arXiv:1909.01269 [hep-th]

2019 G. Cuomo,
"Superfluids, vortices and spinning charged operators in 4d CFT",
JHEP 2002 (2020) 119,
e-Print: arXiv:1906.07283 [hep-th]

2017 G. Cuomo, A. de la Fuente, A. Monin, D. Pirtskhalava, and R. Rattazzi,
"Rotating superfluids and spinning charged operators in conformal field theory",
Phys. Rev.D 97 (2018) no. 4, 045012,
e-Print: arXiv:1711.02108 [hep-th]

2017 G. Cuomo, Denis Karateev, and Petr Kravchuk,
"General Bootstrap Equations in 4DCFTs",
JHEP01, 130, (2018),
e-Print: arXiv:1705.05401 [hep-th]

Online preprints

2020 G. Cuomo, A. Esposito, E. Gendy, A. Khmelnitsky, A. Monin and R. Rattazzi,
"Gapped Goldstones at the cutoff scale: a nonrelativistic EFT",
e-Print: arXiv:2005.12924 [hep-th]

Talks

Talks at conferences and workshops

2019 **Superfluids, vortices and spinning charged operators in CFTs**

- talk for the program "Quantum-Mechanical Systems at Large Quantum Number" at the Simons center for geometry and physics, Stony Brook, USA.

Seminars at universities and research institutes

2019 **Gapped Goldstones at the cutoff scale**
- University of Catania, Catania, Italy
- New York University (NYU), New York, USA
- Columbia University, New York, USA

2019 **Superfluids, vortices and spinning charged operators in CFTs**
- Technical University of Munich (TUM), Munich, Germany

2019-2020 **The epsilon expansion meets semiclassics**
- Yale University, Yale, USA
- Scuola Internazionale Superiore di Studi Avanzati (SISSA), Trieste, Italy
- Ludwig Maximilian University (LMU), Munich, Germany
- Bern University, Bern, Switzerland
- École normale supérieure (ENS), Paris, France
- webinar for the University of Chicago, Chicago, USA

Teaching experience

Student supervision

Nov. 2018–July 2019 **Master thesis co-supervisor**, *EPFL/University of Pisa*,
Student: E. Gendy. Title of the thesis: "On massive Nambu-Goldstone bosons".

Teaching activity

Feb.–May 2019 **Bachelor in Sciences Forensiques UNIL**, *Physique générale II*,
Teaching assistant for the exercise sessions.

Sep.–Dec. 2017 – 2019 **Master in Physics EPFL**, *Quantum field theory I*,
Teaching assistant for the exercise sessions.

Feb.–May 2017 & 2018 **Master in Physics EPFL**, *Quantum field theory II*,
Teaching assistant for the exercise sessions.

Awards and scholarships

2015–2016 **SISSA**.
Scholarship for the admission to the Master Programme (2500 EUR per year).

2013 **University of Catania**.
Merit scholarship awarded to the best bachelor physics students of the University of Catania, first place (1000 EUR).

2011 **Valorizzazione delle eccellenze - Miur**, Italy, national prize.
Italian merit prize for graduating with the maximum mark and honor at high school.

Schools attended

July 2018	**Bootstrap school**, *California Institute of Technology (CALTECH)*, Pasadena.
July 2017	**Prospects in Theoretical Physics (PITP)**, *Institute of Advanced Studies (IAS)*, Princeton.
January 2017	**GGI lectures on the theory of fundamental interactions**, *Galileo Galilei Institute for Theoretical Physics (GGI)*, Firenze.
August 2014	**Utrecht Summer School in Theoretical Physics**, *University of Utrecht*, Utrecht.

Programming languages and technical softwares

`Mathematica`, LaTeX.

Languages

Italian	Mother tongue.
Spanish	Mother tongue.
English	Fluent. CAE (C1) in 2011.
French	Intermediate (speaking, reading); basic (writing).

Lausanne, July 1, 2020.